Excitatory amino acid receptors implicated in neuropathic pain: The role of receptor phosphorylation and adapter proteins

by Emer Garry

Thesis presented for the degree of Doctor of Philosophy

Department of Preclinical Veterinary Sciences
Faculty of Veterinary Medicine
University of Edinburgh

2002

DECLARATION

I hereby declare that the composition of this thesis and the work presented in it are entirely my own with the exception of the biochemical enzyme assay work which was carried out as part of a collaborative study by Dr. Rory Mitchell at the MRC Membrane and Adapter Proteins Co-op, Division of Biomedical and Clinical Laboratory Sciences, University of Edinburgh. Some of this work has been published in abstract form.

Emer Garry

Published Abstract

E. Garry, A. Moss, F. O'Neill, J. Blakemore, J. Bowen, R. Mitchell, H. Husi, S.G.N. Grant, S.M. Fleetwood-Walker (2001) Evidence for a role of the NMDA receptor-interacting protein PSD-95 in neuropathic pain. *Soc Neurosci Abstracts*, 145.

ACKNOWLEDGEMENTS

This work was supported by the Wellcome Trust and a studentship awarded by the Preclinical Veterinary Faculty. I would like to begin by thanking my supervisor Dr Sue Fleetwood-Walker for all her advice, continued support and guidance throughout. I would like to thank Dr. Rory Mitchell at the MRC Membrane and Adapter Proteins Co-op for his expert biochemical and pharmacological assistance. Also, many thanks to Prof. Seth Grant for providing the mutant mice and Dr. Roger Klegg at the Hannah Research Institute in Ayr for kindly donating control myristoylated peptides. I would like to further extend my appreciation to my thesis committee, Mike Shipston and Prof. Vince Molony for their continued encouragement.

Special thanks to members of the lab for teaching me all they know and making the three years immensely enjoyable. In particular, Andrew Moss, James Blakemore, Vicky Wallace, Francis O'Neill and John Wilson. I would also like to thank everyone at the department of Preclinical Veterinary Sciences for their expert assistance. I am especially indebted to all my family and friends for their support which helped me get through the thesis writing!

CONTENTS

LIST OF FIGURES

LIST OF TABLES

ABSTRACT

Ionotropic glutamate receptors play key roles in the spinal processing of nociceptive inputs, especially in chronic pain states, which involve sensitisation of spinal neurones. The resulting hyperalgesia and allodynia are prominent in models of neuropathic pain arising from peripheral nerve injury; a condition poorly treated with currently available analgesics. The NMDA subtype of glutamate receptor is thought to be involved particularly in inducing the central sensitisation that occurs in the spinal cord during chronic pain, while AMPA receptors are more generally believed to have a greater role in acute nociceptive and non-nociceptive processing.

Both NMDA and AMPA receptors have been shown to bind to a number of intracellular adapter proteins, which link the receptors to a variety of proteins with signalling, scaffolding and other roles. As there is little or no functional data for these proteins in spinal cord, studies were carried out to assess whether they play a role in the regulation of ionotropic receptor-mediated mechanisms of neuropathic pain.

We show, using intrathecal drug administration in a rat model of neuropathic pain, that AMPA receptors play a greater role in sensitisation than in normal somatosensory inputs and could represent a novel target for selective intervention in neuropathic hyperalgesia/allodynia. Furthermore, we have implicated for the first time a possible role for the AMPA receptor adapter proteins SAP97, PICK1, GRIP and NSF in neuropathic sensitisation from experiments with cell-permeable blocking peptides for their interaction motifs. In addition, the levels of mRNA and protein for GluR2 and GRIP and the mRNA for another adapter protein, Narp increased in the spinal cord in response to peripheral mononeuropathy. In contrast, GluR1 levels were decreased and no observable difference was seen in NSF or PICK1, or SAP97. Further experiments addressed the effects of nerve-injury on phosphorylation of the AMPA receptor GluR1 subunit and on the association of the GluR2 subunit with GRIP and PICK 1.

Additionally, we show that mutant mice expressing a truncated form of the PSD-95 adapter protein lack the NMDA receptor-dependent reflex sensitisation that is characteristic of neuropathic pain. PSD-95 was found in spinal NMDA receptor complexes and was expressed in lamina II neurons. Biochemical studies indicate that NMDA-mediated Ca^{2+} entry is unaffected in the mutant mice, yet the facilitation of this process that is normally brought about by nerve injury is impaired, with a corresponding deficit in nerve-injury induced phosphorylation of the NMDA receptor NR1 subunit.

These studies suggest new pharmacological targets for chronic pain and a critical involvement of protein: protein complexes associated with the NMDA and AMPA ionotropic glutamate receptors.

ABBREVIATIONS

ABP	AMPA binding protein
AKAP	A kinase anchoring proteins
AMPA	α-amino-3-hydroxy-5-methyl-4-isoxazole proprionic acid
ANOVA	Analysis of variance
BCA	bicinchoninic acid
BLAST	Basic Local Alignment Search Tool
°C	degrees centigrade
Ca^{2+}	calcium
CaMKII	calcium/calmodulin-dependent protein kinase
cAMP	cyclic adenosine 3',5'-monophosphate
CB	choleratoxin B (choleragenoid)
CCI	chronic constriction injury
cDNA	complementary DNA
CGRP	calcitonin gene-related peptide
CNS	central nervous system
Cu^{2+}	copper
dATP	deoxyadenosine triphosphate
DEPC	diethyl pyrocarbonate
dH_2O	distilled water
DMF	dimethylformamide
DNA	deoxyribose nucleic acid
DRG	dorsal root ganglion
DTT	dithiothreitol
EAA	excitatory amino acid
ECL	enhanced chemiluminescence
EDTA	ethylenediamine treat acetic acid
ER	endoplasmic reticulum
GABA	γ-amino-butyric acid
GAL	galanin

GAPDH	glyceraldehyde-3-phosphate dehydrogenase
GRASP	GRIP-associated protein
GRIP	glutamate receptor interacting protein
hr	hour(s)
HRP	horseradish peroxidase
HTM	high threshold mechanoreceptor
IEG	immediate early gene
i.p.	intraperitoneal
ISHH	In situ hybridisation histochemistry
I.T.	intrathecal
K^+	potassium
KN-92	2-[N-(2-hydroxyethyl)-N-(4-methoxybenzenesulfonyl)
	amino-N-(4-chlorocinnamyl)-N-methylbenzylamine (KN-92),
KN-93	3-[N-(4-Methoxybenzenesulfonyl)]amino-N-methylbenzylamine
LTD	long-term depression
LTM	low threshold mechanoreceptor
LTP	long-term potentiation
M; mM	molar; millimolar
mAb	monoclonal antibody
MAGUK	membrane associated guanylate kinase
MIA	mechanically insensitive afferents
min	minute(s)
mg; kg	milli- kilo- gram
Mg^{2+}	magnesium
mGluR	metabotropic glutamate receptor
mm; μm	milli- micro- metres
MNS	motoneurones
mRNA	messenger RNA
myr-AIP	myristoylated autocamtide-2 related inhibitory peptide
Na^+	sodium
NaCl	sodium chloride
Narp	neuronal activity-regulated pentraxin

NBQX	2,3-dihydroxy-6-nitro-7-sulfamoyl-benzo(f)quinoxaline
NCBI	National Centre for Biotechnology Information
NK	neurokinin
NMDA	*N*-methyl-D-aspartate
nNOS	neuronal nitric oxide synthase
NPY	neuropeptide Y
NR	NMDA receptor
NRM	nucleus Raphe magnus
NS	nocispecific dorsal horn neurones
NSAID	non-steroidal anti-inflammatory drug
NSF	*N*-ethylmaleimide-sensitive fusion protein
pAb	polyclonal antibody
PAG	periaqueductal gray
PBS	phosphate buffered saline
PDZ	PSD-95/SAP90, *Dlg*-A, ZO-1 domain
PKA	cAMP-dependent protein kinase
PKC	phospholipid/calcium-dependent protein kinase C
PSD	postsynaptic density
PVDF	polyvinyl difluoridine
PWL	paw withdrawal latency
PWT	paw withdrawal threshold
RA	rapidly adapting
(R)-CPP	3-((*R*)-2-Carboxypiperazin-4-yl)-propyl-1-phosphonic acid
RNA	ribonucleic acid
RNase	ribonuclease
RVM	rostral ventromedial medulla
SA	slowly adapting
SAP	synapse-associated protein
SCT	spinocervical tract
SDS-PAGE	SDS polyacrylamide gel electrophoresis
SEM	standard error of the mean
SMT	spinomesencephalic tract

SOM	somatostatin
SP	substance P
SPA	stimulation-produced analgesia
SPET	suspended paw elevation time
SSC	standard saline citrate buffer
STT	spinothalamic tract
TE	Tris-EDTA
TEA	triethanolamine
tRNA	transfer RNA
VIP	vasoactive intestinal polypeptide
WDR	wide dynamic range dorsal horn neurones
WGA	wheatgerm agglutinin

CHAPTER 1: Introduction

This thesis is concerned with the mechanisms underlying chronic neuropathic pain, a pervasive clinical condition with unsatisfactory therapeutic treatment to date. Specifically, we will examine the two major receptors that are known to contribute to glutamatergic excitatory transmission of nociceptive processing in the central nervous system, the AMPA and NMDA receptors, as well as their newly identified intracellular interacting proteins and consider how they may be involved in neuropathic pain processing in the spinal cord by use of an animal model of mononeuropathy (Bennett and Xie, 1988). First, however, it will be necessary to introduce normal somatosensory processing as well as current views on factors that may contribute to the development and maintenance of neuropathic pain in the central nervous system.

1.1 Chronic pain

Pain is a complex phenomenon. It is more than a mere sensation, representing a highly subjective individual experience involving not only the transduction of injurious environmental stimuli, but also the cognitive, emotional and situational processing of this information. Acute pain is a self-limited normal sensation triggered in the nervous system as an alert to possible injury thus serving a protective mechanism. However, chronic pain is maladaptive and serves no apparent biological advantage, can persist for weeks, months and even years, and is primarily due to hyperexcitability in the nervous system, resulting in spontaneous pain and hypersensitivity.

Chronic pain remains a major health care problem afflicting an estimated 70% of patients with advanced cancer and inflammatory disorders and up to 94% of patients with spinal cord injuries (Grond et al., 1994; Hiraga, Mizuguchi and Takeda, 1991).

The socio-economic impact of chronic pain is vast and there is gaping hole in effective therapeutics.

Officially, pain is defined by the International Association for the Study of Pain (IASP) as:

" An unpleasant sensory and emotional experience associated with potential or actual tissue damage or described in terms of such damage".

-Merskey, 1986

This definition highlights the distinction between *'nociception'*, the physiological detection of tissue damage by specialised cutaneous receptors, and *'pain'*, the perceptual awareness of nociception that is subject to emotional and situational interpretation.

Common chronic pain complaints include headache, low back pain, cancer pain, arthritic pain and neurogenic pain, resulting from damage to the peripheral nerves or to the central nervous system itself (Scadding, 1984). The prevalence of chronic pain is difficult to establish. In the UK, 46.5% of the population report some chronic pain with 14.1% reporting significant chronic pain (Elliot et al., 1999). In Australia, prevalence is estimated at 17-20%, while 15-20% (50 million) of Americans are reported to have some form of chronic pain that costs the economy billion of dollars annually (Rudin, 2001).

1.2 Neuropathic pain

A major cause of chronic pain is trauma to or compression of peripheral nerves. Peripheral neuropathy may be caused by diseases of the nerves or as a result of systemic illnesses. Many neuropathies have well-defined causes such as diabetes, AIDs, or nutritional deficiencies, mechanical pressure such as nerve compression or entrapment as well as direct nerve trauma. A common example of entrapment neuropathy is carpal tunnel syndrome, which has become more common because of repetitive strain inflammatory injury due to the increasing use of computers.

Although the causes of peripheral neuropathy are diverse, they produce common symptoms including weakness, numbness, paraesthesias (abnormal sensations such as burning, tickling, pricking or tingling) and pain (Scadding, 1984). This includes increased responses to normally noxious stimuli (hyperalgesia) and painful responses to normally innocuous stimuli (allodynia), as well as spontaneous pain.

1.3 Available treatments

Drugs have a limited efficacy in the treatment of neuropathic pain and currently the mainstay of pain management depends on opiates, which have a limited use in chronic neuropathic pain treatment where they are largely ineffective and there are associated tolerance and dependence problems. Apart from trigeminal neuralgia, which responds well to the anticonvulsant carbamazepine, pharmacological interventions for neuropathic pain are seriously lacking. There are a number of recognised medications that may aid in the management of chronic pain such as non-opioid analgesic NSAIDs (non-steroidal anti-inflammatory drugs). However, the action of these drugs in the treatment of chronic neuropathic pain is relatively minor and highly variable. The search for adequate analgesics to treat neuropathic pain is ongoing. However, the new compound, gabapentin shows clinical efficacy in chronic pain treatment, although their mechanism of action is unknown at present (Rose and Kam 2002). One focus of research has been the NMDA receptor (which will be dealt with in greater detail later), a major receptor in the nervous system known to be activated following peripheral nerve trauma. Blockade of this receptor with antagonists like dextromethorphan or ketamine appeared initially to be a promising therapeutic development but toxicity, low safety margins and psychotropic side effects are unacceptable and limit their use.

Clearly it is vital to identify novel, more specific targets that alleviate chronic neuropathic pain, without affecting normal acute responses. In order to do this, it is necessary to understand the underlying mechanisms and factors involved in the generation and maintenance of the neuropathic pain state which relies on an

understanding of the normal somatosensory transmission and how this is altered following nerve trauma.

1.4 Normal somatosensory processing in acute pain transmission

Somatosensory systems are concerned with the conversion of environmental to electrochemical stimuli by transduction of cutaneous stimuli via a variety of afferents, which innervate the skin, and relaying that information to the central nervous system (CNS). The glabrous skin contains a complex array of free nerve endings and axons which terminate in specialised end organs. Generally speaking, information from stimuli applied to the skin, evoking sensations like vibration, stretch, touch, itch, pressure and pain are detected by specialised receptors in the skin and transmitted to the spinal cord via afferent sensory axons where they have highly structured termination patterns in the dorsal horn of the spinal cord (Wall, 1960; Brown and Fuchs, 1975). The terminal regions of the primary afferent fibres have receptive fields with discrete innervation territories activated only by stimuli that directly impinge on their receptive fields. Skeletal and visceral innervation are beyond the scope of this work.

1.5 Peripheral nervous system

Mechanoreceptors and nociceptors innervating the skin are the two major components of the peripheral sensory system involved in relaying information about mechanical stimuli (such as light touch, vibration and pressure) and painful stimuli (noxious pressure, pinch or temperature), respectively (Lynn, 1994) with distinct activation thresholds that must be reached by such stimulation before they become activated.

Peripheral nociceptors exist as free nerve endings and are classified according to axon type. Briefly, Aα and Aβ fibres are large myelinated fibres (15-20μm in diameter) with rapid conduction velocities (60-100m/s) that relay information about proprioception (muscle sense) and touch, respectively. These fibres do not normally

contribute to pain but instead are involved with processing innocuous stimuli. Aδ fibres are smaller diameter (1-5μm) myelinated fibres with conduction velocities of ~20m/s that respond to intense mechanical and mechano-thermal stimuli. C-fibres are unmyelinated and so have slower conduction velocities (~2m/s) and respond to a range of noxious mechanical, thermal and chemical stimuli (summarised below). Thus, the normally accepted classification of afferent somatosensory inputs is based on response characteristics to innocuous and noxious stimuli applied to the skin and comprises non-nociceptive mechanoreceptors and thermoreceptors as well as nociceptors.

1.5.1 Non-nociceptive mechanoreceptors

Cutaneous mechanoreceptors are a diverse group of highly sensitive sensory receptors that have the ability to respond to a variety of tactile sensations. Receptors innervating hair follicles in hairy skin respond to hair movements, with D-hair units responding to movement of the fine 'down' hairs with conduction velocities in the Aδ range, G-hair units responding to rapid movement of 'guard' hairs with the highest mechanical thresholds conducting in the large myelinated A fibre range and T-hair units, responding to movements of the least numerous, large 'tylotrich' hairs, are rapidly adapting and conduct in the Aαβ range (Lynn and Carpenter, 1982; Brown and Iggo, 1967).

Rapidly adapting ('RA') Meissner and Pacinian corpuscle receptors are mechanoreceptors responding to light touch, pressure and vibration while slowly adapting ('SA') type I mechanoreceptors associated with Merkel cells and SA type II mechanoreceptors associated with Ruffini corpuscles are involved in stretch perception and shape discrimination, respectively (Willis and Coggeshall, 1991). These are associated with the rapidly conducting Aβ fibres involved in innocuous information transmission. Unmyelinated C-fibre mechanoreceptors have also been identified as responsive to gentle mechanical stimulation and cooling of the skin (Bessou et al., 1971).

Cold and warm thermoreceptors constitute a further class of non-nociceptive receptors responding to small variations in cold sensations (Aδ and cold-specific C-fibres) and to slight warming of the skin in the non-noxious range (30-37°C), respectively (Iggo, 1959).

1.5.2 Nociceptors

The term 'nociceptor' was introduced by Sherrington (1906) who defined nociceptive afferents as '*those primary afferent neurones that can be activated by harmful or potentially harmful stimuli and that give rise to the sensation of pain*'. They are functionally divided into two groups consisting of Aδ mechanical and C-fibre polymodal nociceptors. In general, electrical stimulation of Aδ fibres evokes the rapid, sharp pain sensation ('first pain'), while stimulation of C-fibres produces the dull, diffuse or burning pain ('second pain'; Woolf and Hardy, 1941).

Aδ mechanoreceptors are functionally distinct fibres for recognising mechanical skin stimulation and are excited by high threshold mechanical (HTM) stimulation of the skin, such as pressure and pinch. About 20% of A fibres are HTM (other types of A fibres being RA and SA type I and II, as discussed in the preceding section; Lynn and Carpenter, 1982). Aδ fibres are nociceptive in function and so become activated after strong pressure stimulation that lowers the response threshold and causes spontaneous firing (Burgess and Perl, 1967; Lynn and Shakhanbeh, 1988). A commonly used method to examine myelinated fibres is intracellular labelling with cholera toxin (choleragenoid, CB) that, when conjugated to HRP, only labels the terminals of these medium to large diameter myelinated afferents (Robertson and Grant, 1985).

C-polymodal nociceptors respond to a wide range of stimuli including noxious heat (≥42°C), high threshold mechanical and chemical stimulation (Bessou and Perl, 1969). They differ from other sensory receptors in this ability to respond to multiple stimulus modalities (Treede and Magerl, 1995). C-fibre responses to heat can be increased by a variety of conditioning stimuli, such as capsaicin (the 'hot' factor in

chilli peppers) and mustard oil (allyl isothiocyanate) both of which are considered to selectively activate C-fibre nociceptors (Bevan and Szolcsanyi, 1990, Woolf and Wall, 1986). These compounds, as well as intracellular labelling with wheatgerm agglutinin (WGA) that, when conjugated to HRP, predominantly labels small diameter C-fibre terminals (Robertson and Grant, 1985), are common tools to examine C-fibre properties.

Other types of nociceptors include cold nociceptors, that respond to $<0^{o}C$ stimuli associated with Aδ nociceptors and possibly cold-sensitive C-fibres (Simone and Kajander, 1996). There may also be chemical nociceptors that respond specifically to changes in extracellular pH and acidosis. Finally, 'silent' nociceptors, that require sensitisation before responding to a stimulus, have been identified (Schaible and Schmidt, 1985).

An important feature is that repetitive C-fibre stimulation results in an increased responsiveness of dorsal horn neurones, a phenomenon known as 'wind-up', that lasts several minutes and in normal spinal circuits is NMDA receptor-dependent (Mendell and Wall, 1965; Mendell, 1966, see Section 1.7.3).

1.5.3 Fibre composition of the sciatic nerve

The sciatic nerve of the rodent, which is the target of surgical manipulation in the present work (see Section 1.11.1), is divided into the sural, lateral sural, superficial peroneal and tibial nerves. In consideration of the above types of primary afferents, the fibre composition of the entire rat sciatic nerve at mid-thigh level is estimated at ~27,000 axons, 6% of which are myelinated motor axons, 23% are myelinated A fibres, 48% are unmyelinated C-fibre sensory axons, and 23% are unmyelinated sympathetic axons (Schmalbruch, 1986).

Sensory axons in the peripheral nerves are supported metabolically by their nerve cell body, which resides in the dorsal root ganglia (DRG). Cell bodies with the large diameters in the DRG give rise to the myelinated rapidly conducting Aβ fibres while

small and medium diameter DRG cell bodies give rise to most of the nociceptive Aδ and C-fibres (Willis and Coggeshall, 1991). The sciatic nerve projects to distinct regions in the superficial dorsal horn, mostly to LI and LII, in L4-L6 spinal segments in an orderly topographic pattern (Swett and Woolf, 1985).

1.6 Central nervous system

The first synaptic relay in the dorsal horn occurs between the primary afferent terminals and dorsal horn neurones, a connection governed by attributes in the *presynaptic* peripheral afferent fibres themselves, such as the type of neuropeptides and neurotransmitters released, and the response properties of *postsynaptic* central neurones (whether they are intrinsic or projection neurones) these afferent fibres come into contact with. However, before examining the convergence of these primary afferents and their specific terminations in the spinal cord, it is necessary to explain the lamination pattern in the dorsal horn.

1.6.1 Dorsal horn organisation

The superficial dorsal horn is the first synaptic relay of the fine afferent fibres from skin, described above, and is regarded as the initial processing site for signals directly related to the transmission and modulation of pain (Cervero, 1988). The current view of the spinal cord is based on the work of Rexed (1952) who classified the 'butterfly' shape of the cat spinal cord grey matter into nine laminae, which make up the dorsal and ventral horns of the spinal cord and a tenth lamina that surrounds the central canal. This work has been extended to other species including the rat (Molander, Xu and Grant, 1984; Fig. 1.1a). For the purposes of this work, emphasis will be placed on the architecture of the rat dorsal horn (laminae I-V).

Lamina I (LI, 'marginal zone') is a thin layer extending medially and laterally around the superficial edge of the dorsal horn with loosely distributed small (5x5μm) and large cells (15x5μm, the Marginal cells of Waldeyer). LI is a major site of termination of thinly myelinated (Aδ) fibres, and correspondingly many cells in this

lamina respond to noxious mechanical and/or thermal stimuli (Light and Perl, 1979; Willis and Coggeshall, 1991). LI also contains cells of origin of the spinothalamic tract (STT), which will be dealt with in more detail below (see Section 1.9) (Lima and Coimbra, 1986; Giesler et al., 1976).

Lamina II (LII, 'substantia gelatinosa') lies ventral to LI, has an outer zone (LII_o) with densely packed small cells (5x5μm) and a less compact inner zone (LII_i) distinguished by the relative lack of myelinated fibres. LII is the main termination site for unmyelinated C-afferent fibres from the skin with sparse Aδ input (Light and Perl, 1979; Réthelyi, 1977; Sugiura et al., 1988). Neurones in LII are mostly intrinsic interneurones with extensive local integration. While there is some projection into LI, only ~1% of LII neurones send their axons to the brainstem (Willis and Leonard, 1979; Giesler et al., 1978).

Lamina III (LIII), ventral to LII, is defined by the presence of transversely cut myelinated fibres. LIII cells are less tightly packed than LII and are generally larger (7-8μm x 10-12μm). Large hair follicle afferents (G-, T, and smaller D- hair), Pacinian corpuscles and RA mechanoreceptive afferents terminate in LIII. LIII cell dendrites project to LI and IV, and this lamina contains cells of origin of the spinocervical tract (SCT) and the postsynaptic dorsal column tract (see Section 1.9, Brown, 1981).

Lamina IV (LIV) is thicker than the previous three laminae and is the first layer not to show a lateral bend. LIV has scattered larger cells (10x15μm), and many of their dendrites ascend into LI –III, such that LIV can receive a direct primary afferent input from fibres that enter the superficial layers. A significant number of the larger LIV cells are the cells of origin of the spinocervical tract and the postsynaptic dorsal column tract (see Section 1.9, Brown, 1981).

Lamina V (LV) forms the neck of the dorsal horn and, in comparison to LIV, contains a more heterogeneous neuropil with even larger cells (15x20μm).

Many fine afferent fibres from muscle and viscera as well as some small myelinated afferents from skin nociceptors project directly in LV (Brown, 1981). Together, LIII, IV and the dorsal part of LV make up the 'nucleus proprius' (Brown, 1981). Many of the cells in LV constitute the ascending projection to the thalamus (Giesler et al., 1976).

1.6.2 Dorsal horn neurones and sensory discrimination

The dorsal horn is characterised by a wide range of cells of different sizes and morphological appearances (see Fig. 1.1b). The neurones in the dorsal horn are categorised by their response characteristics to the arriving primary afferent fibre signals from skin and have been classified into three major groups; non-nociceptive (Class 1), multireceptive (Class 2) and nocispecific (Class 3) neurones (Iggo, 1974).

Non-nociceptive neurones in the dorsal horn respond to cutaneous low threshold mechanoreceptor units activated by hair movement, touch and pressure and are thus involved in innocuous information processing (Iggo, 1974).

Multireceptive neurones are sensitive to cutaneous mechanoreceptors and nociceptors, so are said to have a 'wide dynamic range' (Mendell, 1966) and are mainly located in LIV-VI of the dorsal horn with some presence in LI (Woolf and Fitzgerald, 1983; McMahon and Wall, 1983).

Nocispecific neurones are purely excited by nociceptive Aδ and C-fibres activated by noxious stimulation of the skin (Cervero, Iggo and Ogawa, 1976). These are located mainly in LI and less so in LV, some of which will project to the thalamus and brainstem (Christensen and Perl, 1970; Light and Perl, 1979).

There is a fourth class of dorsal horn neurone (Class 4), which are proprioceptive in nature, responding to joint movement and pressure on deep tissues and, as such, are beyond the scope of this work.

Figure 1.1 Laminar organisation of and cutaneous afferent input to the spinal cord

(a) Source: Molander, Xu and Grant (1984)

Schematic representation of the ten laminar divisions of Rexed (1952) in the L5 segment of the rat spinal cord.

Abbreviations:
Liss- Lissauer's tract
Pyr- pyramidal tract
LSN- lateral spinal nucleus
IM- intermedio-medial nucleus
VM- ventro-medial nucleus
I-X- Rexed's ten laminae

(b) Source: Cervero and Iggo (1980)

A hypothetical cross-section of the spinal dorsal horn illustrating the afferent fibres and neuronal endings in LI-IV. Rexed's (1952) laminar divisions are indicated on the right, with the afferent fibre types terminating in each region of the dorsal horn indicated on the left. Some neurone types are also illustrated; a LI marginal cell, a LII limiting cell and two neurones of the nucleus proprius where the neurone illustrated in LIII has dendrites projecting into LII.

(a)

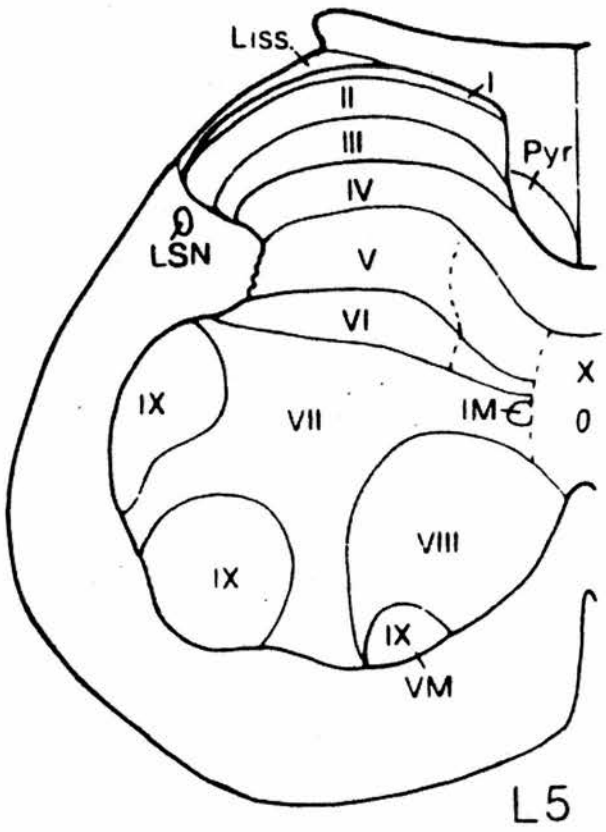
LISS.
I
II
III
IV
V
VI
Pyr
LSN
IX
VII
IM
X
0
IX
VIII
IX
VM
L5

(b)

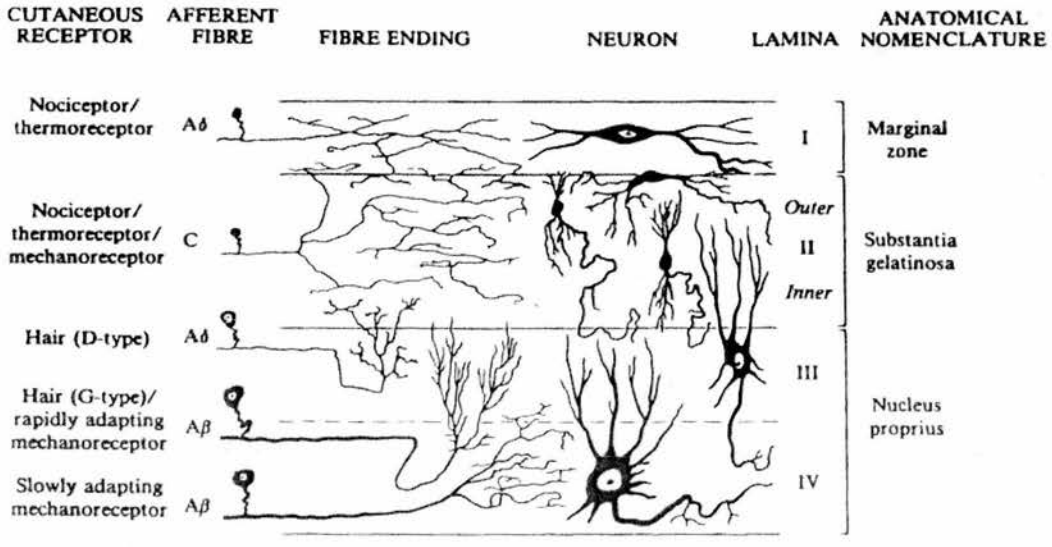
CUTANEOUS RECEPTOR
AFFERENT FIBRE
FIBRE ENDING
NEURON
LAMINA
ANATOMICAL NOMENCLATURE
Nociceptor/ thermoreceptor
Aδ
Nociceptor/ thermoreceptor/ mechanoreceptor
C
Hair (D-type)
Aδ
Hair (G-type)/ rapidly adapting mechanoreceptor
Aβ
Slowly adapting mechanoreceptor
Aβ
I
Outer
II
Inner
III
IV
Marginal zone
Substantia gelatinosa
Nucleus proprius

A variety of neurotransmitters and neuropeptides are released from primary afferent nerve terminals in response to stimulation. These neurotransmitters and neuropeptides act on their respective postsynaptic receptors to alter the response of dorsal horn neurones. Next, we will examine the major excitatory amino acid neurotransmitter, glutamate, and its associated receptors as well as a brief description of some of the neuropeptides that may affect plasticity in the dorsal horn of the spinal cord.

1.7 Excitatory amino acid receptors

Of particular interest here are the excitatory amino acid receptors in the postsynapse that respond to glutamate activation. The presynapse has the machinery for neurotransmitter release while the postsynapse assembles various signalling molecules involved in synaptic plasticity. Cellular plasma membranes are a complex aggregate of lipids, transmembrane proteins and associated cytosolic components that are organised into domains, which have distinct structural and biochemical properties. The synapse is one of the most highly ordered membrane structures, in which transmembrane receptors, ion channels and cytoplasmic signalling proteins are localised in a discrete focal structure that is tightly linked to the cytoskeleton (the postsynaptic density).

The postsynaptic density (PSD)

Glutamate receptors are concentrated in the PSD, a disc-like structure tightly apposed to the postsynaptic membrane first observed in the 1950s by electron microscopy. The PSD may govern the precise alignment between pre- and post-synapses and maintain neurotransmitter receptors and ion channels in their appropriate locations. It is a dynamic structural matrix that consists not only of functional receptors, but also of cytoskeletal frameworks and regulatory proteins, some of which contact the cytoplasmic domains of ion channels in the postsynaptic membrane and contribute to the organisation of Ca^{2+}-dependent and other signal transduction systems beneath the postsynaptic membrane.

1.7.1 Glutamate, the excitatory amino acid neurotransmitter

L-glutamate is an endogenous excitatory amino acid transmitter that is released from the terminals of primary afferent fibres following electrical nerve stimulation (Curtis, Phillis and Watkins, 1960; Rizzoli, 1968; Davies et al., 1979; Duggan and Johnston, 1970). Glutamate has been localised to subpopulations of small and large DRG cells, myelinated and unmyelinated dorsal root axons and fibres in the superficial laminae of the dorsal horn so that it is widely involved as a neurotransmitter of primary sensory afferents (Wanaka et al., 1987; Battaglia and Rustioni, 1988; Weinberg, 1999; Westlund, McNeill and Coggeshall, 1989). Indeed, almost all primary afferents terminating in superficial laminae appear to process glutamate in a fashion consistent with a neurotransmitter role (Rustioni and Weinberg, 1989). Intrathecal administration of glutamate produces an increase in primary afferent-induced nociceptive responses (Woolf, 1986; Coderre and Melzack, 1992) and ionophoretic application of glutamate or its receptor agonists can excite spinal cord and DRG neurones (Curtis, Phillis and Watkins, 1960; Huettner, 1990).

1.7.2 Ionotropic receptors

Glutamate, released from presynaptic nerve terminals, activates ionotropic ligand-gated ion channels and G protein-coupled metabotropic receptors. The various subgroups of glutamate receptors are highly conserved between mammals and constitute the major excitatory transmitter system, the best studied of which are the ligand-gated ion channels ('ionotropic glutamate receptors'), which are permeable to cations (Hollmann and Heinemann, 1994). The ionotropic receptors have been divided into two major classes based on their pharmacological response characteristics; *N*-methyl-D-aspartate (NMDA) and non-NMDA receptors. The non-NMDA class of ligand-gated receptors are further subdivided into α-amino-3-hydroxy-5-methyl-4-isoxazole proprionic acid (AMPA) and kainate receptor subtypes. Glutamate produces a fast excitatory potential at the AMPA receptor site and a long synaptic potential acting at the NMDA receptor site. As ionotropic receptors are focus of this research, more attention will be paid to them here.

Mammals express four AMPA receptor subunits (GluR1, 2, 3 and 4 or GluR-A-D), five high affinity kainate receptor subunits (KA-1, KA-2, GluR5, GluR6 and GluR7) and five NMDA receptor subunits (NR1, NR2A, B, C, and D). Each subunit is a glycosylated membrane-inserted polypeptide of ~900 to 1500 amino acids in length and all subunits contain four hydrophobic transmembrane segments (TM1-4), which determine their transmembrane topology, with an extracellular amino terminus, an intracellular C-terminus and a 'TM2' segment, which forms the channel pore (see Fig. 1.2). Ionotropic receptors are believed to be pentameric in structure (Hollmann and Heinemann, 1994; Seeburg, 1993; Wenthold et al., 1992).

1.7.3 Evidence for a role of ionotropic receptors in pain

Much evidence supports a role for glutamate receptors in both the peripheral and central nervous system. Peripherally, injection of NMDA, AMPA or KA into glabrous skin increases paw withdrawals following both noxious and non-noxious mechanical stimulation and induces biting and scratching behaviour, that may be indicative of pain, and can be blocked with corresponding antagonists (Carlton, Hargett and Coggeshall, 1995; Aanonsen and Wilcox, 1987; Zhou, Bonasera and Carlton, 1996; Jackson et al., 1995). In the CNS, AMPA and NMDA receptor agonists both depolarise spinal nociceptive neurones (Aanonsen, Lei and Wilcox, 1990; Coderre, 1993). In addition, stimulation of Aδ fibres induces non-NMDA receptor-mediated excitatory postsynaptic potentials in LII neurones (Yoshimura and Nishi, 1992).

Several reports suggest that monosynaptic transmission from primary afferents in the spinal cord is mediated mainly by non-NMDA receptors whereas NMDA receptors are more important in the higher order synapses and mediate the wind-up and sensitisation of dorsal horn neurones evoked by C-fibre volleys. Wind-up is mimicked by the application of L-glutamate or the agonist NMDA and is blocked by NMDA receptor antagonists (Zieglgänsberger and Herz, 1971; Davies and Lodge, 1987).

Figure 1.2 General structure of an ionotropic glutamate receptor subunit

Ionotropic glutamate receptor subunits follow the same basic structural pattern with an extracellular N-terminus and an intracellular C-terminus that can be the site of interactions with intracellular proteins. Transmembrane domains (TM) are shown, where theTM2 domain is believed to form the channel pore.

The table shows the currently accepted nomenclature for the NMDA and AMPA subtypes of glutamate receptors.

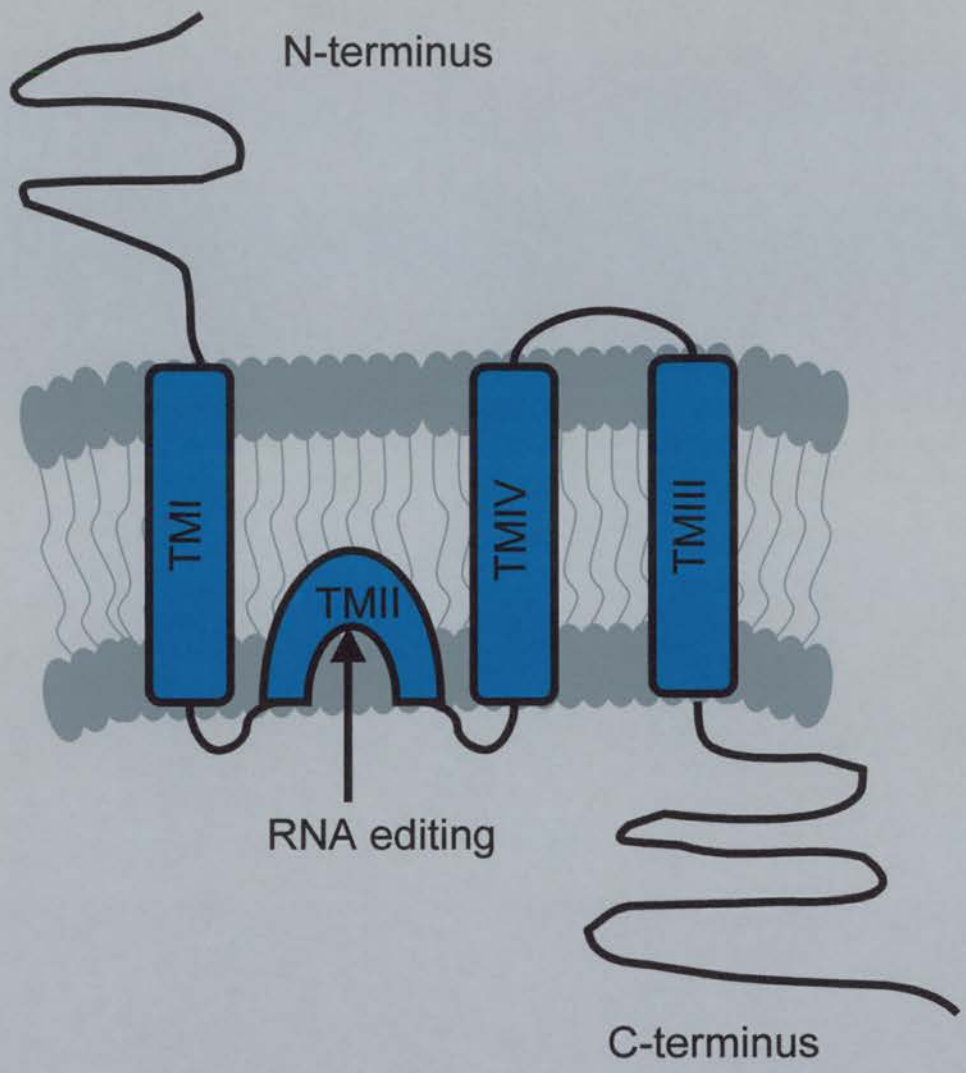

Ionotropic (ligand-gated) glutamate receptor subunits

NMDA		AMPA
NR1	NR2A	GluR1
	NR2B	GluR2
	NR2C	GluR3
	NR2D	GluR4

1.7.4 AMPA receptors

AMPA selectively activates channels with fast kinetics and depolarises spinal nociceptive neurones. Under normal conditions and acute somatosensory processing, activity at the AMPA receptor is dominant. AMPA receptors in the superficial dorsal laminae mediate fast nociceptive transmission in the spinal cord and antagonists disrupt acute nociceptive transmission and prevent the development of hyperalgesia (see Section 1.12.1). AMPA receptor subunits (GluR1-4) can assemble in any combination into both homomeric and heteromeric receptor configurations with distinct functional properties (Boulter et al., 1990; Keinänen et al., 1990; Verdoorn et al., 1991).

High concentrations of AMPA receptor subunits have been demonstrated in neurones of the superficial laminae of the dorsal horn and at synapses (Furuyama et al., 1993; Henley, Jenkins and Hunt, 1993; Tölle et al., 1993; Popratiloff, Weinberg and Rustioni, 1996). All four AMPA receptor subunits are expressed in the spinal cord to varying degrees. GluR1 and GluR2 mRNA and immunoreactivity are dominant in the dorsal horn and are thus of particular interest here, while GluR3 and GluR4 primarily reside in ventral horn (Furuyama et al., 1993; Tölle et al., 1993). GluR1 expression is confined to LI and LII_o (Tölle et al., 1993) while GluR2, a particularly prominent subunit in the dorsal horn, is especially high in LII_i and the superficial part of LI (Henley, Jenkins and Hunt, 1993; Tölle et al., 1993). So, in general terms, the subunit composition of the AMPA receptors appears to be different between neurones conducting nociception (in the dorsal horn) and those conducting other sensations (in the ventral horn).

AMPA Receptor Properties

The GluR2 subunit dominates the properties of ion flow as virtually all GluR2 subunits undergo site selective RNA editing (by adenosine deamination) at the glutamine/arginine (Q/R) site in the channel pore resulting in Ca^{2+} impermeability (Burnashev et al., 1992a; Melcher et al., 1996; Verdoorn et al., 1991). Neurones of mice with genetic mutation of this Q/R site display increased calcium permeabilities

through the AMPA receptor (Feldmeyer et al., 1999). Most AMPA receptors in the CNS are believed to be calcium impermeable due to the nearly ubiquitous inclusion of the GluR2 subunit (Burnashev et al., 1992a), although there is a report of a population of specifically Ca^{2+}-permeable AMPA receptors (presumably lacking the GluR2 subunit) in the superficial dorsal horn, which may mediate the transmission of nociceptive information (Engelman, Allen and MacDermott, 1999). In addition to RNA editing, each of the GluR1-4 subunits exist in two different forms created by alternative splicing, termed 'flip' and 'flop' isoforms, that are equally abundant but show different regional distributions and differ in the efficacy of glutamate in activating the receptor (Sommer et al., 1990; Tölle et al., 1995). The GluR1 and GluR2 subunits have received particular attention of late due to identification of a variety of intracellular proteins differentially interacting with these subunits that may govern AMPA receptor functions in synaptic plasticity (see Section 1.15).

1.7.5 Kainate receptors

Until very recently the lack of specific pharmacological agents discriminating AMPA and kainate receptors has precluded their functional study. Kainate receptors represent a distinct non-NMDA subtype of receptor (Wenthold et al., 1994). Evidence for an AMPA/kainate receptor distinction came from the differential sensitivity of C-fibres to the agonists kainate and quisqualate as compared to AMPA, consistent with the reported concentration of GluR5 on primary afferent C-fibres (Davies et al., 1979; Agrawal and Evans, 1986; Huettner, 1990; Simmons et al., 1998).

The GluR5 subunit of kainate receptor has been the main focus of kainate receptor research regarding somatosensory processing. It is expressed evenly throughout the dorsal horn in LII, LIII-VI (Tölle et al., 1993). GluR5 agonists depress reflexes to afferent C-fibre inputs significantly more than those to A fibres and selective antagonists can prevent capsaicin-induced hyperalgesia and allodynia in humans and animal models with little effect on acute physiological nociceptive responses (Procter et al., 1998; Sang et al., 1998; Simmons et al., 1998).

1.7.6 NMDA receptors

The NMDA receptor has attracted much attention due to the ability of its antagonist AP5 to alter synaptic plasticity, by reducing long-term potentiation (LTP, a model for learning and memory in the hippocampus induced by brief repetitive stimulation of monosynaptic excitatory pathways that results in a persistent enhancement of synaptic transmission lasting from hours to weeks) in the hippocampus and affecting aspects of learning (Morris, 1989; Collingridge, Kehl and McLennan, 1983).

The NMDA receptor consists of two major subunits, NMDA receptor 1 (NR1) and NMDA receptor 2 (NR2A, B, C and D), whereby the NR1 subunit contains a glycine binding site and the NR2 subunits contain the glutamate binding site, both of which must be ligand-bound before ion channel activation can occur (Moriyoshi et al., 1991; Laube et al., 1997). None of the NR2 subunits alone can form functional homomeric ion channels but instead must co-assemble with NR1 to form functional heteromeric receptors (Monyer et al., 1992). In the spinal cord, NMDA receptor antagonists have long been known to reduce frequency-dependent potentiation (wind-up) of cells to repeated C-fibre stimulation and following mustard oil application (Dickenson and Aydar, 1991; Woolf and Thompson, 1991).

NR1 is ubiquitously expressed in the dorsal horn of the spinal cord and NR1 mRNA is also located in sensory neurones known to relay predominantly nociceptive information (in the trigeminal nuclei and spinothalamic tract) as well as those neurones relaying touch and proprioceptive information (dorsal column neurones) (Kus, Saxon and Beitz, 1995). The NR2 subunits of the NMDA receptor are differentially expressed throughout the dorsal horn of the spinal cord (Tölle et al., 1993; Luque et al., 1994). NR2A and NR2B subunits are of particular interest here with widespread NR2A mRNA expression in the spinal cord while NR2B expression is largely restricted to the superficial dorsal horn, LI and II (Luque et al., 1994; Boyce et al., 1999). The NR2 subunits have been the focus of much research regarding the mechanisms of neuronal plasticity due to the identification of molecules interacting at their C-terminal sites affecting ion channel localisation and NMDA-dependent signalling mechanisms (see Section 1.15).

NMDA receptor properties

The NMDA receptor channel complex is uniquely ligand- and voltage- gated and requires a number of events to occur for activation. Under normal (acute) nociceptive transmission, the NMDA receptor is subject to a Mg^{2+} ion block and so is largely inactive. For the channel to open not only must this block be relieved but the NMDA receptor-channel complex requires glutamate and co-agonist glycine binding for channel activation (Kleckner and Dingledine, 1988). Glycine binding sites, other than the strychnine-sensitive inhibitory glycine receptor, co-localise with NMDA binding sites (in brain) and glycine can potentiate NMDA receptor responses in the dorsal horn of the spinal cord (Budai, Wilcox and Larson, 1992).

The NR1 and NR2 subunits contain an asparagine residue in the TM2 pore region homologous to the Q/R site in AMPA receptors, which are crucial for divalent ion permeation and ion block. In heteromeric NR1/2 receptors, Ca^{2+} permeability is thought to be largely controlled by an asparagine residue in NR1 while sensitivity towards Mg^{2+} ions is dominated by the TM2 asparagine in NR2 (Burnashev et al., 1992b). In addition, differential splicing of three distinct exons of NR1 generates eight NR1 splice variants arising through insertion or deletion of three short exon cassettes in the N-terminus (N1) and the C-terminus (C1 and C2) domains. NR1 splice variants differ in their patterns of temporal and spatial expression and pharmacological properties as well as interaction capabilities dictated by C-terminal motifs, which will be dealt with in Chapter 4 (Sugihara et al., 1992; Hollmann et al., 1993; Luque et al., 1994; Zukin and Bennett, 1995).

1.7.7 Metabotropic receptors

The metabotropic receptors (mGluR) are a group of G protein-coupled receptors with seven transmembrane domains classified into three groups based on differential coupling to second messenger molecules. The Group I metabotropic receptors are of particular importance to nociception and will be the focus here. Activation of mGluR1 or mGluR5 (Group I) leads to phosphoinositide hydrolysis, intracellular Ca^{2+} mobilisation and possibly, to a lesser extent, increases in cyclic adenosine 3',5'-

monophosphate (cAMP) accumulation (Abe et al., 1992; Masu et al., 1991; Aramori and Nakanishi, 1992). The remaining metabotropic glutamate receptors are linked to inhibition of cAMP production and can now be distinguished, at least in part, by agonist and antagonist selectivity.

Group I metabotropic receptor subunit mRNAs are concentrated in the superficial dorsal horn LI and II (Jia, Rustioni and Valtschanoff, 1999; Berthele et al., 1999). Ionophoresis of first generation metabotropic glutamate receptor antagonists (AP3, CHPG) was reported to inhibit the excitation of single dorsal horn neurones elicited by the C-fibre specific algogen, mustard oil and to attenuate spinal cord neuronal excitability associated with acute inflammation (Neugebauer, Lucke and Schaible, 1994; Young et al., 1994). The non-selective mGluR agonist, trans-ACPD, facilitates formalin-induced nociception (Coderre and Melzack, 1992). A selective Group I mGluR agonist (RS-DHPG) decreases the latency of behavioural reflex responses to hotplate (48°C), von Frey filaments and tail pinch stimulation (Fisher and Coderre, 1998). However, agonist stimulation of mGluRs alone may be insufficient to cause neuronal firing and there is evidence of a synergistic action with ionotropic glutamate receptors as metabotropic receptors participate in the nociceptive spinal reflex with AMPA and NMDA receptors, where mGluR agonists can facilitate their agonist responses on dorsal horn neurones (Boxall et al., 1996; Bleakman et al., 1992; Cerne and Randić, 1992). In addition, co-administration of AMPA and mGluR agonists results in behavioural hyperalgesia in acute nociceptive tests (Meller, Dykstra and Gebhart, 1993).

1.8 Neuropeptides

In addition to glutamate, various neuropeptides are released from the endings of peripheral afferent fibres. Indeed, the co-release of presynaptic glutamate and neuropeptides has been demonstrated and can cause a variety of (synergistic) effects on the postsynaptic dorsal horn cells in the spinal cord. Specifically, glutamate and substance P co-exist in DRG neurones suggesting co-release in response to primary

afferent stimulation (Battaglia and Rustioni, 1988; DeBiasi and Rustioni, 1988, see below).

Substance P (SP)

SP is a member of the tachykinin family of structurally related peptides that includes neurokinin A (NKA) and neurokinin B (NKB), which preferentially activate NK_1, NK_2 and NK_3 receptors, respectively. SP and NKA have been proposed as primary afferent neurotransmitters based on their distribution in superficial dorsal horn laminae I and II and on the basis of their functional effects in intrathecal and electrophysiological experiments. SP is synthesised in small DRG cells from where it is axonally transported to the dorsal root and sciatic nerve (Barbut, Polak and Wall, 1981; Harmar and Keen, 1982). It is present in ~20% of all DRG neurones (Ju et al., 1987), where it has been shown to co-exist with a number of other substances including calcitonin gene-related peptide (CGRP), somatostatin (SOM) and glutamate (Battaglia and Rustioni, 1988; Ju et al., 1987).

SP is released into the dorsal horn in a Ca^{2+}-dependent manner from primary sensory C-fibres in response to peripheral noxious and inflammatory stimuli where it binds to its receptor, NK_1, which has been localised within the superficial layers of the spinal cord (Helke, Charlton and Wiley, 1986; Quirion et al., 1983; Yashpal, Sarrieau and Quirion, 1991). Immunoreactivity for SP is concentrated in LI and exogenous application of SP increases the excitability of dorsal horn neurones in response to noxious thermal and mechanical stimuli and selectively activates high threshold and multireceptive laminae I and II neurones (Duggan et al., 1987; Wiesenfeld-Hallin, 1986; Henry, 1976; Duggan et al., 1995; Couture et al., 1993). Capsaicin treatment causes the depletion of SP (and other peptides) from small primary afferents in the dorsal horn in conjunction with increasing chemical and mechanical nociceptive thresholds (Hayes, Skingle and Tyers, 1981; Nagy et al., 1981; Yaksh et al., 1979). Indeed, SP release in the superficial dorsal horn has been reported only following noxious heat (52°C), noxious mechanical or chemical stimuli that would be predicted to activate fine (capsaicin-sensitive) afferents (Duggan et al., 1987).

Intrathecal injection of SP or an NK_1 receptor-selective agonist elicits biting and scratching behaviours in mice that may be indicative of pain sensation as well as reports of hyperalgesia induction (Hylden and Wilcox, 1982; Courteix, Lavarenne and Eschalier, 1993). Although mixed affects have been reported (Hayes and Tyers, 1979; Yashpal, Wright and Henry, 1982), NK_1 receptor antagonists are generally not effective at reducing dorsal horn neurone responses to brief noxious stimuli indicating these receptors may be more active in states of persistent pain (Fleetwood-Walker et al., 1990; Couture et al., 1993; Garces et al. 1993; Picard et al., 1993; Seguin, Le Marouille-Girardon and Millan, 1995; Yamamoto and Yaksh, 1992). LII neurones are reportedly insensitive to NK_1 (as well as NK_3) agonists that may be due to a lower NK_1 expression in this region than previously thought (Bleazard, Hill and Morris, 1994). Moreover, NK_1 receptor antagonists have not proved to be efficacious in clinical trials of chronic pain states (Hill, 2000) although there may be a differential involvement of the tachykinins according to the model of neuropathic pain used (Coudore-Civiale et al., 1998; Coderre and Melzack, 1991). More recent evidence using novel, highly potent NK_1 receptor antagonists suggest that NK_1 receptor blockade attenuates the sensitised response elicited by innocuous mechanical stimuli in primate STT cells following capsaicin injection without affecting noxious mechanical responsiveness (Rees et al., 1998).

There are reported NK_2 binding sites in LI and II (Quiron and Dam, 1988) and NK_2 receptor antagonists can attenuate endogenous thermal nociceptive responses (Fleetwood-Walker et al., 1990). The NK_2 ligand, NKA, appears to originate from small diameter primary afferent fibres (Ogawa, Karazawa and Kimura, 1985) and intrathecal application of NKA induces hyperalgesia that can be blocked by NK_2 receptor antagonists (Yashpal, Hui-Chan and Henry, 1996). Whether this is a viable target in neuropathy has not been assessed.

Glutamate and SP

Activation of C-fibres and glutamate release can result in SP and NKA release (Go and Yaksh, 1987; Duggan et al., 1990). In addition, the co-existence of glutamate

and SP in fine afferent fibres and the possibility of co-release may allow sufficient membrane depolarisation for NMDA receptor activation from prolonged activation of peripheral inputs. Indeed, the co-administration of NK_1 and NMDA receptor antagonists results in a synergistic action, whereby their respective inhibitory effects on nociceptive stimulation are enhanced (Coderre and Melzack, 1992). PKC-induced activity following NK_1 receptor activation may provide a mechanism for this synergy via NMDA receptor activity modulation by PKC (Rusin, Ryu and Randić, 1992; Chen and Huang, 1992; Urban et al., 1994). Ionophoresis of SP or NK_1 receptor agonists facilitate NMDA receptor-induced activity, and this increment can be inhibited by antagonists acting at the glycine site of NMDA (Heppenstall and Fleetwood-Walker, 1997; Dougherty and Willis, 1991; Cumberbatch Chizh, and Headley, 1994).

Calcitonin gene-related peptide (CGRP)

CGRP is found in about 30% of DRG cells and is released into spinal cord laminae I, II and V following noxious thermal and mechanical stimulation (Lee et al., 1985; Carlton et al., 1988; Morton and Hutchison, 1989). Subpopulations of CGRP-positive neurones contain SP, SOM or galanin immunoreactivity (Ju et al., 1987). Indeed, a high proportion (~80%) of SP-containing DRG neurones also contain CGRP (Battaglia and Rustioni, 1988; Ju et al., 1987). Intrathecal application of CGRP is reported to decrease the nociceptive threshold for acute mechanical stimulation (Oku et al., 1987) and CGRP synergistically increases the effect of SP on dorsal horn neurones and enhances SP release in spinal cord slices (Oku et al., 1987; Biella et al., 1991).

Vasoactive Intestinal Polypeptide (VIP)

VIP expression is very low under normal conditions and may be restricted to DRG cells though low levels of peptide immunoreactivity can be detected in LI and II (Gibson et al., 1981; Kar and Quirion, 1995, Yashpal, Sarrieau and Quirion, 1991; Knyihár-Csillik et al., 1991). VIP is recognised by the $VPAC_1$, $VPAC_2$ and PAC

receptors (Ishihara et al., 1992; Lutz et al., 1993; Hosoya et al., 1997). Intrathecal application of VIP increases the excitability of the spinal cord to thermal much more than mechanical stimuli suggesting that this neuropeptide may be released by thermosensitive cutaneous afferents that respond poorly to mechanical stimuli (Wiesenfeld-Hallin, 1987; Cridland and Henry, 1988). Aδ and C-fibre stimulation from the sciatic nerve causes the release of VIP and its immunoreactivity increases in the lateral part of the dorsal horn (Klein et al., 1992; Yaksh, Abay and Go, 1982). Ionophoresis of VIP excites nociceptive and non-nociceptive neurones in the rat trigeminal nucleus caudalis and spinal cord LI-VII (Salt and Hill, 1981; Jeftinija et al., 1982) despite the fact that the levels of VIP within the spinal cord appear to be lower than those seen in many other regions of the CNS (Emson et al., 1978; Loren et al., 1979).

Galanin (GAL)

GAL is normally present in approximately 23% of small to medium diameter DRG neurones, where it co-exists with several other neurotransmitters including CGRP and SP (Ju et al., 1987; Zhang, Nicholas and Hökfelt, 1993; Ma and Bisby, 1997). GAL has widespread CNS distribution and can be found in the dorsal horn concentrated in LI-III, with moderate expression in IV-V and primary afferent terminals (Kar and Quirion, 1995). Intrathecal GAL produces brief facilitatory effects at low doses, which become inhibitory as the dose increases (Wiesenfeld-Hallin, Villar and Hökfelt, 1988). In addition, in both electrophysiological and behavioural studies, GAL inhibits the analgesic effect of morphine on noxious thermal and mechanical stimuli (Wiesenfeld-Hallin et al., 1991a), while having no effect alone on these nociceptive inputs. As such, GAL may be a modulator of excitatory peptides as pre-administration of galanin intrathecally has been shown to antagonise the excitatory effects of SP and CGRP on the flexor withdrawal reflex (Wiesenfeld-Hallin et al.,1991b; Xu et al., 1990).

Somatostatin (SOM)

High levels of SOM peptide(s) are found in small diameter primary afferent neurones in a distinct population to those that contain SP (Hökfelt et al., 1976; Nagy and Hunt, 1982). While SOM immunoreactivity is concentrated in LII (Hökfelt et al., 1976), its role in nociceptive processing is unclear as both inhibitory and excitatory responses of dorsal horn neurones to its application have been reported (Murase, Nedeljkov and Randić, 1982; Randić and Miletić, 1978; Salt and Hill, 1983). Intrathecal SOM has been reported to increase the excitability of the spinal cord following mechanical and thermal stimuli (Wiesenfeld-Hallin, 1986).

Neuropeptide Y (NPY)

NPY is found in sympathetic ganglia and may be a major peptide involved in sympathetic neurotransmission (Lundberg et al., 1983). While there appears to be low expression in the DRG under normal conditions, NPY immunoreactivity exists in the spinal cord dorsal and ventral horns that may arise from intrinsic neurones or supraspinal tracts (de Quidt and Emson, 1986; Wakisaka, Kajander and Bennett, 1991). In the spinal cord, NPY may co-exist with GAL or GABA (Zhang, Nicholas and Hökfelt, 1993; Laing et al., 1994; Rowan, Todd and Spike, 1993). However, the functional role of NPY is unclear as intrathecal NPY has revealed a biphasic action for this peptide, where at low doses it appears to be excitatory and at high doses, inhibitory (Xu et al., 1994).

1.9 Ascending pathways

The processing of afferent input at the level of the spinal cord and the convergence of the primary afferents into the central nervous system via the dorsal root ganglion underpin an important regulation of the functional properties of dorsal horn neurones. Many of the dorsal horn cells in the spinal cord are part of neuronal pathways that carry information from cutaneous and subcutaneous mechanoreceptors and nociceptors in ascending projections to brainstem and midbrain structures

including thalamic nuclei and medullary structures, known to be involved in relaying nociceptive signals. In addition, these neurones are also under descending control from these and other areas. Each will be dealt with in turn.

Spinothalamic Tract (STT)

The STT carries information from the dorsal horn to the thalamic nuclei in the brain and is of interest as transection of the STT causes analgesia and is occasionally used to alleviate intractable pain in humans (Dubner and Bennett, 1983). The cells of origin of the STT tract, based on retrograde HRP transport studies, are located in LI, II and IV-VI, most of which are nocispecific or multireceptive neurones (Giesler et al., 1976; Willis, Haber and Martin, 1977). Indeed, the nocispecific neurones of lamina I are a feature of the STT (Dubner and Bennett, 1983; Giesler et al., 1976). Stimulation of various brain regions, such as the nucleus Raphe magnus (NRM) in the rostral ventromedial medulla (RVM) and the periaqueductal grey (PAG), can inhibit the responses of STT cells to both noxious and tactile stimuli originating from myelinated fibres (Willis, Haber and Martin, 1977).

Spinomesencephalic Tract (SMT)

The mesencephalic tegmentum is a target for various somatosensory inputs originating from the spinal cord, and the SMT terminates in numerous areas of this region, including the periaqueductal gray (PAG). Using HRP tracing, the projections of spinal cord neurones to the mesencephalic tegmentum are mostly contralateral from LI and the lateral neck of the dorsal horn (LV-VI) (Menétrey et al., 1982). A significant proportion of lamina I neurones contribute to the SMT and electrophysiological recordings of these neurones indicate that many of them are nociceptive in nature (Menétrey et al., 1982).

Spinocervical Tract (SCT)

Neurones of origin of the SCT are mostly located in LIV, while very few of the SCT neurones, which project ipsilaterally, have been found in LI/II of the spinal cord. The majority of SCT neurones respond to tactile stimuli from hair follicles, though some are activated by intense cutaneous pressure, pinch and thermal nociceptive stimulation (Brown, 1981; Cervero, Iggo and Molony, 1977).

Postsynaptic Dorsal Column system

The postsynaptic dorsal column fibres, primarily located in LIII/IV of the rat spinal cord, project ipsilaterally through the dorsal funiculus to the nucleus gracilis and nucleus cuneatus (Giesler, Nahin and Masden, 1984). There are two types of fibre in this system, some of which are modality specific and respond only to gentle stimulation (these can exert a segmental inhibitory influence on spinal cells relaying high threshold afferent messages) while others are modality convergent and respond more vigorously to noxious cutaneous stimulation (Brown et al., 1983). Polymodal cells of the nucleus gracilis and the fibres of the fasciculus gracilis are exited by innocuous hair movement, pressure, pinching and cooling as well as nociceptive stimuli (Angaut-Petit, 1975).

1.10 Descending inhibition

The spinal cord dorsal horn is under the influence of numerous neuronal pathways that descend from the brain and the activity of these pathways include actions on primary afferent fibres, on neurones that give rise to ascending pathways and on interneurones, and as such provide a feedback system onto the dorsal horn. The existence of a modulatory pain system was alluded to by Melzack and Wall (1965) in the 'Gate Control' theory of pain, which proposed that spinal nociceptive transmission could be inhibited by non-nociceptive inputs. It is now clear that nociceptive processing is modulated by segmental control from intrinsic interneurones, Aβ fibre activity and supraspinal influences, highlighting the fact that

the dorsal horn is not merely a passive transmission station but rather a site where dynamic inhibitory and modulatory events occur.

The finding that electrical stimulation of certain brain areas, such as the PAG could have an analgesic action (stimulation-produced analgesia; SPA), by inhibiting the transmission of nociceptive input at the level of the dorsal horn, clearly demonstrated the existence of descending systems that contribute to pain modulation (Reynolds, 1969). Furthermore, suppression of nociceptive responses is produced by supraspinal administration of narcotic analgesics as well as electrical stimulation at midbrain sites (Hayes et al., 1979). PAG stimulation inhibits the responses of WDR and NS neurones in dorsal horn (Bennett and Mayer, 1979). Indeed, neurones within the dorsal horn are under a modulatory control that involves inhibitions from descending pathways in the brain, local actions of inhibitory interneurones and the various inhibitory neurotransmitters.

1.10.1 Tonic descending inhibition and supraspinal modulation

Excitation of dorsal horn neurones by impulses in unmyelinated primary afferent fibres is subject to a powerful tonic inhibition from supraspinal sites that reduces firing to peripheral noxious stimulation with little effect on responses to non-noxious stimulation, such as hair deflection (Morton, Johnson and Duggan, 1983). The fact that dorsal horn neurones were under tonic descending inhibition was highlighted with the use of a reversible cold block that essentially isolates cells caudal to block from descending inhibitory controls on dorsal horn neurones of the spinal cord (Wall, 1967). This demonstrated that descending systems could change neuronal response properties, whereby dorsal horn neurones previously responsive to low threshold mechanical stimulation can exhibit a greater firing frequency with increased stimulation intensity under cold block condition such that LTMs become responsive to a wide range of stimulus types and so resemble WDR neurones (Wall, 1967; Brown, 1971).

Descending pathways from the brainstem modify spinal function. In recordings from RVM while monitoring tail flick responses to noxious heat, Fields and Heinricher (1985) identified two main classes of cells in this site of SPA. 'On-cells' were consistently excited by noxious heat while 'Off-cells' were inhibited by the same stimuli, and a significant proportion of these cells project to the spinal cord (Fields and Heinricher, 1985). The medullary nucleus Raphe magnus (NRM) provides a major serotonergic input to the dorsal horn LI/II and V cells (Basbaum and Fields, 1978). Also, analgesia to nociceptive responses (with little effect on innocuous transmission) can be produced by electrical stimulation of the serotonin-rich neurones in the central inferior Raphe nucleus region (Guilbaud et al., 1977; Hope et al., 1989; Willis, 1977; Oliveras et al., 1974; Duggan and Griersmith, 1979). These inhibitory effects alter nociceptive transmission in LI, IV-VI, and their associated ascending pathways (SCT and STT) with little apparent effect on LII cells (Cervero, Molony and Iggo, 1979).

There are also a number of endogenous factors contributing to the modulation of nociceptive transmission, including the opioid system, and inhibitory transmitters, such as γ-amino butyric acid (GABA) and glycine, acting either presynaptically, at the level of transmitter/peptide release from primary afferents, and/or postsynaptically, acting directly on dorsal horn neurones. Additionally, inhibitory segmental controls produced by the large diameter Aβ fibres exist that alter the responses of spinal neurones to nociceptive stimulation whereby cutaneous stimulation of large A fibres selectively inhibits C-fibre- and noxious stimulation-evoked excitation of dorsal horn neurones (Woolf and Wall, 1982).

Endogenous Opioids

Major advances in the understanding of physiological pain modulation came with finding that endogenous opioid peptides mimic narcotic analgesics in producing prolonged analgesic effects in animals. Opioid peptides, such as enkephalin and dynorphin are localised (in the spinal cord) to LI-III and LV of the dorsal horn and so highly associated with areas receiving small diameter afferent primary fibres (Glazer

and Basbaum, 1981; Cruz and Basbaum, 1985). After brain stimulation or systemic morphine administration, the nociceptive receptive fields of WDR and NS neurones shrink so that gentle mechanical stimulation can now evoke neuronal discharge. Spinal enkephalin terminals are presynaptic to STT neurones and this arrangement is presumed to underlie an important inhibition of spinal nociceptive transmission (Ruda, 1982). Fields and Heinricher (1985) proposed that brainstem 'Off-cell' activation by morphine underlies opioid suppression of nociceptive transmission, while 'On-cells' are likely to facilitate nociceptive transmission at the dorsal horn level (Fields and Heinricher, 1985). Nociceptin/ orphanin FQ (N/OFQ), the endogenous ligand for the orphan opioid receptor OLR_1, has been reported to have a generalised inhibitory effect on neurones, does not co-localise with opioid receptors and can block opioid analgesia (Yamamoto et al., 1999).

GABA

A role of the postsynaptic inhibitory neurotransmitter GABA in spinal modulation comes from evidence that ionophoresis of GABA can inhibit dorsal horn neurones (Curtis et al., 1970; Zieglgänsberger and Sutor, 1983). Application of a GABA analogue can reduce tonic inhibition after reversible cold block (Foong and Duggan, 1986) and GABA-like immunoreactivity has mostly been localised to LI-III, LIV-VI and it is present in interneurones (Barber, Vaughn and Roberts, 1982; Todd and McKenzie, 1989).

Glycine

Ionophoresis of glycine results in strong depression of the activity of dorsal horn neurones (Curtis, Hosli and Johnston, 1967; Zieglgänsberger and Sutor, 1983). Glycine immunoreactivity can be found in LI-III and most commonly in LIII, such that GABA and glycine co-exist in some LI-III neurones (Todd, 1990). Interestingly, glycine has two opposing actions, an excitatory action, where it is a co-agonist for the excitatory NMDA receptor and an inhibitory action via the strychnine-sensitive glycine receptor (Budai, Wilcox and Larson, 1992).

1.11 Alterations in somatosensory processing following nerve damage

Following nerve damage, there are long-lasting structural, physiological and phenotypic alterations in the peripheral and central nervous system resulting in the generation of a state of hypersensitivity. Alterations in baseline somatosensory sensitivity arise as a result of increased nociceptor sensitivity and are accompanied by the generation of primary afferent impulses at abnormal locations ('*peripheral sensitisation*') as well as increased gain in CNS processing circuits ('*central sensitisation*').

Peripheral neuropathy results in pain hypersensitivity and spontaneous pain, and so manifests as either stimulus-evoked or stimulus-independent pain. Stimulus-evoked pain is exemplified by the behavioural states of hyperalgesia, hypersensitivity to a painful stimulus, and allodynia, a painful response to an innocuous stimulus, such as light touching of the skin. Stimulus-independent pain manifests as spontaneous pain in humans that may also be a feature and is characterised by continuous superficial burning and/or a deep aching pain. In addition, cold allodynia is a striking feature that occurs only in a neuropathic pain condition, although the precise underlying mechanisms are still unknown (Frost et al., 1988). It has been reported that allodynia to cooling is a characteristic of 'reflex sympathetic dystrophies' (Attal et al., 1990a) whereby in humans, cold aching, burning and prickling sensations can be experienced following a cold stimulus (Davis, 1998). Paralleling some aspects of neuropathic sensitisation, noxious skin stimuli intense enough to produce tissue injury generate prolonged sensory disturbances, like continuing pain, increased sensitivity and allodynia. As in neuropathic pain, these changes could result from either sensitisation (a reduction in the thresholds of skin nociceptors) or an increase in the excitability of the CNS so that normal inputs now evoke exaggerated responses.

In an effort to determine the mechanisms of neuropathic pain, various animal models involving a variety of peripheral nerve manipulations have been developed that aim to mimic the behavioural aspects of neuropathic pain reported in humans. Most neuropathic pain patients have a partial nerve injury, and a complete lesion is only

usually seen after amputation, where the special situation of 'phantom limb pain' arises. Partial nerve injury models mimic the most common type of injury seen in humans. The research presented here has utilised the chronic constriction injury model (CCI) of Bennett and Xie (1988), a widely used, highly reproducible model that results in the hallmark behavioural signs of neuropathic pain; hyperalgesia and allodynia.

1.11.1 Chronic constriction injury (CCI) model

The Bennett and Xie model, developed in an effort to reproduce the sensory disorders accompanying human peripheral neuropathies, produces a chronic, painful mononeuropathy. The model involves tying chromic catgut ligatures around the sciatic nerve at mid-thigh level (see Fig. 1.3) and within one week, the cutaneous territory of the sciatic nerve is hyperalgesic, accompanied by the presence of allodynia and spontaneous pain (dysaesthesia) (Attal et al., 1990a; Bennett and Xie, 1988). Importantly, the ligatures constrict but do not sever the sciatic nerve such that there is partial denervation and many axons are left in continuity. The hyperalgesia, allodynia and ongoing pain associated with peripheral nerve injury reflect morphological and physiological changes in the peripheral and central nervous system as well as alterations in the distribution, excitability and/or phenotype of primary afferent neurones and central synapses.

1.11.2 PNS structural reorganisation

CCI selectively injures axons in the sciatic nerve with a substantial degeneration of large myelinated axons and a partial degeneration of thinly myelinated and unmyelinated axons (Basbaum et al., 1991; Coggeshall et al., 1993). The constriction produces a massive loss of myelination of the large Aα and Aβ axons distal to injury as well as reducing the number of functional small myelinated Aδ and C-fibre axons to cause a partial and differential deafferentation of the sciatic nerve territory (Munger, Bennett and Kajander, 1992; Gautron et al., 1990; Nuytten et al., 1992).

Figure 1.3 The Bennett and Xie model of chronic constriction injury

Schematic illustration of the Bennett and Xie model, showing the placement of chromic catgut around the sciatic nerve at mid-thigh level (3 ligatures used for mice and four ligatures for rat) to loosely constrict the nerve, which causes primary afferent demyelination and results in the behavioural manifestations of neuropathic sensitisation: hyperalgesia and allodynia.

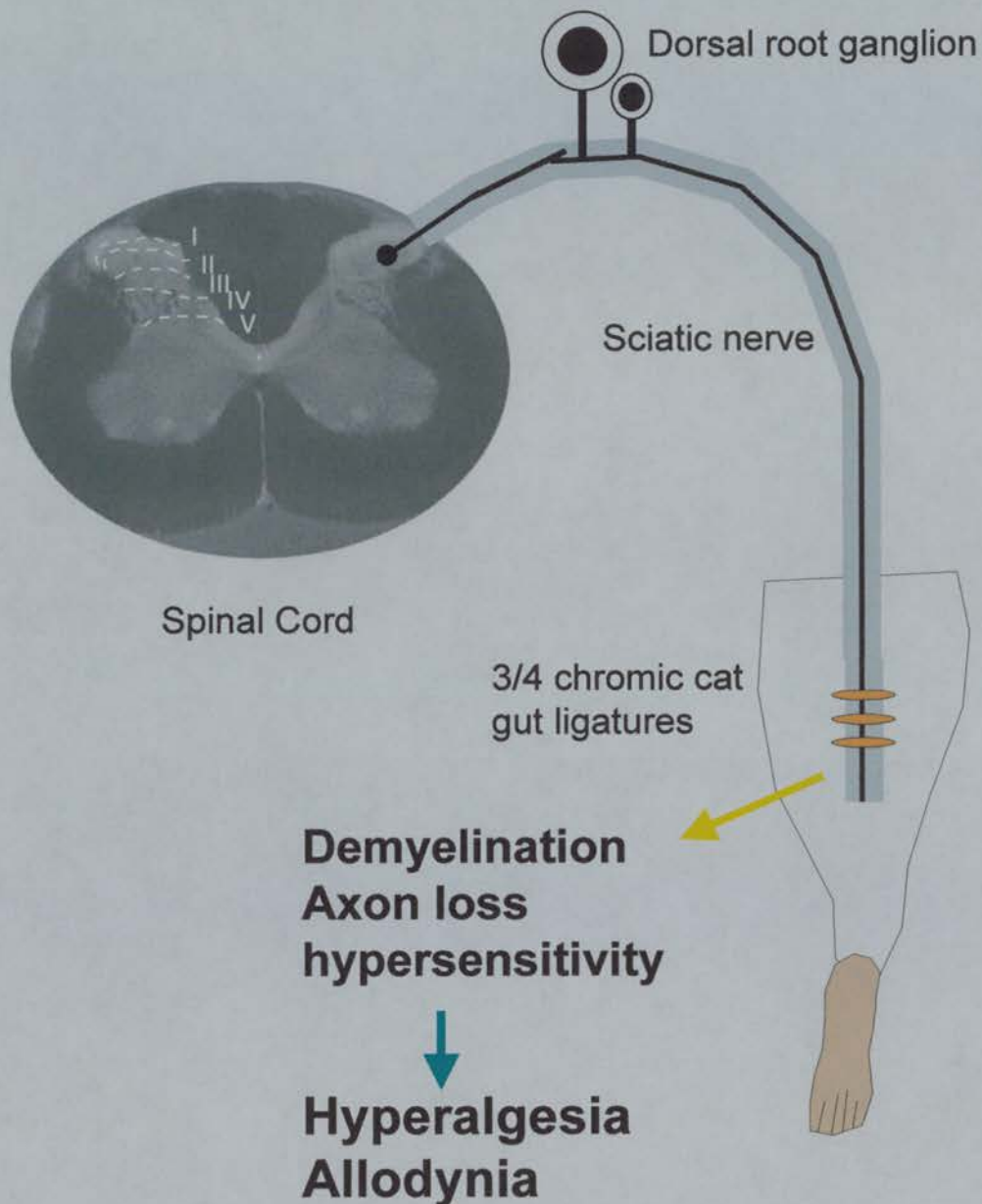
Dorsal root ganglion
I
II
III
IV
V
Sciatic nerve
Spinal Cord
3/4 chromic cat
gut ligatures
Demyelination
Axon loss
hypersensitivity
Hyperalgesia
Allodynia

In the periphery, alterations in the excitability of primary afferent neurones, neuronal degeneration, neuroma formation and the generation of spontaneous inputs occur following CCI. Abnormal pain sensations begin at about the same time as abnormalities in primary afferent function, when large Aβ and Aδ fibres become incapable of conducting impulses through the injury site where, by day three following induction of CCI, 89% of Aβ fibres, 87% of Aδ fibres and 32% of C-fibres are reported to be unable to conduct through the injury site (Kajander and Bennett, 1992). Axons at the injury site can form neuromas which are a source of intense ongoing electrical activity. This 'spontaneous' activity may be due to Na^+ channel accumulation and may arise because the neuromas become abnormally sensitive to various stimuli (Koltzenburg, Torebjörk and Wahren, 1994; Devor, 1991).

Spontaneous firing in DRG and peripheral nerve increases with injury. Fibre cross-excitation by abnormal contacts or ephapses (where impulse activity in one axon activates a neighbouring one) accompanied by crossed afterdischarge, where the activity of a group of neurones asynchronously engages the endogenous repetitive firing capability of their neighbours, also occur (Tal and Eliav, 1996; Kajander and Bennett, 1992). This situation predicts that, in the presence of remaining cutaneous innervation, painful responses may be evoked with normally innocuous gentle to firm mechanical stimulation (Devor and Wall, 1990).

1.11.3 The sympathetic nervous system

Under normal conditions, there is no evidence for communication between postganglionic sympathetic neurones and afferent neurones in the periphery. However, by four days following CCI, sympathetic axons sprout and invade the DRG in parallel with behavioural manifestations of neuropathic sensitivity, providing an anatomical substrate for sympathetic maintenance of pain that may lead to sensitisation of neurones (Jänig, Levine and Michaelis, 1996; Ramer and Bisby, 1997). Following CCI, guanethidine sympathectomy can reduce abnormal reactions to cold and heat (45°C) without affecting responses to mechanical stimulation or the

presence of spontaneous pain (Perrot et al., 1993; Attal et al., 1990b), suggesting a differential sympathetic involvement in the different modalities of neuropathic pain.

1.11.4 CNS structural reorganisation

The peripheral injury of CCI is associated with structural and functional changes in the CNS, changes in somatosensory processing in the spinal cord and a chronic rearrangement of the highly ordered laminar termination of primary afferents within somatotopically appropriate regions of the dorsal horn. Many of these alterations could readily outlast nerve regeneration and reinnervation (Sugimoto, Bennett and Kajander, 1990).

The spinal cord is bombarded by high levels of spontaneous discharge from many of the injured nerve's afferents triggering central changes and consequently a long lasting increase in the excitability of dorsal horn cells with abnormal characteristics, such as an increase in the spatial extent of the cutaneous receptive fields of dorsal horn neurones, amplified responses, threshold reductions and high spontaneous activity; i.e. the state of central sensitisation (Woolf, 1983; Wall, 1991). Altered central processes are believed to underlie the phenomenon of secondary hyperalgesia, whereby a zone of mechanical hyperalgesia develops in uninjured skin surrounding a local cutaneous injury in the absence of alterations in the sensitivity of afferents (LaMotte et al., 1991; Hardy, Wolff and Goodell, 1950).

Aβ fibres under normal conditions signal light touch, vibration and position sense, but never pain. However, following CCI, sprouting of low threshold Aβ fibre terminals from LIII into LII occurs and if this redistribution results in the establishment of functional contacts with cells that would normally receive C-nociceptor input, this may explain abnormal responsiveness to innocuous stimuli, allodynia (Woolf, Shortland and Coggeshall, 1992). Such new Aβ activation of previously nociceptive cells might affectively bypass the inhibitory controls that large myelinated fibres (and other influences) usually confer on small afferent fibre inputs (Gautron et al., 1990). This may be a mechanism whereby large diameter

LTM afferents can elicit the sensation of nociception through central changes after nerve injury that strengthen the synaptic ties between central pain signalling pathways and LTMs (Woolf 1983; Cook et al., 1987; Campbell et al., 1988).

1.12 Ionotropic glutamate receptors following nerve injury

Central sensitisation is accompanied by a number of alterations in the expression of neuropeptides, neurotransmitters and their respective receptors in primary afferent neurones and in the spinal cord that may contribute to hyperexcitability.

There may be a differential role for ionotropic receptors in the generation and maintenance of chronic pain states. NMDA receptors have been implicated in nociceptive inputs for Aδ and C-fibres, suggesting they are involved in a hyperalgesia response, while AMPA and kainate receptors may be important in Aδ, C- and large myelinated fibre inputs and may mediate both hyperalgesia and normal responses (Dougherty et al., 1992; Gerber and Randić, 1989; Dickenson and Sullivan, 1990). The co-activation of AMPA and NMDA receptors is thought to produce thermal hyperalgesia induced by peripheral nerve injury (Mao et al., 1992a). On the other hand, when AMPA and Group I metabotropic receptors are co-activated, mechanical hyperalgesia is produced (Meller, Dykstra and Gebhart, 1993). NMDA and non-NMDA, but not metabotropic, antagonists inhibit flexion withdrawal during normal sciatic nerve stimulation (Silva, Cleland and Gebhart, 1997).

1.12.1 AMPA receptors

It has been reported that GluR1 and GluR2/3 subunit densities are upregulated following CCI (Harris et al., 1996) and downregulated following inflammation, deafferentation or contusive spinal cord injury (Pellegrini-Giampetro et al., 1994; Helgren et al., 1999; Florenzano and DeLuca, 1999; Grossman et al., 1999). AMPA receptor antagonists prevent the development of hyperalgesia in rats with CCI (Harris et al., 1996) as well as attenuating responses to noxious mechanical/thermal,

and/or non-noxious mechanical stimuli (Budai and Larson 1994; Cumberbatch, Chizh and Headley, 1994; Dougherty et al., 1992). The enhancement may be due to increased sensitivity of AMPA/kainate receptors to glutamate, which may result from the activity of PKC and CaMKII in the postsynaptic neurone, causing direct phosphorylation of glutamate receptors.

1.12.2 Kainate receptors

While there is still little information regarding a role for kainate receptors following CCI, it has been reported that selective antagonists of the GluR5 subunit of kainate receptor can attenuate the frequency of responses to mechanical stimuli and the latency of response to thermal stimuli that occur following CCI with no effect on normal rats (Sutton, Maccecchini and Kajander, 1999).

1.12.3 NMDA receptors

During normal nociceptive processing AMPA receptors mediate the fast excitatory transmission in the spinal cord, while the NMDA receptor ion pore is subject to a Mg^{2+} block. As mentioned, during brief excitation of nociceptors and following the afferent barrage produced by neuropathic pain, co-release of glutamate and SP is thought to depolarise postsynaptic cells via AMPA, metabotropic and/or neurokinin receptors. Indeed, in the spinal dorsal horn simultaneous activation of the multiple receptors NMDA, NK_1 and NK_2 is required for LTP induction by natural noxious stimulation (Rusin et al., 1993; Liu and Sandkühler, 1995). Depolarisation will result in the elimination of the Mg^{2+} NMDA receptor block, activating the ion channel and allowing Ca^{2+} entry and it is likely that the alterations in intracellular calcium and its downstream targets contribute to persistent changes in dorsal horn excitability (Coderre, 1993; Coderre and Melzack, 1992).

NMDA receptor-ligand binding sites and NR1 protein levels are reduced in the superficial dorsal horn following CCI (Hama et al., 1995). Ionophoresis of the NMDA receptor antagonist MK-801 in the spinal cord of rats with CCI reduces

noxious-evoked responses (Sotgui and Biella, 2000; Mao et al., 1992a) and MK-801, as well as the selective NMDA antagonist D-CPP, can reverse the facilitated behavioural withdrawal reflexes seen following mustard oil and conditioning electrical stimulation of afferents (Woolf and Thompson, 1991). In addition, intrathecal injection of selective NR2B subunit selective antagonists can inhibit CCI-induced facilitated responses and wind-up (Boyce et al., 1999).

At most glutamatergic synapses calcium influx through NMDA receptors, AMPA receptors or calcium release from intracellular stores (e.g. triggered by metabotropic and/or tachykinin receptors) may also be involved.

Such calcium influx following depolarisation and its release from intracellular stores leads to the activation of kinases, such as protein kinase C (PKC) and Ca^{2+}/calmodulin-dependent kinase (CaMK). Ca^{2+}/calmodulin also activates some isoforms of adenylate cyclase, which increase cAMP and activate protein kinase A (PKA). These kinases may modulate AMPA and NMDA receptors by phosphorylating specific residues that regulate channel function. Here, we will briefly examine some evidence implicating these kinases in nociceptive processing.

1.13 Involvement of kinases in nociceptive sensitisation

PKA has been implicated in central hyperexcitability. Application of cAMP or the catalytic subunit of PKA can enhance dorsal horn responses to glutamate-gated ion channel activation and result in hyperalgesia (Cerne, Jiang and Randić, 1992; Aley and Levine, 1999) and mutant mice with a knockout of the RIβ subunit of PKA have normal acute nociceptive responses but have a reduction in response during the second phase of the formalin test implicating at least one subunit of PKA in inflammatory hyperexcitability (Malmberg et al., 1997a).

Little is known about a role for CaMKII in nociceptive processing although presynaptic injection of CaMKII itself increases neurotransmitter release in the hippocampus (Llinás et al., 1985). Mutant αCaMKII mice are deficient in both

spatial learning and LTP (Silva et al., 1992) and CaMKII antagonists can prevent the induction of LTP (Bortolotto and Collingridge, 1998). Moreover, the active autophosphorylated form of CaMKII can increase excitatory transmission in dorsal horn neurones (Kolaj et al., 1994). In addition, spinal neuronal responses to mustard oil application are reduced following ionophoresis of CaMKII inhibitors (Young et al., 1995).

There is substantial evidence supporting a role for PKC in regulating persistent pain. Application of PKC activators can results in an enhancement of nociceptive responses and there are increases in PKC ligand binding in the spinal cord following peripheral nerve injury and noxious stimulation (Munro, Fleetwood-Walker and Mitchell, 1994; Coderre, 1993; Mao, et al., 1992b). PKCε and PKCγ mutant mice fail to develop behavioural correlates of neuropathic pain behaviour while normal acute nociception is retained (Khasar et al., 1999; Malmberg et al., 1997b). In addition, sustained dorsal horn neuronal activity following mustard oil application is reduced following ionophoresis of PKC inhibitors (Young et al., 1995).

Activation of these kinases leads to post-translational changes that modulate activity of both AMPA and NMDA receptors and this will be dealt with in further detail in Chapters 3 and 4, respectively.

1.14 Neuropeptide changes in neuropathic pain

In addition to the structural and physiological alterations that occur following peripheral nerve injury, neurochemical alterations occur in many afferent neurones such that they may switch their phenotype and so exaggerate the central response to innocuous stimuli (Hökfelt, Zhang and Wiesenfeld-Hallin, 1994, see Fig. 1.4). In this way, there may be a qualitative change in function, which could explain how presynaptic transmitter changes may initiate new postsynaptic alterations in ion channel excitability and expression levels (Wall, 1991). Although this is not an exhaustive list, the main changes observed include a down-regulation of the excitatory peptides SP and CGRP as well as decreased SOM, while levels of VIP,

NPY and GAL are all seen to increase such that these peptides are differentially regulated following nerve damage and inflammation, but we will focus on nerve injury here.

SP, CGRP and SOM

SP and CGRP are among the two main peptides that decrease their expression following nerve damage. Under normal conditions ~30% of small to medium diameter neurones in the DRG express SP (Ju et al., 1987; Smith, Seckl and Harmar, 1993). There is a significant decrease in the expression of SP mRNA in these DRG neurones that is accompanied by depleted SP binding and mRNA in the dorsal and ventral horn after unilateral nerve section, ligation or dorsal rhizotomy (Jessell et al., 1979; Barbut, Polak and Wall, 1981; Nahin et al., 1994; Kajander and Xu, 1995). However, SP immunoreactivity has been reported to increase in a model of partial nerve injury in spared DRG neurones (Ma and Bisby, 1998). Furthermore, NK_1 receptor immunoreactivity and mRNA is upregulated in the LI and LII following sciatic nerve section and ligation (Abbadie et al., 1996; Aanonsen et al., 1992).

However as mentioned in Section 1.8, mixed effects for NK_1 receptor antagonists in neuropathic pain have been reported and clinical trials with NK_1 receptor antagonists have proved disappointing (Hill, 2000) although trials with more potent NK_1 receptor antagonists as analgesic agents are currently in progress (Walpole et al., 1998). NK_2 receptor antagonists have been reported to be anti-hyperalgesic following nerve ligation and involved in the maintenance of hyperexcitability during inflammation (Neugebauer, Rumenapp and Schaible, 1997).

CGRP is abundant in DRG neurones under normal conditions but following CCI, there is a marked decrease in the expression of CGRP mRNA in small to medium DRG neurones as well as decreased levels of CGRP immunoreactivity in the superficial dorsal horn (Nahin et al., 1994; Kajander and Xu, 1995). SOM is normally present in approximately 20% of small to medium diameter DRG (Ju et al.,

Figure 1.4 Schematic of the principal changes in the CNS following peripheral nerve injury

Schematic representation of a small and large primary afferent sensory neurone in a dorsal root ganglion sending a central branch to the dorsal horn of the spinal cord and a peripheral branch which has been injured by axotomy. Arrows indicate changes in the levels of neuropeptides and their receptors.

In small diameter DRG neurones, SP, CGRP and SOM peptide levels are decreased, as is NPY receptor mRNA, while levels of VIP GAL, CCK and NPY are increased. In large diameter DRG there is an increase in NPY and NPY receptor along with smaller increases in VIP and GAL, while CRGP peptide and opioid receptor levels decrease. Summaries of the structural and physiological changes from the peripheral to the central nervous system are indicted.

(Adapted from Hökfelt, Zhang and Wiesenfeld-Hallin, 1994).

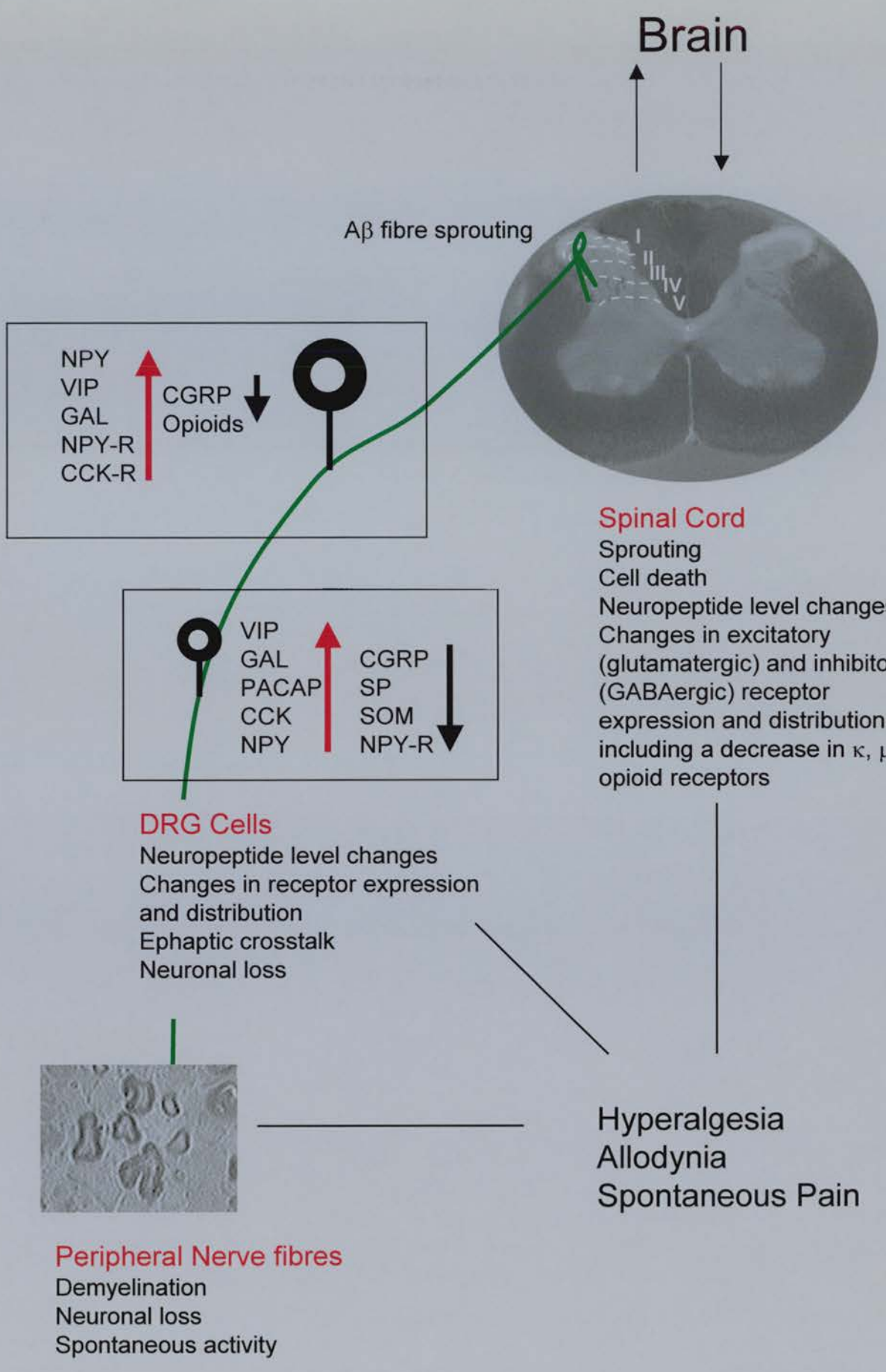
Brain
Aβ fibre sprouting
I
II
III
IV
V
NPY
VIP
GAL
NPY-R
CCK-R
CGRP
Opioids
VIP
GAL
PACAP
CCK
NPY
CGRP
SP
SOM
NPY-R
Spinal Cord
Sprouting
Cell death
Neuropeptide level changes
Changes in excitatory (glutamatergic) and inhibitory (GABAergic) receptor expression and distribution including a decrease in κ, μ, δ opioid receptors
DRG Cells
Neuropeptide level changes
Changes in receptor expression and distribution
Ephaptic crosstalk
Neuronal loss
Hyperalgesia
Allodynia
Spontaneous Pain
Peripheral Nerve fibres
Demyelination
Neuronal loss
Spontaneous activity

1987; Smith, Seckl and Harmar, 1993), however following nerve transection there is a marked decrease in the production of SOM by primary afferent neurones with a corresponding decrease in SOM immunoreactivity in the superficial dorsal horn (Shehab and Atkinson, 1986; Villar et al., 1989; Zhang et al., 1993).

VIP, GAL and NPY

Following CCI, there is a reported ipsilateral spinal cord increase in VIP, GAL and NPY mRNA in DRG (Nahin et al., 1994). VIP expression is relatively low in the superficial dorsal horn and primary afferent neurones under normal conditions (Knyihar-Csillik et al., 1991; Fuji et al., 1983). Following axotomy and crush, there is a significant increase in VIP expression in small to medium diameter DRG neurones, where it is often co-localised with GAL, with a corresponding increase in VIP immunoreactivity in the superficial dorsal horn (Nahin et al., 1994; Zhang et al. 1995; Knyihar-Csillik et al., 1991; Shehab and Atkinson, 1986). In addition, following CCI, spinal $VPAC_2$ receptor mRNA increases ipsilateral to CCI while there is a decrease in $VPAC_1$ receptor mRNA and no change in PAC_1 receptor mRNA expression (Dickinson et al., 1999). VIP predominantly has an excitatory role and so it is possible that this peptide takes over the role of SP as a primary neurotransmitter within the CNS of neuropathic animals.

Galanin is upregulated in medium and large DRG neurones after complete and partial sciatic nerve transection and in ipsilateral dorsal horn after CCI (Ma and Bisby, 1997; Hökfelt et al., 1987; Villar et al., 1989; Colvin, Mark and Duggan, 1997). The pattern of co-expression of GAL with other neuropeptides also changes following nerve injury with an increase in the co-existence of GAL with NPY and VIP (Nahin et al., 1994). In addition, intrathecal GAL alleviates mechanical and cold allodynia following ischemic peripheral nerve injury (Hao et al., 1999). The expression of NPY in the DRG is low under normal conditions (Gibson et al. 1984), but following nerve injury, NPY is upregulated in laminae III-V of the dorsal horn and expression is induced in many large or medium diameter primary afferent neurones (Kar and Quirion, 1995; Nahin et al., 1994; Zhang et al., 1995).

1.15 Ionotropic glutamate receptor interacting proteins

While there is a vast body of information for the role of the AMPA and NMDA receptor ion channels in the plasticity of neuropathic pain, there is little information regarding their underlying mechanisms and second messenger cascades.

Over the last few years, biochemical indices have identified a number of intracellular proteins that interact with the intracellular C-termini of AMPA and NMDA receptors that may mediate their localisation and ability to interact with intracellular signal transduction machinery. These proteins are of two types, those that contain PDZ domains (discussed below) of which there are specific examples that interact with either AMPA or NMDA receptors, and those that do not contain PDZ domains, largely interacting with AMPA receptors. Together with their respective glutamate receptor ion channels and associated molecules, these proteins form large complexes that may regulate neuronal transmission and plasticity. In general, it is believed that the AMPA receptor and the NMDA receptor exist as distinct macromolecular complexes.

PDZ domain-containing proteins

PDZ domains mediate protein: protein interactions, and were first recognised as repeats of ~90 amino acids in the amino terminus of the PSD-95 (MAGUK) family of cytoplasmic proteins where they are thought to have an organising function at sites of cell-to-cell contact (Kennedy, 1997). PDZ domains are named after three proteins with these repeats (PSD-95/SAP90, *Dlg*-A and tight junction proteins, ZO-1) and are found throughout phylogeny in diverse organisms.

Multiple PDZ domains are modular protein-binding domains that have at least two distinct mechanisms for binding: they can bind to specific recognition sequences at the carboxyl termini of proteins or they can dimerise with other members of the MAGUK family via N-terminal interactions and indeed seem to be able to do both at the same time (Fanning and Anderson, 1996). Many cytosolic signalling proteins and cytoskeletal proteins are composed of modular units of small protein: protein

interaction domains that allow reversible and regulated assembly into larger protein complexes.

PDZ domains have been observed in many cytosolic proteins and may co-operate to enhance binding to their common targets or help to bind simultaneously to multiple different targets as well as showing specificity of binding (Sonyang et al., 1997). PDZ domain-containing proteins may be crucial for the maintenance of clusters of glutamate receptors at synapses in dendritic spines (Rao et al., 1998) though they are not essential in cluster formation (Migaud et al., 1998) or directly in the translocation of these clusters to synaptic sites (van Rossum and Hanisch, 1999).

The Membrane Associated Guanylate Kinase (MAGUK) protein family members use multiple domains (including PDZ domains) to cluster ion channels, receptors, adhesion molecules and cytosolic signalling proteins at synapses. All MAGUKs are associated with the plasma membrane. Distinct MAGUKS interact with the intracellular C-termini of both the GluR1 AMPA and NR2 NMDA receptor subunits. This will be discussed in more detail in Chapters 3 and 4, respectively.

There is a growing list of proteins that do not belong to this MAGUK family, although they do contain PDZ domains. A protein called GRIP (Glutamate Receptor Interacting Protein) interacts with the C-terminal of GluR2 subunits of AMPA receptors and may be important for receptor clustering as well as coupling AMPA receptors to signalling and cytoskeletal molecules. Other identified GluR2 interaction partners include PICK1, a PDZ protein that binds to the α isoform of PKC and may regulate AMPA receptor modulation, and NSF, a non-PDZ domain-containing protein with an identified role in vesicle trafficking. These will be discussed in more detail in Chapters 3.

1.16 Aims

The aims of the present work were to further examine the underlying mechanisms of both the AMPA and NMDA subtypes of glutamate receptors in central neuropathic

sensitisation by an examination of their interacting partners and the potential changes in function that they may have in the CCI model (Bennett and Xie, 1988).

We have used the CCI model to investigate GluR2-interacting proteins such as GRIP, PICK1 and NSF, by examination of expression levels in the spinal cord under normal conditions and following CCI, as well as the effects of inhibiting these interactions by use of intrathecally-applied blocking peptides. In addition, we will examine functional modulations affecting the AMPA receptor by an analysis of the effects of GluR1 serine residue phosphorylation by kinases such as PKA and PKC/CaMKII in the spinal cord following CCI. These results are presented in Chapter 3.

Hypotheses

1: Given that non-selective AMPA receptor antagonists have been reported to reduce behavioural sensitivity following nerve injury, we tested the possibility that highly selective AMPA receptor antagonists would have a similar effect when administered locally by intrathecal injection in the spinal cord following CCI.

2: Based on the assumption from previous in vitro work, whereby blocking particular proteins that interact with the intracellular C-terminus of the GluR1 and GluR2 subunits of AMPA receptors (such as SAP97, GRIP/PICK1 and NSF) causes reduced receptor clustering and localisation as well as a run-down of AMPA receptor mediated currents, we tested the possibility that such specifically targeted C-terminal myristoylated peptides will disrupt AMPA receptor involvement in neuropathic pain.

3: If the second hypothesis proves to be the case, then it would be expected that there will be a regulation of expression of receptor subunit levels and associated adapter proteins in the spinal cord following CCI. For this, mRNA analysis via in situ hybridisation and protein analysis via Western blotting will be carried out.

4: We will also set out to examine how the mechanism of action of AMPA receptor subunits may be altered following CCI and the effects of phosphorylation by kinases on this by use of subunit selective phosphorylation-specific antibodies.

To examine any functional effects of NMDA receptor interactions during neuronal plasticity following CCI, we have used mice with a mutation in the best-characterised PDZ domain-containing protein, PSD-95, which interacts with NR2 subunits of NMDA receptors, and characterised the development of behavioural neuropathy following CCI. We show that in the mutant mice there is a striking failure to develop neuropathic sensitisation and some of the possible underlying mechanisms are investigated. In addition, an examination of NMDA receptor channel modulation by PKA and PKC was undertaken to establish any alteration in NMDA receptor phosphorylation following CCI. These results will be presented in Chapter 4.

Hypotheses:

1: Learning and memory in the hippocampus and central sensitisation in the spinal cord share the common mechanism of NMDA receptor dependence. Given the effect of a PSD-95 mutation on tests of learning and memory, we predict that PSD-95 mutant mice will also show an altered phenotype for the behavioural sensitivity following the induction of CCI.

2: The NMDA receptor dependence factor of any findings from hypothesis 1 will be tested using NMDA receptor antagonists following CCI and the activation of the NMDA receptor via application of an agonist in naïve mice.

3: Based on the finding that NMDA receptor activation can result in calcium entry through the ion channel and a cascade of Ca^{2+} associated kinases, we will test the possibility, via enzyme activity or phospho-specific antibodies, that any alterations in the phenotype observed from Hypothesis 1 will be NMDA receptor dependent and/or mediated via the closely associated protein kinases such as CaMKII and PKA which are known not only to be involved in hippocampal behavioural paradigms but also are involved in behavioural sensitisation in the spinal cord.

CHAPTER 2: Materials/Methods

2.1: Supplier information

Company	Product
Amersham Biotech, Ltd., Amersham Place, Little Chalfont, Buckinghamshire, HP7 9NA.	Hypercoat LM-1 Emulsion, Hyperfilm ECL, 7.5% homogeneous gels, PhastSystem
AstraZeneca Ltd., Macclesfield, Cheshire.	Hibitane, Fluothane
BDH Chemical Company, Merck House, Poole, BH1 1TD.	OCT mounting medium, Polylysine ® microscope slides, acetic anhydride, TEA, gluteraldehyde, ammonium acetate, PerTex microscopy mountant
Becton Dickinson (BD), UK Ltd., PO Box 17663, London, SE1 4ZT.	U-100 insulin 12.7mm 0.5ml syringes, 25.1 G Terumo syringes
BioRad Laboratories, BioRad House, Marylands Avenue, Hemel Hempstead, Herts HP2 7TD.	10% cross-linked polyacrylamideTRIS-HCL resolving/4% stacking ready gels, immunoblot PVDF membrane, analytical grade mixed bed anion exchange resin
Boehringer Mannheim Ltd., Bell Lane, Lewes, E. Sussex, BN7 11G.	Glycogen

Calbiochem-Novabiochem UK Ltd., Boulevard Industrial Park, Padge Road, Beeston, Boulevard Industrial Park, Nottingham, NG9 2JR.	2-[N-(2-hydroxyethyl)-N-(4 methoxybenzenesulfonyl) amino-N-(4-chlorocinnamyl)-N methylbenzylamine (**KN-92**), 2-[N-(2-hydroxyethyl)-N-(4-methoxybenzenesulfonyl) amino-N-(4-chlorocinnamyl)-N-methylbenzylamine, phosphate (**KN-93**), myristoylated autocamtide-2 related inhibitory peptide, calmodulin
Cambridge Bioscience, Signet Court, Newmarket Road, Cambridge, CBS 8LA.	Monoclonal anti-CaMKII mouse IgG
Chemicon International Ltd., 2 Admiral House, Cardinal Way, Harrow, HA3 5UT.	Polyclonal anti-GluR1 rabbit IgG, polyclonal anti-GluR2 rabbit IgG, polyclonal anti-NSF rabbit IgG, polyclonal anti-NR2B rabbit IgG, monoclonal anti-GAPDH mouse IgG, Re-Blot antibody-stripping reagent
Fisher Scientific UK Ltd., Bishop Meadow Road, Loughborough, Leicestershire, LE11 5RE.	Mini borosilicate glass homogenisers
Genus Xpress (Ethicon), 10 Castings Court, Falkirk, KK2 9HJ.	Coated vicryl, 13mm, curved needle 4/0(5/0), 75cm, chromic catgut 17mm 4/0(5/0) 45cm
Gibco Life Technologies Ltd., Inchinnan Park, Paisley, PA4 9RP.	20x Standard saline citrate

HA West X-Ray Ltd., 41 Watson Crescent, EH11 1ES.	Liquid fixer Ilford Hypam, Developer powder D-19
Linton Instrumentation, No.1 Forge Business Centre, Norfolk, IP22 1AD.	Plantar test and heat flux infrared radiometer, compartment rat enclosure
Merck Ltd., Merck House, Poole, Dorset, BH15 1TD.	DPX mountant for microscopy, coverslips (22x50cm)
Millipore UK Ltd., The Boulevard, Blackmoor Lane, Watford, Herts, WD1 8YW.	Immobilon (polyvinyl difluoridine; PVDF) membranes
NEN Life Science UK Ltd., PO Box 66, Hounslow, TW5 9RT.	[α-^{35}S]-dATP radiolabel specific activity <1250 Ci/mol
New England Biolabs (NEB) UK Ltd., Hitchin, Herts, SG4 0TY.	Luminol, HRP-linked secondary antibodies
Oswell DNA Service, Medical & Biological Sciences Building, University of Southampton, Boldrewood, Southampton SO16 7PX.	GluR1 (45 mer) antisense mRNA GluR2 (45 mer) antisense mRNA GRIP2 (39 mer) antisense mRNA NSF (45 mer) antisense mRNA Narp (48 mer) antisense mRNA
Pepsyn Ltd., University of Liverpool, School of Biological Sciences, University of Liverpool, Liverpool L69 72B.	Myristoylated peptides: myr-NVYGIESVKI myr-SGMPLGATGL myr-AKRMKVAKNAQ

Pierce, 3747 N. Meridian Road, PO Box 117, Rockford, IL 61105, USA.	BCA Protein assay reagent kit
Promega UK Ltd., Delta House, Chilworth Research Centre, Southampton SO16 7NS.	Tdt enzyme and buffer
Rhone Merieux Ltd., Harlow, Essex, CM19 5TS.	Sagatal
Roche Diagnostics Ltd., Bell Lane, Lewes, East Sussex, BN7 1L6.	Sephadex G-25 quickspin columns
Santa Cruz Biotech, Inc., **(Autogen Bioclear UK, Ltd.)** Holly Ditch Farm, Mile Elm, Calne, Wiltshire, SN11 0PY.	Monoclonal anti-hDlg (SAP97) mouse IgG, monoclonal anti-PICK1 mouse IgG, polyclonal anti-NRζ1 goat IgG, monoclonal anti-AKAP150 mouse IgG
Sigma-Aldrich Company Ltd., Fancy Road, Poole, Dorset, BH12 4QH.	All other chemicals
Stoelting 620 Wheat Lane, Woodale, IL60191.	von Frey filaments
Upstate Biotechnology Inc., **(TCS Biologicals),** Park Keys, Botolph, Claydon, Buckinghamshire, MK18 2LR.	Polyclonal anti-phospho-Ser^{897}-NR1 rabbit IgG, polyclonal anti-phospho-Ser^{896}-NR1 rabbit IgG, polyclonal anti-NR1 rabbit IgG, polyclonal anti-NR2A rabbit IgG, polyclonal anti-phospho-Ser^{831}-GluR1 rabbit IgG, polyclonal

	anti-phospho-Ser^{845}-GluR1 rabbit IgG, polyclonal anti-GluR1 rabbit IgG
Tocris Cookson Ltd., Northpoint, Fourth Way, Avonmouth, Bristol, BS11 8TA.	2,3-dihydroxy-6-nitro-7-sulfamoyl benzo(f)quinoxaline (NBQX), (±)-4-(4-Aminophenyl)-1,2-dihydro-1-methyl-2-propylcarbamoyl-6,7-methylenedioxphalazine (SYM2206) 3-((*R*)-2-carboxypiperazin-4-yl)-propyl-1-phosphonic acid ((R)-CPP)
Transduction Labs. Inc., (Becton Dickinson, UK, Ltd.), PO Box 17663, London, SE1 4ZT.	Monoclonal anti-GluR2/4 mouse IgG, monoclonal anti-PKA-RIIα mouse IgG, polyclonal anti-PKA-RIIβ rabbit IgG, monoclonal anti-GRIP mouse IgG, monoclonal anti-PSD-95 mouse IgG, U-100 insulin 12.7mm 0.5ml syringes, 25.1 G Terumo syringes

2.2: Methods common to Chapter 3 and 4

2.2.1 Animals

Adult male Wistar rats were used for the experiments described in Chapter 3 (150-200g; Charles River, UK). They were housed in standard laboratory cages in groups of four, with food and water supplied *ad libitum*. Adult C57/BL6/MF1 mice, either wild-type or PSD-95 mutant strains (Gift from Prof. Seth Grant, Dept. Neuroscience, University of Edinburgh) were used in the experiments described in Chapter 4. They were housed in standard laboratory conditions with littermates, with food and water supplied *ad libitum*. All experiments were carried out in accordance with the UK Animals (Scientific Procedures) Act 1986.

2.2.2 Surgical preparation of animals with chronic constriction injury (CCI)

Rats and mice were initially anaesthetised with sodium pentobarbital (Sagatal; 0.01ml/kg, i.p., for mice was diluted by 1:10 in dH_2O; Rhône Mérieux, UK) and this was then supplemented with halothane O_2 (AstraZeneca, Ltd.). Under aseptic conditions, using the method of Bennett and Xie for rat (Bennett and Xie, 1988), the sciatic nerve was exposed at the mid-thigh level proximal to the sciatic trifurcation. Four chromic catgut ligatures (4.0 for rats; Ethicon, Edinburgh) separated by 1mm were tied loosely to constrict the tibial branch as viewed under 40x magnification. A slight modification of the Bennett and Xie CCI model was developed for mice, whereby three chromic catgut ligatures (5.0 for mice; Ethicon, Edinburgh) were applied to the sciatic nerve in the same manner as described above. Vascular supply was not compromised. The overlying muscle and skin were sutured and the animals were placed in a recovery cage. A sham operation was performed as a control and followed the same procedure, except that no ligatures were tied around the sciatic nerve.

2.2.3 Behavioural testing

Behavioural testing was carried out to assess the development and progression of the neuropathic pain sensitivity characteristic to the CCI model, as indicated by the presence of hyperalgesia and allodynia. Testing procedures were the same for rats and mice. To eliminate bias, the experimenter was blind to genotype/drug treatment.

(i) Thermal Hyperalgesia

Thermal hyperalgesia was monitored using a Hargreave's Thermal Stimulator (Linton Instrumentation, USA). A radiant thermal stimulus of infrared intensity 30 or 15 (manufacturer's scale) for rats and mice, respectively (>50°C; Hargreaves et al., 1988) was applied to the mid-plantar surface of the hindpaw. The withdrawal response was characterised as a brief paw flick. The latency of withdrawal was recorded for the ipsilateral (injured) and the contralateral (uninjured) hindpaws ('PWL', paw withdrawal latency). The means of between 5 and 10 readings were recorded at 3-5 min intervals, which ensured no hypersensitivity to the test was established (see Fig. 2.1a).

(ii) Mechanical Allodynia

Mechanical allodynia was measured as the withdrawal threshold to calibrated Semmes-Weinstein von Frey filaments (Stoelting, Wood Dale, IL) with a bending force of 8.41-4830.62mN.mm^{-2}. Animals were placed on a wire cage and the filaments were applied to the mid-plantar surface of the hindpaw from beneath until the filament started to bend. This stimulus was repeated 8-10 times at 1-2 sec intervals for both the injured and uninjured hindpaws. The mean threshold required to elicit a withdrawal response was recorded ('PWT', paw withdrawal threshold). The filaments were applied in ascending order, and responses were characterised as a brief paw flick. The withdrawal threshold was defined from the lower of two consecutive von Frey filaments that elicited a response. Data were expressed as the

Figure 2.1 Photographic description of behavioural tests

(a) Shows a mouse placed in a Perspex box on the Hargreaves thermal stimulator, where the animal withdraws the hindpaw following noxious thermal stimulation

(b) Shows a mouse placed in a wire cage box and a von Frey filament was applied to the hindpaw, until the filament started to bend

(c) Shows a rat (mouse reactions are too rapid for photographic capture) placed in a glass tank on an elevated metal grid floor covered (~1cm) with a mixture of ice and water (3-4^{o}C). The hindpaw is elevated above the water level under conditions of neuropathic pain.

a

b

c

threshold indentation pressure (i.e. the bending force/ per cross-sectional area at the tip of the filament; see Fig. 2.1b).

(iii) Cold Allodynia

In order to test for the presence of cold allodynia, animals were placed in a glass tank with an elevated metal grid floor. This was covered (~1cm) with a mixture of ice and water (3-4°C), which ensured both the glabrous and hairy skin of the foot was covered with water. Animals were placed in the tank for a 30 sec period, the first 10 sec of which were to allow the animals to acclimatise. During the remaining 20 sec, measurements were made of the amount of time the animal elevated the injured paw above the water level, defined as the Suspended Paw Elevation Time (SPET). To ensure paws returned to body temperature, testing was carried out only every 10 min (see Fig. 2.1c).

2.2.4 Intrathecal injections

Baseline measurements were recorded for thermal hyperalgesia (Hargreave's test) and mechanical allodynia (von Frey filament test) in animals that had undergone chronic constriction injury and were at the peak of neuropathic reflex sensitisation. Animals were briefly anaesthetised with halothane and O_2. Drugs (see Table 2.1 for details of compounds used) were injected intrathecally (in 50µl saline vehicle for rat or 10µl saline vehicle for mice), at the L4 level of the spinal cord (Hylden and Wilcox, 1982) using a 25.1G syringe or a U-100 microfine insulin syringe (for rat and mouse injections, respectively; Becton Dickenson, Ltd.). The experimenter was blind to the content of the injections so as to eliminate bias. 15 min following injection, animals were re-tested using the same procedures and measurements were taken to determine the effects of drug on hyperalgesic and allodynic behaviours. Animals were tested every 5 min until readings returned to baseline levels.

-Drugs

The drugs used for blocking the AMPA receptor were NBQX, an AMPA/kainate antagonist with 50 fold selectivity for AMPA over kainate, the selective AMPA receptor antagonist NS-257 and SYM 2206, a highly potent AMPA receptor antagonist. The vehicle, saline, was used in control injections. In addition, a number of myristoylated peptides (for increased cell permeability) designed to block specific regions on the GluR2 and GluR1 C-termini were designed for use in intrathecal injections, myr-NVYGIESVKI, myr-AKRMKVAKNAQ, myr-SGMPLGATGL. The inactive myristoylated peptide, myr-GRRNAIHDE' (Gift from Dr. Roger Clegg, Hannah Research Institute, Ayr) was used in control injections. The agonist AMPA was used to examine activation of spinal AMPA receptors. (R)-CPP, the highly selective NMDA receptor antagonist and NMDA, the NMDA receptor ligand were used to examine the basic pharmacology of the NMDA receptor in vivo. In addition, the CaMKII inhibitors, myristoylated autocamtide-2-related inhibitory peptide, KN-93 and its inactive structural analogue, KN-92 and the vehicle, saline, were used in control injections (see Table 2.1 for a summary of drugs and specific doses).

2.2.5 Statistics

In each behavioural study, data were pooled, either for each test day (for the development of neuropathic reflex sensitivity), or for test block minutes (following intrathecal injection). Data were displayed as the average ± the standard error of the mean (SEM). In the test of thermal hyperalgesia, paired Student's t-tests were performed to determine any significant differences between ipsilateral and contralateral hindlimb values, while a one-way ANOVA followed by a Dunnett's post-hoc test were used to examine any alteration of post-treatment responses to pre-treatment baseline responses. In the test of mechanical allodynia, Mann-Whitney Rank sum tests were performed to determine any significant differences between ipsilateral and contralateral hindlimb values, while a Kruskal-Wallis ANOVA followed by a Dunn's post-hoc test were used to examine any alteration of post-treatment responses to pre-treatment baseline responses.

Table 2.1 Compounds used for intrathecal injections

This table provides a brief summary of the compounds used for the intrathecal injection experiments, stating specific dose ranges and general information of the site of compound activity.

Compounds	Dose	Activity
AMPA receptor antagonists		
NBQX	1.5, 5, 13 nmol	*Non-competitive antagonist*
NS-257	28, 83, 166 nmol	*Competitive antagonist*
SYM 2206	1.5 nmol	*Potent non-competitive antagonist*
AMPA receptor agonist		
AMPA	50μmol	*AMPA receptor ligand*
Myristoylated inhibitory peptides		
myr-NVYGIESVKI	4.5nmol	*Blocks PICK1/GRIP site on GluR2*
myr-AKRMKVAKNAQ	4.5nmol	*Blocks NSF site on GluR2*
myr-SGMPLGATGL	4.5nmol	*Blocks SAP97 site on GluR1*
myr-GRRNAIHDE	4.5nmol	*Inactive control peptide*
NMDA receptor antagonist		
(R)-CPP	100ρmol	*Competitive antagonist*
NMDA receptor agonist		
NMDA	0.25nmol	*NMDA receptor ligand*
CaMKII inhibitors		
KN-93	120ρmol	*Blocks calmodulin binding site*
KN-92	120ρmol	*Inactive structural analogue of KN-93*
myr-AIP	1nmol	*Potent inhibitor of CaMKII*

2.2.6 Western blotting

(i) Tissue Preparation

A laminectomy (L3-6) was performed on anaesthetised animals (n=3-6) at the peak of behavioural neuropathic sensitivity and the spinal cord was hemisected to separate contralateral from ipsilateral sides. This was then immediately gently homogenised, in a hand–held homogeniser (Fisher Scientific, Ltd.) at 4°C containing freshly prepared Laemmli buffer.

(ii) Solutions

SDS Laemmli lysis buffer (5x stock)
0.625M Tris-Cl, pH 6.8; 2% (w/v) SDS
0.1% (w/v) bromophenol blue
50% (v/v) glycerol

Phosphate buffered saline (PBS)
0.1M $Na_2HP0_42H_2O$, 0.1M $NaH_2P0_42H_2O$, 150mM NaCl; pH 7.4

SDS-PAGE electrophoresis buffer
1M Tris base, 0.1M glycine

Protein transfer buffer
0.1M Tris base, 0.5M glycine, 0.01% (w/v) SDS

(iii) SDS polyacrylamide gel electrophoresis (SDS-PAGE)

Polyacrylamide gel electrophoresis was performed using the Tris-glycine buffer system for protein separation described by Laemmli (1970). Pre-cast polyacrylamide ready gels (4% stacking, 10% resolving, 15 wells; BioRad) were placed in a buffer chamber and wells were cleared of gel fragments by washing with buffer prior to sample loading. Electrophoresis running buffer (1x) was added to the buffer chamber. Samples and molecular weight marker proteins were loaded into the wells of the stacking gel and electrophoretically separated at a constant voltage of 100V until the samples passed into the resolving gel, at which point the voltage was increased to 150V and run until the samples reached the bottom of the gel.

(iv) Transfer of proteins

PVDF membranes were wetted by briefly soaking in methanol, which was then removed with several brief dH_2O washes. The gel was removed from the stabilising backing plate, placed in 1x transfer buffer and sandwiched between filter paper and sponges. This 'sandwich' was placed in the buffer chamber, immersed in transfer buffer and cooled with an ice block. Electro-blotting was performed at 100V for 45 min using BioRad Protean II Gel Transfer apparatus.

(v) Protein loading

Prior to immunoblotting, membranes were temporarily stained with PhastGel Blue R (Amersham Biotech, Ltd.) to ensure even protein loading of the lanes. This stain was removed with methanol prior to membrane blocking. As a further control for protein level normalisation, membranes were stripped ("Re-Blot" reagent, Chemicon International, Ltd.) and reprobed for the ubiquitous housekeeping enzyme glyceraldehyde-3-phosphate dehydrogenase (GAPDH) where possible. GAPDH has previously been shown to serve as a stable and consistent housekeeping protein whose cellular levels are unaltered for example in cases of spinal cord and brain insult (Medhurst et al., 2000).

(vi) Immunoblotting

Membranes were blocked overnight at 4°C in 4% Marvel/0.1% Tween-20. Following blocking treatment, membranes were incubated in primary antibody (made up to the desired concentration in 4% Marvel/0.1% Tween-20) for 1-2 hr at room temperature in a sealed bag on a rotator (See Tables 2.2 and 2.3 for primary antibody details). Membranes were washed five times in wash buffer (PBS, 0.1% (v/v)/ Tween-20) for 5 min at room temperature and incubated with the relevant horseradish peroxidase (HRP)-conjugated secondary antibody for 45 min at room temperature on a shaker, followed finally five times in wash buffer for 5 min at room temperature.

(vii) Enhanced chemiluminescence detection

To detect bound antibody, membranes were incubated with a minimal volume of enhanced chemiluminescence (ECL) detection reagent (Amersham Biotech, Ltd.) for 1 min at room temperature. Excess reagent was drained off the membranes which were then wrapped in cling-film, placed in a cassette and exposed to X-ray film for varying amounts of time (30 sec-20 min) depending on signal strength.

(viii) Densitometry Analysis

X-ray films were scanned using '*Colour It*' scanning software. Densitometry was performed using '*Scan Analysis*' software whereby grey levels of positive protein bands and background grey levels were quantitatively measured. Where possible, the grey levels of the protein of interest were normalised against GAPDH levels.

While quantitative measurement of the levels of protein expression was carefully made by ECL film image densitometry (and compared to GAPDH expression) the relationship between this and protein concentration is not necessarily strictly linear so values should formally be considered as a comparative estimate of protein levels.

Table 2.2 Antibodies used for Western blots and immunoprecipitations of spinal cord (Chapter 3)

This table provides a brief summary of the antibodies used for Western blotting and immunoprecipitation experiments specific to Chapter 3, stating specific primary antibody details and dilutions as well as secondary antibody details and dilutions.

Primary antibody	Dilution	Secondary antibody	Dilution
Polyclonal anti-GluR1 rabbit IgG (UBI)	1:100	HRP-linked anti-rabbit (Chemicon)	1:5,000
Polyclonal anti-phospho-Ser^{831}-GluR1 rabbit IgG (UBI)	1:100	HRP-linked anti-rabbit (Chemicon)	1:5,000
Polyclonal anti-phospho-Ser^{845}-GluR1 rabbit IgG (UBI)	1:100	HRP-linked anti-rabbit (Chemicon)	1:5,000
Monoclonal anti-hDlg (SAP97) mouse IgG (Santa Cruz Biotech.)	1:250	HRP-linked anti-mouse (NEB)	1:2,000
Polyclonal anti-GluR2 rabbit IgG (Chemicon)	1:100	HRP-linked anti-rabbit (NEB)	1:2,000
Monoclonal anti-GluR2+4 mouse IgG (BD)	1:50	HRP-linked anti-mouse (Chemicon)	1:10,000
Monoclonal anti-PICK1 mouse IgG (Santa Cruz Biotech.)	1:200 (1:75 for ip)	HRP-linked anti-mouse (NEB)	1:2,000
Monoclonal anti-GRIP mouse IgG (Transduction Labs.)	1:500	HRP-linked anti-mouse (NEB)	1:2,000
Polyclonal anti-NSF rabbit IgG (Chemicon)	1:1,000	HRP-linked anti-rabbit (NEB)	1:2,000
Monoclonal anti-GAPDH mouse IgG (Chemicon)	1:750	HRP-linked anti-mouse (NEB)	1:2,000

Table 2.3 Antibodies used for Western blots and immunoprecipitations of spinal cord (Chapter 4)

This table provides a brief summary of the antibodies used for Western blotting and immunoprecipitation experiments specific to Chapter 4, stating specific primary antibody details and dilutions as well as secondary antibody details and dilutions.

Primary antibody	Dilution	Secondary antibody	Dilution
Polyclonal anti-NRζ1 goat IgG (Santa Cruz Biotech.)	1:100	HRP-linked anti-goat (Santa Cruz Biotech)	1:100
Polyclonal anti-NR1 rabbit IgG (UBI)	1:100	HRP-linked anti-rabbit (Chemicon)	1:5,000
Polyclonal anti-phospho-Ser^{896}-NR1 rabbit IgG (UBI)	1:100	HRP-linked anti-rabbit (Chemicon)	1:5,000
Polyclonal anti-phospho-Ser^{897}-NR1 rabbit IgG (UBI)	1:100	HRP-linked anti-rabbit (Chemicon)	1:5,000
Polyclonal anti-NR2A rabbit IgG (UBI)	1:500	HRP-linked anti-Rabbit (Chemicon)	1:5,000
Polyclonal anti-NR2B rabbit IgG (Chemicon)	1:500	HRP-linked anti-rabbit (Chemicon)	1:5,000
Monoclonal anti-PSD-95 mouse IgG (Transduction Labs.)	1:500	HRP-linked anti-mouse (NEB)	1:2,000
Monoclonal anti-AKAP150 mouse IgG (Santa Cruz)	1:1,000	HRP-linked anti-mouse (NEB)	1:2,000
Monoclonal anti-PKA RIIα mouse IgG (Transduction Labs.)	1:200	HRP-linked anti-mouse (NEB)	1:2,000
Polyclonal anti-PKA RIIβ rabbit IgG (Transduction Labs.)	1.500	HRP-linked anti-rabbit (Chemicon)	1:5,000

2.3: Methods specific to Chapter 3

2.3.1 In situ hybridisation histochemistry (ISHH)

Unless otherwise stated, all solutions were made up in dH_2O that had been treated with the nuclease inhibitor, DEPC. RNase contamination was minimised by using sterile glassware, DEPC-treated dH_2O, and all surfaces were treated with RNase Zap ® (Sigma).

(i) Oligonucleotide Probes

Oligonucleotide probes for GluR1, GluR2, GRIP2, NSF and Narp mRNA were designed on the basis of previous publications and/or confirmed by homology screening with the Basic Local Alignment Search Tool (BLAST) online at the National Centre for Biotechnology Information (NCBI). Probes were synthesised and HPLC purified by Oswell Chemicals (University of Southampton) and each probe was dissolved in 1ml of sterile water, at a given concentration (µg/ml). All probes were aliquoted into 200µl samples and stored at -70°C until required. A summary of all probes is given in table 2.4, showing the length and mRNA sequence site complementary probes were designed against. Probe sequences can be seen in Figure 2.2.

Table 2.4 Oligonucleotide probe details

Summary of oligonucleotide probes used against GluR1, GluR2, GRIP2, NSF and Narp mRNA showing details of probe length, target sequence identification and probe concentration. Probes were based on either the details of previous publications where possible, and where not possible, confirmed by homology screening with Blast online at NCBI.

Probe	Size	Target Sequence	Concentration (μg/ml)	Reference	Accession No.
GluR1	45 mer	1893-1937	780	Keinänen et al. (1990)	X17184
GluR2	45 mer	2032-2076	795	Keinänen et al. (1990)	M85035
GRIP2	39 mer	2148-2186	987	Brückner et al. (1999)	AF072509
NSF	45 mer	76-120	416	BLAST sequence specificity	AF189019
Narp	48 mer	671-717	282	BLAST sequence specificity	S82649

Figure 2.2 Sequence and design of oligonucleotide probes

DNA sequence is shown in black from the 5' to the 3' region for each of GluR1 and GluR2 AMPA receptor subunits, as well as that for GRIP2, NSF and Narp. The antisense oligonucleotide is shown in red and the complementary base probes were highly selective for each target as determined by BLAST screening at NCBI. GluR1, GluR2 and GRIP2 probes were based on previous publications (Keinänen et al., 1990; Brückner et al., 1999), while the probes for NSF and Narp were generated using BLAST screening at NCBI, with high selectivity for NSF and Narp mRNA.

GluR1 (45 mer) mRNA; nucleotides 1893-1937 (Keinänen et al. 1990)

5'CACAGCGA AGAGTTTGAA GAGGGACGAG ACCAGACAAC CAGTGAC3'

3'GTCACTGG TTGTCTGGTC TCGTCCCTCT TCAAACTCTT CGCTGTG5'

GluR2 (45 mer) mRNA; nucleotides 2032-2076 (Keinänen et al., 1990)

5'CACACTGAG GAATTTGAAG ATGGAAGAGA AACACAAAGT AGTGAA3'

3'TTCACTACT TTGTGTTTCT CTTCCATCTT CAAATTCCTC AGTGTG5'

GRIP2 (39 mer) mRNA; nucleotides 2148-2186 (Brückner et al., 1999)

5'CAC CATCTCCGGT ACAGAGGAAC CTTTTGACCC CATCAT 3'

3'ATG ATGGGGTCAA AAGGTTCCTC TGTACCAGAG ATGGTG 5'

NSF (45 mer) mRNA; nucleotides 76-120

5' GAACG AAAAGGATTA CCAGTCTGGC CAGCATGTGA TGGTGAGGAC 3'

3' GTCCT CACCATCACA TGCTGGCCAG ACTGGTAATC CTTTTCGTTC 5'

Narp (48 mer) mRNA; nucleotides 671-717

5' GAAGACGAGA AGTCCCTGCT CCACAATGAG ACCTCGGCTC ACCGGCAG 3'

3' CTGCCGGTGA GCCGAGGTCT CATTGTGGAG CAGGGACTTC TCGTCTTC 5'

(ii) Tissue preparation

Neuropathic rats at the peak of behavioural reflex sensitivity and sham and age-matched controls (n=4 for each condition) were anaesthetised with a gaseous mixture of halothane and O_2, a laminectomy (L3-6) was performed, and the fresh spinal cord tissue was snap frozen in isopentane (-40 to –45°C) and mounted vertically (rostral end down) on a cryostat chuck with mounting medium (OCT, BDH, UK) and orientation for the ipsilateral side was noted. 10μm thick frozen transverse cryostat sections were taken and maintained at –18°C using a Cryotechnics Bright cryostat and thaw-mounted onto Polylysine ® microscope slides (BDH, UK). Tissue was stored at –70°C.

(iii) Probe labelling

All probes were labelled with deoxyadenosine α[^{35}S]-triphosphate ([^{35}S-dATP], specific activity <1250 Ci/mol; NEN Dupont) at their 3' ends using recombinant terminal deoxynucleotidyl transferase (rTdT) to yield a specific activity of approximately 2x10^6 cpm per sample in 100μl of hybridisation buffer. The reaction was carried out for 90 min at 37°C in an autoclaved eppendorf tube containing the following: x μl of the appropriate oligonucleotide probe (calculated to ensure 3x more ρmol [^{35}S]-dATP than oligonucleotide), 10μl of potassium cacodylate tailing buffer (TdT buffer), 4μl rTdT enzyme (15 units/μl), 4μl [^{35}S]-dATP (70ρmol; 1.5-2 x 10 Ci/mmol) made up to a final volume of 40μl DEPC H_2O. Prior to incubation the mixture was vortexed briefly then spun down (13,000 x g, 3 min). Following the initial incubation period, a further 2μl of [^{35}S]-dATP and 2μl of rTdT enzyme were added to the reaction mixture to optimise conditions, vortexed and incubated for a further 30 min after which the reaction was stopped by cooling on ice for 15 min. 2 x 1μl of pre-spun samples were taken.

The resultant labelled probe was separated from incorporated nucleotides by purification through a Nu-Clean D25 (Sepharose) disposable spun column and centrifuged for 4 min at 4,000 x g. Duplicate aliquots (2x1μl) of the pre- and post-

spun mixture were β-emission counted by liquid scintillation in 1ml of Optiphase scintillation cocktail to calculate the specific activity and percentage incorporation of radioactivity (all probes showed between 50-65% incorporation). The labelled probe was then stored at -70°C until required (for a maximum of 14 days).

(iv) Post-fixing

Slides were brought to room temperature and immediately fixed in 4% paraformaldehyde in PBS (0.1 M; pH 7.4) for 10 min, then rinsed in two washes of fresh PBS (0.1 M; pH 7.4) for 5 min each. Non-specific binding of the probe to the glass and tissue was reduced by treating the slides for 10 min in ethanolamine solution (0.1M TEA and 0.026M acetic anhydride). Subsequently, the sections were dehydrated through increasing concentrations of ethanol (50%, 70%, 80%, 90% and 100%), each buffered with ammonium acetate (0.3M) for 2 min each, with a final 2 min stage in 100% unbuffered ethanol. Slides were thoroughly dried for 1-2 hr prior to hybridisation.

(v) Hybridisation

Previously prepared stock solutions of hybridisation buffer and de-ionised formamide (stored at –20°C) were brought to room temperature, then aliquoted together to obtain a 1x hybridisation buffer/40% de-ionised formamide solution: dextran sulphate (10%; w/v), sodium chloride (600mM), Tris pH 7.6 (10mM), EDTA (1mM), Denhardt's solution (0.1%; w/v), salmon sperm DNA (0.01%; w/v), Baker's yeast tRNA (0.005%; w/v) glycogen (0.0005%; w/v) and formamide (40%; w/v). The radiolabelled probes were then added in a volume that gave a final count number of 2 x 10^6cpm/100µl hybridisation buffer. The resulting hybridisation mixture was heated to 60-70°C for 10 min, and then subsequently cooled on ice for 1 min before the reducing agent, dithiothreitol (DTT; 10mM), was added. This helped to protect the [^{35}S]-dATP from oxidation and ensured that the probe remained in a single-stranded state even after the solution had been cooled. 100µl of this final solution

was then carefully pipetted onto slides and a DEPC-treated coverslip was lowered gently onto the solution. Hybridisation was carried out in sealed containers containing 2 sheets of Whatman (No. 1) filter paper saturated with a solution of 50% de-ionised formamide: 50% 4x Standard saline citrate (SSC) solution, at 37°C for 18 hr.

(vi) Post-hybridisation washes

Following the overnight incubation, the coverslips were removed, slides were placed into racks and washed in decreasing concentrations of SSC solutions (2xSSC; 1xSSC; 0.5xSSC; pH 7) at 40°C for 2 hr each, to remove any excess hybridisation buffer solution and any non-specifically bound probe, and dehydrated through ascending concentrations of ethanol buffered with 0.3M ammonium acetate (50%, 70%, 80%, 90%, 100%) for 2 min each and lastly in 100% absolute ethanol for 2 min, before being left to air dry overnight. Slides were exposed to Hyperfilm β-max in a dark room and left to develop in a sealed autoradiographic cassette with intensifying screen for approximately 10 days at 4°C. The film was then developed using a standard X-ray Film developing machine (X-Omatic, MRC Membrane and Adapter Proteins Co-Op, Division of Biomedical and Clinical Laboratory Sciences, Edinburgh). The intensity of the latent image was used as an indicator for the length of slide exposure to autoradiographic emulsion that was required prior to final developing.

(vii) Emulsion coating

Under darkroom conditions, the dried slides were dipped in 20ml (1:10 diluted with dH_2O) of Ilford K5 liquid autoradiographic emulsion at 43°C for approximately 5 seconds, blotted lightly then left to dry in an upright position overnight in the dark before being sealed in light-tight Kartell boxes containing silica gel desiccant, wrapped in black plastic and stored at 4°C for 6-12 weeks, depending on the intensity of the autoradiographic image developed previously.

(viii) Developing and staining

Following the assigned exposure time, slides were brought to room temperature, and the exposed silver grains were developed under safe-light conditions at 15°C in Kodak D-19 developer for 4 min, rinsed in distilled water for 30 sec, then fixed in Ilford Hypam K5 fixer (diluted 1:5 (v/v) with distilled water) for 5 min. All traces of fixer were removed with excess washing in dH_2O. Slides were lightly counter-stained with Mayer's haematoxylin (4 min) and 5% eosin (2-3 sec), with distilled water washes between each stain, before being dehydrated through 50%, 70%, 90% and 100% ethanol (2 min each). The slides were then placed in fresh xylene solution (2 min) and finally mounted in DePeX mounting medium.

(ix) Controls

Data for each rat were obtained from a number of parallel assays to minimise experimental variation, whereby hybridisations using coronal brain sections (where expression for each probe has been documented) acted as positive controls to verify the sensitivity of the ISHH methodology. Controls used to demonstrate specificity of the respective oligonucleotide consisted of (1) pre-treating sections with RNase A (1 mg/ml; Sigma, Poole, UK) for 1 hr prior to hybridisation and (2) co-incubation of the [^{35}S]-labelled oligonucleotide in the hybridisation medium with a 100-fold excess of unlabelled oligonucleotide.

(x) Analysis

-Cell counts

The number of cells positively hybridised for each probe within lateral and mediolateral locations of laminae I-V was calculated at x40 magnification (total grid area 175 x 175 μm). Cells were considered to be positively labelled if the silver grains showed a dense pattern around the nucleus and were 5-fold denser than a typical non-expressing cell within the same field area or background levels. The total number of positively hybridised cells was determined for each spinal cord section,

(n=5 sections) and these values were used to calculate the mean number of positively hybridised cells per unit area in the lumbar spinal segments L3-6 (neuropathic, n=4; sham-operated, n=4; naïve, n=4).

-Silver grain density

To assess any changes in the relative expression of mRNA following chronic constriction injury, the mean silver grain density per positively labelled cell was measured using '*Image 1.44*' software (Improvision, U.K.) with video input from a CCD camera (Sony, Japan) mounted on a Zeiss Axioscope microscope (x40 magnification). For each section, counts were made both ipsilateral and contralateral to the nerve injury in lateral and mediolateral zones. A minimum of five positively hybridised cells was counted in each region and a pixel count was obtained, which was converted to a silver grain number via a pre-determined calibration procedure. The mean number of silver grains per cell was calculated for each section (n=5 sections) and was compared using a Student's t-test.

2.3.2 Immunoprecipitation of the AMPA receptor subunits

Due to resultant smaller samples achieved with immunoprecipitation, the PhastSystem was used for all immunoprecipitations, as it requires less sample loading. Immunoprecipitation (IP) was achieved using a method adapted from Schopperle et al. (1998).

(i) Tissue preparation

A laminectomy was performed on anaesthetised rats and the spinal cord was hemisected to separate contralateral from ipsilateral sides following CCI or following the application of AMPA (50μM) or saline vehicle, that were applied in a volume of 500μl for 15 min before rapid removal to cold buffer on ice. This was then immediately gently homogenised in a hand–held homogeniser containing freshly prepared 2.0ml IP buffer (PBS pH 7.5, 1% CHAPS, 0.75% sodium deoxycholate, 2μg/ml aprotinin, 4μg/ml leupeptin, 1mM AEBSF, 2μg/ml pepstatin, 1mM vanadate, 1mM sodium fluoride, 5mM sodium molybdate and soya bean trypsin inhibitor (50μg/ml)). The homogenate was transferred into eppendorf tubes and incubated (with rolling) at 4°C for 1 hr. The samples were then centrifuged at 12,000 x g for 15min at 4°C to remove particulate material.

(ii) Protein estimation

The bicinchoninic acid (BCA) Protein Assay Reagent Kit (Pierce) was used to quantify protein concentrations between samples. This is based on the affinity of BCA for Cu^{2+}, produced by protein reacting with Cu^{2+} in an alkaline medium. The reaction produces a purple precipitate that exhibits absorbance at 540nm and was carried out in MaxiSorb 96-well microtitre plates (NUNC). Aliquots of 200μl of the reaction mix were added to the wells followed by the addition of 10μl of sample, according to manufacturer's supplied protocol. Absorbance at 540nm was measured using a SpectraMax 250 microtitre plate reader. Known concentrations of bovine serum albumin were used to create a standard curve, and the average protein concentration was calculated from this.

(iii) Immunoprecipitation of GluR2

Supernatants were pre-cleared with Protein G-Sepharose 4B fast flow (Sigma-Aldrich Co Ltd, UK) (20µl/ml) (1:1 beads:IP buffer) for 45 min at 4°C. The following two controls were processed in parallel: (1) IP buffer replaced the sample supernatant and (2) the GluR2 antibody was replaced with normal immune mouse serum. After a pulse spin to concentrate the beads (Eppendorf microfuge, 10 sec, 13, 000 x g) the supernatant was removed to another Eppendorf tube containing a mouse monoclonal GluR2 antibody (0.5µg/ml diluted to 1:50) (BD, UK). The antibody and Protein G-Sepharose (1:1) 40µl/ml were pre-incubated together ~1 hr before addition of supernatant and the mix left overnight (with rolling) at 4°C. The beads were pulse spun, washed once in IP buffer and twice in PBS before 40µl of x2 Laemmli buffer was added per ml of original supernatant. Western blots were performed on the resulting samples to detect immunoprecipitated and co-immunoprecipitated proteins.

(iv) Immunoblotting for GluR2-interacting proteins

The IP pellets previously resuspended in 2x Laemmli buffer (2% sodium dodecyl sulphate (SDS), 20 mM Tris, 5% mercaptoethanol) were boiled for 5 min. SDS-PAGE was carried out on pre-cast 7.5% SDS polyacrylamide gels followed by electroblotting on to polyvinylidene fluoride membrane (ImmobilonP^{SQ}), (Millipore UK Ltd.) using the PhastSystem (Amersham Biotech, Ltd.). Before immunoblotting was carried out, blots were temporarily stained with PhastGel Blue R (Amersham Biotech UK Ltd) to check that protein loading of the lanes was even.

The blots were blocked with 5% Marvel in PBS to reduce non-specific background. Immuno-detection was carried out as described previously (Johnson et al., 2000) using a rabbit polyclonal antibody to GluR2 or GluR1 receptor (0.1µl/ml diluted to 1:100; Chemicon International Ltd.) followed by pre-absorbed HRP-conjugated anti-rabbit secondary antibody (Chemicon International Ltd.). Visualisation of antibody bands was carried out using Luminol (NEB, UK Ltd.) followed by exposure of the blots to ECL film (Amersham Biotech UK Ltd.).

For GluR2 immunoprecipitations, the blots were stripped ("Re-Blot" reagent, Chemicon International Ltd.) and re-probed with either a mouse monoclonal antibody to GRIP (250μg/ml diluted 1:500; Transduction Labs, UK Ltd.) or a rabbit polyclonal antibody to PICK1 (200μg/m diluted 1:75; Santa Cruz Biotechnology Inc.).

(v) Immunoprecipitation for phospho-GluR1

Hemisected spinal cords from rats at the peak of neuropathic behavioural sensitivity were homogenised at 4°C in 20mM Na Hepes, pH 7.5, with 5% glycerol, 1mM EGTA, 1mM DTT, 1mM AEBSF, 2μg/ml aproptinin, 10μg/ml leupeptin, 2μg/ml pepstatin, 50μg/ml SBTI, 25mM Na β-glycerophosphate, 1mM Na-orthovanadate, 1mM NaF, 1μM calyculin A, 1μM cypermethrin. The extract (0.5 ml) was incubated for 1 hr on ice and clarified by centrifugation at 13, 000 x g for 1 hr at 4°C. The clarified supernatant was incubated for 4 hr at 4°C with 3.5 μg/ml of rabbit anti-GluR1 IgG, (UBI) before precipitation with Protein G Sepharose CL-4B (15μl) and the samples were kept under constant agitation overnight at 4°C. Samples were washed five times with 0.5 ml cold extraction buffer before solubilisation in Laemmli buffer. Protein samples were subjected to reducing SDS-PAGE and transferred to PVDF membrane at 4°C for 90 min at 75 V in 10% (v/v) methanol, 10 mM CAPS pH 11.0. Blots were probed with pan-GluR1 (UBI, 1:100), phospho-Ser^{831}-GluR1 and phospho-Ser^{845}-GluR1 antibodies (UBI, 1:100). Signal detection was carried out using a pre-absorbed rabbit HRP-conjugate (1:5,000, Chemicon) secondary antibody enhanced chemiluminescence.

2.4: Methods specific to Chapter 4

2.4.1 β-galactosidase staining in heterozygous PSD-95 mutant mice

(i) Perfusion

Heterozygous PSD-95 mutant mice (n=3, naïve) were deeply anaesthetised with halothane until breathing had ceased but cardiovascular function was still evident. An incision into the thoracic cavity was made, the heart was exposed and a 25.1G needle was inserted transcardially. Initially, heparinised saline (0.9% NaCl/ 0.25% (v/v) heparin) was infused before perfusion with 4% paraformaldehyde in 0.1M PBS for 5min. A laminectomy was performed and the spinal cord, DRG, sciatic nerve and brain were dissected out and placed in ascending concentrations of sucrose in PBS at 4°C (5%, 30min; 10%, 2 hr; 25%, overnight). Following snap freezing in isopentane at –40°C, tissue samples were mounted on a cryostat chuck (spinal cord mounted vertically with rostral end down or in longitudinal orientation, and transverse sections for all other tissues) and embedded in OCT (BDH). 10μm thick cryostat sections were cut at –22°C, thaw mounted onto Polylysine ® microscope slides and stored at –70°C overnight.

(ii) Solutions

Detergent wash	β-galactosidase stain
0.1M PBS	0.1M Detergent wash
0.041% (v/v) MgCl	0.05% (w/v) potassium ferrocyanide
0.01% (w/v) Na-deoxycholate	0.05% (w/v) potassium ferricyanide
0.02% (v/v) NP40	0.01% (w/v) X-Gal in DMF

(iii) Tissue staining

Slides were placed in small plastic slide holders (10ml capacity) to minimise reagent usage and 7ml of the detergent wash was gently pipetted onto the back end of the slides and placed on ice for 15 min. The excess was poured off and the wash was repeated (3x15 min). Sections were then rinsed with 0.1M PBS/2mM $MgCl_2$ for 10 min at 4°C. This was poured off and 7ml of the stain solution was added and slides were incubated in the dark at 37°C for 4-6 hr. Slides were then washed with 0.1M PBS/2mM $MgCl_2$ at room temperature (2x5 min), dH_2O (10 min), dehydrated in 50, 70, 100% of ethanol for 5 min each, placed in xylene (2x5 min) and coverslipped with Pertex. Slides were stored under darkroom conditions before viewing under a microscope.

(iv) Light microscopy

Positively stained sections were viewed under a Zeiss Axioscope microscope at x40 magnification to qualitatively determine the presence and location of β-galactosidase positive regions and photographs were taken.

2.4.2 Molecular composition of NMDA receptor complexes in spinal cord

To determine the presence of a basic PSD-95: NMDA receptor complex in the spinal cord, a laminectomy was performed on deeply anaesthetised wild-type mice (n=4) and whole spinal cord was homogenised at 4°C in 50 mM Tris pH 9.0, with 1% Na deoxycholate, 50 mM NaF, 20μM $ZnCl_2$, 1mM Na-orthovanadate, 0.5 mM PMSF, 2 μg/ml aprotinin and 2 μg/ml leupeptin. The extract (0.5 ml) was incubated for 1 hr on ice and clarified by centrifugation at 13, 000 x g for 1 hr at 4°C. As described previously (Husi et al., 2000), MAP-NR1 IgG, PSD-95 IgG, NR2A IgG or NR2B IgG were incubated with extract for 4 hr at 4°C. Protein G-Sepharose (15 μl) was subsequently added and the samples were kept under constant agitation overnight at 4°C. Alternatively, an affinity reagent based on the C-terminal 6 amino acids of NR2B (SIESDV; 'pep6', Husi et al., 2000) was used directly. Samples were washed

five times with 0.5 ml cold extraction buffer before solubilisation in Laemmli buffer. Protein samples were subjected to reducing SDS-PAGE and transferred to PVDF membrane at 4°C for 90 min at 75 V in 10% (v/v) methanol, 10 mM CAPS pH 11.0. Primary antibodies used to probe blots were as described previously (Husi et al., 2000) and signal detection was carried out using peroxidase-linked secondary antibody enhanced chemiluminescence.

2.4.3 Light microscopy to examine myelinated fibres in the sciatic nerve

(i) Perfusion

PSD-95 mutant mice and matched wild-type littermates (n=3, naïve; n=3 CCI, in each case) were deeply anaesthetised with Sagatal (dose) and perfused transcardially initially with heparinised saline before being perfused with 4% paraformaldehyde in 0.1M PBS for 5 min (see section 2.4.1 (*i*)).

(ii) Analysis

1µm resin-embedded transverse (Reichert Ultracut UCT ultramicrotome) sections of the tibial branch distal to CCI were stained with toluidine blue and examined using '*Image 1.44*' software (NIH). The cross-sectional area of the tibial nerve was measured at x100 magnification in 5 randomly generated regions on each nerve section, which were chosen using a 4x4 grid. For analysis, 30 myelinated fibres closest to the centre of the screen were selected and the axon areas, external areas, and G ratios (axon diameter/ external diameter) were measured to quantify myelin thickness (adapted from method used by Coggeshall et al., 1993; see Fig. 2.3).

2.4.4 Electron microscopy to examine unmyelinated fibres in the sciatic nerve

(i) Perfusion

PSD-95 mutant mice and matched wild-type littermates (n=3, naïve; n= 3 CCI, in each case) were deeply anaesthetised with halothane and perfused transcardially

initially with heparinised saline, as above, before being perfused with 2.5% gluteraldehyde, 2% paraformaldehyde, 0.1M Na^+ cacodylate buffer, pH 7.3, 1mM $CaCl_2$ for 5 min. Sciatic nerve distal to CCI was removed and fixed for 2 hr in the same fixative, post-fixed in OsO_4 and embedded in araldite. Ultra-thin 80nm transverse sections were stained with uranyl acetate and lead citrate, mounted onto copper slot grids and examined in a transmission electron microscope (Phillips BioTwin Electron Microscope).

(ii) Analysis

25 random areas were photographed at x2300 magnification and then printed at a final magnification of x5750, which was used to count all the myelinated and unmyelinated fibres. For analysis, five negatives were chosen at random and scanned using a flat bed scanner for computer analysis using '*Image 1.44*' (see Fig. 2.3). The axon diameters/areas of 30 unmyelinated C-fibres were measured from each of the photomicrographs, the fibres being selected from clusters consisting solely of unmyelinated fibres.

Figure 2.3 Morphological analysis of the sciatic nerve

(a) Light microscopy analysis of myelinated fibres

(i) Shows the tibial branch of a toluidine-stained transverse section of the sciatic nerve with a total area of 96058mm^2.

(ii) Illustrates the grid used for random and unbiased selection of regions of the nerve to be analysed.

(iii) Computer-captured image of tibial nerve at x100 (oil immersion) magnification.

(iv) Image analysis threshold of the same region of nerve shown in (iii) from which axon diameters, external diameters, and G ratios were measured.

(b) Electron microscopy analysis of unmyelinated C-fibres

(i) Photomicrograph selected for C-fibre cluster analysis.

(ii) Computer-generated threshold of the fibres represented in (i).

a

(i)

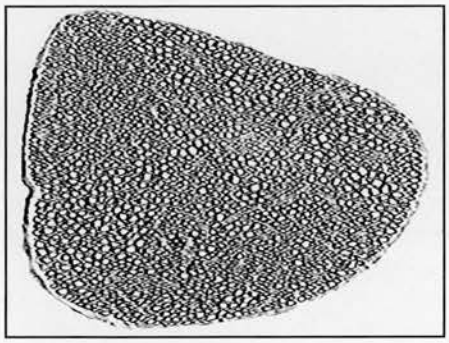

(ii)

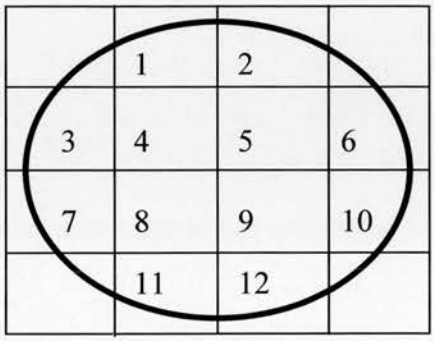

(iii)

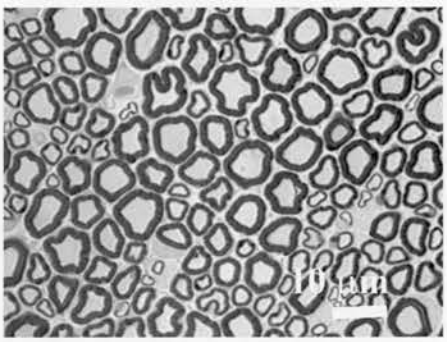

(iv)

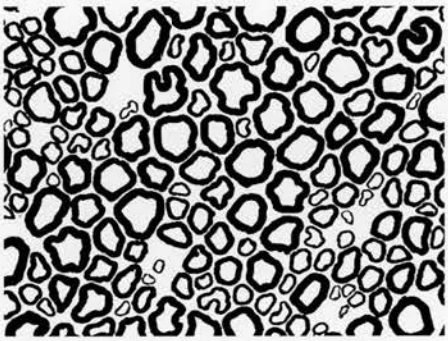

b

(i)

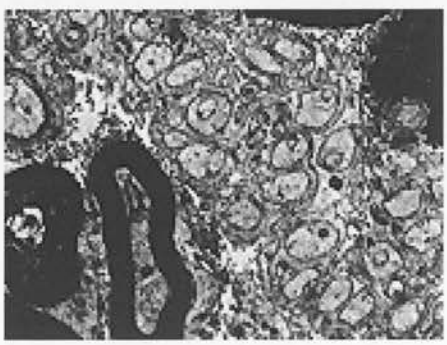

(ii)

2.4.5 *Ex vivo* CaMKII activity assays

Spinal cord tissue was rapidly homogenised in buffer with protease/phosphatase inhibitors, solubilised with CHAPS and cleared prior to immunoprecipitation of CaMKII with mouse monoclonal IgG/Protein G Sepharose. [^{33}P] phosphotransferase activity of immunoprecipitates was measured using autocamtide-2 as a substrate and conventional separation by phosphocellulose binding. The protein content of the original homogenate was determined by the Coomassie binding method (see section 2.3.2 (*ii*)).

Following lumbar L3-6 laminectomy under anaesthesia, PSD-95 mutant (naïve, n=3; CCI, n=4) and wild-type mice (naïve, n=3; CCI, n=4) were treated by topical application of agents to the dorsal surface of the spinal cord. NMDA (500 μM) with the co-agonist glycine (100 μM), ionomycin (10 μM), (R)-CPP (10 μM) or saline vehicle were applied in a volume of 500μl for 15 min before rapid removal to cold buffer on ice. Constitutive (autophosphorylated) and Ca^{2+}/calmodulin-elicited activity of CaMKII (Hanson et al., 1989; Jones and Persaud, 1998) were measured by the following procedure. Samples were rapidly homogenised on ice in 20 mM Na HEPES pH 7.5 with 5% glycerol, 1mM EGTA, 1mM dithiothreitol, 1mM AEBSF (4-(2-aminoethyl) benzene sulphonyl fluoride), 2 μg/ml^{-1} aprotinin, 10 μg/ml leupeptin, 2 μg/ml pepstatin, 50 μg/ml soybean trypsin inhibitor, 25 mM Na β-glycerophosphate, 1mM Na-orthovanadate, 1mM NaF, 1 μM calyculin A, 1 μM cypermethrin. Following a 30 min incubation on ice with 0.25% CHAPS (3-([3-cholamidopropyl] dimethylammonio)-1-propanesulphonate) and clarification, samples were incubated at 4°C for 2 hr with 3 μg/ml mouse anti-α-CaMKII IgG (clone CBα-2; Zymed) and then with excess Protein G-Sepharose for 1 hr. Aliquots of washed immunoprecipitates were incubated for 20 min at 30°C (linear range of assay) with 50 μM autocamtide-2, 50 μM ATP (with [^{33}P]γ-ATP to 0.25 μCi/tube), 10 mM $MgCl_2$ and 8 μg/ml purified bovine calmodulin, in the presence of 0.5 μM PKC-α_{19-31} and 0.5 μM PKI_{6-22} amide (to suppress any PKC and PKA-mediated activity, respectively) before termination with cold TCA (to 10% w/v), centrifugation and spotting of the supernatant onto P81 phospho-cellulose paper (Whatman).

Samples were washed extensively in 75 mM H_3PO_4 and dried before scintillation counting. Constitutive and maximal Ca^{2+}-evoked activity was measured in the absence and presence of 2 mM $CaCl_2$, respectively. Zero time and substrate-free blanks were less than 2% of maximal activity. Parallel immunoblotting experiments were attempted with phospho-specific antisera for Thr^{286}-CaMKII (the key autophosphorylation site), but gave insufficient signal: noise ratios for further use.

2.4.6 Immunoblotting for phospho-NR1

Spinal cord samples were initially homogenised in the buffer as for CaMKII assays (without CHAPS) and a membrane fraction was prepared. This was solubilised in 1% deoxycholate-containing buffer for 1 hr at 4°C and then the clarified supernatant was incubated for 4 hr at 4°C with 3.5 µg/ml of goat anti-NR1 IgG, (SC-1467, Santa Cruz) before precipitation with Protein G-Sepharose CL-4B for 1 hr at 4°C. After washing, bead-attached proteins were solubilised in Laemmli buffer prior to SDS-PAGE separation and transfer on to Immobilon P (Millipore) membranes and detection by peroxidase-linked secondary antibody enhanced chemiluminescence (ECL).

Blots were probed with pan-NR1 (Chemicon, 1:100), phospho-Ser^{897}-NR1 and phospho-Ser^{896}-NR1 antibodies (Upstate Biotech, 1:100). Mean relative phospho-Ser^{897}-NR1:pan-NR1 immunoreactivity ratios were calculated in each case.

CHAPTER 3: A role for the AMPA receptor and its interacting proteins in neuropathic pain behaviour

3.1: Introduction

As mentioned in the general introduction, the AMPA receptor comprises four main subunits, GluR1-4. The GluR2/3 subunits of AMPA receptors have received particular attention due to the identification of a number of intracellular proteins found to interact with the extreme intracellular C-terminus of these subunits to provide a mechanism for clustering receptors in the plasma membrane and to direct kinases and phosphatases to their sites of action (O'Brien, Lau and Huganir, 1998; Scannevin and Huganir, 2000).

GluR2/3 subunits of AMPA receptor have a consensus PDZ binding motif (IESVKI) in their extreme C-terminus which interacts with several proteins including GRIP1, (Glutamate Receptor Interacting Protein 1) (Dong et al., 1997), ABP (AMPA receptor Binding Protein) and its splice variant, ABP-L (also called GRIP2) (Srivastava et al., 1998; Brückner et al., 1999; Dong et al., 1999a; Wyszynski et al., 1999) and PICK1 (Protein Interacting with C Kinase 1) (Xia et al., 1999; Dev et al., 1999). NSF (*N*-ethylmaleimide-Sensitive Fusion protein) interacts with a different site on the GluR2 C-terminus (VAKNAQ). These interacting proteins may be involved in trafficking the receptor from the cell body to synapses, play a role in AMPA receptor stabilisation at the synaptic plasma membrane and possibly link the receptor to downstream signalling pathways (Torres et al., 1998; Ye et al., 2000). The GluR2 C-terminal 5 residues represent the interaction site for GRIP, ABP and PICK1 and are also thought to be essential for AMPA receptor stabilisation at the synaptic plasma membrane (see Fig. 3.1 for summary).

3.1.1 Glutamate receptor interacting protein (GRIP) family

The first protein described to interact with AMPA receptors was isolated in yeast 2-hybrid screens by Dong et al. (1997) and named GRIP (Glutamate Receptor Interacting Protein, now termed GRIP1) characterised as containing seven PDZ domains. Several splice variants have since been identified and are known as ABP (AMPA receptor Binding Protein), a shorter splice variant of GRIP1 and ABP-L/GRIP2 (hereafter referred to as GRIP2). There is a 68% homology between GRIP1 and GRIP2 (Wyszynski et al., 1999).

The 4th and 5th PDZ domains of GRIP1 and GRIP2 and the 4th 5th and 6th PDZ domains of ABP interact with the consensus motif 'IESVKI' specific to the GluR2/3 subunit C-termini. Although enriched in the PSD at synapses, a large proportion of GRIP appears to be cytosolic (Wyszynski et al., 1998) and located in post-Golgi vesicles suggesting that GRIP may be involved in AMPA receptor transport to the plasma membrane and perhaps also its localisation in dendrites (Dong et al., 1999). The interaction between GluR2 and GRIP is crucial for precise apposition of GluR2 at the postsynaptic membrane (Dong et al., 1997).

The splice variants of GRIP differ in their developmental regulation and expression profiles. Although GRIP1 co-localises with AMPA receptors at excitatory synapses, it has also been localised at synapses presynaptically positive for GAD (a marker of GABAergic input) suggesting that GRIP may well have additional AMPA-independent functions (Wyszynski et al., 1999). Both GRIP1 and GRIP2 are expressed in the spinal cord but the precise localisation has not been documented and GRIP2 is believed to be the predominant form expressed in adult nervous system (Dong et al., 1999b; Brückner et al., 1999).

3.1.2 PICK1

PKC phosphorylation of Serine residue 880 (IESVKI) in the GluR2 C-terminus prevents GRIP binding and so is suggestive of a potential role for protein phosphorylation in the regulation of the GluR2:GRIP interaction (Matsuda et al.,

1999). Since AMPA receptors are regulated by PKC phosphorylation, PICK1, a PDZ domain-containing protein that docks both GluR2/3-containing AMPA receptors and PKCα, may mediate this regulation. PICK1, originally identified by its interaction with PKCα, interacts with the same motif in the C-terminus of GluR2/3 as GRIP, although the site of interaction of GluR2 and PKCα on PICK1 is different, suggesting that PICK1 can bind both GluR2 and PKCα at the same time (Xia et al., 1999; Dev et al., 1999). PICK1 itself is an efficient substrate for PKC phosphorylation both in vitro and in vivo and can induce GluR2 clustering on the plasma membrane through interaction of the receptor C-terminus with the PDZ domain of PICK1 (Staudinger, Lu and Olsen, 1997).

PICK1 may function to localise activated PKCα to the plasma membrane and so bring the kinase in proximity with specific substrates, including the AMPA receptor (Staudinger, Lu and Olsen, 1997). Indeed, the co-expression of PICK1 and GluR2 results in both proteins being much more closely localised in their intracellular distribution (Xia et al., 1999). PKC activation in neurones increases the phosphorylation of Ser^{880} on GluR2 and induces internalisation of the GluR2 subunits suggesting that the regulation of the GluR2 interaction with PDZ proteins by phosphorylation may modulate surface expression of AMPA receptors during synaptic plasticity (Chung et al., 2000). The presence and distribution of PICK1 in spinal cord has not been specifically documented.

In addition to interacting with PDZ domain-containing proteins such as GRIP and PICK1, the GluR2 subunit also interacts with proteins that do not have PDZ domains, such as NSF (N-ethylmaleimide-Sensitive Fusion protein) and Narp (Neuronal activity-regulated pentraxin).

3.1.3 *N*-ethylmaleimide-sensitive fusion protein (NSF)

NSF, a hexameric ATPase essential for various membrane fusion events, is enriched in the PSD and can form a protein complex with the AMPA receptor GluR2 C-terminus at a site distinct from the GRIP/ABP/PICK1 binding site (Osten et al.,

1998; Song et al., 1998). The function of this interaction, given the established role of NSF in vesicle cycling and fusion, may be in the insertion and/or stabilisation of AMPA receptors at the postsynaptic membrane and such a role may be important for surface expression of AMPA receptors in the postsynaptic membrane (Noel et al., 1999). NSF is expressed in the spinal cord and DRG although precise localisation has not been carried out (Püschel, O'Connor and Betz, 1994).

Infusion of an inhibitory peptide that blocks the NSF:GluR2 interaction in hippocampal neurones reduces AMPA receptor current magnitude and abundance at the synapse, and therefore the NSF binding region appears to be a functional domain of the C-terminus involved in receptor trafficking and/or stabilisation at the synapse (Song et al., 1998; Lüthi et al., 1999). The NSF:GluR2 interaction appears to be essential for the maintenance of stable synaptic excitatory currents in hippocampal neurones (Nishimune et al., 1998; Song et al., 1998) as well as surface expression of AMPA receptors (Noel et al., 1999).

3.1.4 Neuronal activity-regulated pentraxin (Narp)

Narp is an IEG, its mRNA is enriched in the brain and, like other IEGs, it is activity-regulated, and rapidly induced by seizure (Tsui et al., 1996; Reti and Baraban, 2000). Narp is thought to be completely extracellular and so it is present both pre-and post-synaptically. Although no direct interaction between Narp and the AMPA receptor has so far been elucidated in detail, Narp has been found in GluR1, 2 and 3 co-immunoprecipitations. Narp has no PDZ domains neither does it have access to the intracellular domains of the AMPA receptor so it is likely to interact with extracellular AMPA receptor domains. However, it is enriched at excitatory glutamatergic synapses and is reported to induce AMPA receptor clustering (Fong and Craig, 1999; O'Brien et al., 1999). Narp is expressed in the spinal cord, although its precise localisation has not so far been documented, and it may contribute to the clustering of GluR1 subunits in cultured spinal neurones where 73% of GluR1 clusters have associated Narp immunostaining (O'Brien et al., 1999).

3.1.5 GluR1 interactions

All of the above interactions occur at the GluR2/3 C-terminus but recent evidence suggests that the GluR1 subunit of AMPA receptor can bind to a PDZ domain containing protein known as SAP97 (Synapse Associated Protein 97), a member of the MAGUK family of proteins (which will be discussed in more detail in Chapter 4). SAP97 binds to the extreme C-terminus of GluR1 and does not appear to interact with GluR2/3 (Leonard et al., 1998). AMPA receptor complexes (in brain) contain SAP97 and SAP97 is closely associated with GluR1 in the plasma membrane and may be co-localised with AMPA receptors at postsynaptic sites (Leonard et al., 1998). There is little functional information relating to this interaction so far, but targeting of PKA to GluR1, which facilitates the phosphorylation of Ser^{845} in the GluR1 C-terminus, may occur via a SAP97: AKAP79/150 protein scaffold (Colledge et al., 2000, see Section 3.1.6).

Figure 3.1 Schematic representation of the GluR1 and GluR2 adapter proteins

This schematic diagram shows the AMPA receptor subunits GluR1 and GluR2 in the postsynaptic membrane. The C-terminus of the GluR1 subunit binds to SAP97 via a specific GluR1 C-terminal peptide 'SGMPLGATGL' (although the PDZ domain of SAP97 mediating this interaction is unknown). Narp, an extracellular protein, can cause clustering of GluR1 in particular, though a direct interaction between Narp and AMPA receptors has not been shown.

The C-terminal sequence IESVKI interacts with GRIP via PDZ4 and PDZ5 domains and with PICK1, via its single PDZ domain. NSF (a non-PDZ domain-containing protein) also interacts near the GluR2 C-terminus at an internal site distinct from that of GRIP/PICK1 binding, 'VAKNAQ'.

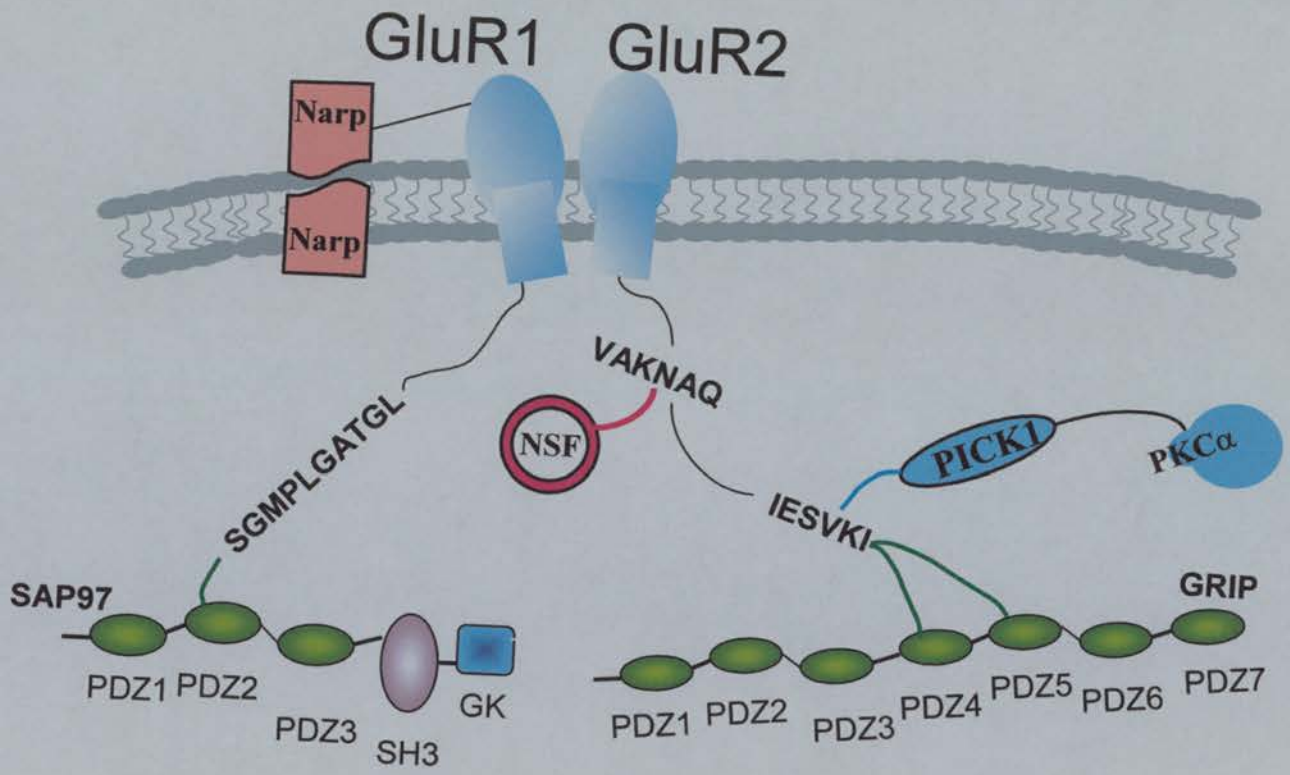
GluR1
GluR2
Narp
Narp
VAKNAQ
NSF
SGMPLGATGL
PICK1
PKCα
IESVKI
SAP97
GRIP
PDZ1 PDZ2
PDZ3
SH3
GK
PDZ1 PDZ2 PDZ3 PDZ4 PDZ5 PDZ6 PDZ7

3.1.6 AMPA receptor phosphorylation

AMPA receptors are modulated by phosphorylation and this may play a role in the expression of synaptic plasticity at central excitatory synapses. The GluR1 subunit phosphorylation sites have been identified (see below) and phosphorylation here may alter single channel properties of the AMPA receptor or act to convert a non-conducting (silent) receptor channel to a conducting (active) one. An increase in the responsiveness of postsynaptic AMPA receptors subsequent to Ca^{2+} influx has been proposed to induce LTP (Lee et al., 2000) and AMPA receptor phosphorylation by Ca^{2+}-activated protein kinases is believed to play a pivotal role in LTP expression (Lee et al., 2000).

The PKA (Ser^{845}) and CaMKII/PKC (Ser^{831}) phosphorylation sites located in the intracellular C-terminal domain of GluR1 have been identified (Roche et al., 1996; Mammen et al., 1997). Phosphorylation of Ser^{831} by CaMKII potentiates GluR1 current (Derkach, Barria and Soderling, 1999) while PKA activity at Ser^{845} increases AMPA responsiveness through a modulation of channel gating and channel open probability without affecting channel conductance (Banke et al., 2000).

AMPA receptors are constitutively phosphorylated (and therefore potentiated) by PKA owing to the specific targeting of PKA to the synapse by AKAP79/150 mediated by SAP97 (Rosenmund et al., 1994; Colledge et al., 2000). PKA localisation is required for the modulation of AMPA/kainate currents and AKAP: PKA interactions are important in the regulation of synaptically-activated AMPA channels. PKA has been associated with both LTP and LTD (Lee et al., 2000) and its phosphorylating activity increases when the kinase is targeted to the channel via a SAP97: AKAP79/150 complex. A mutation in the PDZ binding site in the tail of GluR1, which uncouples the receptor from SAP97, reduces the basal level of Ser^{845} phosphorylation. This is interesting given the recent evidence implicating a GluR1: PDZ domain interaction in the delivery of AMPA receptors into synapses (Colledge et al., 2000; Hayashi et al., 2000).

While PKA has been implicated as underlying both LTD and LTP, CaMKII phosphorylation appears to be essential for the induction of LTP. LTP induction or increased CaMKII activity induces delivery of AMPARs into synapses that is thought to require the predicted PDZ domain interaction motif but is not dependent on the GluR1 CaMKII phosphorylation site, Ser^{831} (Hayashi et al., 2000).

To date, evidence for the functional significance of proteins interacting with the C-terminus of GluR2 subunits is largely lacking. GluR1 subunit phosphorylation has, however, been implicated in synaptic plasticity in the hippocampus. Here, we addressed the possibility that interactions of these adapter proteins with the GluR2 subunit and phosphorylation of the GluR1 subunits may have a functional role in the establishment and/or maintenance of neuropathic pain.

3.2: Results

Chapter 2 (sections 2.2 and 2.3) contains the details of methods used in this chapter.

3.2.1 Intrathecal injection of AMPA receptor antagonists

The AMPA receptor is believed to play a role in both the acute and chronic sensitisation following afferent nerve damage. To examine the question of a role for the AMPA receptor in neuropathic pain conditions, we assessed the contribution of spinal AMPA receptors to CCI-induced (see Section 2.2.2 and 2.2.3, pgs. 56-60) changes in somatosensory behavioural reflexes by the local administration of the AMPA receptor antagonists, NBQX (Fig. 3.2 and 3.3), NS-257 (Fig. 3.5 and 3.6) and SYM 2206 (Fig. 3.8). Intrathecal injection of the AMPA/kainate receptor antagonist, NBQX, and the highly selective AMPA receptor antagonists, NS-257 and SYM 2206 (see Section 2.2.4 for intrathecal injections and Table 2.1 for drug details, pgs 60-63) in rats at the peak of behavioural reflex sensitivity attenuated the ipsilaterally sensitised behavioural measures of thermal hyperalgesia (Fig. 3.2, 3.5 and 3.8a, respectively). The AMPA receptor antagonists had similar but somewhat less marked effects on mechanical allodynia following CCI. NBQX significantly alleviated mechanical allodynia at all doses tested (Fig. 3.3), and the single dose of SYM 2206 had a similar affect (Fig. 3.8b). Intrathecal NS-257 significantly reversed the ipsilateral mechanical allodynia for the two highest doses used (Fig. 3.6b and c).

These antagonists differentially attenuated thermal and mechanical neuropathic reflexes, as all three antagonists had a significant though short lasting effect (~60 min) on thermal hyperalgesia while NBQX and SYM 2206 had a more pronounced effect at alleviating mechanical allodynia than did NS-257. The effects were dose-dependent, restricted to reflexes ipsilateral but not contralateral to nerve injury and none of the drugs had any detectable effect in naïve animals (Fig. 3.4, 3.7, and 3.9). At the highest doses used for NBQX and NS-257, there was variation in the baseline contralateral withdrawal responses, possibly indicative of ventral horn AMPA

receptors effecting motor co-ordination perhaps representing the possibility of side effects at these higher doses. Intrathecal injection of saline vehicle had no appreciable effect on thermal hyperalgesia or mechanical allodynia following CCI (Fig. 3.10a and b, respectively). These data indicate a key role for the AMPA receptor in the CNS in mediating nociceptive transmission following peripheral nerve damage.

Figure 3.2 Effects of the intrathecal administration of the AMPA receptor antagonist NBQX on thermal hyperalgesia in rats at the peak of neuropathic reflex sensitivity

Data represent the average hindlimb withdrawal latency ± SEM to a noxious thermal stimulus (n=6) for each time point following the intrathecal injection of 1.5nmol (a), 5nmol (b) or 13nmol (c) of NBQX.

Rats at the peak of ipsilateral thermal hyperalgesia, as determined by a significant reduction in ipsilateral paw withdrawal latency ('PWL') compared to contralateral withdrawal latency (*, $p<0.05$, Student's t-test), were intrathecally injected with NBQX (at arrow). 10 min following injection, 1.5nmol (a), 5nmol (b) or 13nmol (c) of NBQX significantly attenuated ipsilateral thermal hyperalgesia in comparison to pre-injection ipsilateral values (†, $p<0.05$, One-way ANOVA followed by a Dunnett's test), while there was no significant alteration in the pre-/post-injection contralateral responses. The duration of the drug effect varied in a dose-dependent manner, with 1.5nmol and 5nmol NBQX reversing the sensitisation of ipsilateral paw withdrawal for 30-50 min, whereas 13nmol NBQX had significant effects for up to 80 min, although variations in the contralateral withdrawal latency (c) indicate activation of ventral AMPA receptors which implies effects on motor co-ordination. As the drug effect wore off, ipsilateral PWL returned to baseline withdrawal latencies indicative of thermal hyperalgesia.

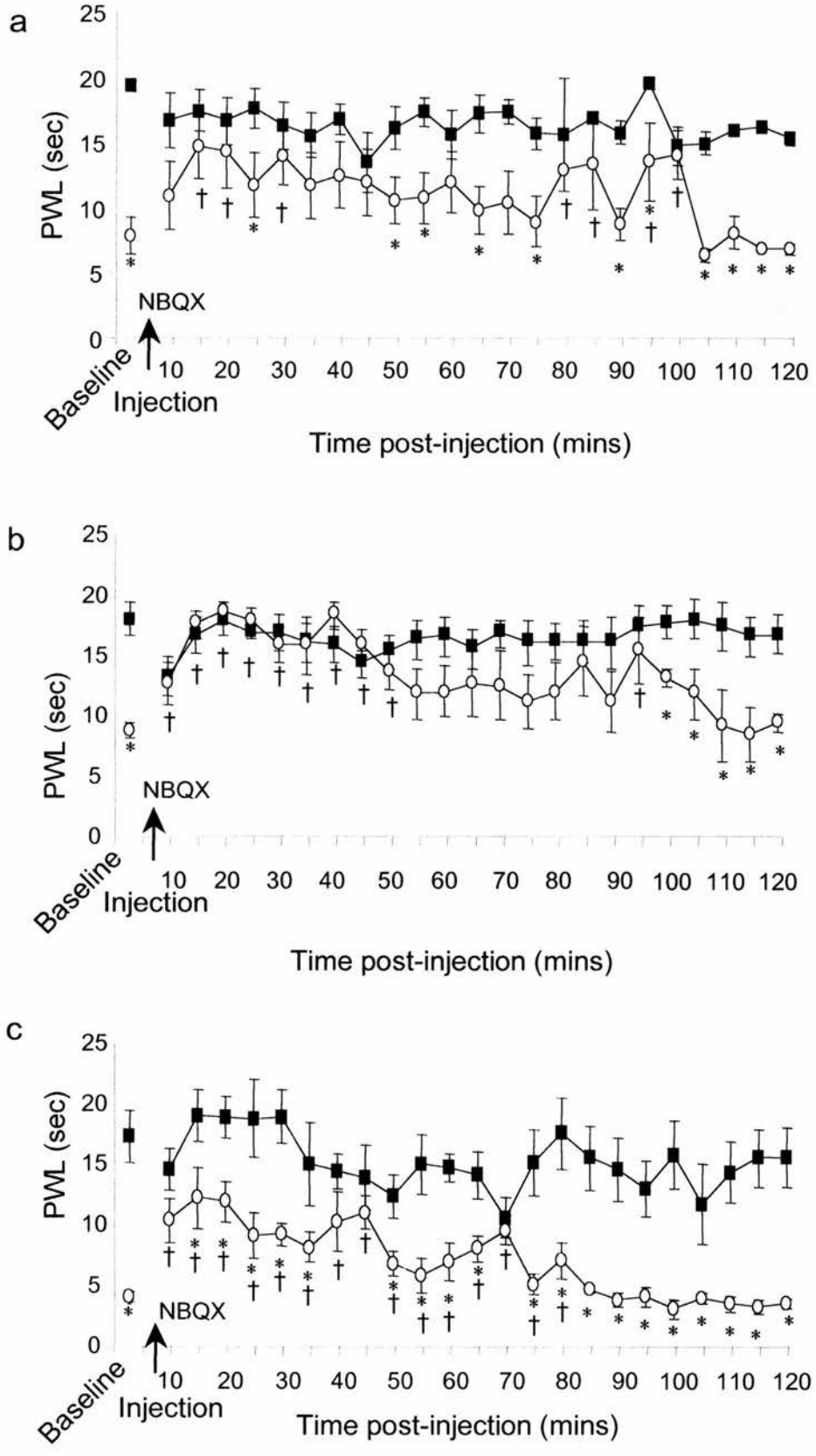
a
b
c
PWL (sec)
25
20
15
10
5
0
NBQX
Baseline
Injection
10 20 30 40 50 60 70 80 90 100 110 120
Time post-injection (mins)

Figure 3.3 Effects of the intrathecal administration of the AMPA receptor antagonist NBQX on mechanical allodynia in rats at the peak of neuropathic reflex sensitivity

Data represent the average hindlimb withdrawal threshold ± SEM to a normally innocuous mechanical stimulus (n=6) for each time point following the intrathecal injection of 1.5nmol (a), 5nmol (b) or 13nmol (c) of NBQX.

Rats at the peak of ipsilateral mechanical allodynia, as determined by a significant reduction in ipsilateral paw withdrawal threshold ('PWT') compared to contralateral withdrawal threshold (*, $p<0.05$, Mann-Whitney Rank Sum test), were intrathecally injected with NBQX (at arrow). 10 min following injection, 1.5nmol (a), 5nmol (b) or 13nmol (c) of NBQX significantly attenuated ipsilateral mechanical allodynia in comparison to pre-injection ipsilateral values (†, $p<0.05$, Kruskal-Wallis ANOVA followed by a Dunn's test), while there was no significant alteration in the pre-/post-injection contralateral responses. The duration of the drug effect was in the range of 45-50 min for all doses of NBQX tested. As the drug effect wore off, ipsilateral PWT returned to baseline withdrawal thresholds indicative of mechanical allodynia.

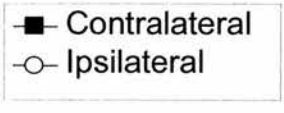

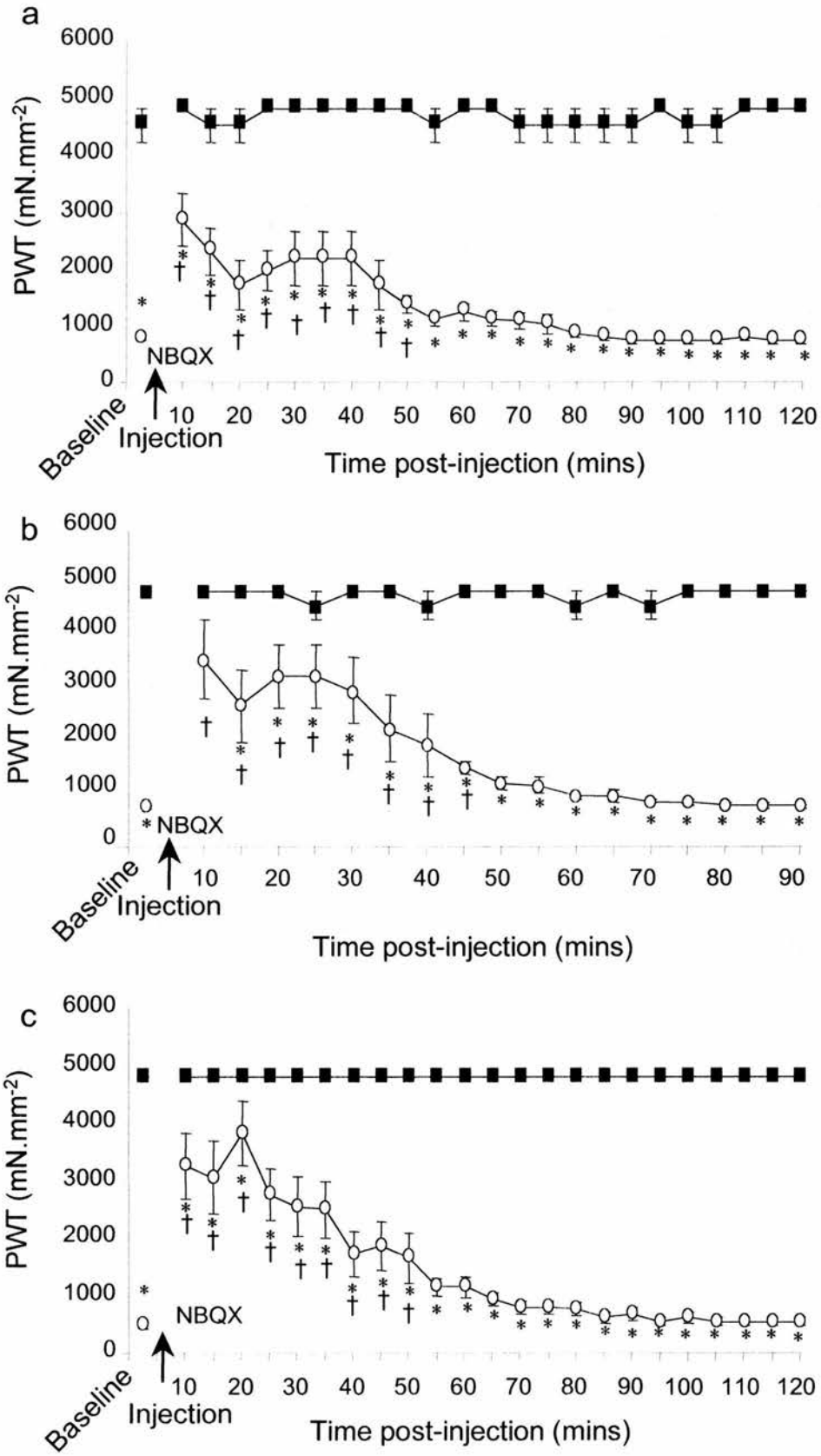
a
b
c
PWT (mN.mm-2)
6000
5000
4000
3000
2000
1000
0
NBQX
Baseline
Injection
10 20 30 40 50 60 70 80 90 100 110 120
Time post-injection (mins)
10 20 30 40 50 60 70 80 90

Figure 3.4 Effects of the intrathecal administration of the AMPA receptor antagonist NBQX in naïve rats

Data represent the average (a) hindlimb withdrawal latency to noxious heat and (b) withdrawal threshold to mechanical (von Frey filament) stimuli ± SEM for each time point in naïve, untreated rats (n=5) following the intrathecal injection of 5nmol NBQX.

There was no significant difference withdrawal latency (a) of either hindpaw in naïve rats when testing resumed 10 min following injection, except at the latest time points at 55-60 min where there was a significant reduction in PWL in both left and right hindpaws (†, $p<0.05$, One-way ANOVA followed by a Dunnett's test). The intrathecal injection of NBQX (arrow) had no appreciable effect on the withdrawal threshold in either hindlimb (b, Mann-Whitney Rank Sum test).

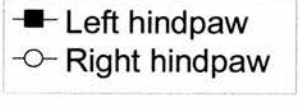

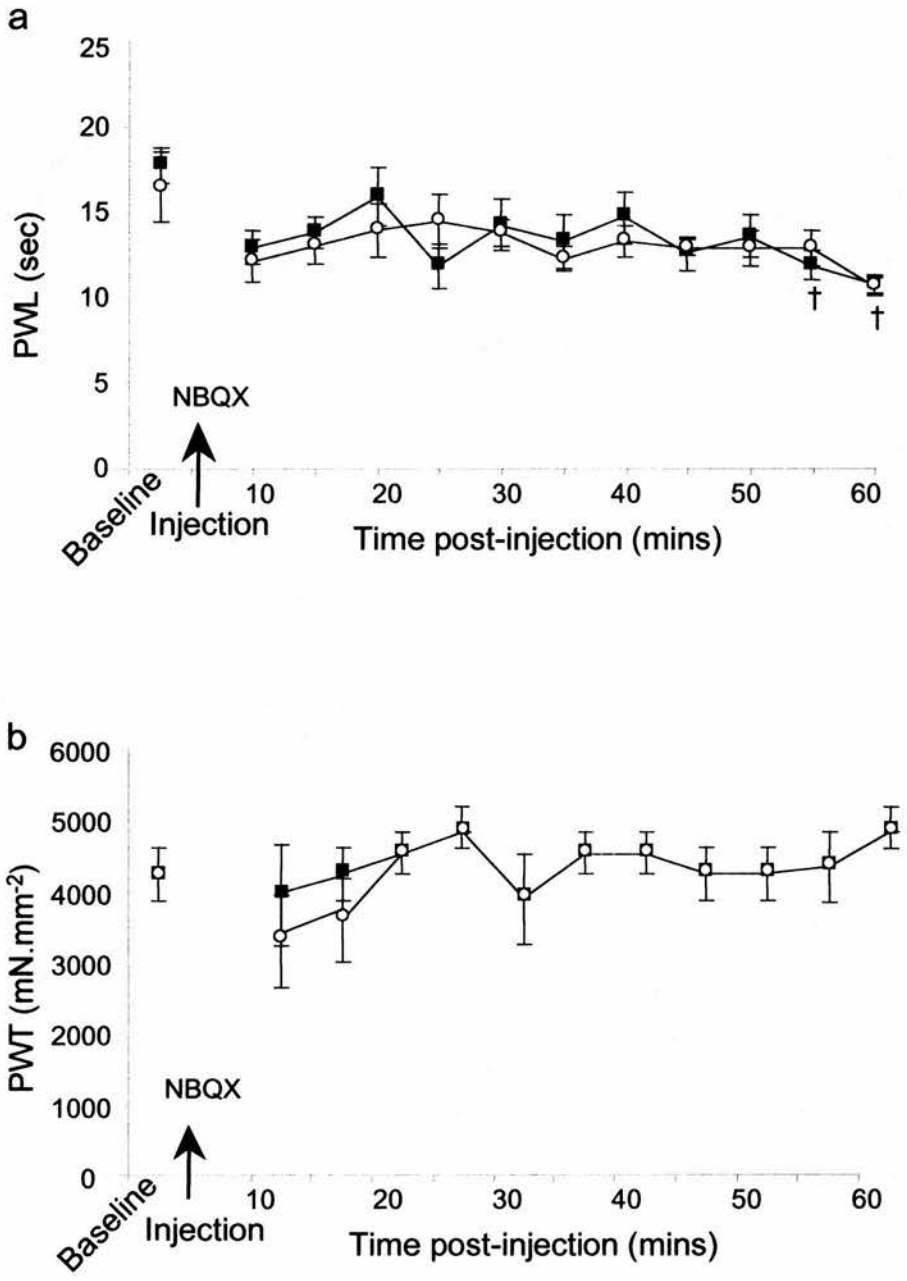
a
PWL (sec)
25
20
15
10
5
0
NBQX
Baseline
Injection
10
20
30
40
50
60
Time post-injection (mins)
†
†
b
PWT (mN.mm-2)
6000
5000
4000
3000
2000
1000
0
NBQX
Baseline
Injection
10
20
30
40
50
60
Time post-injection (mins)

Figure 3.5 Effects of the intrathecal administration of the selective AMPA receptor antagonist NS-257 on thermal hyperalgesia in rats at the peak of neuropathic reflex sensitivity

Data represent the average hindlimb withdrawal latency ± SEM to a noxious thermal stimulus (n=6) for each time point following the intrathecal injection of 28nmol (a), 83nmol (b) or 166nmol (c) of NS-257.

Rats at the peak of ipsilateral thermal hyperalgesia, as determined by a significant reduction in ipsilateral paw withdrawal latency ('PWL') compared to contralateral withdrawal latency (*, $p<0.05$ Student's t-test), were intrathecally injected with NS-257 (at arrow). 10 min following injection, 28nmol (a), 83nmol (b) or 166nmol (c) of NS-257 significantly attenuated ipsilateral thermal hyperalgesia in comparison to pre-injection ipsilateral values (†, $p<0.05$, One-way ANOVA followed by a Dunnett's test), while there was no significant alteration in the pre/post-injection contralateral responses. The duration of the drug effect varied in a dose-dependent manner, with 28nmol and 83nmol NS-257 reversing the sensitisation of ipsilateral paw withdrawal for 40-60 min, whereas 166nmol NS-257 had significant effects for up to 85 min, although variations in the contralateral withdrawal latency (c) indicate activation of ventral AMPA receptors which implies effects on motor co-ordination. As the drug effect wore off, ipsilateral PWL returned to baseline withdrawal latencies indicative of thermal hyperalgesia.

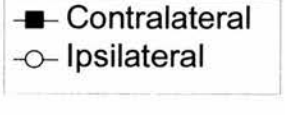

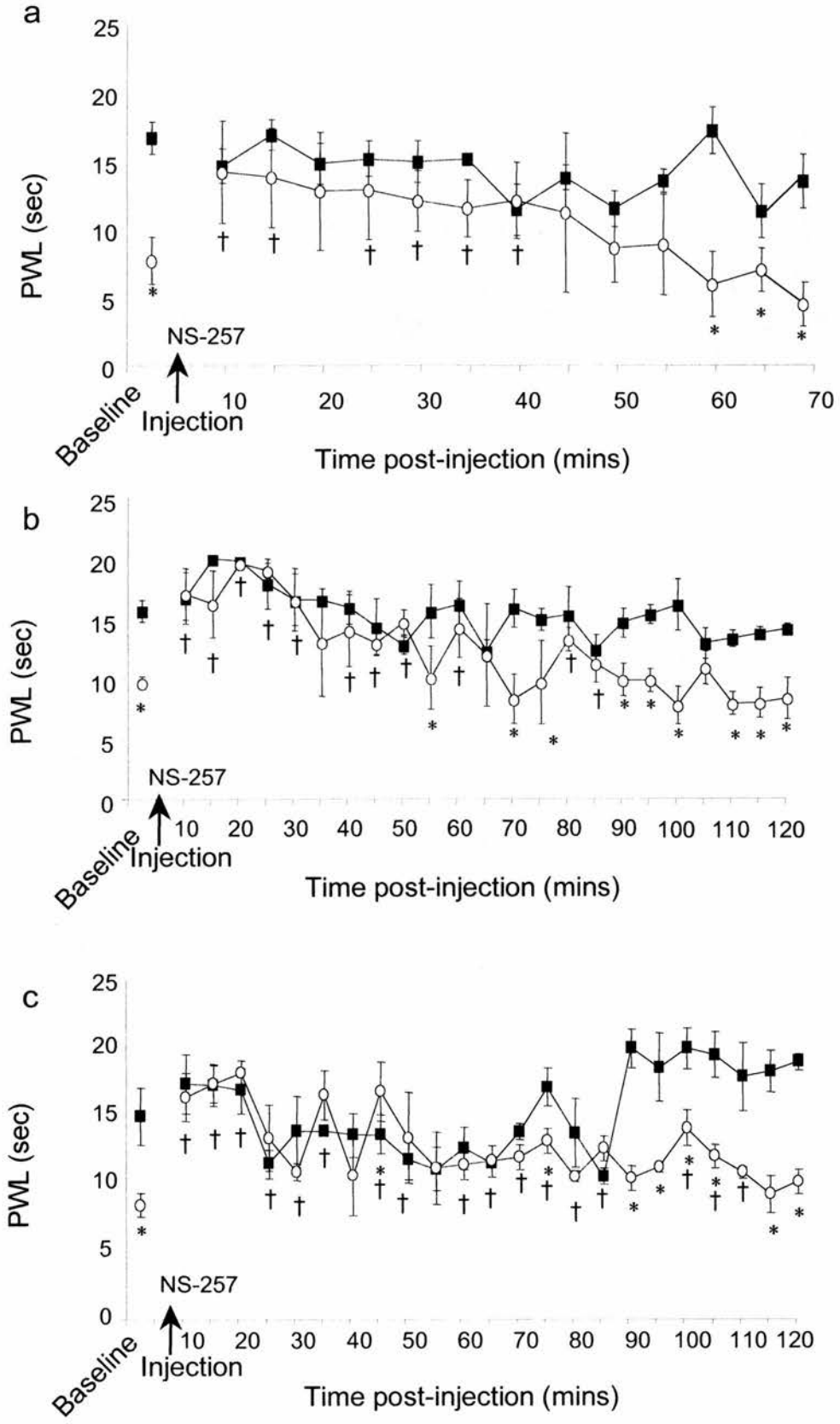
a
PWL (sec)
25
20
15
10
5
0
NS-257
Baseline
Injection
10
20
30
40
50
60
70
Time post-injection (mins)
b
PWL (sec)
25
20
15
10
5
0
NS-257
Baseline
Injection
10
20
30
40
50
60
70
80
90
100
110
120
Time post-injection (mins)
c
PWL (sec)
25
20
15
10
5
0
NS-257
Baseline
Injection
10
20
30
40
50
60
70
80
90
100
110
120
Time post-injection (mins)

Figure 3.6 Effects of the intrathecal administration of the selective AMPA receptor antagonist NS-257 on mechanical allodynia in rats at the peak of neuropathic reflex sensitivity

Data represent the average hindlimb withdrawal threshold ± SEM to a normally innocuous mechanical stimulus (n=6) for each time point following the intrathecal injection of 28nmol (a), 83nmol (b) or 166nmol (c) of NS-257.

Rats at the peak of ipsilateral mechanical allodynia, as determined by a significant reduction in ipsilateral paw withdrawal threshold ('PWT') compared to contralateral withdrawal threshold (*, $p<0.05$, Mann-Whitney Rank Sum test), were intrathecally injected with NS-257 (at arrow). 10 min following injection, 28nmol (a), 83nmol (b) or 166nmol (c) of NS-257 significantly attenuated ipsilateral mechanical allodynia in comparison to pre-injection ipsilateral values (†, $p<0.05$, Kruskal-Wallis ANOVA followed by a Dunn's test), while there was no significant alteration in the pre-/post-injection contralateral responses. The duration of the drug effect varied in a dose-dependent manner, as both 28nmol and 83nmol NS-257 reversed ipsilateral withdrawal only within the first 25-35 min, whereas 166nmol NS-257 had significant effects for up to 50 min. As the drug effect wore off, ipsilateral PWT returned to baseline withdrawal thresholds indicative of mechanical allodynia.

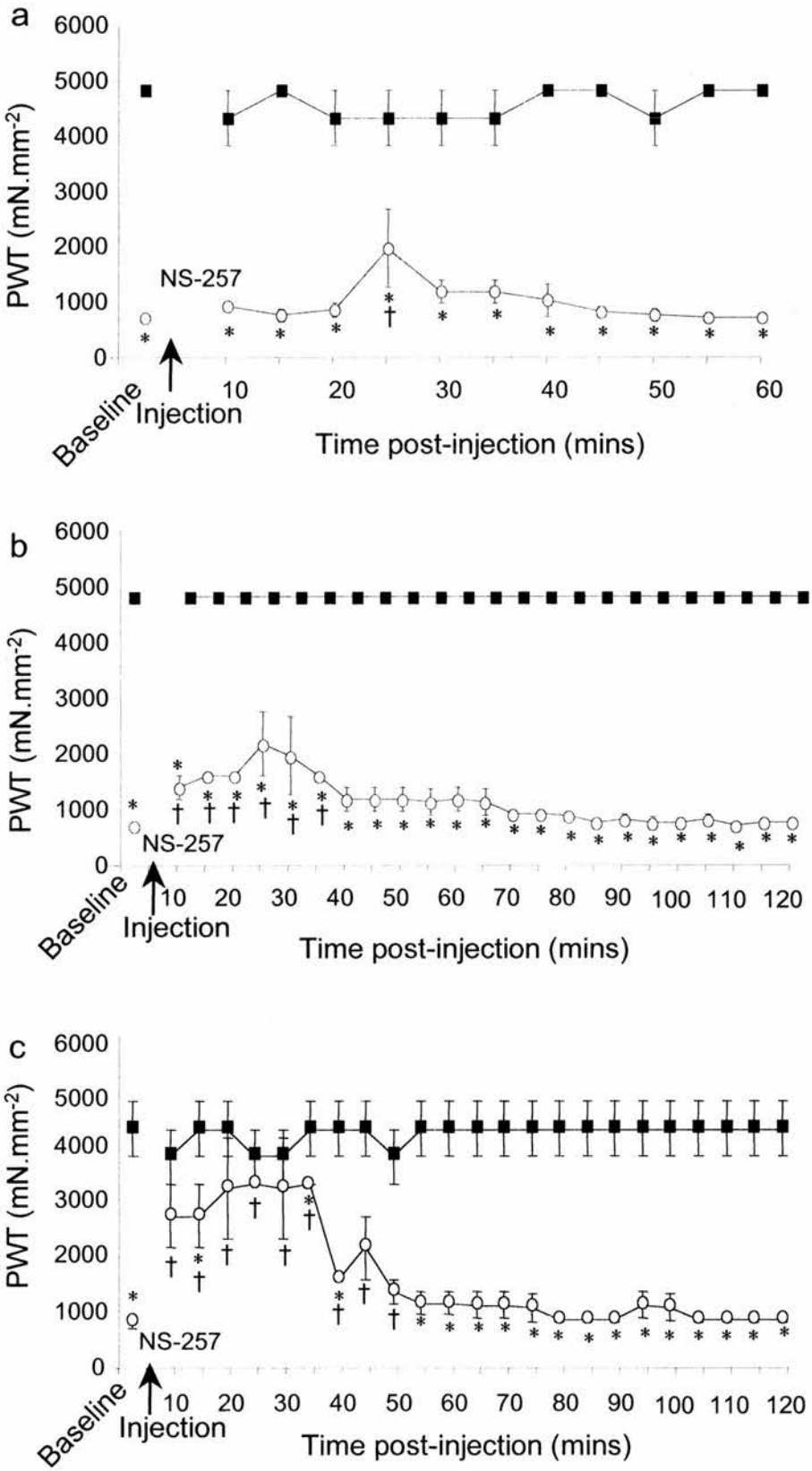
a
b
c
PWT (mN.mm-2)
6000
5000
4000
3000
2000
1000
0
NS-257
Baseline
Injection
10
20
30
40
50
60
70
80
90
100
110
120
Time post-injection (mins)

Figure 3.7 Effects of the intrathecal administration of the selective AMPA receptor antagonist NS-257 in naïve rats

Data represent the average (a) hindlimb withdrawal latency to noxious heat and (b) withdrawal threshold to mechanical (von Frey filament) stimuli ± SEM for each time point in naïve, untreated rats (n=5) following the intrathecal injection of 83nmol NS-257.

There was no significant difference in either withdrawal latency or threshold (a and b, respectively) of either hindpaw in naïve rats when testing resumed 10 min following injection (Student's t-test and Mann-Whitney Rank Sum test, respectively). The intrathecal injection of NS-257 (arrow) had no appreciable effect on the withdrawal latency or the withdrawal threshold in either hindlimb.

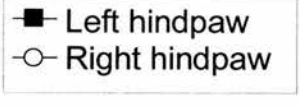

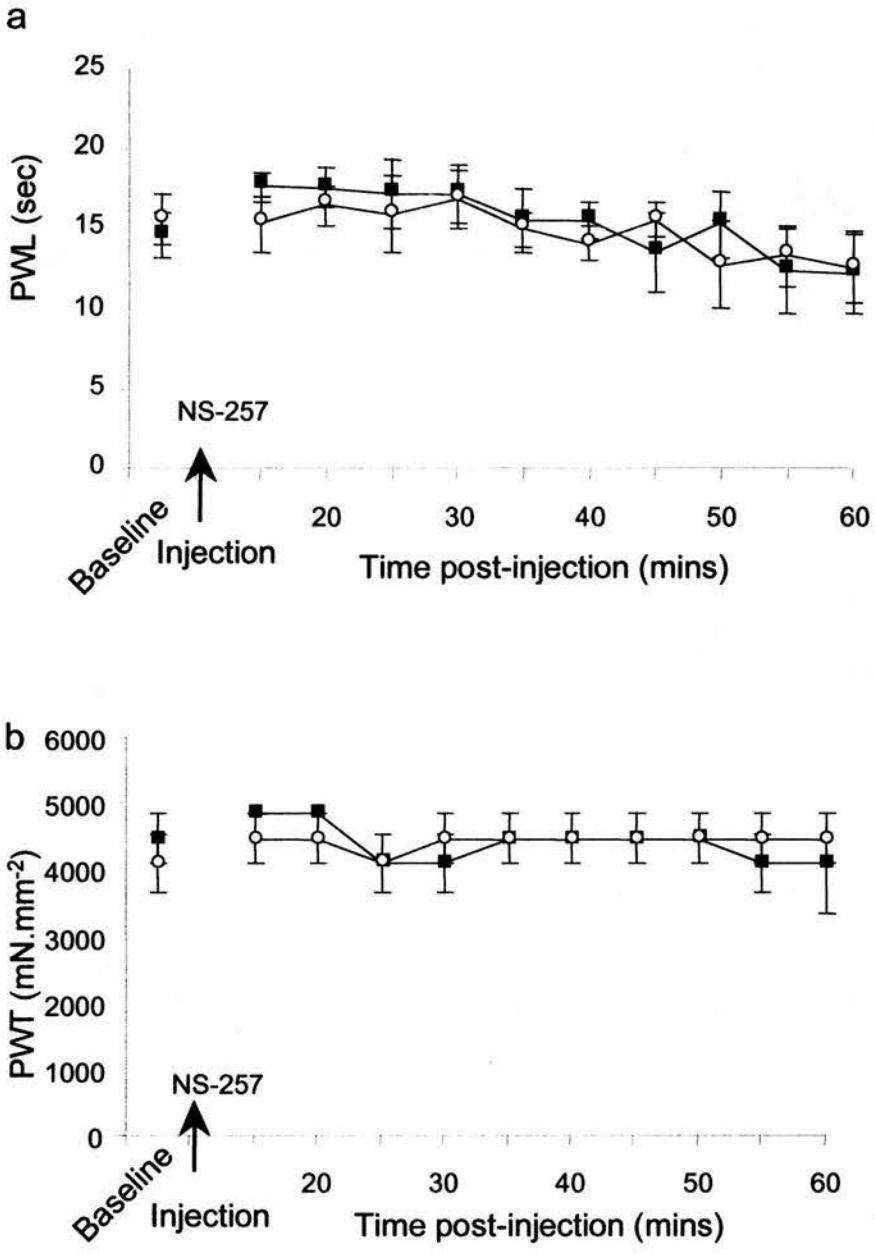
a
PWL (sec)
25
20
15
10
5
0
NS-257
Baseline
Injection
20
30
40
50
60
Time post-injection (mins)
b
PWT (mN.mm-2)
6000
5000
4000
3000
2000
1000
0
NS-257
Baseline
Injection
20
30
40
50
60
Time post-injection (mins)

Figure 3.8 Effects of the intrathecal administration of the selective AMPA receptor antagonist SYM 2206 on thermal hyperalgesia and mechanical allodynia in rats at the peak of neuropathic reflex sensitivity

Data represent the average hindlimb withdrawal latency (a) and withdrawal threshold (b) ± SEM to a noxious thermal or normally innocuous mechanical stimulus (n=6) for each time point following the intrathecal injection of 1.5nmol SYM 2206.

Rats at the peak of ipsilateral thermal hyperalgesia, as determined by a significant reduction in ipsilateral paw withdrawal latency (a, 'PWL'; *, $p<0.05$ Student's t-test) or paw withdrawal threshold (b, 'PWT'; *, $p<0.05$ Mann-Whitney Rank Sum test) compared to contralateral withdrawal latency, were intrathecally injected with SYM 2206 (at arrow). 10 min following injection, 1.5nmol SYM 2206 significantly attenuated ipsilateral thermal hyperalgesia in (a) in comparison to pre-injection ipsilateral values (†, $p<0.05$, One-way ANOVA followed by a Dunnett's test) while there was no significant alteration in the contralateral response. In (b), the ipsilaterally reduced paw withdrawal threshold to mechanical stimulation was significantly increased (†, $p<0.05$, Kruskal-Wallis ANOVA followed by a Dunn's test) with no change in contralateral responses. The effect of SYM 2206 lasted for up to 60 min for the thermal test and 40 min for the mechanical test before the ipsilateral withdrawal returned to pre-injection baseline values indicative of hyperalgesia/ allodynia.

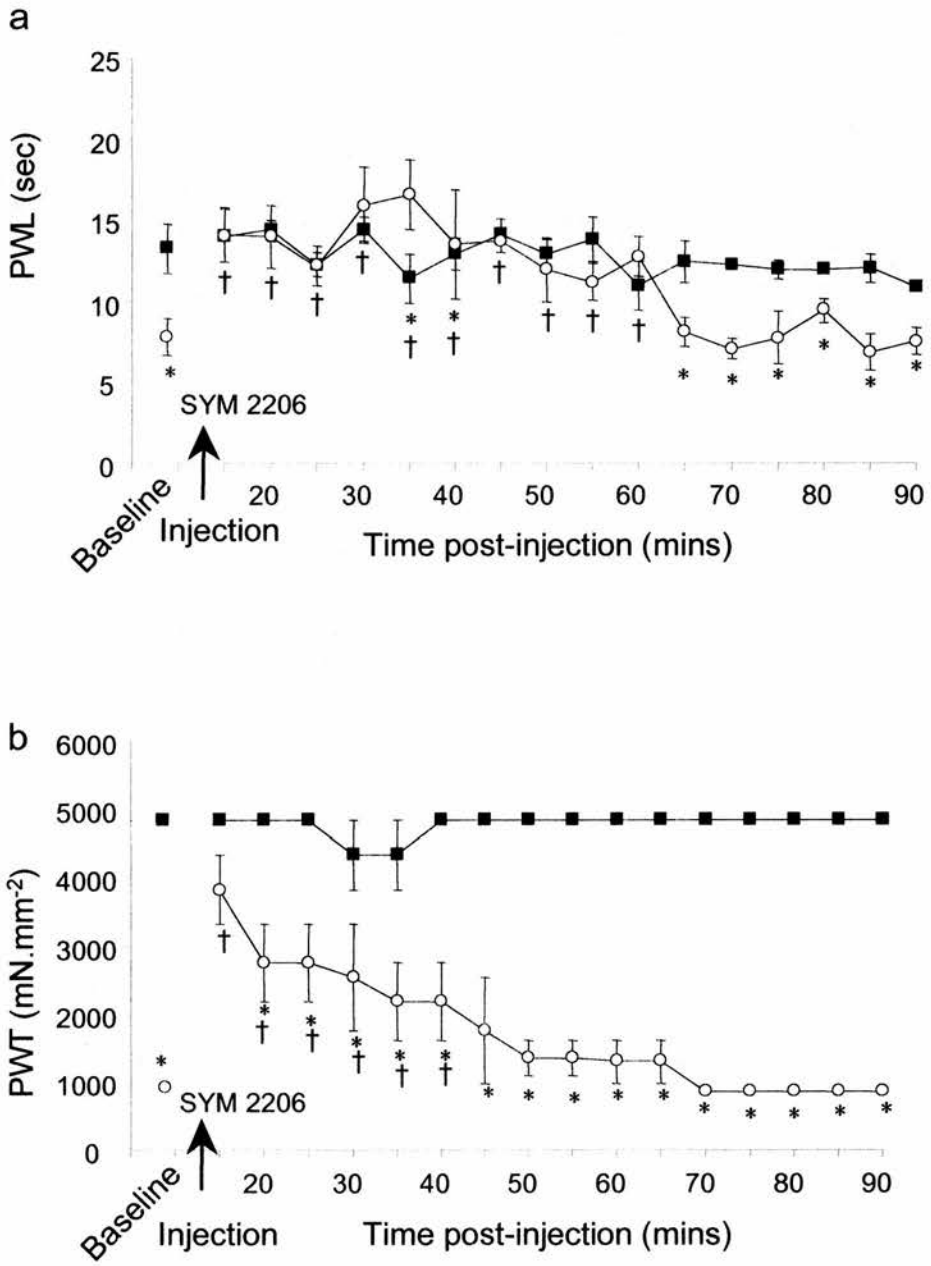
a
PWL (sec)
25
20
15
10
5
0
SYM 2206
Baseline
Injection
20
30
40
50
60
70
80
90
Time post-injection (mins)
b
PWT (mN.mm-2)
6000
5000
4000
3000
2000
1000
0
SYM 2206
Baseline
Injection
20
30
40
50
60
70
80
90
Time post-injection (mins)

Figure 3.9 Effects of the intrathecal administration of the selective AMPA receptor antagonist SYM 2206 in naïve rats

Data represent the average (a) hindlimb withdrawal latency to noxious heat and (b) withdrawal threshold to mechanical (von Frey filament) stimuli ± SEM for each time point in naïve, untreated rats (n=5) following the intrathecal injection of 1.5nmol SYM 2206.

There was no significant difference in either withdrawal latency or threshold (a and b, respectively) of either hindpaw in naïve rats when testing resumed 10 min following injection (Student's t-test and Mann-Whitney Rank Sum test, respectively). The intrathecal injection of SYM 2206 (arrow) had no appreciable effect on the withdrawal latency or the withdrawal threshold in either hindlimb.

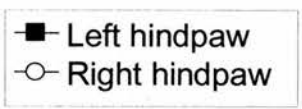

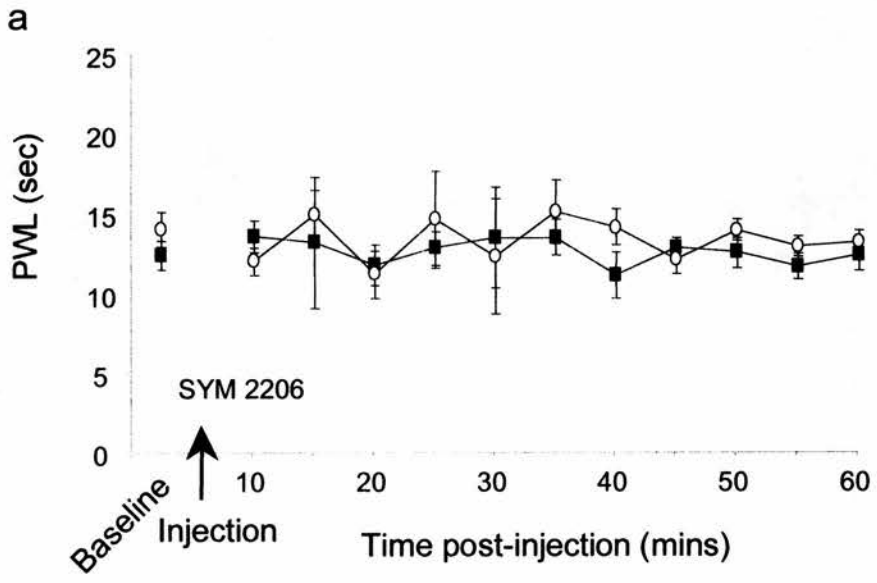
a
PWL (sec)
25
20
15
10
5
0
SYM 2206
Baseline
Injection
10
20
30
40
50
60
Time post-injection (mins)

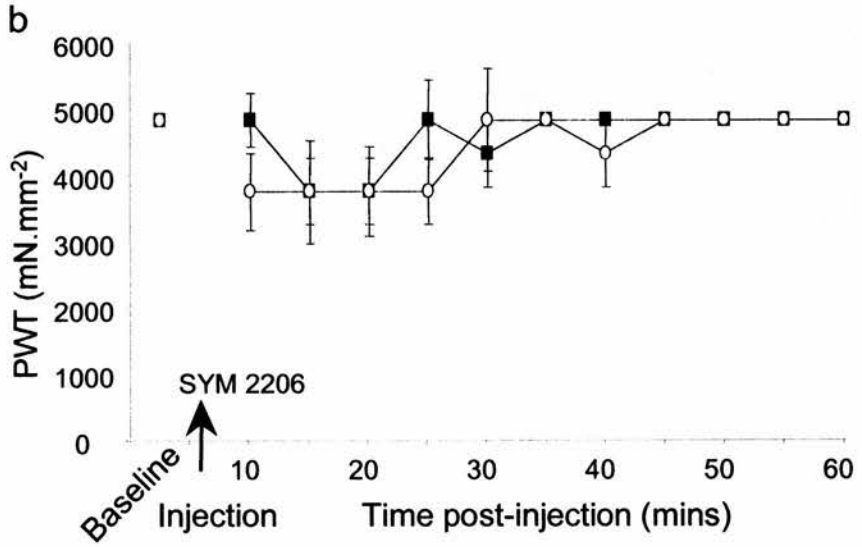
b
PWT (mN.mm-2)
6000
5000
4000
3000
2000
1000
0
SYM 2206
Baseline
Injection
10
20
30
40
50
60
Time post-injection (mins)

Figure 3.10 Effects of the intrathecal administration of saline on thermal hyperalgesia and mechanical allodynia in rats at the peak of neuropathic reflex sensitivity

Data represent the average hindlimb withdrawal latency (a) and withdrawal threshold (b) ± SEM to a noxious thermal or normally innocuous mechanical stimulus (n=6) for each time following the intrathecal injection saline vehicle.

Rats at the peak of ipsilateral thermal hyperalgesia as determined by a significant reduction in ipsilateral paw withdrawal latency (a, 'PWL'; *, $p<0.05$ Student's t-test) or paw withdrawal threshold (b, 'PWT'; *, $p<0.05$ Mann-Whitney Rank Sum test) compared to contralateral withdrawal latency were intrathecally injected with saline (at arrow). Saline had no discernible effect on the withdrawal latency or the withdrawal threshold in either hindlimb when testing resumed 10 min following injection and there was no significant effect on hindlimb withdrawal post-injection when compared to pre-injection, baseline withdrawal.

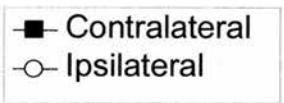

a

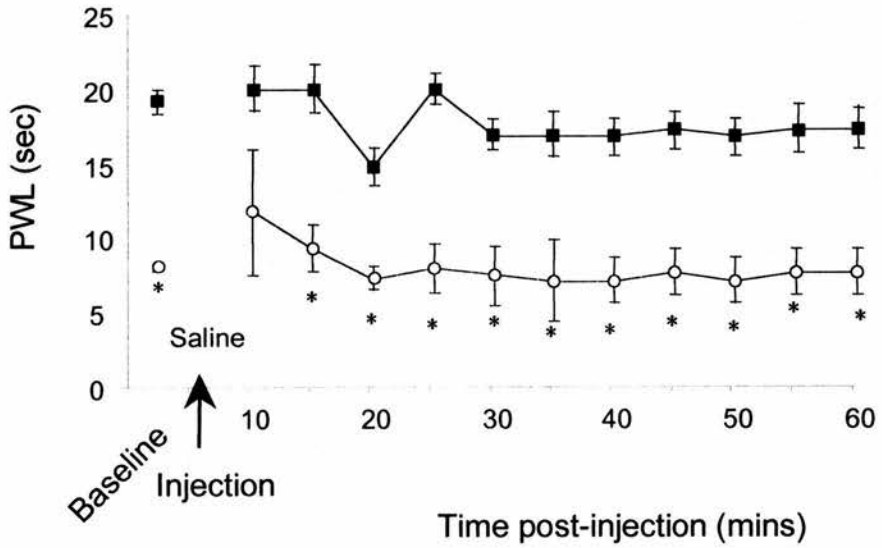
25
20
15
10
5
0
PWL (sec)
Saline
Baseline
Injection
10
20
30
40
50
60
Time post-injection (mins)

b

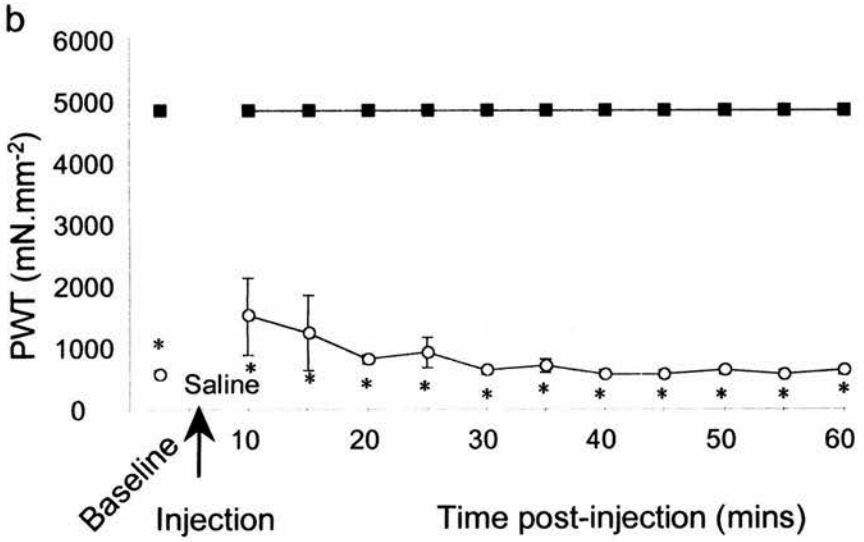
6000
5000
4000
3000
2000
1000
0
PWT (mN.mm-2)
Saline
Baseline
Injection
10
20
30
40
50
60
Time post-injection (mins)

3.2.2 Intrathecal injection of myristoylated C-terminal inhibitory peptides

As there is little in vivo functional evidence to date on the proteins that interact with the C-termini of GluR2 and GluR1 AMPA receptor subunits, we assessed the effects of strategies designed to block the interactions of the GluR2 subunit with GRIP/ PICK1 or NSF, and also any effects of blocking the GluR1 interaction with SAP97. For this, we investigated the effects of the local application of myristoylated peptides (see Section 2.2.2 and 2.2.3, pgs. 56-60), mimicking the site of the C-terminal interaction site of each of these proteins, on CCI-induced changes (see Section 2.2.4 for intrathecal injections and Table 2.1 for drug details, pgs. 60-63).

Intrathecal injection of myr-NVYGIESVKI (to block the site of GRIP/ABP/PICK1 binding on the extreme GluR2/3 C-terminus) markedly alleviated previously developed ipsilateral thermal hyperalgesia in rats following CCI for up to 50 min following injection (Fig. 3.11a), but had little effect on mechanical allodynia (Fig. 3.11b). No effects were seen on reflexes in naïve rats (Fig. 3.12). The inhibitory peptide blocking the NSF binding site, myr-AKRMKVAKNAQ, had a moderate effect in attenuating the thermal hyperalgesic state for up to 35 min (Fig. 3.13a) but had a much smaller and shorter lasting effect on the allodynic state (Fig. 3.13b). This peptide had no detectable effects in naïve rats (Fig. 3.14). In contrast, blocking the SAP97 site on the GluR1 C-terminus with the inhibitory peptide myr-SGMPLGATGL, had a significant effect in the reversal of thermal hyperalgesia lasting 55 min (Fig. 3.15a) but also had a clear effect on the reversal of the allodynic behaviour for up to 60min following injection (Fig. 3.15b). This peptide had no effect on thermal or mechanical reflex tests in naïve animals (Fig. 3.16).

This suggests there may be a role for GluR1: SAP97 interactions in the maintenance of mechanical allodynia, whereas the GluR1: SAP97 and the GluR2: GRIP/PICK1, GluR2: NSF interactions may all contribute to the maintenance of thermal hyperalgesia. Only myr-SGMPLGATGL had a significant effect on the contralateral response while neither myr-NVYGIESVKI or myr-AKRMKVAKNAQ had any significant effect on contralateral responses and none of the inhibitory peptides had any significant effect when tested in naïve rats (Fig. 3.12, 3.14 and 3.16). In addition,

an inactive control myristoylated peptide (myr-GRRNAIHDE) had no effect on the thermal hyperalgesia or mechanical allodynia following CCI (Fig. 3.17a and b). These data indicate, for the first time, a functional in vivo role for the AMPA receptor interacting proteins in persistent neuropathic pain. The functional effects varied according to which part of the GluR2/3 C-terminus or the GluR1 C-terminus was blocked. No distinction was made here between GRIP, ABP and PICK1 which all bind to the same motif in the GluR2/3 C-terminus.

Figure 3.11 Effects of the intrathecal administration of the GluR2: GRIP/PICK1 motif-directed myristoylated inhibitory peptide 'myr-NVYGIESVKI' on thermal hyperalgesia and mechanical allodynia in rats at the peak of neuropathic reflex sensitivity

Data represent the average (a) hindlimb withdrawal latency to noxious heat and (b) withdrawal threshold to von Frey filament stimuli ± SEM (n=6) for each time point before and following the intrathecal injection of 4.5nmol myr-NVYGIESVKI.

Rats at the peak of ipsilateral thermal hyperalgesia, that displayed a significant reduction in ipsilateral paw withdrawal latency (a, 'PWL'; *, $p<0.05$ Student's t-test) or paw withdrawal threshold (b, 'PWT'; *, $p<0.05$ Mann-Whitney Rank Sum test) compared to contralateral withdrawal latency, were intrathecally injected with myr-NVYGIESVKI (at arrow). 15 min following injection, myr-NVYGIESVKI significantly attenuated ipsilateral thermal hyperalgesia (a) in comparison to pre-injection ipsilateral values (†, $p<0.05$, One-way ANOVA followed by a Dunnett's test) while there was no significant alteration in the contralateral response. The effect lasted for up to 50 min for the thermal test before the ipsilateral withdrawal returned to pre-injection, baseline latencies (*, $p<0.05$ Student's t-test). In contrast, myr-NVYGIESVKI had no significant effect on ipsilateral mechanical allodynia with ipsilateral withdrawal remaining at pre-injection, baseline thresholds (b).

a

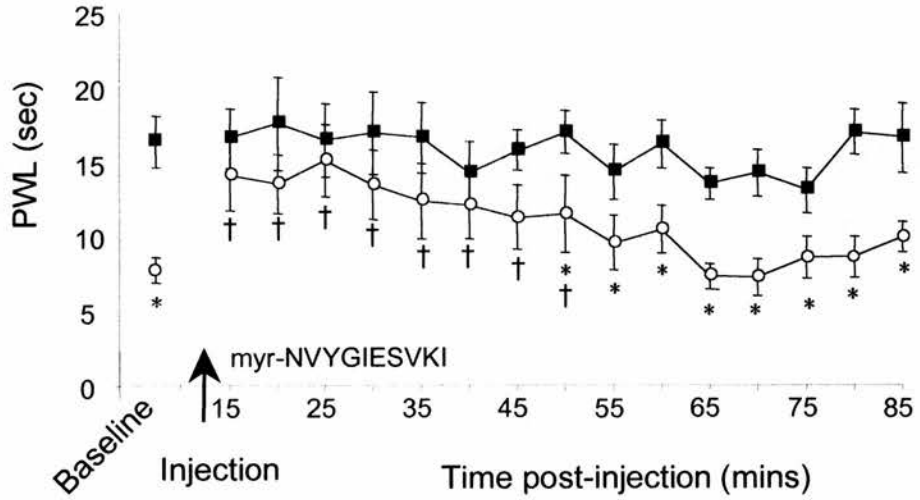
PWL (sec)
25
20
15
10
5
0
myr-NVYGIESVKI
15
25
35
45
55
65
75
85
Baseline
Injection
Time post-injection (mins)

b

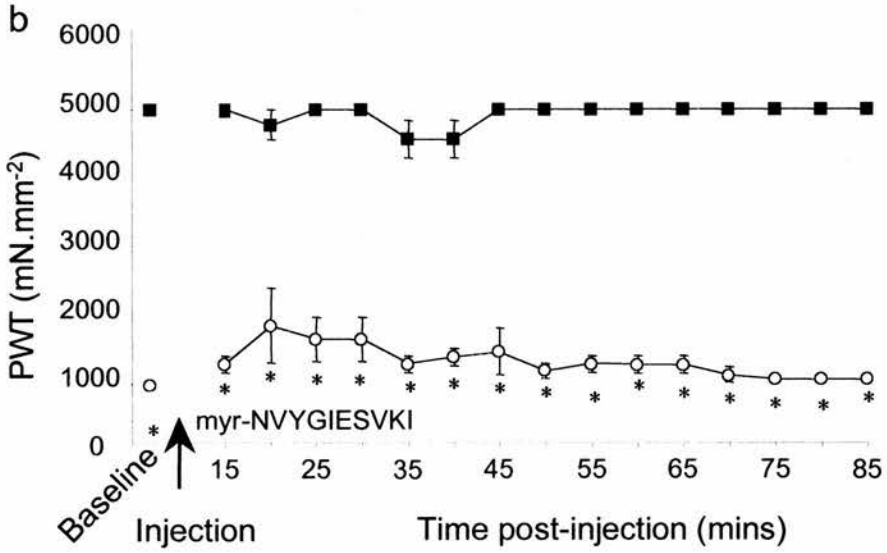
PWT (mN.mm-2)
6000
5000
4000
3000
2000
1000
0
myr-NVYGIESVKI
15
25
35
45
55
65
75
85
Baseline
Injection
Time post-injection (mins)

Figure 3.12 Effects of the intrathecal administration of the selective GluR2: GRIP/PICK1 motif-directed myristoylated inhibitory peptide 'myr-NVYGIESVKI' in naïve rats

Data represent the average (a) hindlimb withdrawal latency to noxious heat and (b) withdrawal threshold to von Frey filament stimuli ± SEM in naïve, untreated rats (n=5) for each time point before and following the intrathecal injection 4.5nmol myr-NVYGIESVKI.

There was no significant difference in either withdrawal latency or threshold (a and b, respectively) between hindpaws in naïve rats (Student's t-test and Mann-Whitney Rank Sum test, respectively). The intrathecal injection of myr-NVYGIESVKI (arrow) had no effect on the withdrawal latency or the withdrawal threshold in either hindlimb when testing resumed 10 min following injection, except at one time point (†, $p < 0.05$, One-way ANOVA followed by a Dunnett's test and Kruskal-Wallis ANOVA followed by a Dunn's test, respectively).

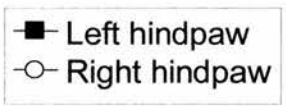

a

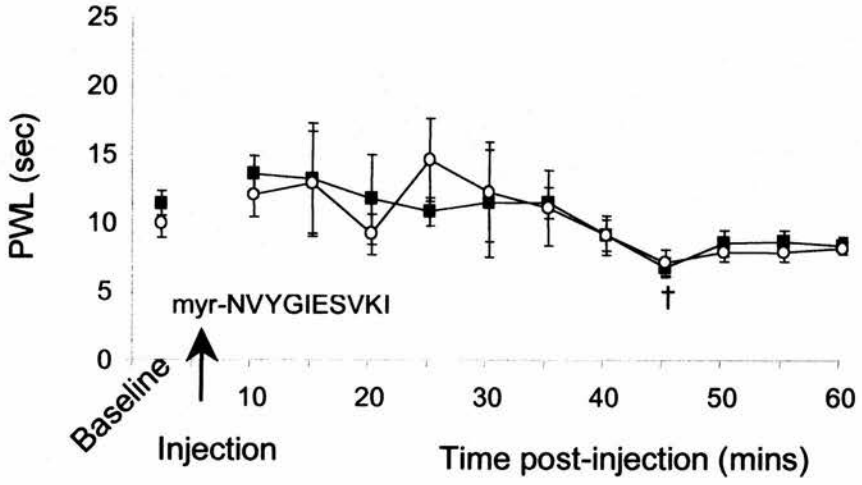
25
20
15
10
5
0
PWL (sec)
myr-NVYGIESVKI
†
Baseline
Injection
10
20
30
40
50
60
Time post-injection (mins)

b

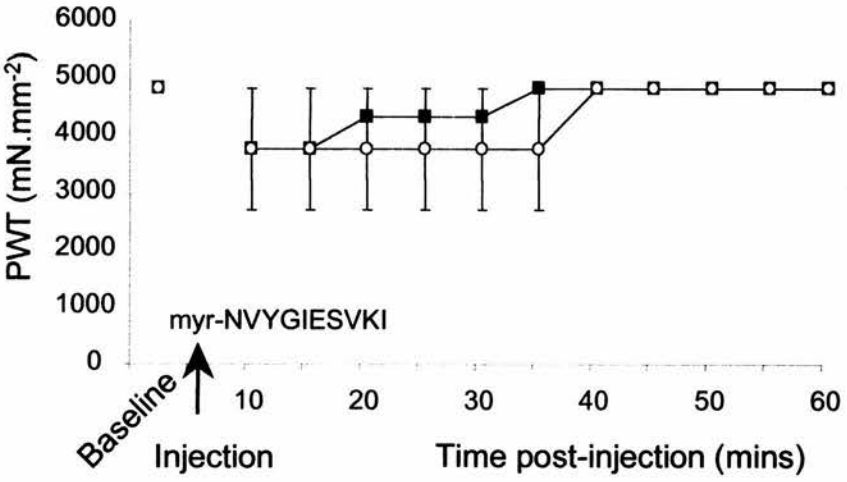
6000
5000
4000
3000
2000
1000
0
PWT (mN.mm-2)
myr-NVYGIESVKI
Baseline
Injection
10
20
30
40
50
60
Time post-injection (mins)

Figure 3.13 Effects of the intrathecal administration of the GluR2: NSF motif-directed myristoylated inhibitory peptide 'myr-AKRMKVAKNAQ' on thermal hyperalgesia and mechanical allodynia in rats at the peak of neuropathic reflex sensitivity

Data represent the average (a) hindlimb withdrawal latency to noxious heat and (b) withdrawal threshold to von Frey filament stimuli ± SEM (n=6) for each time point before and following the intrathecal injection of 4.5nmol myr-AKRMKVAKNAQ.

Rats at the peak of ipsilateral thermal hyperalgesia, that displayed a significant reduction in ipsilateral paw withdrawal latency (a, 'PWL'; *, $p<0.05$ Student's t-test) or paw withdrawal threshold (b, 'PWT'; $p<0.05$ Mann-Whitney Rank Sum test) compared to contralateral withdrawal latency, were intrathecally injected with myr-AKRMKVAKNAQ (at arrow). 15 min following injection, myr-AKRMKVAKNAQ significantly attenuated ipsilateral thermal hyperalgesia (a) in comparison to pre-injection ipsilateral values (†, $p<0.05$, One-way ANOVA followed by a Dunnett's test) while there was no significant alteration in the contralateral response. The effect lasted for up to 35 min for the thermal test before the ipsilateral withdrawal returned to pre-injection, baseline latencies (*, $p<0.05$ Student's t-test). In contrast, myr-AKRMKVAKNAQ had a minimal effect on ipsilateral mechanical allodynia with ipsilateral withdrawal returning to pre-injection, baseline thresholds within 20 min (b).

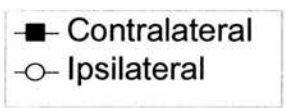

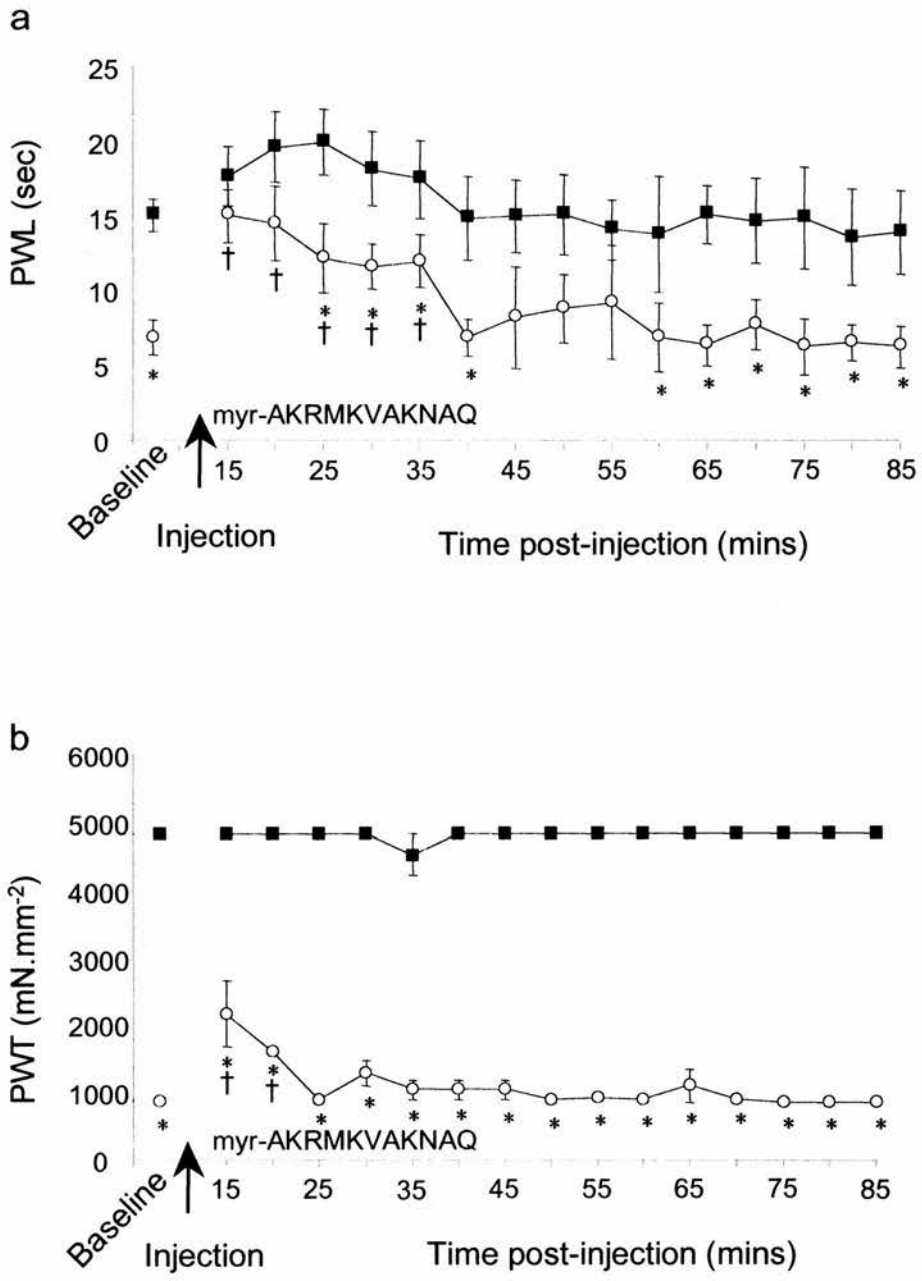
a
PWL (sec)
25
20
15
10
5
0
myr-AKRMKVAKNAQ
Baseline
15
25
35
45
55
65
75
85
Injection
Time post-injection (mins)
b
PWT (mN.mm-2)
6000
5000
4000
3000
2000
1000
0
myr-AKRMKVAKNAQ
Baseline
15
25
35
45
55
65
75
85
Injection
Time post-injection (mins)

Figure 3.14 Effects of the intrathecal administration of the GluR2: NSF motif-directed myristoylated inhibitory peptide 'myr-AKRMKVAKNAQ' in naïve rats

Data represent the average (a) hindlimb withdrawal latency to noxious heat and (b) withdrawal threshold to von Frey filament stimuli ± SEM in naïve, untreated rats (n=5) for each time point before and following the intrathecal injection of 4.5nmol myr-AKRMKVAKNAQ.

There was no significant difference in either withdrawal latency or threshold (a and b, respectively) between hindpaws in naïve rats (Student's t-test and Mann-Whitney Rank Sum test, respectively). The intrathecal injection of myr-AKRMKVAKNAQ (arrow) had no effect on the withdrawal latency or the withdrawal threshold in either hindlimb when testing resumed 10 min following injection (One-way ANOVA followed by a Dunnett's test and Kruskal-Wallis ANOVA followed by a Dunn's test, respectively).

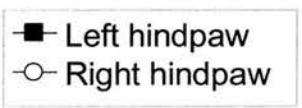

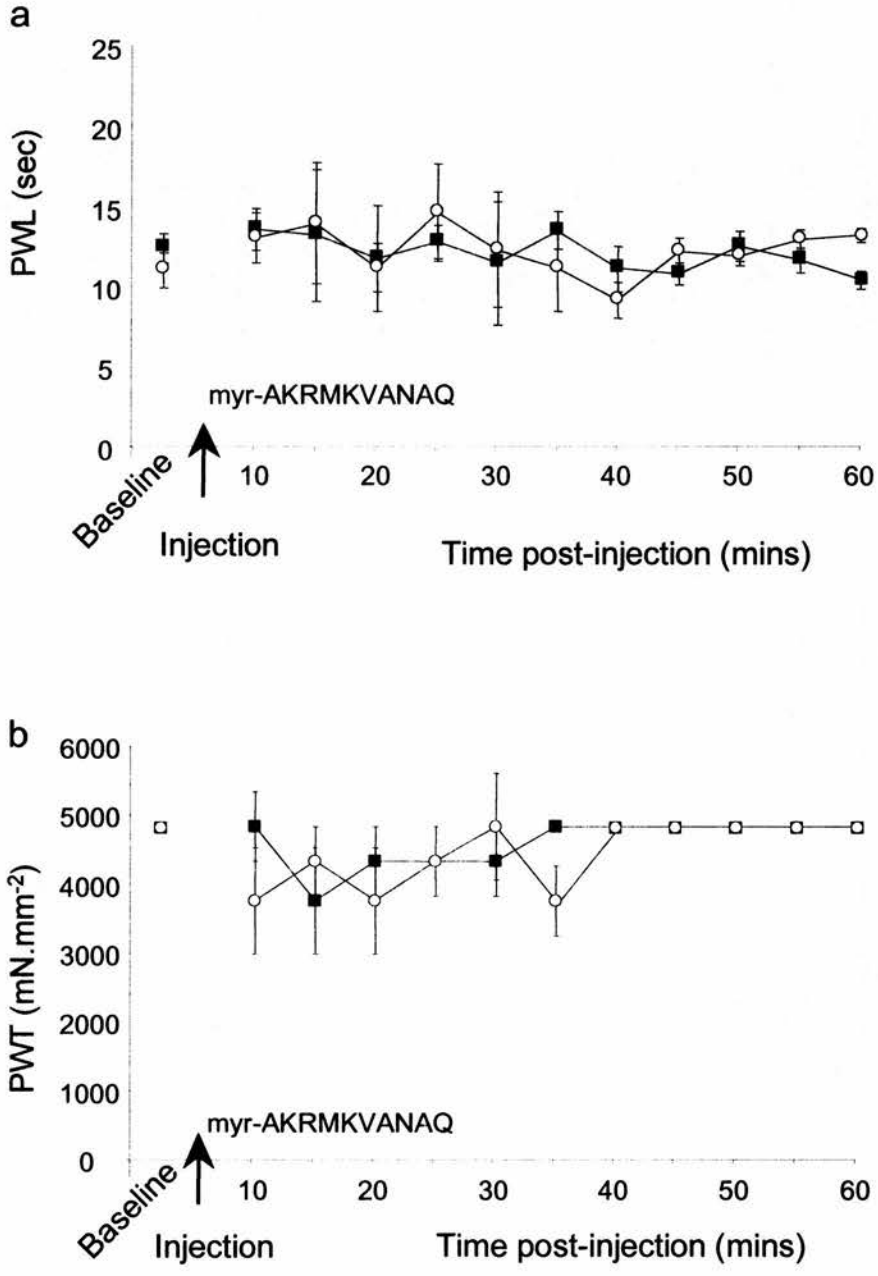
a
25
20
15
10
5
0
PWL (sec)
myr-AKRMKVANAQ
Baseline
Injection
10
20
30
40
50
60
Time post-injection (mins)
b
6000
5000
4000
3000
2000
1000
0
PWT (mN.mm-2)
myr-AKRMKVANAQ
Baseline
Injection
10
20
30
40
50
60
Time post-injection (mins)

Figure 3.15 Effects of the intrathecal administration of the GluR1: SAP97 motif-directed myristoylated inhibitory peptide 'myr-SGMPLGATGL' on thermal hyperalgesia and mechanical allodynia in rats at the peak of neuropathic reflex sensitivity

Data represent the average (a) hindlimb withdrawal latency to noxious heat and (b) withdrawal threshold to von Frey filament stimuli ± SEM (n=6) for each time point before and following the intrathecal injection of 4.5nmol myr-SGMPLGATGL.

Rats at the peak of ipsilateral thermal hyperalgesia displayed a significant reduction in ipsilateral paw withdrawal latency (a, 'PWL'; *, $p<0.05$ Student's t-test) or paw withdrawal threshold (b, 'PWT'; $p<0.05$ Mann-Whitney Rank Sum test) compared to contralateral withdrawal latency were intrathecally injected with myr-SGMPLGATGL (at arrow). 15 min following injection, myr-SGMPLGATGL significantly attenuated ipsilateral thermal hyperalgesia (a) in comparison to pre-injection ipsilateral values (†, $p<0.05$, One-way ANOVA followed by a Dunnett's test) although there was a significant reduction in the contralateral response in comparison to baseline contralateral values (‡, $p<0.05$, One-way ANOVA followed by a Dunnett's test). The effect lasted for up to 55 min for the thermal test before the ipsilateral withdrawal returned to pre-injection, baseline latencies (*, $p<0.05$ Student's t-test). In (b), the ipsilaterally reduced paw withdrawal threshold to mechanical stimulation was significantly increased (†, $p<0.05$, Kruskal-Wallis ANOVA followed by a Dunn's test) following injection of myr-SGMPLGATGL with no change in contralateral responses. The effect lasted for up to 60 min for the mechanical test before the ipsilateral withdrawal returned to pre-injection, baseline thresholds indicative of mechanical allodynia.

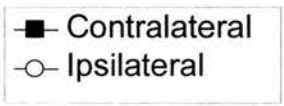

a

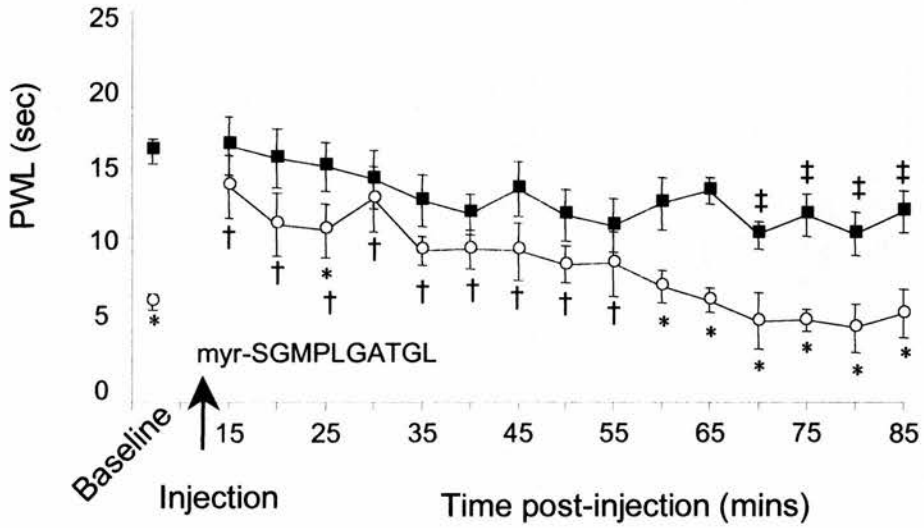
PWL (sec)
25
20
15
10
5
0
myr-SGMPLGATGL
Baseline
15
25
35
45
55
65
75
85
Injection
Time post-injection (mins)

b

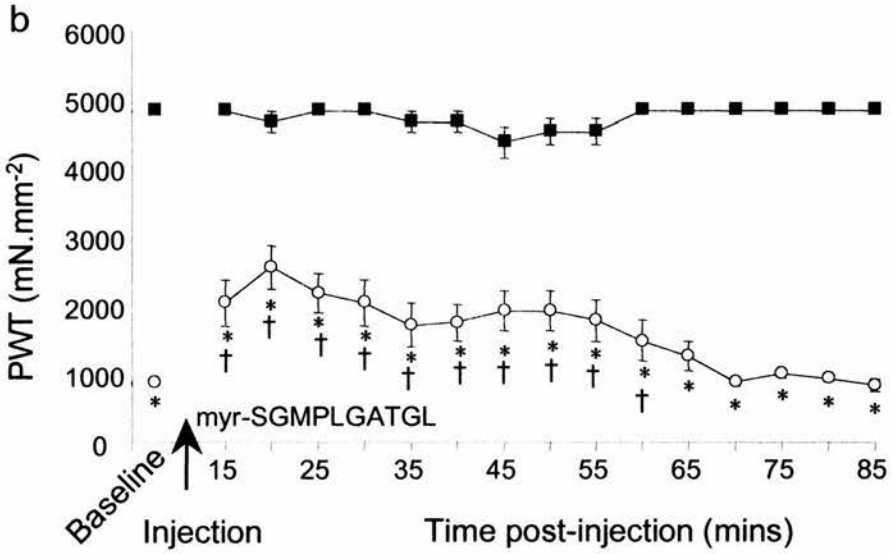
PWT (mN.mm-2)
6000
5000
4000
3000
2000
1000
0
myr-SGMPLGATGL
Baseline
15
25
35
45
55
65
75
85
Injection
Time post-injection (mins)

Figure 3.16 Effects of the intrathecal administration of the GluR1: SAP97 motif-directed myristoylated inhibitory peptide 'myr-SGMPLGATGL in naïve rats

Data represent the average (a) hindlimb withdrawal latency to noxious heat and (b) withdrawal threshold to von Frey filament stimuli ± SEM in naïve, untreated rats (n=5) for each time point before and following the intrathecal injection of 4.5nmol myr-SGMPLGATGL.

There was no significant difference in either withdrawal latency or threshold (a and b, respectively) between hindpaws in naïve rats (Student's t-test and Mann-Whitney Rank Sum test, respectively). The intrathecal injection of myr-SGMPLGATGL (arrow) had no effect on the withdrawal latency or the withdrawal threshold in either hindlimb (One-way ANOVA followed by a Dunnett's test and Kruskal-Wallis ANOVA followed by a Dunn's test, respectively).

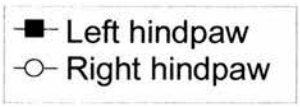

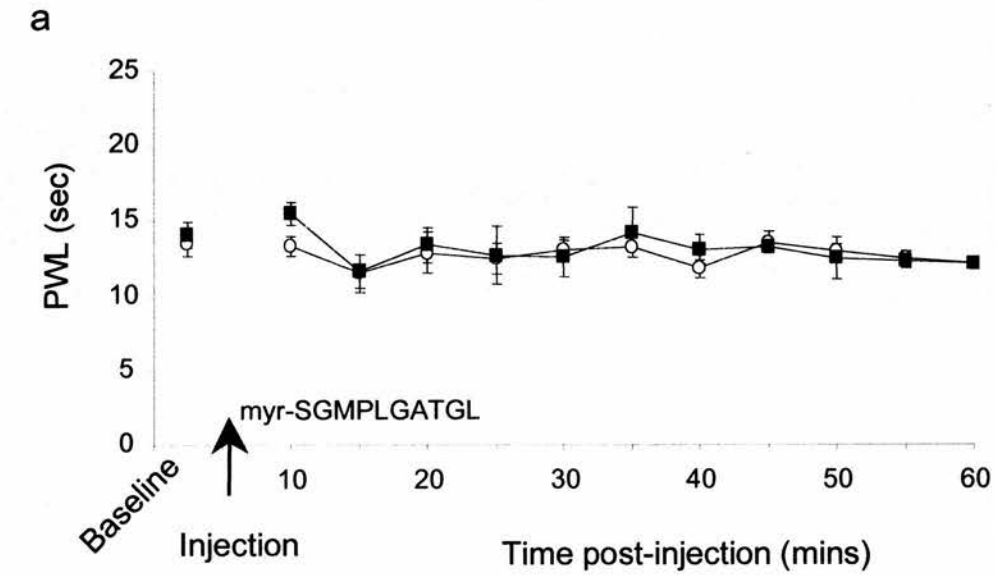
a
25
20
15
10
5
0
PWL (sec)
myr-SGMPLGATGL
Baseline
10
20
30
40
50
60
Injection
Time post-injection (mins)

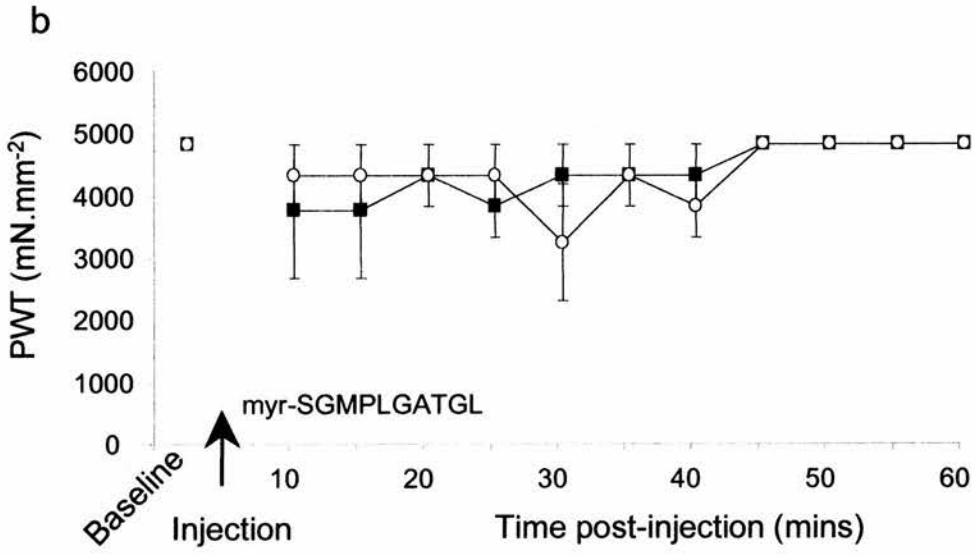
b
6000
5000
4000
3000
2000
1000
0
PWT (mN.mm-2)
myr-SGMPLGATGL
Baseline
10
20
30
40
50
60
Injection
Time post-injection (mins)

Figure 3.17 Effects of the intrathecal administration of an inactive myristoylated control peptide 'myr-GRRNAIHDE' in rats at the peak of neuropathic reflex sensitivity

Data represent the (a) average hindlimb withdrawal latency to noxious heat and (b) withdrawal threshold to von Frey filament stimuli ± SEM in naïve, untreated rats (n=5) for each time point following the intrathecal injection of 4.5nmol of the myristoylated control peptide.

There was no significant difference in either withdrawal latency or threshold (a and b, respectively) between hindpaws in naïve rats (Student's t-test and Mann-Whitney Rank Sum test, respectively). The intrathecal injection of the myristoylated control peptide (arrow) had no discernible effect on the withdrawal latency or the withdrawal threshold in either hindlimb (One-way ANOVA followed by a Dunnett's test and Kruskal-Wallis ANOVA followed by a Dunn's test, respectively).

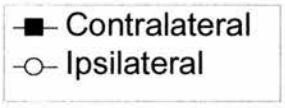

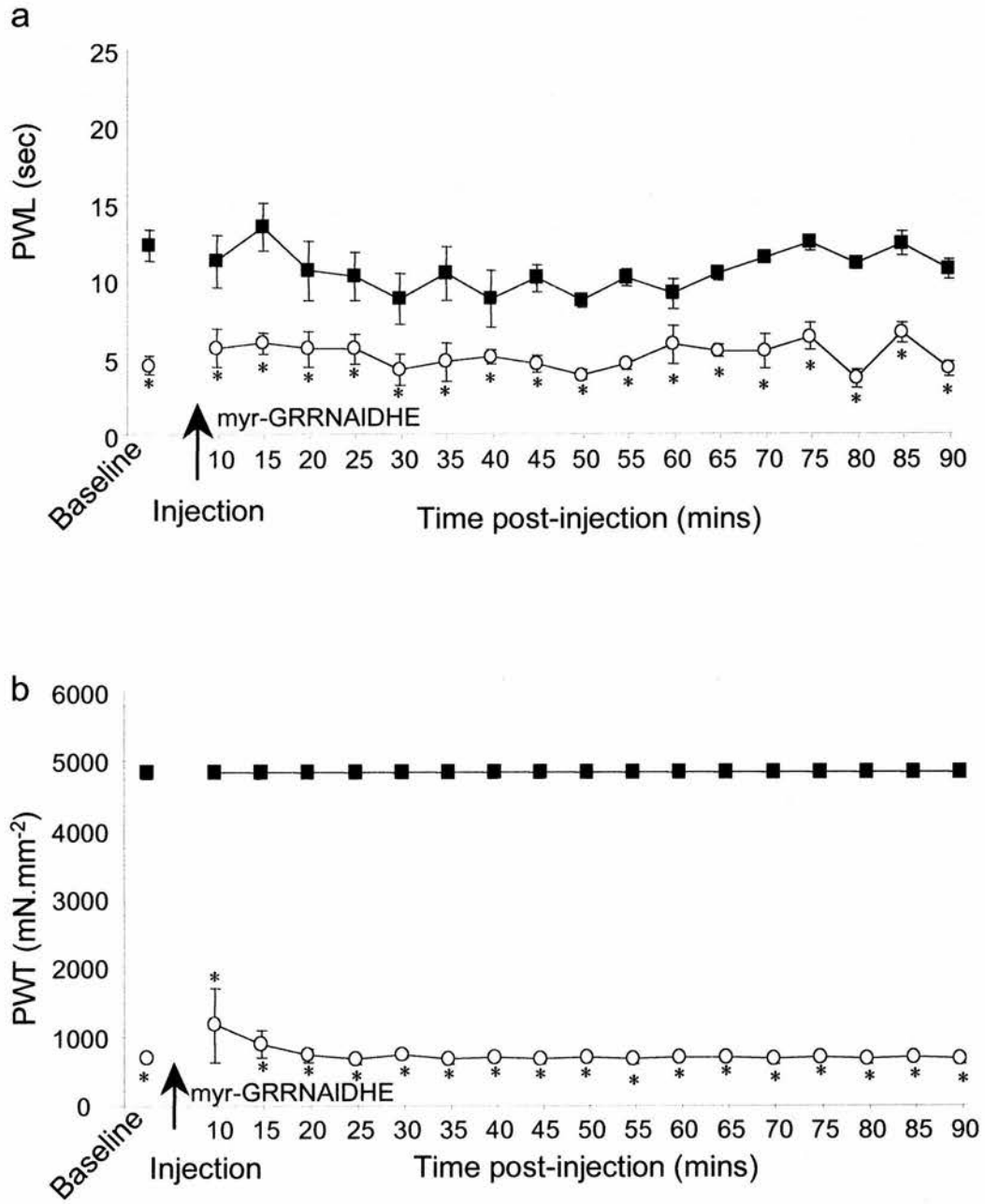
a
PWL (sec)
25
20
15
10
5
0
myr-GRRNAIDHE
Baseline
Injection
10 15 20 25 30 35 40 45 50 55 60 65 70 75 80 85 90
Time post-injection (mins)
b
PWT (mN.mm-2)
6000
5000
4000
3000
2000
1000
0
myr-GRRNAIDHE
Baseline
Injection
10 15 20 25 30 35 40 45 50 55 60 65 70 75 80 85 90
Time post-injection (mins)

3.2.3 In situ hybridisation histochemistry

The distribution of the AMPA receptors in the spinal cord has been previously documented under normal conditions although there is little evidence for the distribution following neuropathic pain conditions (Furuyama et al., 1993; Tölle et al., 1993; Harris et al., 1996). Indeed, there is almost no evidence for the specific localisation of GluR2 interacting proteins in the spinal cord and it was of interest to determine whether there were any alterations in expression levels following the establishment of neuropathic sensitivity. Here, we show an analysis of GluR2, GRIP2, NSF, GluR1 and Narp mRNA in the spinal cord following CCI (see Section 2.3.1, Table 2.4 and Fig. 2.2 for probe details, pgs. 71-80). No probe for PICK1 was readily available, as the rat cDNA has not been cloned.

(i) GluR2

There was a high basal level of GluR2 mRNA expression in the spinal cord, in terms of both the density of expression (Fig. 3.18a and b) and the number of expressing cells (Table 3.1). These findings were similar in untreated and sham animals, and were in agreement with previously published work (Furuyama et al., 1993; Tölle et al., 1993). Labelled neurones were mostly located in the dorsal horn, particularly LI, III-V with moderate expression in LII. Few labelled cells were found in the ventral horn of the spinal cord or the white matter. Following CCI, ipsilateral to injury in the spinal cord there was a significant increase in the levels of GluR2 mRNA in the superficial dorsal horn laminae I and II at the sites of primary afferent termination, both laterally and mediolaterally (Fig. 3.18a and b). The increase in mRNA was seen for the density of labelling while there was no significant increase in the number of cells expressing GluR2 mRNA (Table 3.1). A representative example of this increase in LII neurones is shown photographically in Figure 3.19 (a) in comparison to contralateral (Fig. 3.19b), sham-operated (Fig. 3.19c) and naïve (Fig. 3.19d) samples from the same region. No marked alterations in expression levels were seen in the lower laminae III-V or indeed in the ventral horn motoneurones (MNS). There was little variation in GluR2 mRNA in expression between contralateral, sham-operated or naïve samples.

Figure 3.18 In situ hybridisation measurement of GluR2 mRNA expression per cell in the spinal cord following CCI compared to sham-operated and naïve rats

Data represent the mean density (± SEM) of silver grains per cell expressing GluR2 mRNA for the mediolateral (a) and lateral (b) dorsal horn laminae I-V (LI-V) and motoneurones (MNS) ipsilateral and contralateral to CCI, compared to sham-operated and naïve animals (n=4 rats, 5 sections per condition for each rat).

Ipsilateral to CCI, there was a significant increase in the number of silver grains per cell in LI and II in both mediolateral and lateral zones when compared to contralateral levels (*, $p<0.05$ Student's t-test) and when compared to sham and naïve levels (†, $p<0.05$, One-way ANOVA followed by a Dunnett's test) There was no significant variation in the number of silver grains per cell in the lower dorsal horn laminae III-V or in motoneurones following CCI. For all laminae examined, there was no significant difference in the relative expression of GluR2 mRNA when comparing the contralateral to sham or naïve values, or when comparing sham to naïve values.

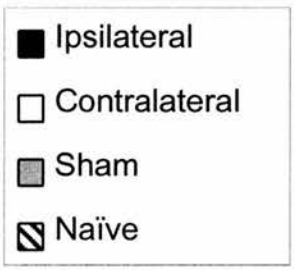

a

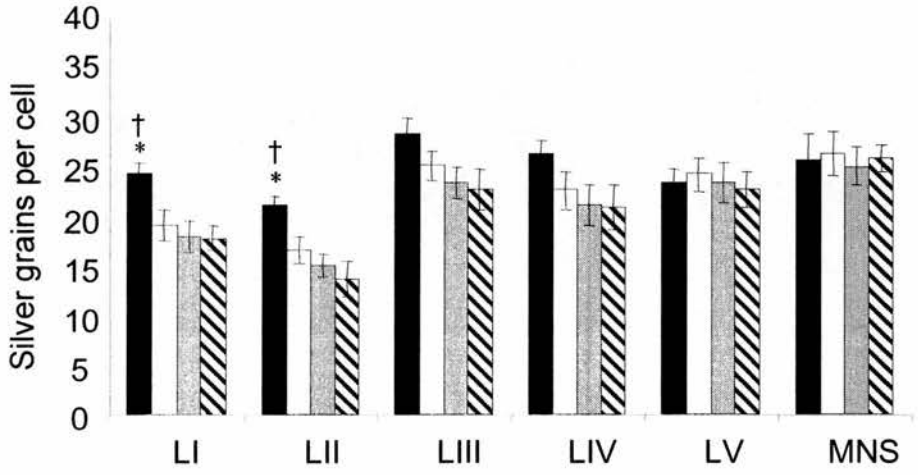
Silver grains per cell
40
35
30
25
20
15
10
5
0
†
*
†
*
LI
LII
LIII
LIV
LV
MNS

b

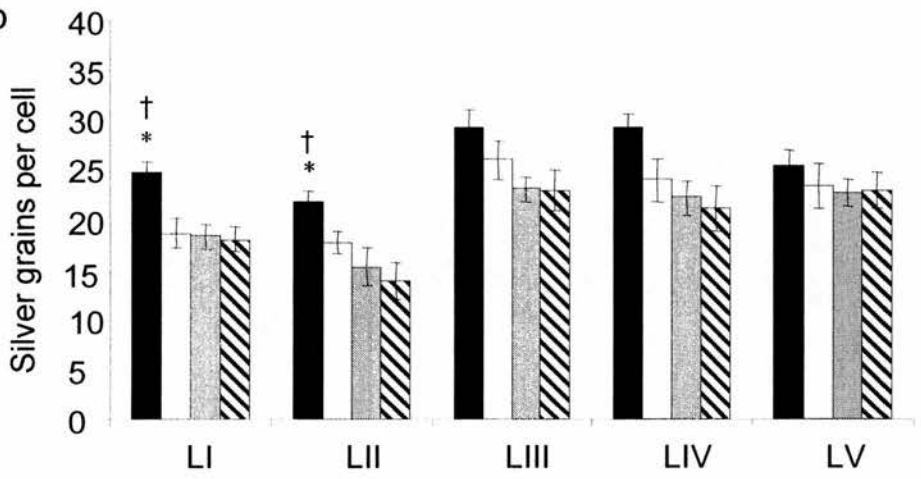
Silver grains per cell
40
35
30
25
20
15
10
5
0
†
*
†
*
LI
LII
LIII
LIV
LV

Table 3.1 In situ hybridisation measurement of GluR2 mRNA expressing cells in the spinal cord following CCI compared to sham-operated and naïve rats

Data represent the mean number of cells (± SEM) expressing GluR2 mRNA for the mediolateral and lateral dorsal horn laminae I-V (LI-V) and motoneurones (MNS) ipsilateral and contralateral to CCI, compared to sham-operated and naïve animals (n=4 rats, 5 sections per condition for each rat).

There was no significant alteration in the number of cells expressing GluR2 mRNA ipsilateral to CCI when compared to the contralateral dorsal horn (Student's t-test). For all laminae examined, there was no significant difference in the relative expression of GluR2 mRNA when comparing the contralateral to sham or naïve values, or when comparing sham to naïve values (One-way ANOVA).

GluR2	Mean number of hybridising cells							
	Mediolateral				Lateral			
	Ipsilateral	Contralateral	Sham	Naïve	Ipsilateral	Contralateral	Sham	Naïve
LI	31.3 ± 1.7	29.9 ± 1.4	30.6 ± 2.0	28.6 ± 1.0	32.9 ± 2.5	29.1 ± 1.9	30.8 ± 1.7	31.6 ± 1.0
LII	27.5 ± 1.3	29.7 ± 2.0	31.4 ± 1.7	29.9 ± 0.9	29.9 ± 1.7	28.9 ± 1.3	29.3 ± 1.0	30.9 ± 0.9
LIII	32.0 ± 2.4	29.6 ± 1.2	30.3 ± 1.9	31.0 ± 1.0	31.0 ± 1.1	29.5 ± 1.5	30.4 ± 2.2	28.0 ± 2.4
LIV	41.3 ± 1.3	41.6 ± 1.5	39.2 ± 0.9	37.8 ± 0.7	39.4 ± 0.8	40.8 ± 1.3	38.9 ± 1.6	39.8 ± 0.7
LV	40.4 ± 1.3	38.6 ± 2.7	41.3 ± 1.4	40.1 ± 1.0	40.7 ± 1.0	37.1 ± 1.3	39.6 ± 0.7	40.1 ± 0.9
MNS	21.8 ± 1.5	22.0 ± 1.6	23.8 ± 2.1	19.5 ± 1.3				

Figure 3.19 Photomicrographs of GluR2 mRNA expression in lamina II of the spinal cord of CCI, sham-operated and naïve rats

High power light field photomicrographs showing in situ hybridisation identification of GluR2 mRNA expression in the medial zone of the superficial dorsal horn at the site of the most marked changes in lamina II ipsilateral to CCI (a). Corresponding regions are shown contralateral to CCI (b), following sham operation (c) and in naïve animals (d).

Scale bar = 10 μm

a

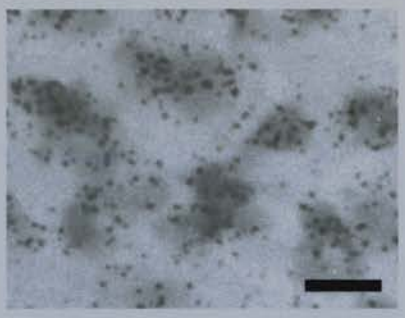

b

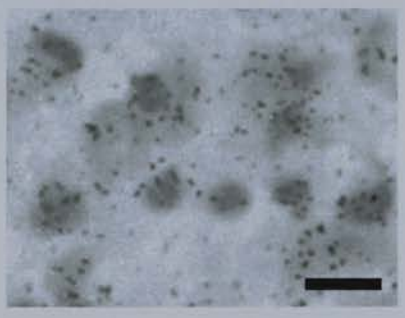

c

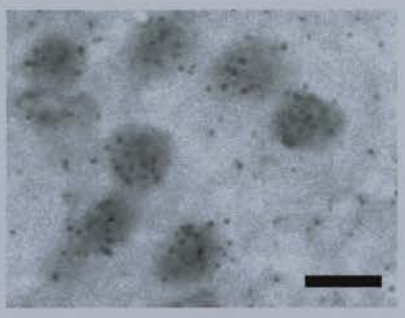

d

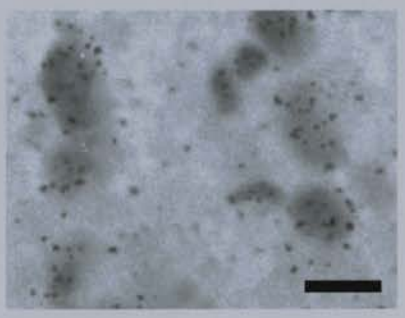

(ii) GRIP2

Here, GRIP2 mRNA was examined as it is reported to be the predominant form in adult nervous system (Brückner et al., 1999) (see Section 2.3.1, Table 2.4 and Fig. 2.2 for probe details, pgs. 71-80). GRIP2 mRNA expression was readily detected throughout the spinal cord, with slightly greater expression in the lower laminae III-V in naïve and sham-operated tissue and with motoneurones showing moderate labelling (Fig. 3.20).

Following CCI, ipsilateral to injury in the spinal cord there was a significant increase in the levels of GRIP2 mRNA in the superficial dorsal horn laminae I and II (at the sites of primary afferent termination) mainly mediolateral in location (Fig. 3.20a). There was an increase in the density of mRNA expression (Fig. 3.20) as well as an increase in the number of cells expressing GRIP2 mRNA in LI and II with little alteration in the lower laminae III-V (Table 3.2). A representative example of this increase in GRIP2 mRNA expression ipsilateral to CCI in LII neurones is shown photographically in Figure 3.21 as well as comparisons to corresponding regions from contralateral CCI (Fig. 3.21b), sham-operated (Fig. 3.21c) and naïve (Fig. 3.21d) animals. Minimal alterations in expression levels were seen in the lower laminae (III-V) or indeed in the ventral horn motoneurones (MNS). The level of GRIP2 mRNA did not significantly differ between contralateral, sham-operated or naïve animals.

(iii) NSF

Under basal conditions the expression of NSF appeared to be relatively low in the superficial dorsal horn in comparison to that for GluR2 or GRIP2. The predominant expression of NSF mRNA was found in LII-V, with motoneurones showing moderate labelling (Fig. 3.22).

Following CCI, there was a small though significant decrease in the density of NSF mRNA ipsilateral to injury in the lateral zone of the superficial dorsal horn (Fig. 3.22b), specifically in LI while there was no detectable alteration in the number of

cells expressing NSF mRNA (Table 3.3). A representative example of this lateral LI decrease in NSF mRNA is shown in Figure 3.23a in comparison to corresponding samples from contralateral CCI (Fig. 3.23b), sham-operated (Fig. 3.23c) and naïve (Fig. 3.23d) animals. The level of NSF mRNA did not significantly differ between contralateral, sham-operated or naïve animals.

Figure 3.20 In situ hybridisation measurement of the density of GRIP2 mRNA expression per cell in the spinal cord following CCI compared to sham-operated and naïve rats

Data represent the mean density of silver grains (± SEM) per cell expressing GRIP2 mRNA for the mediolateral (a) and lateral (b) dorsal horn laminae I-V (LI-V) and motoneurones (MNS) ipsilateral and contralateral to CCI, compared to sham-operated and naïve animals (n=4 rats, 5 sections per condition for each rat).

Ipsilateral to CCI, there was a significant increase in the number of silver grains per cell in LI and II in the mediolateral zone (a) and LII in the lateral zones when compared to contralateral levels (*, $p<0.05$ Student's t-test) and when compared to sham and naïve levels (†, $p<0.05$, One-way ANOVA followed by a Dunnett's test). There was no significant variation in the number of silver grains per cell in the lower dorsal horn laminae III-V or in motoneurones following CCI. For all laminae examined, there was no significant difference in the relative expression of GRIP2 mRNA when comparing the contralateral to sham or naïve values, or when comparing sham to naïve values.

a

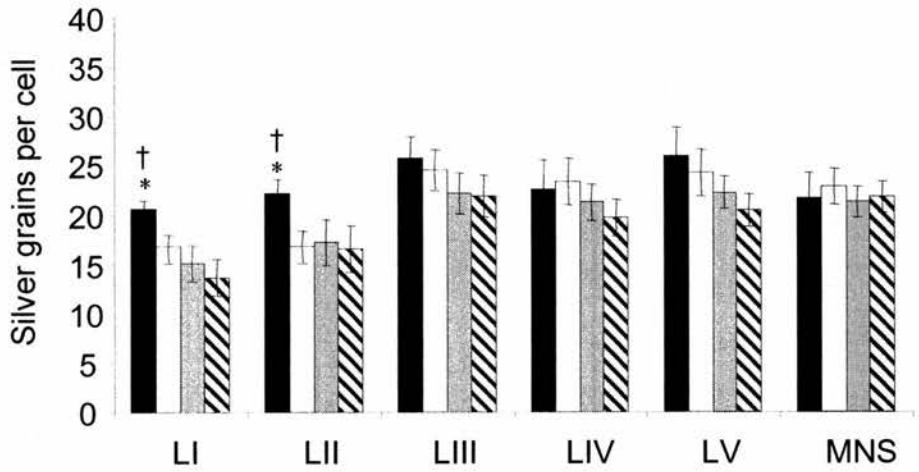
Silver grains per cell
40
35
30
25
20
15
10
5
0
†
*
†
*
LI
LII
LIII
LIV
LV
MNS

b

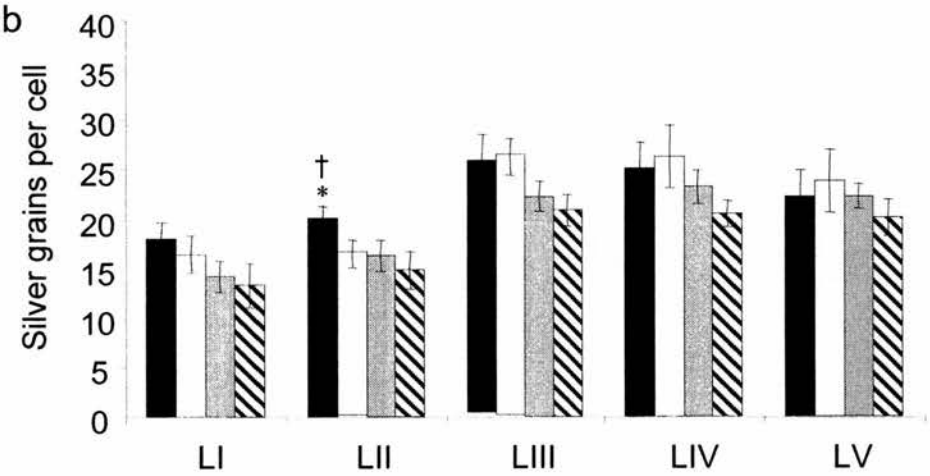
Silver grains per cell
40
35
30
25
20
15
10
5
0
†
*
LI
LII
LIII
LIV
LV

Table 3.2 In situ hybridisation measurement of GRIP2 mRNA expressing cells in the spinal cord following CCI compared to sham-operated and naïve rats

Data represent the mean number of cells (± SEM) expressing GRIP2 mRNA for the mediolateral and lateral dorsal horn laminae I-V (LI-V) and motoneurones (MNS) ipsilateral and contralateral to CCI, compared to sham-operated and naïve samples (n=4 rats, 5 sections per condition for each rat).

There was a significant increase in the number of cells expressing GRIP2 mRNA in the mediolateral superficial dorsal horn LI and II ipsilateral to CCI when compared to the contralateral dorsal horn (*, $p<0.05$, Student's t-test) and when ipsilateral values were compared to sham and naïve values (†, $p<0.05$, One-way ANOVA followed by a Dunnett's test). For all laminae examined, there was no significant difference in the relative expression of GRIP2 mRNA when comparing the contralateral to sham or naïve values, or when comparing sham to naïve values (One-way ANOVA).

GRIP2	Mean number of hybridising cells							
	Mediolateral				Lateral			
	Ipsilateral	Contralateral	Sham	Naïve	Ipsilateral	Contralateral	Sham	Naïve
LI	30.5 ± 1.3*†	25.8 ± 1.9	27.9 ± 1.0	26.3 ± 1.4	28.2 ± 1.4	27.3 ± 2.0	26.8 ± 1.3	26.4 ± 1.7
LII	32.5 ± 1.1*†	27.3 ± 1.8	28.3 ± 0.9	26.8 ± 1.2	30.4 ± 1.7	28.7 ± 1.9	27.2 ± 1.1	28.3 ± 1.6
LIII	29.2 ± 1.1	28.7 ± 2.0	29.9 ± 1.6	30.6 ± 1.4	29.4 ± 1.3	30.9 ± 1.8	34.4 ± 2.3	28.2 ± 2.2
LIV	40.4 ± 1.8	39.3 ± 1.1	44.3 ± 1.9	42.9 ± 2.0	38.6 ± 2.0	39.4 ± 1.3	37.1 ± 1.8	42.5 ± 2.0
LV	39.3 ± 1.6	41.4 ± 1.6	42.4 ± 1.3	44.2 ± 1.1	40.1 ± 0.9	39.8 ± 1.5	38.3 ± 2.0	40.8 ± 1.8
MNS	25.9 ± 1.4	27.2 ± 1.5	29.8 ± 1.9	27.5 ± 1.8				

Figure 3.21 Photomicrographs of GRIP2 mRNA expression in lamina II of the spinal cord of CCI, sham-operated and naïve rats

High power light field photomicrographs showing in situ hybridisation identification of GRIP2 mRNA in the medial zone of the superficial dorsal horn at the site of the most significant changes in lamina II ipsilateral to CCI (a). Corresponding regions are shown contralateral to CCI (b), following sham operation (c) and in naïve animals (d).

Scale bar = 10 μm

a

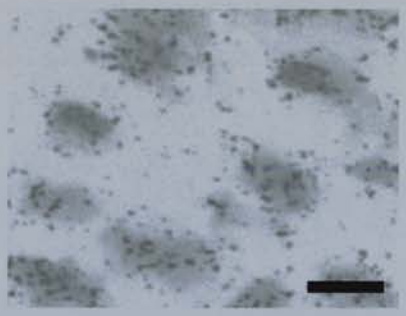

b

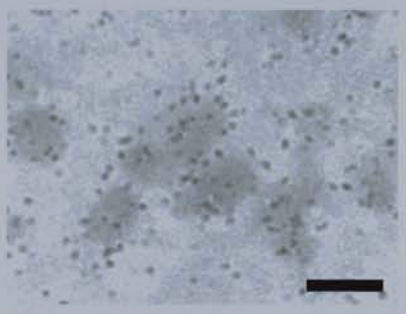

c

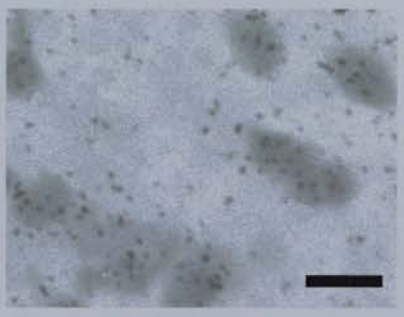

d

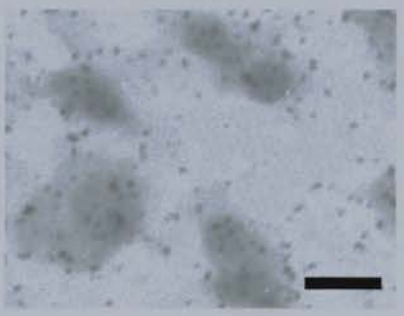

Figure 3.22 In situ hybridisation measurement of NSF mRNA expression per cell in the spinal cord following CCI compared to sham-operated and naïve samples

Data represent the mean density (± SEM) of silver grains per cell expressing NSF mRNA for the mediolateral (a) and lateral (b) dorsal horn laminae I-V (LI-V) and motoneurones (MNS) ipsilateral and contralateral to CCI, compared to sham-operated and naïve animals (n=4 rats, 5 sections per condition for each rat).

Ipsilateral to CCI there was a significant decrease in the number of silver grains per cell in LI and II in the lateral zone only (b) when compared to contralateral levels (*, $p<0.05$ Student's t-test) and when compared to sham and naïve levels (†, $p<0.05$, One-way ANOVA followed by a Dunnett's test). There was no significant variation in the number of silver grains per cell in the lower dorsal horn laminae III-V or in motoneurones following CCI. For all laminae examined, there was no significant difference in the relative expression of NSF mRNA when comparing the contralateral to sham or naïve values, or when comparing sham to naïve values (One-way ANOVA).

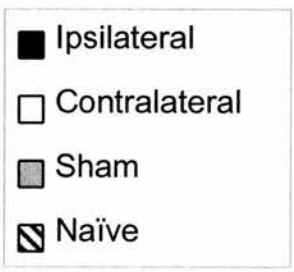

a

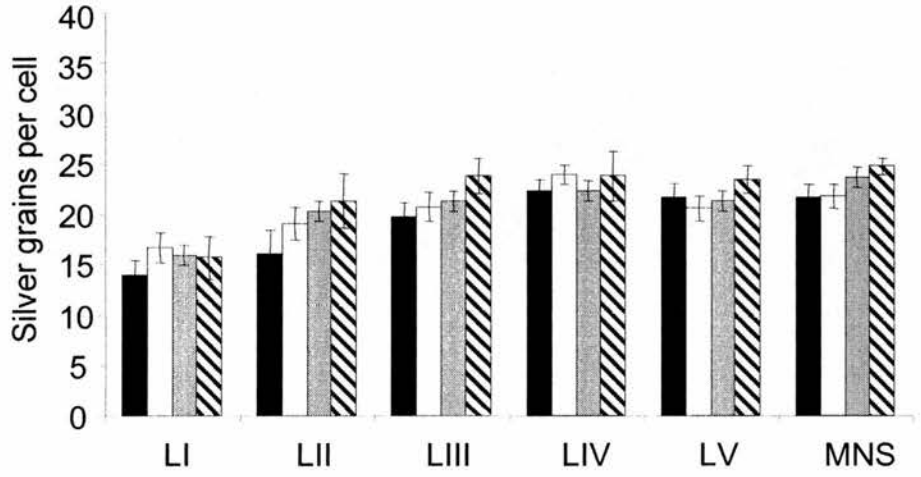
Silver grains per cell
40
35
30
25
20
15
10
5
0
LI
LII
LIII
LIV
LV
MNS

b

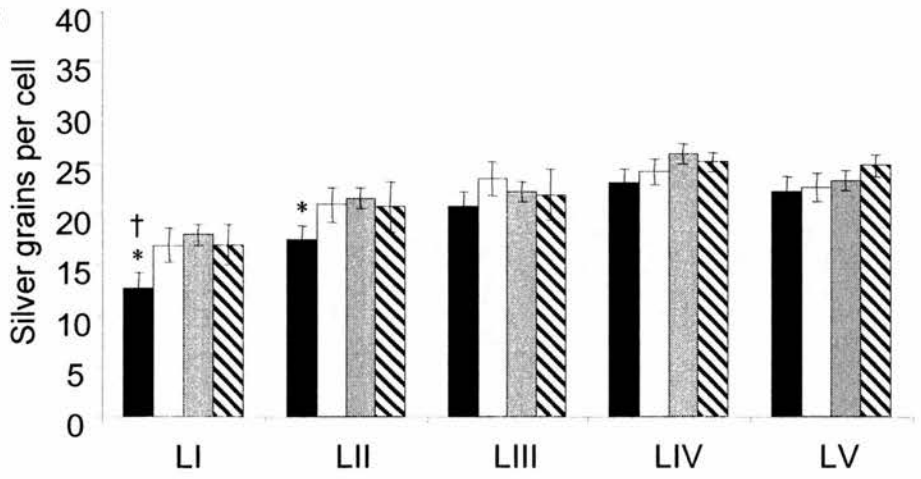
Silver grains per cell
40
35
30
25
20
15
10
5
0
†
*
*
LI
LII
LIII
LIV
LV

Table 3.3 In situ hybridisation measurement of NSF mRNA expressing cells in the spinal cord following CCI compared to sham-operated and naïve rats

Data represent the mean number of cells (± SEM) expressing NSF mRNA for the mediolateral and lateral dorsal horn laminae I-V (LI-V) and motoneurones (MNS) ipsilateral and contralateral to CCI, compared to sham-operated and naïve samples (n=4 rats, 5 sections per condition for each rat).

There was no significant alteration in the number of cells expressing NSF mRNA in the mediolateral superficial dorsal horn LI and II ipsilateral to CCI when compared to the contralateral dorsal horn (Student's t-test) or when compared to sham and naïve levels (One-way ANOVA). For all laminae examined, there was no significant difference in the relative expression of NSF mRNA when comparing the contralateral to sham or naïve values, or when comparing sham to naïve values (One-way ANOVA).

NSF	Mean number of hybridising cells							
	Mediolateral				Lateral			
	Ipsilateral	Contralateral	Sham	Naïve	Ipsilateral	Contralateral	Sham	Naïve
LI	32.3 ± 1.2	35.2 ± 1.8	34.1 ± 2.0	34.7 ± 1.8	31.4 ± 1.6	35.0 ± 1.9	37.8 ± 1.5	33.4 ± 1.8
LII	31.3 ± 2.0	32.8 ± 1.5	33.8 ± 1.7	34.1 ± 1.1	31.5 ± 0.9	33.4 ± 1.1	34.0 ± 1.6	33.7 ± 1.2
LIII	31.9 ± 1.8	36.3 ± 2.1	32.9 ± 2.1	33.8 ± 1.7	32.2 ± 0.8	32.9 ± 1.2	33.8 ± 1.4	33.3 ± 2.0
LIV	42.2 ± 1.5	43.0 ± 0.9	43.3 ± 1.9	40.2 ± 0.8	42.7 ± 1.3	43.4 ± 2.8	39.2 ± 1.8	44.7 ± 1.6
LV	46.0 ± 1.8	44.2 ± 1.9	44.7 ± 1.7	44.3 ± 1.6	44.3 ± 1.9	43.8 ± 1.4	43.6 ± 1.2	45.1 ± 2.3
MNS	27.3 ± 2.3	26.4 ± 2.0	26.7 ± 1.7	26.3 ± 1.4				

Figure 3.23 Photomicrographs of NSF mRNA expression in lamina I of the spinal cord of CCI, sham-operated and naïve rats

High power light field photomicrographs showing in situ hybridisation identification of NSF mRNA in the medial zone of the superficial dorsal horn at the site of the most significant changes in lamina I ipsilateral to CCI (a). Corresponding regions are shown contralateral to CCI (b), following sham operation (c) and in naïve animals (d).

Scale bar = 10 μm

a

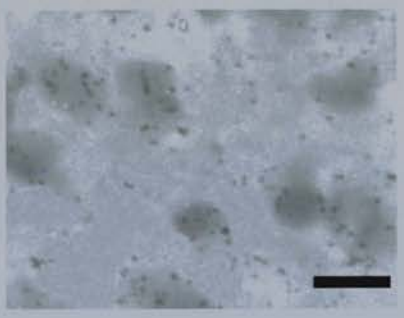

b

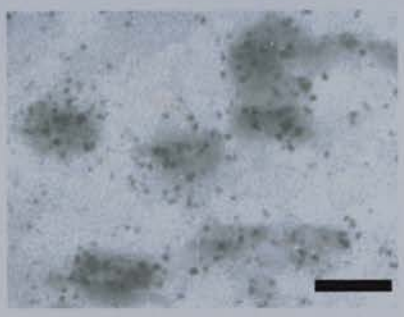

c

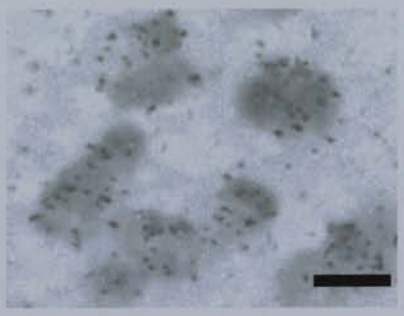

d

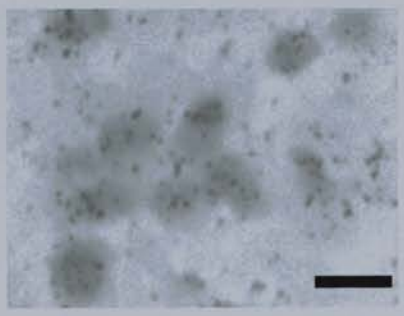

(iv) GluR1

The pattern of constitutive expression of GluR1 mRNA under basal conditions broadly matched that of previous reports (Tölle et al., 1993, Harris et al., 1996) with high expression throughout the dorsal horn especially in LIII-V (Fig. 3.24, (see Section 2.3.1, Table 2.4 and Fig. 2.2 for probe details, pgs. 71-80). There was a slightly lower expression in the ventral horn compared to deep dorsal horn and few labelled cells were found in the white matter. Following CCI, a decrease in the density of GluR1 mRNA ipsilateral to injury was seen specifically in the superficial dorsal horn LI and II in both lateral and mediolateral zones (Fig. 3.24a and b, respectively). In addition, there was a small but significant decrease in the number of cells expressing GluR1 mRNA in the ipsilateral superficial dorsal horn (Table 3.4). A representative example of this lateral LII decrease in GluR1mRNA ipsilateral to CCI is shown in Figure 3.25a in comparison to corresponding regions contralateral to CCI (Fig. 3.25b), and in sham-operated (Fig. 3.25c) and naïve (Fig. 3.25d) animals. The level of GluR1 mRNA did not significantly differ between contralateral, sham-operated and naïve animals.

(v) Narp

The constitutive level of Narp mRNA expression in the superficial dorsal horn LI and II was low under normal conditions and was predominantly concentrated in LIII/IV. Relatively low expression was observed in ventral horn, and motoneurones were labelled. Ipsilateral to CCI injury, there was a marked increase in the expression of Narp mRNA in the superficial dorsal horn laminae I and II in both mediolateral and lateral zones (Fig. 3.26 a and b), with examples represented in Figure 3.27, while there was no change in expression of Narp mRNA in contralateral, sham-operated or naïve dorsal horn samples. The ipsilateral increase was seen in both the density of Narp mRNA (Fig. 3.26) and in the number of cells expressing Narp mRNA (Table 3.5).

These data indicated a differential regulation of the AMPA receptor subunits GluR1 and GluR2 in the spinal cord following the establishment of neuropathy, as GluR1

was apparently downregulated in the superficial dorsal horn, while GluR2 mRNA levels increased. In addition, while NSF was diminished in the dorsal horn of the spinal cord following CCI, there was a marked increase in the levels of GRIP and Narp mRNA expression.

Figure 3.24 In situ hybridisation measurement of GluR1 mRNA expression per cell in the spinal cord following CCI compared to sham-operated and naïve rats

Data represent the mean density (± SEM) of silver grains per cell expressing GluR1 mRNA for the mediolateral (a) and lateral (b) dorsal horn laminae I-V (LI-V) and motoneurones (MNS) ipsilateral and contralateral to CCI, compared to sham-operated and naïve animals (n=4 rats, 5 sections per condition for each rat).

Ipsilateral to CCI, there was a significant decrease in the number of silver grains per cell in LI and II in the lateral zone only (b) when compared to contralateral levels (*, $p<0.05$ Student's t-test) and when compared to sham and naïve levels (†, $p<0.05$, One-way ANOVA followed by a Dunnett's test). In addition there was a moderate decrease in the number of silver grains per cell in LIII when compared to contralateral values only (*, $p<0.05$, Student's t-test). There was no significant variation in the number of silver grains per cell in the lower dorsal horn laminae IV-V or in motoneurones following CCI (One-way ANOVA). For all laminae examined, there was no significant difference in the relative expression of GluR1 mRNA when comparing the contralateral to sham or naïve values, or when comparing sham to naïve values (One-way ANOVA).

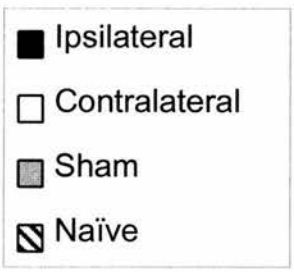

a

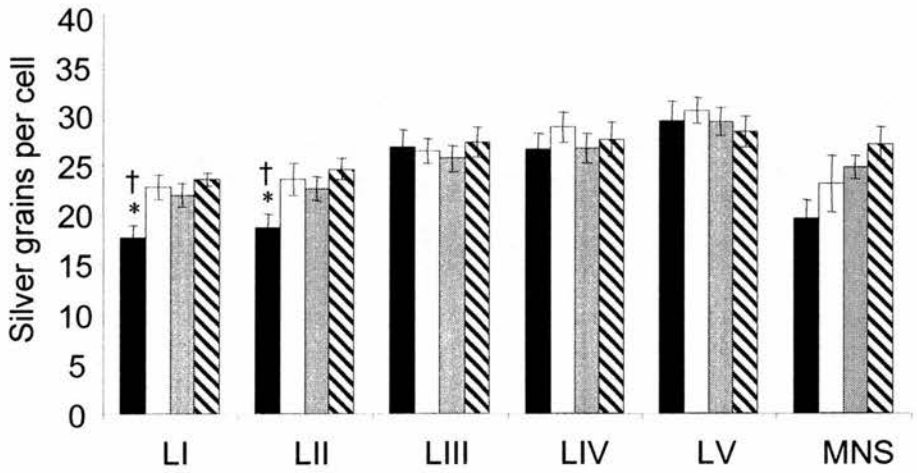
Silver grains per cell
40
35
30
25
20
15
10
5
0
†
*
†
*
LI
LII
LIII
LIV
LV
MNS

b

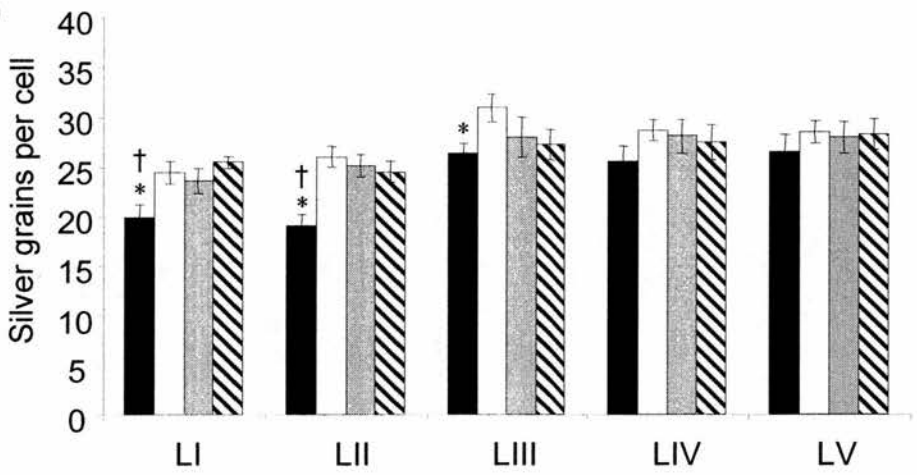
Silver grains per cell
40
35
30
25
20
15
10
5
0
†
*
†
*
*
LI
LII
LIII
LIV
LV

Table 3.4 In situ hybridisation measurement of GluR1 mRNA expressing cells in the spinal cord following CCI and compared to sham-operated and naïve rats

Data represent the mean number of cells (± SEM) expressing GluR1 mRNA for the mediolateral and lateral dorsal horn laminae I-V (LI-V) and motoneurones (MNS) ipsilateral and contralateral to CCI, compared to sham-operated and naïve samples (n=4 rats, 5 sections per condition for each rat).

There was a significant decrease in the number of cells expressing GluR1 mRNA in the mediolateral superficial dorsal horn LI and II ipsilateral to CCI when compared to the contralateral dorsal horn (*, $p<0.05$, Student's t-test) and when compared to sham and naïve levels (†, $p<0.05$, One-way ANOVA followed by a Dunnett's test). For all laminae examined, there was no significant difference in the relative expression of GluR1 mRNA when comparing the contralateral to sham or naïve values, or when comparing sham to naïve values (One-way ANOVA).

GluR1	Mean number of hybridising cells							
	Mediolateral				Lateral			
	Ipsilateral	Contralateral	Sham	Naïve	Ipsilateral	Contralateral	Sham	Naïve
LI	29.1 ± 1.7*†	35.8 ± 2.1	33.6 ± 1.8	37.3 ± 1.0	17.2 ± 1.3 *	28.0 ± 1.5	30.9 ± 1.8	29.3 ± 1.1
LII	28.2 ± 1.5*†	33.1 ± 2.4	35.9 ± 1.6	35.8 ± 0.9	20.5 ± 1.8	22.1 ± 1.3	21.6 ± 1.7	21.8 ± 0.9
LIII	35.6 ± 1.1	39.9 ± 1.5	38.3 ± 1.8	30.8 ± 1.2	33.4 ± 1.8	32.5 ± 1.1	31.4 ± 2.0	30.8 ± 1.5
LIV	41.5 ± 1.5	41.5 ± 1.1	39.8 ± 1.4	41.2 ± 1.0	40.5 ± 0.8	41.9 ± 1.0	43.2 ± 2.1	41.3 ± 1.5
LV	42.2 ± 1.4	44.0 ± 0.4	44.3 ± 2.0	41.7 ± 0.8	41.7 ± 2.5	40.0 ± 1.1	42.9 ± 1.4	41.7 ± 0.8
MNS	18.6 ± 1.3	23.3 ± 1.0	21.3 ± 1.5	20.9 ± 0.9				

Figure 3.25 Photomicrographs of GluR1 mRNA expression in lamina II of the spinal cord of CCI, sham-operated and naïve rats

High power light field photomicrographs showing in situ hybridisation identification of GluR1 mRNA in the medial zone of the superficial dorsal horn at the site of the most significant changes in lamina I ipsilateral to CCI (a). Corresponding regions are shown contralateral to CCI (b), following sham operation (c) and in naïve animals (d).

Scale bar = 10 μm

a

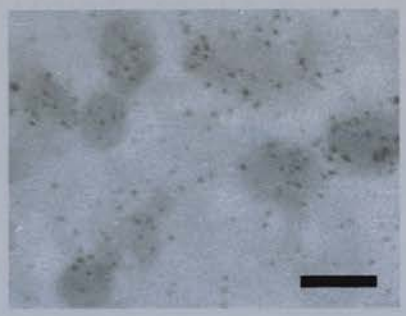

b

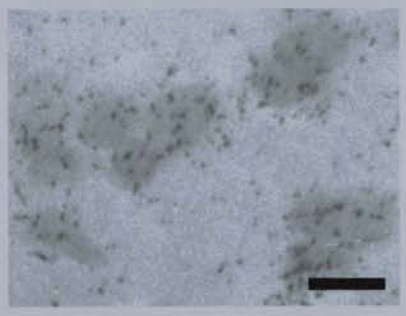

c

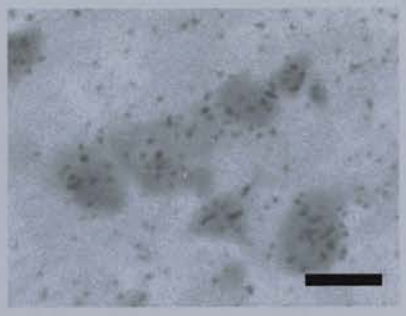

d

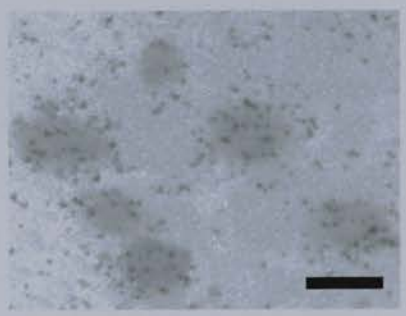

Figure 3.26 In situ hybridisation measurement of Narp mRNA expression per cell in the spinal cord following CCI compared to sham-operated and naïve rats

Data represent the mean density (± SEM) of silver grains per cell expressing Narp mRNA for the mediolateral (a) and lateral (b) dorsal horn laminae I-V (LI-V) and motoneurones (MNS) ipsilateral and contralateral to CCI, compared to sham-operated and naïve animals (n=4 rats, 5 sections per condition for each rat).

Ipsilateral to CCI, there was a significant increase in the number of silver grains per cell in LI and II in both mediolateral and lateral zones when compared to contralateral levels (*, $p<0.05$ Student's t-test) and when compared to sham and naïve levels (†, $p<0.05$, One-way ANOVA followed by a Dunnett's test). There was no significant variation in the number of silver grains per cell in the lower dorsal horn laminae III-V or in motoneurones following CCI (One-way ANOVA). For all laminae examined, there was no significant difference in the relative expression of Narp mRNA when comparing the contralateral to sham or naïve values, or when comparing sham to naïve values (One-way ANOVA).

a

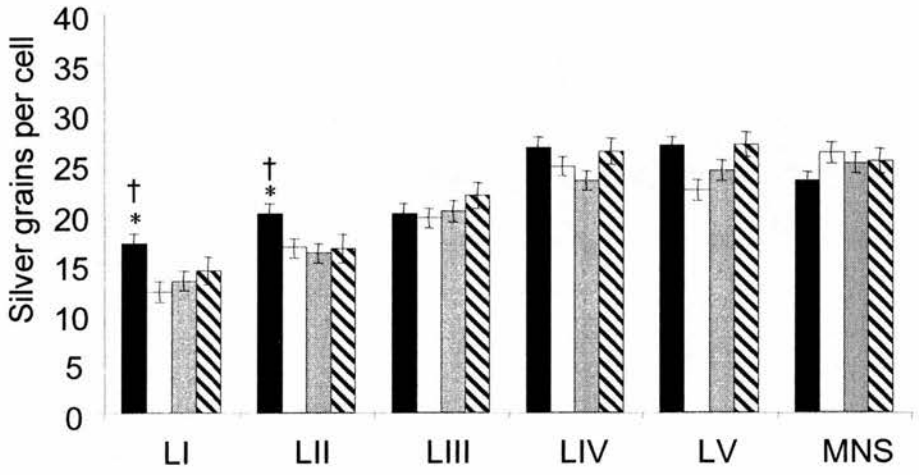
Silver grains per cell
40
35
30
25
20
15
10
5
0
†
*
†
*
LI
LII
LIII
LIV
LV
MNS

b

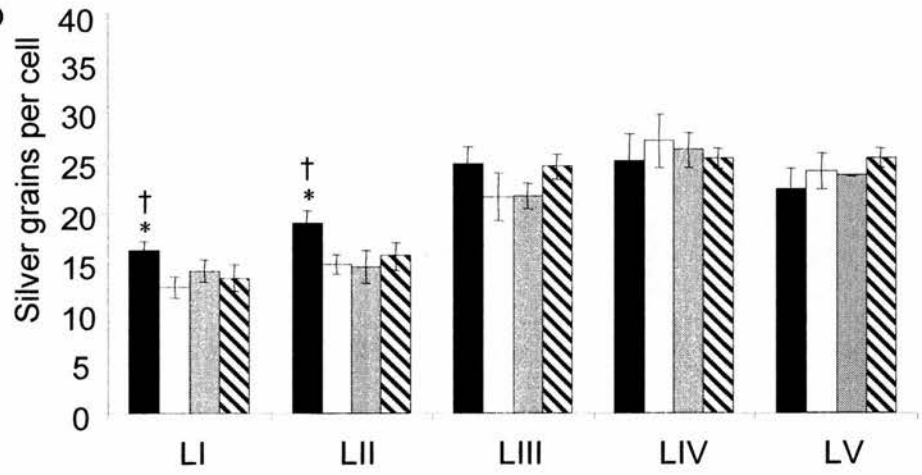
Silver grains per cell
40
35
30
25
20
15
10
5
0
†
*
†
*
LI
LII
LIII
LIV
LV

Table 3.5 In situ hybridisation measurement of Narp mRNA expressing cells in the spinal cord following CCI compared to sham-operated and naïve rats

Data represent the mean number of cells (± SEM) expressing Narp mRNA for the mediolateral and lateral dorsal horn laminae I-V (LI-V) and motoneurones (MNS) ipsilateral and contralateral to CCI, compared to sham-operated and naïve animals (n=4 rats, 5 sections per condition for each rat).

There was a significant increase in the number of cells expressing Narp mRNA in the mediolateral and lateral superficial dorsal horn LI and II ipsilateral to CCI when compared to the contralateral dorsal horn (*, $p<0.05$, Student's t-test) and compared to sham and naïve levels (†, $p<0.05$, One-way ANOVA followed by a Dunnett's test). For all laminae examined, there was no significant difference in the relative expression of Narp mRNA when comparing the contralateral to sham or naïve values, or when comparing sham to naïve values (One-way ANOVA).

Narp	Mean number of hybridising cells							
	Mediolateral				Lateral			
	Ipsilateral	Contralateral	Sham	Naïve	Ipsilateral	Contralateral	Sham	Naïve
LI	34.5 ± 1.7*†	27.8 ± 1.1	25.4 ± 1.3	26.3 ± 0.8	35.8 ± 1.6 *	24.2 ± 1.0	25.0 ± 1.7	27.9 ± 2.1
LII	34.8 ± 1.4*†	28.5 ± 1.6	27.0 ± 1.8	27.7 ± 1.9	36.7 ± 1.4 *	25.9 ± 1.7	24.3 ± 1.4	26.1 ± 1.8
LIII	28.2 ± 2.0	26.9 ± 1.7	27.1 ± 1.4	27.3 ± 2.2	26.3 ± 1.9	27.0 ± 1.6	30.3 ± 2.0	25.9 ± 2.3
LIV	40.4 ± 1.9	42.3 ± 2.1	39.7 ± 0.9	38.9 ± 0.6	37.1 ± 2.0	36.4 ± 0.8	40.8 ± 1.5	37.2 ± 1.4
LV	38.5 ± 1.7	36.3 ± 2.6	39.3 ± 1.9	40.3 ± 1.6	33.8 ± 1.9	34.8 ± 2.2	36.4 ± 1.7	38.3 ± 1.6
MNS	23.0 ± 1.1	25.3 ± 1.8	24.7 ± 2.1	25.5 ± 1.4				

Figure 3.27 Photomicrographs of Narp mRNA expression in lamina II of the spinal cord of CCI, sham-operated and naïve rats

High power light field photomicrographs showing in situ hybridisation identification of Narp mRNA expression in the medial zone of the superficial dorsal horn at the site of the most marked changes in lamina II ipsilateral to CCI (a). Corresponding regions are shown contralateral to CCI (b), following sham operation (c) and in naïve animals (d).

Scale bar = 10 μm

a

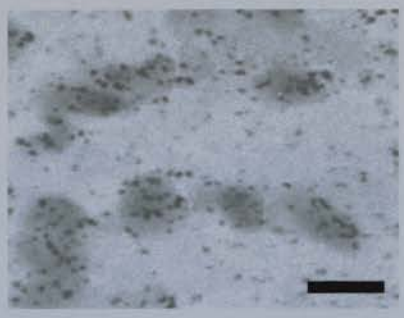

b

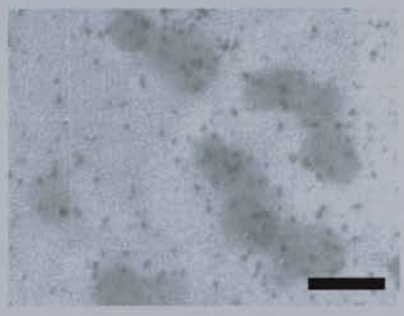

c

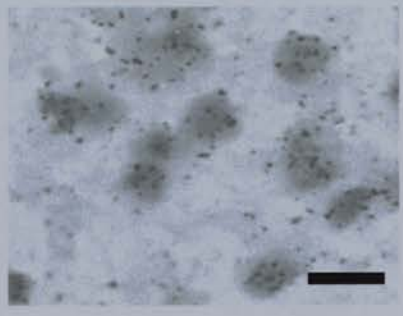

d

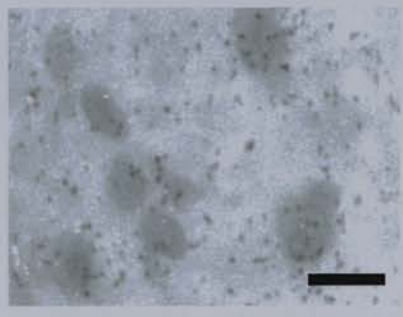

3.2.4 Immunoblotting for AMPA receptor and associated proteins

In order to further examine expression levels following CCI, semi-quantitative protein analysis was carried out using Western blotting for GluR2, GRIP, NSF, PICK1 and SAP97 ipsilateral and contralateral to CCI injury and compared to sham-operated and naïve spinal cord levels (see Section 2.2.6 and antibody details in Table 2.2, pgs. 64-68). Expression levels were compared to that of GAPDH, a ubiquitous and constitutively expressed housekeeping enzyme, the expression of which does not change following peripheral nerve damage (see Chapter 2, section 2.2.6 (*v*)).

Spinal cord segments L4-6 were hemisected into ipsilateral and contralateral sides for animals following CCI at the peak of neuropathy and sham and naïve animals were used as controls. We found that levels of GluR2 (Fig. 3.28 a, lane 1 'I') and GRIP (Fig. 3.28b, lane 1 'I') were significantly increased in the spinal cord ipsilateral to injury with little variation in protein levels between contralateral ('C'), sham ('S') and naïve ('N') samples. Blots were stripped and reprobed for GAPDH (lower panels) to ensure equivalent sample loading (as was also confirmed by Coomassie staining of proteins). These increases in protein levels of GluR2 and GRIP are in agreement with our results of the mRNA by ISHH for these molecules that also significantly increased ipsilateral to CCI (Fig. 3.18 and 3.20, respectively).

No significant difference was seen in the levels of either PICK1 (Fig. 3.28c) or the GluR1-interacting protein, SAP97 (Fig. 3.29) under the same conditions. In contrast to this, and in agreement with mRNA analysis for NSF (Fig. 3.22) levels of NSF protein (Fig. 3.28d) were slightly decreased ipsilateral to injury ('I') compared to contralateral side and sham and normal controls. Again GAPDH served as an internal control. These data indicate that while GluR2 and GRIP protein levels are increased following peripheral nerve injury, there is a decrease in the overall levels of NSF ipsilateral to injury, with no apparent change in PICK1 or SAP97 protein.

Figure 3.28 Western blot analysis of GluR2, GRIP, PICK1 and NSF in the spinal cord following CCI compared to sham-operated and naïve samples

Western blot analysis (n=3) of GluR2 (a), GRIP (b), PICK1 (c) and NSF (d) in spinal cord lysate ipsilateral ('I') and contralateral ('C) to CCI in comparison to sham-operated ('S') and naïve ('N') samples. The ubiquitous housekeeping enzyme GAPDH was used as an internal control in each case (lower panels).

Densitometric analysis (e) indicated that there was a significant increase in the levels of GluR2 and GRIP protein in the ipsilateral spinal cord when compared to the contralateral side (*, $p<0.05$, Student's t-test), while there was no significant difference in the levels of GluR2 or GRIP protein in the contralateral compared to either sham or naïve spinal cord extract. There was no significant change in the levels of PICK1 protein in response to CCI. A small though significant decrease in the levels of NSF protein was seen ipsilateral to CCI when compared to the contralateral spinal cord (*, $p<0.05$, Student's t-test) while there was no significant difference in contralateral, sham or naïve levels. The minor additional bands seen in some samples, particularly with the NSF and GluR2 antibodies, were not consistent findings and are likely to represent non-specific interactions.

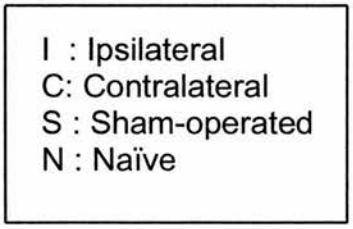

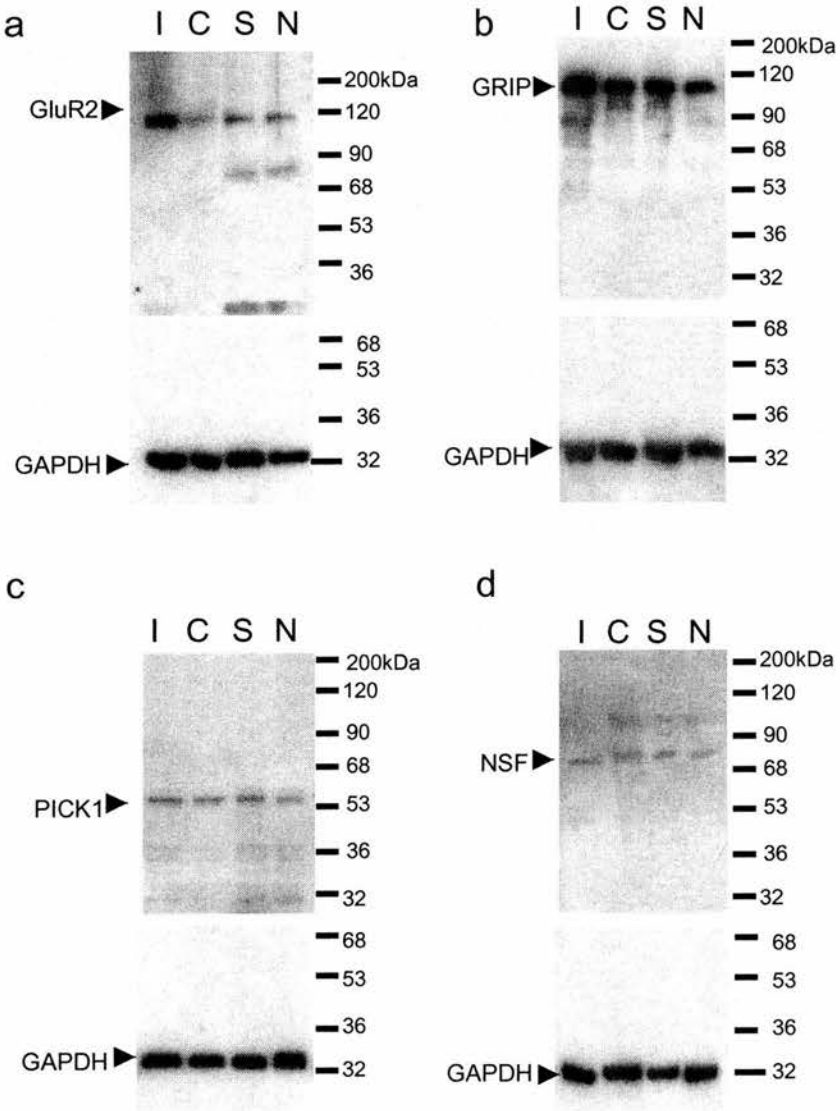

e

Densitometric analysis of the expression of GluR2 and GluR2-interacting proteins in the spinal cord as a % of GAPDH expression

	Ipsilateral CCI	Contralateral CCI	Sham	Naïve
GluR2	55.8 ± 1.9 *	41.6 ± 2.9	43.2 ± 2.9	43.5 ± 3.4
GRIP	126.6 ± 3.5*	98.9 ± 3.1	96.4 ± 2.5	97.8 ± 3.8
PICK1	17.5 ± 2.6	15.4 ± 2.4	14.1 ± 2.2	17.4 ± 2.8
NSF	08.5 ± 2.0*	11.2 ± 1.8	12.4 ± 6.5	14.3 ± 4.5

Figure 3.29 Western blot analysis of the GluR1-interacting protein SAP97 in the spinal cord following CCI compared to sham-operated and naïve samples

Western blot analysis of SAP97 (a) in spinal cord lysate ipsilateral ('I') and contralateral ('C) to CCI in comparison to sham-operated ('S') and naïve ('N') samples. The ubiquitous housekeeping enzyme GAPDH was used as an internal control (lower panels).

Densitometric analysis (b) indicated that there was no significant change in the levels of SAP97 in response to CCI and there was no significant difference in contralateral, sham or naïve levels. The minor additional bands seen in some samples were not consistent findings and are likely to represent non-specific interactions.

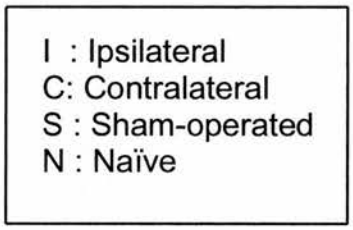

a

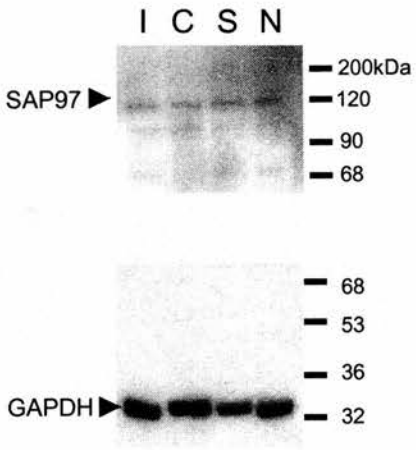

b

Densitometric analysis of the expression of the GluR1-interacting protein SAP97 in the spinal cord as a % of GAPDH expression				
	Ipsilateral CCI	Contralateral CCI	Sham	Naïve
SAP97	41.2 ± 4.3	40.3 ± 3.9	37.7 ± 1.6	41.6 ± 4.6

3.2.5 Direct association of GluR2 with GRIP and PICK1

In order to investigate direct association between GluR2 and GRIP and PICK1 in the spinal cord, we carried out a pilot experiment (n=2) with GluR2 immunoprecipitations on spinal cord extracts solubilised under relatively mild detergent conditions (see methodology in Section 2.3.2 and antibody details in Table 2.2, pgs. 67, 81-83). Extracts were immunoprecipitated with a pan-GluR2 antibody (directed against an N-terminal epitope) before probing Western blots for levels of the GluR2 C-terminus-interacting proteins GRIP and PICK1 (See Fig. 3.30).

Whereas ISSH and Western blot analysis of GRIP in whole lysate of spinal cord following CCI showed an ipsilateral increase, the amount of GRIP associated with GluR2 appeared to diminish bilaterally following CCI (Fig. 3.30b). Similarly, the amount of PICK1 associated with GluR2 appeared to decrease after CCI, but in this case selectively on the ipsilateral side (Fig. 3.30d). GluR2 was used in each case as an internal control for GRIP and PICK1 (Fig. 3.30a and c, respectively). Since the levels of GRIP and PICK1 immunoreactivity associated with these immunoprecipitates were extremely low, a degree of caution is needed in the interpretation of these results. We next examined the possibility that the amount of GRIP and PICK1 present in the membrane fraction of the spinal cord (and thus available to interact with GluR2 receptors) might be altered in response to the GluR2 activation that is likely to occur in CCI or other intense afferent stimulation (see Section 3.2.6).

Figure 3.30 Association of GRIP and PICK1 with GluR2 immunoprecipitates from spinal cord of CCI and naïve rats

Proteins were solubilised from spinal cord samples under mild detergent conditions and immunoprecipitated for GluR2 using an N-terminally-directed antibody followed by collection with Protein G-Sepharose. Following SDS-PAGE and transfer to PVDF, membranes were probed for the presence of GRIP and PICK1 immunoreactivity and for GluR2, using an independent antibody from that used in the immunoprecipitation.

(a) shows the levels of GluR2 in the GluR2-directed immunoprecipitates as a control for (b) which shows that ipsilateral to CCI ('I'), there was an apparent decrease in the amount of GRIP associated with the GluR2 receptor (see table, e) when compared to the contralateral ('C') of naïve samples ('N'). Non-immune IgG ('NI IgG') or IP buffer only (buffer) served as negative controls.

(c) shows the levels of GluR2 in the GluR2-directed immunoprecipitates as a control for (d) which shows that, ipsilateral to CCI, there was also an apparent decrease in the levels of PICK1 protein associated with the GluR2 subunit in the spinal cord ('I') when compared to the contralateral ('C') or naïve ('N') samples. Again, non-immune IgG ('NI IgG') or IP buffer only (buffer) served as negative controls.

(e) Densitometric analysis of the association of GRIP/PICK1 with GluR2 immunoprecipitates. Data are expressed as the density grey scale of GRIP or PICK1 immunoreactive bands as a percentage of corresponding GluR2 immunoreactivity in the same samples. Values are the means (with individual values in parentheses) from two independent experimental series based on tissue from 2 and 3 CCI animals respectively.

I : Ipsilateral
C: Contralateral
N : Naïve

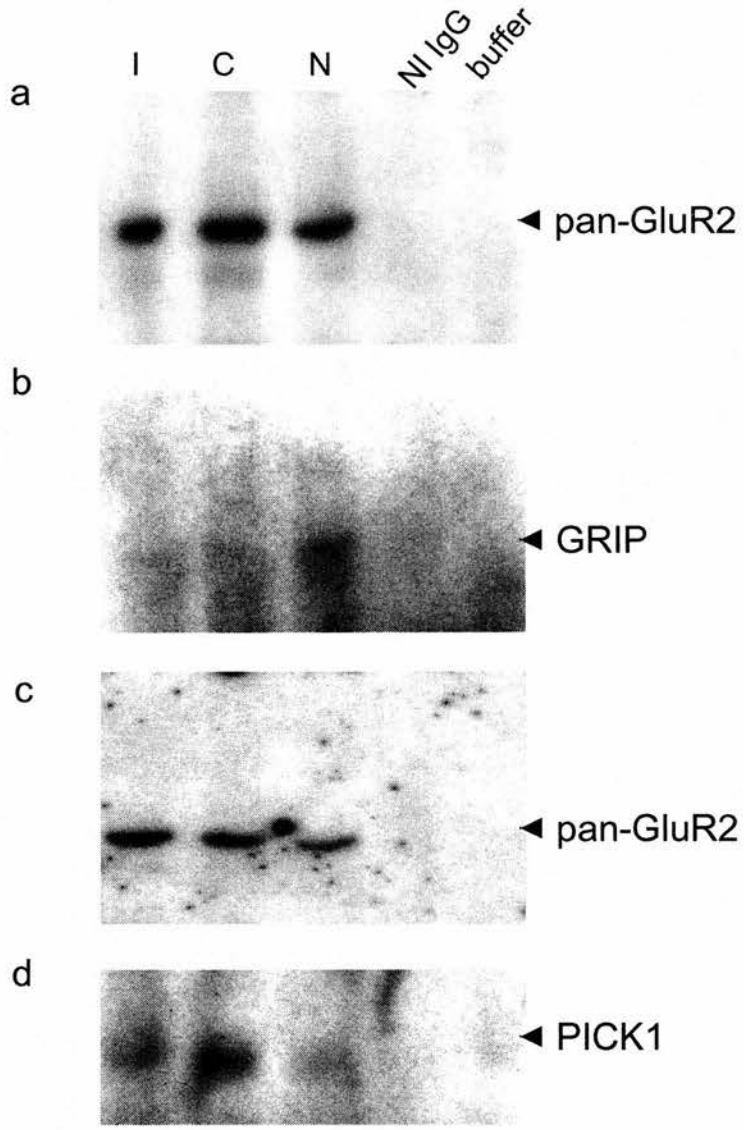

e

% Association of GRIP and PICK1 with GluR2 in GluR2 directed membrane immunoprecipitations		
	GRIP	PICK1
Ipsilateral CCI	20.0 (15/25.0)	46.7 (48.5/44.8)
Contralateral CCI	21.6 (24.7/18.4)	111.8 (125.3/98.3)
Normal	98.6 (116.5/80.7)	88.6 (104.0/73.2)

3.2.6 Alterations in the subcellular distribution of GRIP and PICK1 in spinal cord following topical AMPA treatment

Given the apparent decrease in the levels of both GRIP and PICK1 associated with the GluR2 subunit of AMPA receptor ipsilateral to CCI, we examined any alterations in the proportion of GRIP and PICK1 at the membrane and in the cytosol in response to AMPA receptor stimulation. Membrane and cytosolic preparations originating from the same spinal cord homogenates were used to assess GRIP and PICK1 immunoreactivity (see Section 2.3.2 and antibody details in Table 2.2, pgs. 67, 82-83). AMPA was topically administered to the dorsal surface of the spinal cord in naïve, anaesthetised rats. In whole spinal cord lysate the levels of both GRIP and PICK1 were similar in either saline or AMPA-treated animals (Fig. 3.31).

Interestingly, in membrane preparations, there was a significant decrease in the amount of GRIP associated with the membrane after AMPA receptor stimulation when compared to saline treatment, while there was little effect of AMPA receptor stimulation on the levels of cytosolic GRIP (Fig. 3.31). A similar effect was found for PICK1 protein levels, with a significant decrease in membrane-bound PICK1 in response to spinal AMPA receptor stimulation with little alteration in cytosolic PICK1 protein levels (Fig. 3.31).

So, under normal conditions, there appeared to be a similar membrane and cytosolic content of both proteins in the spinal cord. However, following AMPA receptor stimulation there was a significant movement of both GRIP and PICK1 from the membrane to the cytosol. This may indicate that following excessive AMPA receptor stimulation, such as following direct activation via agonist activity or following CCI, GRIP and PICK1 may no longer be associated with GluR2, at least at membrane sites in the postsynaptic density.

Figure 3.31 Investigation of the translocation of GRIP and PICK1 from the membrane to the cytosol following AMPA receptor activation in naïve rats

Western blots for (a) GRIP and (b) PICK1 following topical application of either AMPA (500µl of 50µM AMPA in saline) or saline vehicle to the dorsal surface of the spinal cord. Whole spinal cord lysates showed no apparent difference in expression levels of GRIP or PICK1 following either saline vehicle or AMPA topical administration. Samples of the spinal cord homogenate from which the whole lysates were prepared were centrifuged at 12, 000 x g for 30 min at 4°C to prepare corresponding membrane and cytosolic fractions. Membrane preparations showed a marked reduction in the content of GRIP and PICK1 following AMPA receptor stimulation in comparison to saline vehicle treatment.

Cytosolic preparations showed similar levels of the content of both proteins following either saline or AMPA topical application.

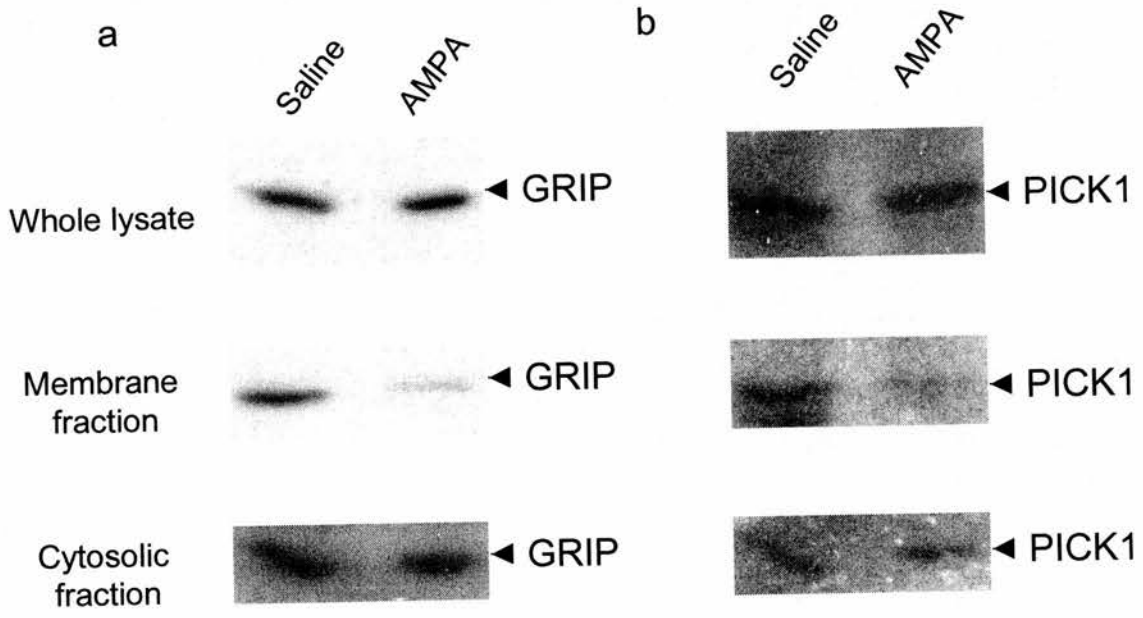
a
Saline
AMPA
Whole lysate
GRIP
Membrane fraction
GRIP
Cytosolic fraction
GRIP
b
Saline
AMPA
PICK1
PICK1
PICK1

3.2.7 Measurement of GluR1 phosphorylation in response to CCI in GluR1 immunoprecipitates

AMPA receptors can be modulated by phosphorylation and specifically the AMPA receptor interacting proteins' ability to bind to the receptor may be regulated by kinases such as PKA, CaMKII and PKC. We have shown (Fig. 3.29) that the levels of the GluR1-interacting protein SAP97 did not appear to be altered following CCI. Nevertheless, SAP97 may function to bring PKA into close proximity with GluR1 via AKAP79/150 (Colledge et al., 2000) and thereby might potentially serve to facilitate GluR1 phosphorylation at the PKA target site in The GluR1 C-terminus, Ser^{845}. In order to assess whether the phosphorylation state of the GluR1 subtype of the AMPA receptor was altered following CCI, we utilised phospho-specific antibodies for key channel-regulating residues in GluR1 at Ser^{831} and Ser^{845} (CaMKII and PKA targets, respectively, see Section 2.3.2 and antibody details in Table 2.2, pgs 67, 83).

There was a consistent decrease in the levels of pan-GluR1 immunoreactivity ipsilateral to injury when compared to contralateral, sham or naïve spinal cord (Fig. 3.32a (i) and b). In contrast, levels of phospho-Ser^{831}-GluR1 immunoreactivity increased ipsilateral to injury when compared to contralateral, sham or naïve spinal cord (Fig. 3.32a (ii) and b). There were, however, no consistently detectable alterations in the levels of phospho-Ser^{845}-GluR1 immunoreactivity as a consequence of CCI (Fig. 3.30b).

Figure 3.32 Immunoblots for phospho-Ser^{831}-GluR1, phospho-Ser^{845}-GluR1 and pan-GluR1 in GluR1 immunoprecipitates from rats following CCI surgery

Western blot analysis of hemisected spinal cord pan-GluR1 immunoprecipitates following sciatic nerve CCI induced 12 days previously. Spinal cord extracts were immunoprecipitated with a pan-GluR1 antibody before probing blots for levels of phospho-Ser^{831}-GluR1, phospho-Ser^{845}-GluR1 or pan-GluR1 immunoreactivity.

Immunoprecipitates probed with the pan-GluR1 antibody showed a decrease in levels of GluR1 in the spinal cord ipsilateral to CCI injury a) (i) lane A when compared to the contralateral (lane B) sham (lane C and D) and naïve (lane E) samples. Lane 'F' is a direct lysate of naïve spinal cord to confirm the correct protein molecular weight and demonstrates the increase in intensity of GluR1 signal following immunoprecipitation with the GluR1 antibody. a) (ii) shows levels of phospho-Ser^{831}-GluR1 immunoreactivity in the same samples. There was a consistent increase in the ratio of phospho-Ser^{831}-GluR1: pan GluR1 immunoreactivity in the spinal cord ipsilateral to CCI (lane 'A') when compared to contralateral, sham and naïve immunoprecipitates (lanes B, C, D and E, respectively).

Only low levels of phospho-Ser^{845}-GluR1 immunoreactivity could be detected and no consistent changes were observed. Non-specific bands seen at ~40-70 kDa represent secondary antibody cross-reactivity with the immunoprecipitating IgG and were similar in all samples and in extract-free blanks. b) shows independent confirmation of the reduced levels of GluR1 immunoreactivity ipsilateral to CCI.

A: CCI Ipsi
B: CCI Contra
C: Sham Ipsi
D: Sham Contra
E: Naïve
F: Naïve, direct Western blot

a (i)

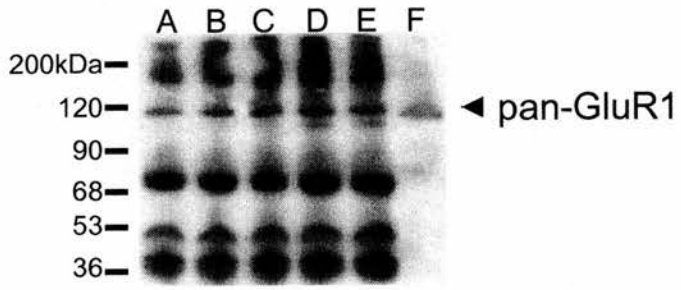
A B C D E F
200kDa
120
90
68
53
36
pan-GluR1

a (ii)

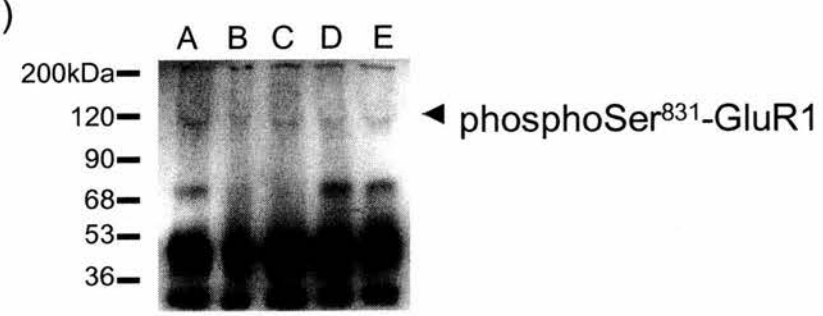
A B C D E
200kDa
120
90
68
53
36
phosphoSer831-GluR1

b

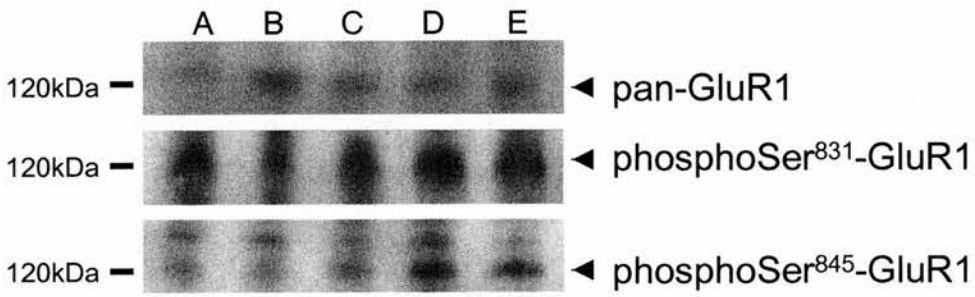
A B C D E
120kDa
pan-GluR1
120kDa
phosphoSer831-GluR1
120kDa
phosphoSer845-GluR1

3.3: Discussion

AMPA receptors in the superficial horn of the spinal cord mediate fast nociceptive transmission under normal conditions and so can contribute to acute nociceptive inputs (Yoshimura and Jessel 1990). Administration of AMPA depolarises nociceptive neurones in the spinal cord and increases responses from noxious and innocuous stimulation (Zhou, Bonasera and Carlton, 1996) and AMPA receptor antagonists can disrupt acute nociceptive processing (Aaonensen, Lei and Wilcox, 1990; Mao et al., 1992a; Procter et al., 1998; Paleckova et al., 1992).

AMPA receptor antagonists also prevent both hyperalgesia and allodynia following CCI (Mao et al., 1992a; Budai and Larson, 1994; Cumberbatch, Chizh and Headley, 1994; Harris et al., 1996). Studies utilising the intrathecal injection of AMPA receptor antagonists confirmed this, whereby NBQX, NS-257 and SYM 2206 showed a dose-dependent and reversible inhibition of neuropathic hyperalgesia with less marked, but still clear effects on mechanical allodynia. This may be consistent with reports that co-activation of AMPA and metabotropic receptors are required for the development of mechanical allodynia (Meller, Dykstra and Gebhart, 1993). Subunit selective antagonists are limited at this time, although a recent report suggests that Joro spider toxin, a Ca^{2+}-permeable AMPA/kainate receptor antagonist, may alleviate mechanical allodynia in a model of secondary hyperalgesia (Sorkin, Yaksh and Doom, 1999).

It has been previously shown that GluR1 and GluR2 mRNA and immunoreactivity are expressed in the dorsal horn of the spinal cord predominantly in laminae I and II. We confirmed this in the present study using in situ hybridisation. Quantitative analysis indicated that there was a significant increase in the density of GluR2 mRNA in spinal cord LI and II cells from rats at the peak of behavioural reflex sensitivity, while there was no significant change in the number of cells expressing GluR2 mRNA in this region. Similarly, Western blot analysis of whole spinal cord lysate from rats following CCI, confirmed the increase in GluR2 at the protein level.

In contrast to one previous report (Harris et al., 1996), we found a decrease in the density and number of cells labelling for GluR1 mRNA ipsilateral to CCI specifically in LI and II, although basal levels of GluR1 expression matched those of previous reports (Harris et al., 1996; Al Ghoul et al., 1993; Popratiloff, Weinberg and Rustioni, 1998). The reason for this discrepancy is unclear. Inflammation, deafferentation and contusive spinal cord injury have all been reported to cause a downregulation of GluR1 subunits (Pellegrini-Giampietro et al., 1994; Helgren et al., 1999; Florenzano and DeLuca, 1999; Grossman et al., 1999). Harris et al. (1996) carried out immunohistochemistry studies in the spinal cord following CCI and found a specific superficial dorsal horn increase in GluR1 immunoreactivity. Western blot analysis carried out here agreed with the in situ data and indicated a decrease in GluR1 levels. It is possible that the Western blot analysis of whole spinal cord homogenate masked a lamina-specific alteration in GluR1 levels in ipsilateral dorsal horn. However, as mentioned, regionally identified GluR1 mRNA levels were also diminished ipsilateral to CCI. While alterations in mRNA do not necessarily imply similar alterations in protein levels, the consistent decrease in both GluR1 protein and mRNA in the ipsilateral dorsal horn following CCI here seems to be at odds with the report of Harris et al. (1996).

The functional impact of blocking the shared GRIP/PICK1 site on the GluR2 C-terminus was examined by the intrathecal injection of a myristoylated peptide corresponding to the interaction motif. This reagent was striking in its attenuation of thermal hyperalgesia following CCI though we could not distinguish between the GRIP and PICK1 interaction using the myristoylated blocking peptide. The effects on mechanical allodynia were, however, minimal.

A significant increase in both the density and number of cells expressing GRIP2 mRNA was found in the dorsal horn LI and II ipsilateral to CCI. Although the presence of GRIP in the spinal cord has been previously documented (Dong et al., 1999; Brückner et al., 1999), the precise localisation has to date been unknown. Western blot analysis of spinal cord following CCI confirmed the increase in the overall levels of GRIP protein ipsilateral to injury (see Fig. 3.33 for summary).

Due to the lack of a cDNA sequence for rat PICK1, in situ hybridisation analysis of PICK1 mRNA expression could not be carried out and localisation could not be determined. However, an examination of PICK1 protein levels indicated that there was no apparent alteration in its level in rats at the peak of behavioural reflex sensitivity. Nevertheless, we cannot rule out the possibility of some role for PICK1 in contributing to neuropathic pain.

In contrast to the increase in the overall levels of GRIP mRNA and protein in the spinal cord ipsilateral to CCI, there appeared to be a general decrease of GRIP protein directly associated the GluR2 subunit following CCI. While there was no apparent alteration in the overall levels of PICK1 protein that binds to the same site as GRIP on the GluR2 C-terminus, ipsilateral to CCI in the spinal cord, the amount of PICK1 protein directly associated with GluR2 was decreased ipsilateral to CCI (see Fig. 3.33 for summary). Further experiments would be needed to confirm the apparent contrast in bilateral/ipsilateral changes for GRIP and PICK1, respectively, especially as very low levels of adapter protein immunoreactivity were present in the receptor immunoprecipitates. The functional implications of these preliminary findings are not yet clear, but it could be envisaged that the situation might arise as a result of GluR2 receptor subunit activation.

The determinants of preferential binding of either GRIP or PICK1 to GluR2 are not fully clear. Matsuda et al. (1999) have shown that the interaction between GRIP and GluR2 may be regulated by kinases. Mutation of Ser^{880} (IE<u>S</u>VKI) within the GluR2 C-terminus PDZ motif, a site known to be phosphorylated by PKC, can disrupt the GRIP: GluR2 interaction while having no effect on PICK1 binding (Matsuda et al., 1999; Chung et al., 2000; Osten et al., 2000). This would hypothetically allow for a functional differentiation in the regulation of GRIP/ABP or PICK1 interaction with the same site on GluR2/3 and is suggestive of a potential role for protein phosphorylation in the regulation of the GluR2: GRIP interaction (Matsuda et al., 1999). We could not examine a role for this site in neuropathic pain due to the lack of availability of phospho-specific-Ser^{880} antibodies.

The GluR2: GRIP interaction may also be disrupted by the activation of the calcium-activated proteinase calpain which can truncate GRIP and cause dissociation of its C-terminal interaction with GluR2 (Lu et al., 2001). Calpain activity has been reported to increase following spinal cord injury (perhaps as a result of elevated Ca^{2+} levels) and blocking calpain may inhibit apoptosis following spinal cord injury (Ray et al., 2000).

The PICK1 PDZ domain is reported to be less selective (T/SXV) than GRIP (ESVKI) and may result in a preferential binding of PICK1 to GluR2 (Chung et al., 2000). However, recent evidence suggests that PKC phosphorylation of Ser^{880} reduces GluR2 binding to GRIP without affecting PICK1: GluR2 binding and causes an internalisation of surface expressed GluR2 subunits (Chung et al., 2000; Matsuda et al., 2000). Moreover, LTD induction in hippocampal slices and cerebellar Purkinje cells increases Ser^{880} phosphorylation and infusion of a peptide that disrupts the binding of PICK1 can inhibit hippocampal LTD expression (Kim et al., 2001; Matsuda et al., 2000). The lack of alteration in PICK1 levels following CCI may theoretically have implications for the ability of PKC to modulate the AMPA receptor. However, the increases in phospho-Ser^{831}-GluR1 immunoreactivity seen ipsilateral to CCI (the CaMKII/PKC phosphorylation site on GluR1) indicate that this change occurs irrespective of unaltered levels of PICK1 expression.

The functional significance of GluR2/3-PDZ domain protein interactions in sensory synaptic transmission has been examined by disruption with synthetic peptides (as we used) by perfusion into cultured spinal neurones and suggests that PKC and interactions of the GluR2/3 C-terminus are important for unmasking silent glutamatergic synapses between sensory afferents and spinal cord dorsal horn neurones (Li et al., 1999). In addition, peptides corresponding to the phosphorylated motif in the GluR2 tail (which selectively blocks PICK1) and the dephosphorylated motif (which blocks binding of both GRIP/ABP and PICK1) have been reported to attenuate cerebellar LTD (Xia, 2000; Matsuda et al., 2000).

Figure 3.33 Summary schematic of the main changes observed in GluR1- and GluR2-associated proteins in the spinal cord ipsilateral to CCI

This schematic represents a summary of the results presented in this chapter. The expression of GluR1 mRNA decreased ipsilateral to CCI, while phosphorylation of its C-terminal tail at Ser^{831} by PKC/CaMKII was increased indicating greater regulation of this subunit by CaMKII/PKA following CCI which may lead to an enhancement of AMPA receptor responsiveness. Levels of Narp mRNA, reported to cause clustering of GluR1 in dissociated spinal neurones increased ipsilateral to CCI. No change was seen in GluR1 regulation by PKA as indicated by a lack of alteration of Ser^{845} expression. As the anchoring protein SAP97 reportedly facilitates PKA localisation to sites of action, we examined expression and functional inhibition of SAP97. However, while a SAP97 targeted site-specific inhibitory myristoylated peptide caused reduced hyperalgesia and allodynia following CCI, there was no detectable change in the expression of SAP97 protein.

The expression of GluR2 increased ipsilateral to CCI indicative of decreased ion permeability through AMPA receptors containing this subunit. There was decreased expression of the classical fusion protein NSF ipsilateral to CCI which may imply less AMPA receptor cycling and blocking the NSF binding site on the GluR2 C-terminus decreased hyperalgesia following CCI possibly as a result of a reduction in AMPA receptor current. At a different site on the GluR2 C-terminus, the IESVKI site binds to both PICK1 and GRIP. The expression of PICK1 is unchanged following CCI, while there is a marked upregulation in the levels of GRIP. Blocking the binding site with a myristoylated peptide reduces hyperalgesia following CCI.

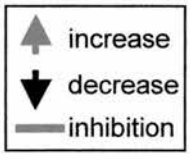

Narp:
Increased Narp expression may lead to an increase in AMPA receptor clustering and facilitate receptor responsiveness

GluR2:
Increased GluR2 receptor expression may have implications for AMPA receptor permeability by limiting Ca^{2+} flow through the channel

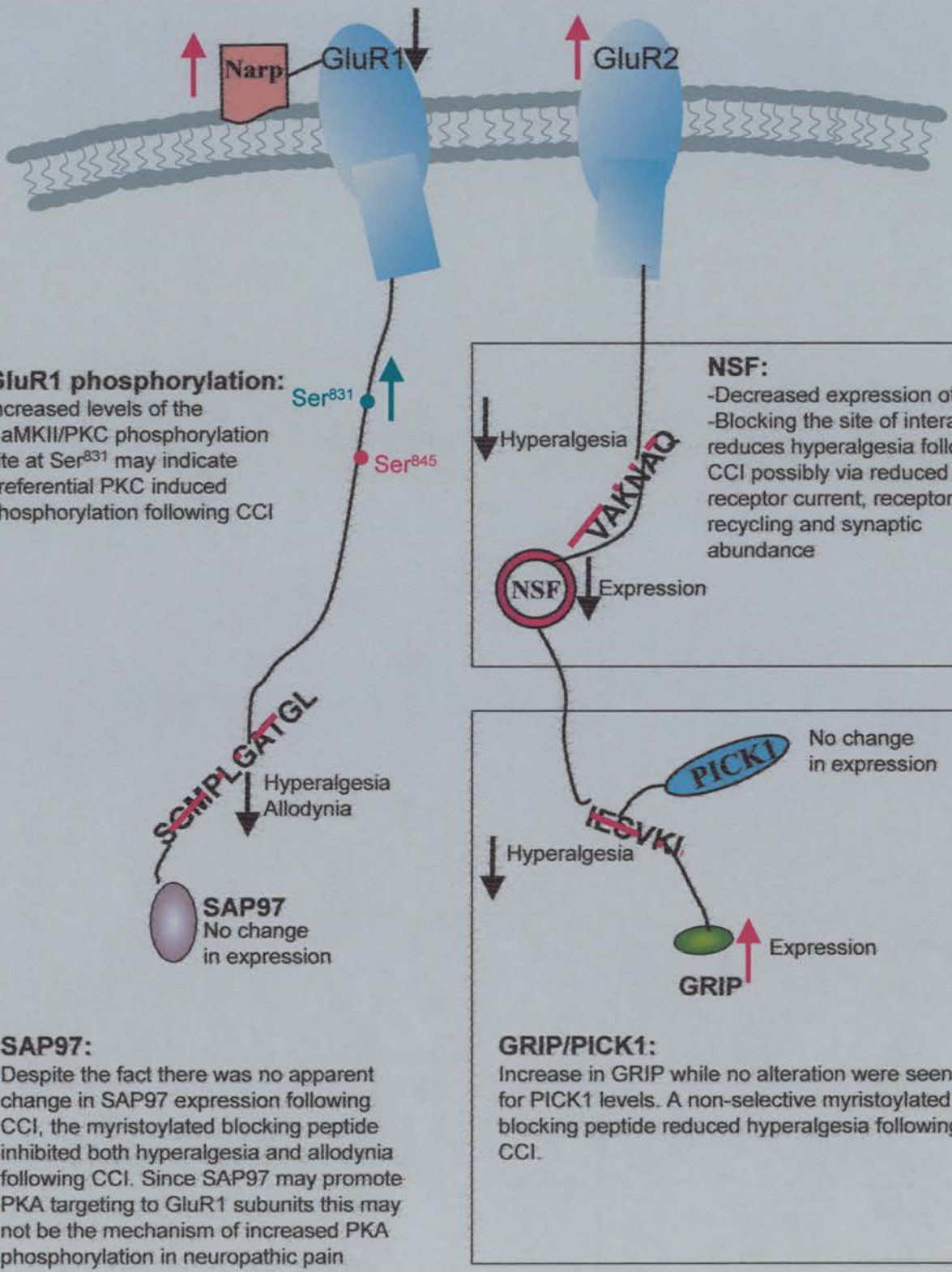

GluR1 phosphorylation:
Increased levels of the CaMKII/PKC phosphorylation site at Ser^{831} may indicate preferential PKC induced phosphorylation following CCI

NSF:
-Decreased expression of NSF
-Blocking the site of interaction reduces hyperalgesia following CCI possibly via reduced AMPA receptor current, receptor recycling and synaptic abundance

SAP97:
Despite the fact there was no apparent change in SAP97 expression following CCI, the myristoylated blocking peptide inhibited both hyperalgesia and allodynia following CCI. Since SAP97 may promote PKA targeting to GluR1 subunits this may not be the mechanism of increased PKA phosphorylation in neuropathic pain

GRIP/PICK1:
Increase in GRIP while no alteration were seen for PICK1 levels. A non-selective myristoylated blocking peptide reduced hyperalgesia following CCI.

Several GRIP-associated proteins (GRASPs) have been identified that bind to distinct PDZ domains within GRIP. GRASP-1 is a neuronal RasGEF associated with GRIP and AMPA receptors in vivo and may regulate neuronal Ras signalling and contribute to the regulation of AMPA receptor distribution (Ye et al., 2000). Overexpression of GRASP-1 in cultured neurones downregulates synaptic AMPA receptor clusters (Ye et al., 2000). The function of the remaining PDZ domains of GRIP are unknown at present though they are likely to mediate distinct interactions, possibly anchoring the AMPA receptor to cytoskeletal proteins or coupling the receptor to intracellular enzymes.

Blocking the distinct NSF interaction site on the GluR2 C-terminus alleviated the thermal hyperalgesia characteristic of the CCI model with little effect on mechanical allodynia. Infusion of this same inhibitory peptide in hippocampal neurones reduces AMPA receptor current and synaptic abundance. Given the role of NSF in vesicular trafficking, blocking this site may affect AMPA receptor transport to the synapse that could affect the receptor's ability to relay nociceptive information (Song et al., 1998; Lüthi et al., 1999). The levels of NSF mRNA decreased in density ipsilateral to injury specifically in LI while there was no detectable alteration in the number of cells expressing NSF mRNA. NSF protein also decreased in the spinal cord ipsilateral to CCI. The functional implications of this are not clear and it seems likely that only one facet of the change in NSF is likely to relate to the role of GluR2. One possibility is that a downregulation of NSF may imply a reduction in AMPA receptor recycling and this hypothetical lack of rundown of AMPA receptor activity could influence the maintenance of the persistent pain state. Loading of peptides corresponding to the NSF-binding domain of GluR2 into rat hippocampal CA1 pyramidal neurones results in a marked, progressive decrement of AMPA receptor-mediated synaptic transmission (Nishimune et al., 1998). This reduction in synaptic transmission is also observed when an anti-NSF monoclonal antibody is loaded into CA1 neurones. These results demonstrate a previously unsuspected functional interaction in the postsynaptic neurone between two major proteins, AMPA and NSF, involved in synaptic transmission and suggest that a rapid NSF-dependent modulation of AMPA receptor function may occur in vivo.

We report a marked increase in both the density and number of cells expressing Narp mRNA in the superficial dorsal horn LI and II ipsilateral to CCI. As no antibodies for this molecule are commercially available, Western blot analysis could not be carried out. The functional impact of an increase in Narp mRNA in neuropathic pain is difficult to interpret, given the limited knowledge about Narp in general, and since no specific site of interaction of Narp with either the GluR1 or GluR2 subunits has been established, this could not be examined in vivo.

Narp is enriched at excitatory synapses on neurones from both the hippocampus and spinal cord and its overexpression increases the number of excitatory but not inhibitory synapses in cultured spinal neurones. In particular, Narp can function as an extracellular aggregating factor for AMPA receptors (O'Brien et al., 1999). It has been reported that >90% of GluR1 clusters on spinal neurones had associated Narp immuno-staining and that Narp over-expression can increase the number of pre-synaptic terminals in spinal neurones (O'Brien et al., 1999). Because Narp is dramatically upregulated in neurones in response to patterned synaptic activity and is expressed at relatively high levels in developing and adult brain, Narp may play a critical role in linking activity with the development and plasticity of excitatory synapses. Also, inhibitory axons do not appear to express Narp (O'Brien et al., 1999). With this in mind, it is plausible that an increase in Narp following the development of neuropathic pain behaviours in CCI could lead to an increase in AMPA receptor-related synapses in neurones in the spinal cord and facilitate their responsiveness.

The presence of GluR2 in an AMPA receptor assembly will limit calcium flow through the ion channel and may serve a neuroprotective role. The proteins interacting with the GluR2 C-terminus may contribute to its regulation, localisation and proximity to signalling pathways. However, the effects of the PDZ domain protein interactions with GluR2 on ion flow, if any, are not known. The high levels of GluR2 in LII may have implications for nociceptive transmission due to the calcium impermeability conferred by this subunit (Burnashev et al., 1992b). AMPA receptors can exist in the absence of GluR2 subunit, as functional AMPA receptors are present (in CA1 at least) in GluR2 knockout mice, which display enhanced LTP

and increased calcium permeability, indicating that this subunit may not be essential for AMPA receptor function (Jia et al., 1996). Cells expressing Ca^{2+}-permeable AMPA receptors (so presumably lacking the GluR2 subunit) can be found in LI and LII_o of the superficial dorsal horn, while there are low numbers of Ca^{2+}-permeable AMPA receptors in LII_i corresponding to the high expression of GluR2 subunits in this region (Engleman, Allen and MacDermott, 1999) and calcium flow through AMPA receptors is likely to activate downstream second messenger pathways that feedback onto the receptor and modulate its activity by mechanisms such as phosphorylation.

Although no direct examination of ion flow through AMPA receptors was carried out here, we examined the ability of the intracellular kinases, CaMKII/PKC and PKA to activate their respective target serine residues on the GluR1 C-terminus following CCI. The afferent barrage produced following the induction of CCI (causing the over-activation or sensitisation of dorsal horn neurones) could therefore potentially result in increased AMPA receptor ion permeability and increased activation of second messenger pathways.

Kinases themselves have been shown to be involved in dorsal horn nociceptive transmission mediated by the activation of postsynaptic glutamate receptors, and excitatory transmission in LII of the spinal cord can be enhanced by intracellularly-applied CaMKII (Kolaj et al., 1994). Activators of PKC and PKA also facilitate spinal neurone responsiveness to inputs (Cerne, Rusin and Randić, 1993). Immunoprecipitates probed with a pan-GluR1 antibody showed a decrease in levels of GluR1 in the spinal cord ipsilateral to CCI injury and a relative increase in phospho-Ser^{831} protein levels ipsilateral to CCI when compared with controls. In agreement with a recent report of increased brainstem phospho-Ser^{831}-GluR1 immunoreactivity following inflammation in pain modulatory regions (Guan et al., 2001), this suggests that AMPA receptors can be modulated by phosphorylation during chronic pain.

It is possible that SAP97 may function to bring PKA into proximity with GluR1 via AKAP79/150 to modulate phosphorylation at Ser^{845}. However, we report that the levels of SAP97 protein appear to be unaltered following CCI and the phosphorylation state of the GluR1 subtype of AMPA receptor at Ser^{845} is similarly unaltered ipsilateral to CCI. However, blocking the site of interaction of SAP97 within the GluR1 C-terminus using the synthetic myristoylated peptide attenuated both thermal hyperalgesia and mechanical allodynia following CCI. Thus, the functional role of the SAP97 interaction with AMPA receptor subunit GluR1 appears to participate in the maintenance of neuropathic pain although the mechanism by which this acts is unclear.

Bidirectional changes in the efficacy of neuronal synaptic transmission, such as hippocampal long-term potentiation (LTP) and long-term depression (LTD), are thought to be mechanisms for information storage in the brain. Aspects of LTP and LTD may be mediated by the modulation of AMPA receptor phosphorylation. LTP and LTD reversibly modify the phosphorylation of the AMPA receptor GluR1 subunit. However, contrary to the hypothesis that LTP and LTD are the functional inverse of each other, LTP and LTD are associated with the phosphorylation and dephosphorylation, respectively, of distinct GluR1 phosphorylation sites. LTD induction in naïve synapses dephosphorylates the major cyclic-AMP-dependent protein kinase (PKA) site, whereas in potentiated synapses the major CaMKII site is dephosphorylated. Conversely, LTP induction in naïve synapses and depressed synapses increases phosphorylation of the CaMKII site and the PKA site, respectively. LTP is differentially sensitive to CaMKII and PKA inhibitors depending on the history of the synapse such that identical stimulation conditions recruit different signal-transduction pathways depending on previous synaptic events (Lee et al., 2000). AMPA receptor function can be rapidly regulated during the forms of synaptic plasticity known as long-term potentiation and depression (LTP and LTD) and this regulation is sensitive to manipulation of PDZ domain interactions, suggesting that AMPA-PDZ interaction may be a key factor in dynamic regulation of receptor function (Li et al., 1999).

The fact that GluR1 and GluR2 subunits of AMPA receptor interact with different sets of PDZ domain containing proteins may well imply a differential role for each subunit and our results indicate a differential regulation of the AMPA receptor subunits GluR1 and GluR2 in the spinal cord following the establishment of neuropathic sensitisation, as GluR1 was apparently downregulated in the superficial dorsal horn, while GluR2 mRNA and protein levels increased. In addition, while NSF was diminished in the dorsal horn of the spinal cord following CCI, there was a marked increase in the levels of GRIP and Narp mRNA expression. Although it is difficult to elucidate the precise function of PDZ domain-containing proteins and other interacting partners of the GluR2 receptor, GRIP/PICK1 and NSF appear likely to play some functional role in the modulation of AMPA receptor- dependent nociceptive transmission during neuropathic pain.

CHAPTER 4: Lack of neuropathic pain behaviour and disruption of spinal NMDA receptor function in PSD-95 mutant mice

4.1: Introduction

A signalling complex of ~2000 kDa can be isolated from mouse forebrain, comprising the NMDA receptor linked to adapter proteins, signalling, cytoskeletal and cell adhesion proteins (Husi et al., 2000; Husi and Grant, 2001). As mentioned in the general introduction, the NMDA receptor (NR) is composed of two main subunits whereby the NR1 subunit is the key functional subunit of all NMDA receptor assemblies, while the NR2 subunits determine the subtype-specific channel characteristics (Chen, Luo and Raymond, 1999). NR2 subunits possess a long intracellular C-terminus enabling them to interact with the membrane associated guanylate kinase (MAGUK) family of proteins, which so far contains PSD-95/SAP90, Chapsyn-110/PSD-93, hDlg/SAP97 and SAP102. The MAGUKs contain three amino-terminal PDZ domain repeats, a Src homology 3 (SH3) domain and a guanylate kinase (GK)-like domain (Kennedy, 1997) and are 70-80% homologous in sequence (Kim and Sheng, 1996).

The best characterised MAGUK protein is PSD-95, which interacts with the NR2 subunits of NMDA receptor. The interaction occurs via the first and second PDZ domains of PSD-95 and the NR2 C-terminal peptide sequence, 'SIESDV' (Kornau et al., 1995; Niethammer, Kim and Sheng, 1996).

4.1.1 MAGUK family of proteins

Interest began with the discovery, using yeast 2-hybrid screening, that MAGUKs acted as interaction partners for the C-terminus of NMDA receptor subunits and K^+ channels (Kornau, Seeburg and Kennedy, 1997). Domain analysis of PSD-95 defined the PDZ repeats as modular protein-binding sites that recognise short consensus

peptide sequences in the NR2 C-termini. PSD-95 interacts most strongly with the NR2B subunit and both of these proteins are highly enriched in the PSD (Moon, Apperson and Kennedy, 1994; Kennedy, 1997).

PSD-95 is believed to cluster and immobilise the NMDA receptor at the postsynaptic membrane via interactions with the cytoskeleton, and to function as a bridge or molecular scaffold for signalling to downstream pathways (Niethammer, Kim and Sheng, 1996; Craven and Bredt, 1998). Some mechanisms by which PSD-95 can stabilise the NMDA receptor complex have been identified. Members of the PSD-95 family can multimerise by two distinct mechanisms via the formation of N-terminal disulfide bridges or via PDZ: PDZ domain interactions (Hsueh, Kim and Sheng, 1997; Kim et al., 1996; Craven, El-Husseini and Bredt, 1999). This is thought to result in the local grouping of ion channels and may be a simple mechanism for clustering a specific mixture of ion channels.

N-terminal palmitoylation of PSD-95 may regulate association of PSD-95 with the membrane (Topinka and Bredt, 1998). The neuronal cell adhesion molecule, neuroligan, whose extracellular regions tightly bind to β-neurexins on the presynaptic terminal membrane to form intercellular junctions, binds to PDZ3 of PSD-95 (Irie et al., 1997). In addition, PSD-95 may immobilise the NMDA receptor via its secondary interactions with the microtubule and actin cytoskeleton. For example, CRIPT and MAP1A, both microtubule-binding proteins, bind to PSD-95 providing a direct link to microtubules that may affect synaptic clustering of receptors (Passafaro et al., 1999; Brenman et al., 1998) and an interaction between the actin binding protein, α-actinin-2 with the NR1 subunit may anchor the NMDA receptor to the actin cytoskeleton (O'Brien, Lau and Huganir, 1998).

Proteins known to interact with the SH3/GK domains include guanylate kinase-associated protein (GKAP), MAP1A, the KA2 kainate receptor subunit and the kinase/phosphatase scaffolding adapter AKAP79/150 (Naisbitt et al., 1997; Brenman et al., 1998; Garcia et al., 1998; Colledge et al., 2000; Kim et al., 1995). Another novel protein, Cypin, may act as a cytosolic regulator of PSD-95 and Cypin

overexpression in hippocampal neurones can disrupt PSD-95 postsynaptic trafficking (Firestein et al., 1999).

4.1.2 MAGUK-associated signalling machinery

Various signalling molecules interact with PSD-95 bringing them into close proximity with the NMDA receptor in the postsynaptic membrane (Sheng, 1996). Citron, a protein target for the activated form of the small GTP-binding protein Rho, binds to PDZ3 of PSD-95 and is present at glutamatergic synapses in a complex with PSD-95 and NMDA (Furuyashiki et al., 1999; Zhang et al., 1999). SynGAP, an abundant synaptic Ras GTPase-activating protein, can bind to all 3 PDZ domains of PSD-95. SynGAP can be phosphorylated by CaMKII, which is reported to reduce its GAP activity (Chen et al., 1998). In addition, PSD-95 can assemble a postsynaptic protein complex containing nNOS and NMDA receptors, where nNOS can bind to PSD-95 via a PDZ: PDZ domain interaction (Christopherson et al., 1999).

4.1.3 Functional modulation of NMDA receptors

NMDA receptor subunits are functionally modulated by serine/threonine and tyrosine kinases, which has implications for receptor activity. The functional influence of kinases on the NMDA receptor may be as a result of direct phosphorylation or phosphorylation of associated proteins. Either may involve adapters such as the PDZ domain-containing proteins. NMDA receptor signalling is mediated by the combined functions of the NR1 and NR2 receptor-channel subunits together with their associated proteins. The C-terminal domains of the NR1 and NR2 subunits all contain sites of PKA and PKC phosphorylation, while tyrosine kinase phosphorylation sites are believed to be limited to NR2 subunits (Tingley et al., 1997; Leonard and Hell, 1997; Lau and Huganir, 1995).

CaMKII and calcium-dependent regulation

Calcium regulation of NMDA receptors has been proposed to involve a linkage between the receptor and the cytoskeleton that may be facilitated by interactions with PSD-95 (Rosenmund and Westbrook, 1993). Calmodulin binds, in a calcium-dependent manner, to the C-terminus of NR1 subunits and α-actinin-2 can bind to the C-terminus of both NR1 and NR2B subunits (Ehlers et al., 1996; Wyszynski et al., 1997). In vitro, α-actinin-2 and calmodulin bind competitively to the initial 30 amino acids of the NR1 C-terminus, to a segment known as C0 that is common to all NR1 splice variants (Wyszynski et al., 1997; Ehlers et al., 1996; Hollmann and Heinemann, 1994, Section 1.7.6). Calmodulin binding to NR1 has been proposed to mediate a calcium-dependent inactivation of the NMDA receptor causing a reduction in the channel open probability (Legendre, Rosenmund and Westbrook, 1993; Krupp et al., 1998) and this channel inactivating effect of calmodulin can be prevented by co-expression of α-actinin-2 (Zhang et al., 1998; Hisatsune et al., 1997).

Furthermore, the NMDA receptor: PSD-95 complex in the forebrain incorporates the Ca^{2+}-dependent protein kinase, CaMKII, which docks to NR2 subunits, where it is predicted to respond readily to NMDA receptor-mediated Ca^{2+} entry (Gardoni et al., 1999; Husi and Grant, 2001). After activation by Ca^{2+}/calmodulin, CaMKII has Ca^{2+}-independent activity (by autophosphorylating at a threonine reside at position 286, Thr^{286}) that prolongs its activation even after the intracellular Ca^{2+} concentration returns to basal levels (Hanson et al., 1989; Fukunaga, Rich and Soderling, 1989). Both αCaMKII and PSD-95 bind to the NR2 subunits in a mutually competitive manner (Gardoni et al., 1999). NR2B but not NR2A or NR1 are believed to be responsible for the autophosphorylation-dependent targeting of CaMKII, this modification inducing a direct high-affinity binding to the NR2B C-terminus (Strack and Colbran, 1998). Inhibitors of the serine/threonine phosphatases PP1 and PP2A have been reported to increase the phosphorylation and activity of CaMKII and CaMKIV, while inhibitors of PP2B (calcineurin) only increase the phosphorylation and activity of CaMKIV (Kasahara, Fukunga and Miyamoto, 1999).

CaMKII activity also has implications for NMDA receptor-mediated stimulation of the Ras-MAPK pathway. SynGAP, a regulatory protein that binds to PSD-95, stimulates the GTPase activity of Ras suggesting that it negatively regulates Ras activity (Kim et al., 1998). Inhibition of SynGAP by CaMKII will stop inactivation of GTP-bound Ras and may be one of the modulatory influences in the activation of the MAPK pathway (Chen et al., 1998).

PKA and PKC

Regulatory phosphorylation of NMDA receptor subunits by kinases such as PKC and PKA may increase the degree of Ca^{2+} entry evoked by NMDA receptor stimulation (Tingley et al., 1997; Westphal et al., 1999). Electrophysiological responses of spinal neurones to NMDA are known to be facilitated by PKC and PKA (Cerne, Jiang and Randić 1992; Heppenstall and Fleetwood-Walker, 1997). Whole cell current responses to NMDA are enhanced by cAMP analogs and by intracellular application of cAMP or a catalytic subunit of PKA (Cerne, Rusin and Randić, 1993). NR1, NR2A and NR2B subunits are all substrates for PKC and PKA where PKC phosphorylates serine residues Ser^{890} and Ser^{896} on NR1 and PKA phosphorylates serine residue Ser^{897} (Tingley et al., 1997; Leonard and Hell, 1997). It has been shown that levels of NR1 phosphorylated protein at Ser^{897} in spinothalamic tract cells are increased in the spinal cord following capsaicin injection (Zou, Lin and Willis, 2000). Furthermore, PKC-mediated phosphorylation of NR1 may decrease its affinity for calmodulin and so attenuate calmodulin-dependent inactivation of the receptor (Hisatsune et al., 1997).

Signalling enzymes may be recruited to NMDA receptors through simultaneous association with two A-kinase anchoring proteins (AKAPs), AKAP79/150 and Yotiao (Colledge et al., 2000; Lin et al., 1998). AKAP79/150 has been shown to bind to PSD-95, which could provide a mechanism to favour NMDA receptor (or ion channel) phosphorylation through preferential recruitment of regulatory kinases (Colledge et al., 2000). AKAP79/150 provides a scaffold for PKA, PKC, and calcineurin (PP2B). Interestingly, PSD-95 competes with calcineurin for binding to

AKAP79/150 in vitro and interaction of AKAP79/150 with PSD-95 appears to exclude the phosphatase calcineurin from the complex, suggesting that this AKAP may preferentially target kinases but not phosphatases to NMDA receptors at the PSD (Colledge et al., 2000).

Through interaction with the C1 splice variant of NR1, the anchoring protein Yotiao targets both PKA (via RII subunits) and the phosphatase PP1 to NMDA receptor complexes, conferring bi-directional regulation of NMDA receptor activity (Lin et al., 1998; Feliciello et al., 1999; Westphal et al., 1999). When PP1 is anchored to Yotiao, it is active and so limits NMDA receptor channel activity. Activation of PKA can overcome PP1 activity and enhance NMDA receptor currents (Westphal et al., 1999). In addition, stimulation of NMDA receptors leads to reduced PP2A phosphatase activity, whereas association of PP2A with NMDA receptors increases its phosphatase activity and dephosphorylates Ser^{897} of NR1 (Chan and Sucher, 2001).

Tyrosine Kinases

Members of the tyrosine kinase family, such as Src and Fyn have also been implicated in NMDA receptor modulation, whereby protein tyrosine kinases can increase NMDA receptor currents (Wang and Salter, 1994). Src co-immunoprecipitates with NMDA and regulates the function of NMDA receptors at hippocampal synapses and in dorsal horn neurones (Yu et al., 1997). In addition, PKC enhancement of NMDA receptor currents can be blocked with tyrosine kinase inhibitors and Src mutant mice lack this PKC-dependent upregulation of NMDA receptor function (Lu et al., 1999). PSD-95 is believed to promote Fyn phosphorylation of NR2A and mutant mice with a Fyn deficit have been shown to display reductions in this phosphorylation (Tezuka et al., 1999). The NR1 subunit is not believed to contain tyrosine phosphorylation sites (Lau and Huganir, 1995).

4.1.4 In vivo function of PSD-95

To date, there has been limited functional information for the role of PSD-95 in vivo. In cultured cortical neurones, antisense PSD-95 can attenuate NMDA receptor-mediated excitotoxicity and blocks Ca^{2+}-activated nitric oxide production specifically without affecting NMDA channels currents (Sattler et al., 1999). Furthermore, PSD-95 binds to neuronal NOS (nNOS), an interaction that is competitively inhibited by an nNOS C-terminal ligand known as CAPON (Carboxy-terminal PDZ ligand of nNOS). Axotomy decreases PSD-95 and CAPON mRNA in facial motoneurones while nNOS levels increase (Che, Tamatani and Tohyama, 2000). Disruption of PSD-95 impairs the induction of synaptic plasticity and forms of learning in the hippocampus (Migaud et al., 1998). A possible cause for this may an uncoupling of the NMDA receptor from PSD-95, which will disrupt links to other cytosolic signalling proteins that propagate or modify the signal generated by the receptor. Despite the pronounced effects on NMDA receptor-mediated plasticity, PSD-95 mutations did not affect synaptic NMDA receptor currents, indicating that the intracellular signalling components of the complex, that have been outlined above, may participate selectively in neuronal plasticity.

The truncated mutation of PSD-95 was located midway through PDZ3, thus rendering the SH3 and GK domains (and possibly the PDZ domain itself) ineffective in mediating associated signalling pathways. The LacZ reporter gene was inserted here as a marker for transcription (Fig. 4.1). Here, using these PSD-95 mutant mice, we have addressed the possibility that the neuropathic sensitisation of spinal dorsal horn neurones may depend on adapter-mediated mechanisms of NMDA receptor function.

Figure 4.1 Schematic representation of the site of PSD-95 mutation

This schematic shows the NMDA (NR1 and NR2) receptors in the postsynaptic membrane. The C-termini of the NR2 subunits bind to PSD-95 via a specific C-terminal peptide 'SIESDV' to PDZ1 and PDZ2 of PSD-95. The truncating mutation in the PSD-95 mutant mice occurred in PDZ3, downstream of the NR2 interaction site, as illustrated by the site of insertion of the LacZ reporter gene.

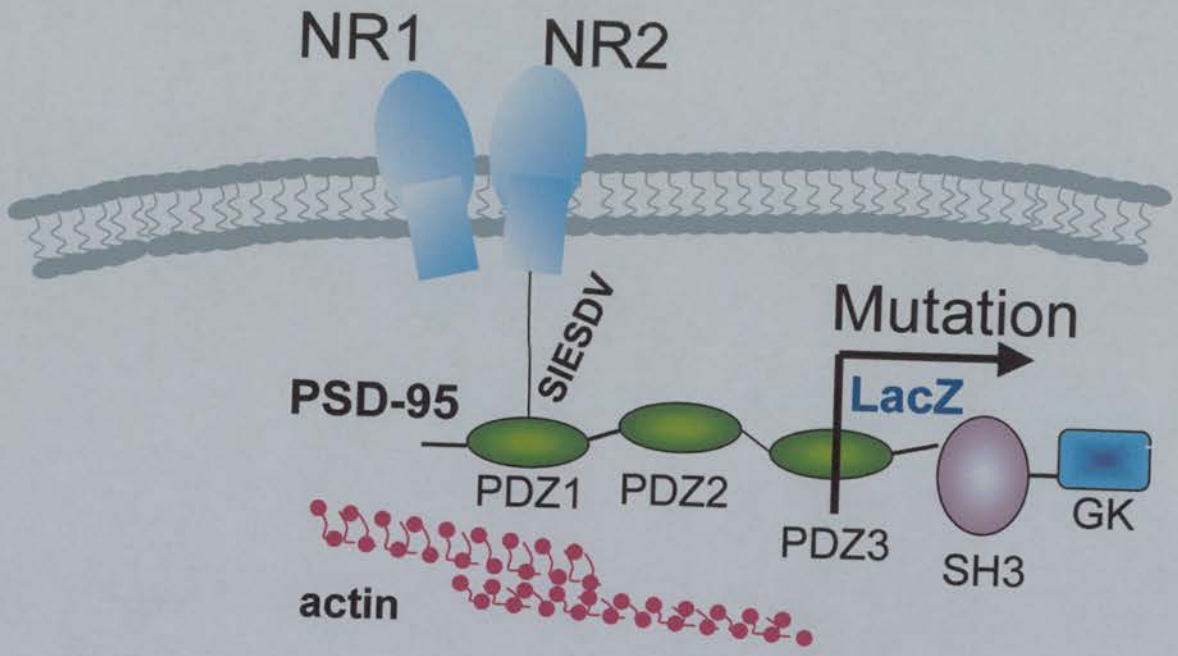
NR1
NR2
SIESDV
Mutation
LacZ
PSD-95
PDZ1
PDZ2
PDZ3
SH3
GK
actin

4.2: Results

Chapter 2 (sections 2.2 and 2.4) contains the details of methods used in this chapter.

4.2.1 Expression of the hybrid PSD-95 (truncated): β-galactosidase protein

Since the NMDA receptor is implicated in neuropathic pain and the PSD-95-docking NR2B subunit of the receptor is selectively expressed in superficial dorsal horn (Boyce et al., 1999) while the NR2A subunit of the NMDA receptor shows a more widespread dorsal horn distribution (Ma and Hargreaves, 2000), we first examined whether PSD-95 is expressed in the adult mouse spinal cord and, if so, where it is localised.

In (heterozygous) mice carrying a targeted mutation in the PSD-95 gene and a LacZ reporter of PSD-95 gene expression (Migaud et al., 1998) histochemical analysis of the expression of β-galactosidase (see Section 2.4.1, pgs. 84-85) showed specific staining in the superficial dorsal horn of the spinal cord with β-galactosidase-positive cells restricted to lamina II (Fig. 4.2a and b). This expression ranged throughout lumbar and thoracic spinal cord, extending undiminished throughout longitudinal sections (Fig. 4.2c).

Dorsal root entry zones showed no expression of the reporter gene (Fig. 4.2d). Further analysis of the peripheral nervous system provided no evidence for expression of β-galactosidase in dorsal root ganglion DRG or sciatic nerve (Fig. 4.2e and f, respectively), indicating that PSD-95 expression is restricted to the CNS. Hippocampus was used as a control for positive expression (Fig. 4.2g). This dorsal horn distribution is coincident with the distribution of NR2A and B subunits with which PSD-95 interacts most strongly (Boyce et al., 1999; Shibata et al., 1999). The specific expression of PSD-95 in lamina II with NMDA receptor subunits suggests the potential involvement of PSD-95-mediated signals in neuropathic pain.

Figure 4.2 β-galactosidase expression in the lumbar spinal cord (L3-L6) of heterozygous PSD-95 mutant mice

(a) 10 μm transverse section, showing specific localisation of β-galactosidase positive cells (blue) in lamina II of the superficial dorsal horn at x10 magnification.

(b) Inset of (a), showing positive cells at higher (x40) magnification.

(c) 10μm thick longitudinal sections cut though the region of positive expression in lamina II showing the spread of β-galactosidase positive cells in segments L3-L6. Expression extended through out lumbar, thoracic and cervical segments with moderate expression in brainstem (not shown).

(d) 10μm longitudinal spinal cord section equivalent to that in (c) but showing the site of peripheral dorsal root entry (arrow) where no β-galactosidase positive cells were observed.

(e) Transverse section of dorsal root ganglion showing no β-galactosidase expression.

(f) Transverse section of sciatic nerve (tibial branch) showing no β-galactosidase expression.

(g) Positive staining was confirmed in the hippocampal region of the brain.

Data are typical of results from 4 mice.

Scale bar =10μm

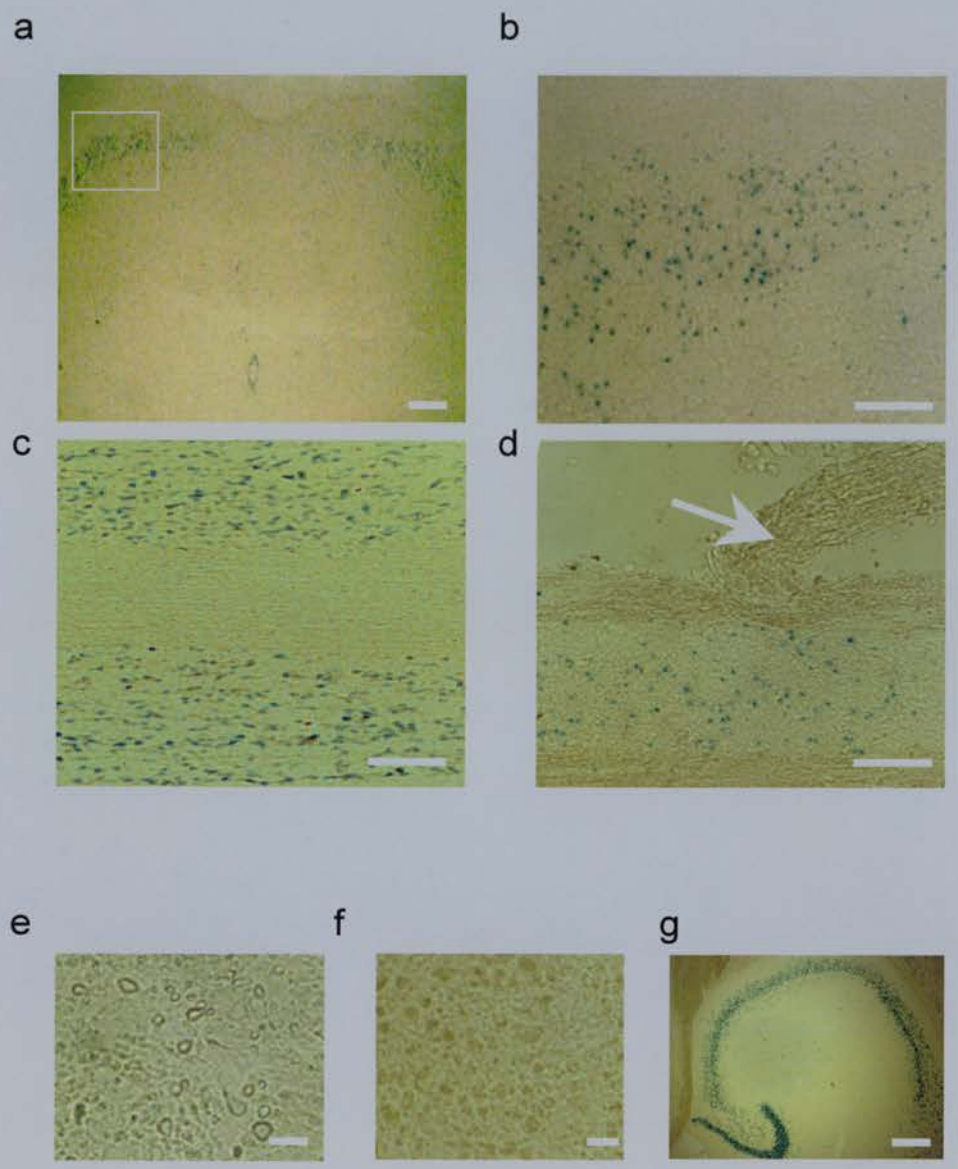
a
b
c
d
e
f
g

4.2.2 NMDA receptor complex in spinal cord

The NMDA receptor present in the spinal cord may be in complexes with PSD-95 as previously shown in forebrain structures (Husi et al., 2000). This possibility was tested by isolating spinal cord multiprotein complexes using both antibody- and peptide-based affinity separations (see Section 2.4.2, pgs. 85-86), which target either NMDA receptor subunits or PSD-95 (Husi and Grant, 2001; Husi et al., 2000). Wild-type spinal cord extracts contained NR1, NR2A, NR2B and PSD-95 (Fig. 4.3a). Experiments which were carried out to assess the composition of spinal NMDA receptor complexes in wild-type spinal cord (as described previously for forebrain, Husi et al., 2000) confirmed that spinal NR1, NR2B and PSD-95-directed immunoprecipitates contained immunoreactivity for NR1, NR2B and PSD-95 (Fig. 4.3b). Forebrain extract was used as a positive control (Fig. 4.3c).

4.2.3 The effects of PSD-95 mutation on the development of neuropathic reflex sensitivity following CCI

Since PSD-95-associated NMDA receptor complexes were present in spinal cord at a major site of nociceptive primary afferent termination in lamina II, we examined the CCI model of neuropathic pain in homozygous PSD-95 mutant mice (see Sections 2.2.1, 2.2.2 and 2.2.3 and Fig. 2.1, pgs 56-60).

Following CCI, wild-type mice progressively developed marked ipsilateral thermal hyperalgesia, mechanical allodynia and cold allodynia while responses of the contralateral paw remained at baseline levels (Fig. 4.4a, b and c, respectively). Significant differences for thermal hyperalgesia measured as the paw withdrawal latency ('PWL' in secs) are shown between pre-operative compared to post-operative values on the same side (Fig. 4.4a) and ipsilateral and contralateral values following CCI (Fig. 4.4a). Paw withdrawal to mechanical stimulation (paw withdrawal threshold, 'PWT') for wild-type mice showed significant differences between pre- and post-operative values on the ipsilateral side (Fig. 4.4b) and between ipsilateral

Figure 4.3 Association of PSD-95 with NMDA receptor subunit proteins in wild-type spinal cord

(a) Direct immunoblots of 100μg whole spinal cord extract in wild-type mice (n=8) probed with NR1, NR2A, NR2B and PSD-95 antibodies showing expression of all proteins in the spinal cord.

(b) Directed affinity separations with an NR2B C-terminal hexapeptide reagent ('pep 6' SIESDV targeting motif on NR2 subunits), or antibodies for NR1, NR2B and PSD-95 subsequently probed with NR1, NR2A, NR2B and PSD-95 antibodies showing physical association of these proteins with each other in spinal tissue.

(c) 50μg forebrain extract are shown for comparison.

The antibodies used for probing blots are listed to the left of the panels.

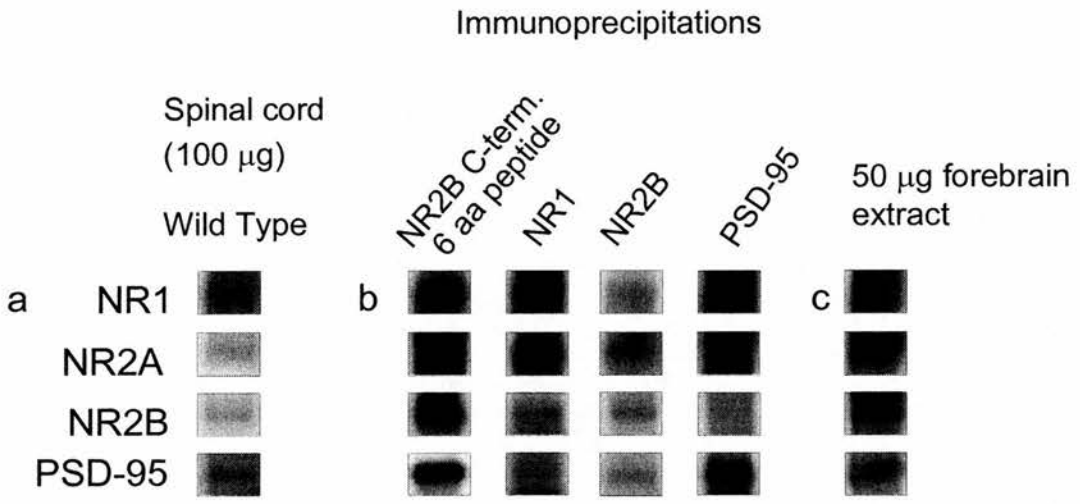
Immunoprecipitations
Spinal cord
(100 μg)
Wild Type
NR2B C-term.
6 aa peptide
NR1
NR2B
PSD-95
50 μg forebrain
extract
a
NR1
NR2A
NR2B
PSD-95
b
c

and contralateral values (Fig. 4.4b). The Suspended Paw Elevation Time (SPET) in response to a cold (4°C) thermal stimulus in wild-type mice showed significant differences between pre- and post-operative values (Fig. 4.4c) and between ipsilateral and contralateral responses (Fig. 4.4c).

The alteration in sensitivity in wild-type mice was evident as early as day 4, with maximal changes occurring at day 8/9 onwards. All CCI-evoked changes in behavioural reflex responses had resolved spontaneously within 22-23 days. Neither thermal hyperalgesia nor mechanical allodynia could be detected at any time point in PSD-95 mutant mice that had undergone identical CCI surgery (Fig. 4.4d and e, respectively), while cold allodynia was severely attenuated, reaching statistical significance at only one time point (Fig. 4.4f). The basal latencies for thermal nociceptive responses were similar in PSD-95 mutant compared to wild-type mice (Fig. 4.4a and d, respectively). There was, however, a lowered mechanical withdrawal threshold in wild-type mice when compared to PSD-95 mutant mice (Fig. 4.4b and e, respectively). Paw withdrawal tests for both mutant and wild-type mice were consistent with previously reported values for mice (Gillespie et al., 2000). These data indicate a key role for PSD-95 in the CNS in the sensitisation of behavioural reflex responses that is characteristic of the neuropathic pain state.

4.2.4 Morphological analysis of the sciatic nerve

In order to exclude the possibility that any of these changes were associated with abnormalities in the pattern of myelination in sciatic afferents, we examined axon diameter and myelin thickness profiles by light and electron microscopy (see Sections 2.4.3, 2.4.4 and Fig. 2.3, pgs. 86-89), firstly in naïve wild-type and homozygous PSD-95 mutant mice prior to constriction injury.

The axon diameters of fibres (Aδ and Aβ class) were similar in naïve wild-type and homozygous PSD-95 mutant mice (Fig. 4.5a and d, respectively) and no significant differences were observed (Chi^2 test and Kolmogorov-Smirnov test for normality). In addition, the myelin thickness profiles for myelinated fibres expressed in terms of G-

Figure 4.4 Behavioural analyses of wild-type and PSD-95 mutant mice with chronic constriction injury to the sciatic nerve

Data represent the average hindlimb withdrawal latency ± SEM from a noxious thermal stimulus (paw withdrawal latency, 'PWL' a and d), a normally innocuous mechanical stimulus (paw withdrawal threshold, 'PWT' b and e) or a cold (4°C) thermal stimulus (suspended paw elevation threshold, 'SPET', c and f) for each day prior to and following CCI (n=8, wild-type; n=9, PSD-95 mutant mice).

Wild-type mice (a), showed significant differences between pre- and post-operative values on the ipsilateral side for the noxious thermal stimulus (†, $p \leq 0.05$; ‡, $p \leq 0.01$, One-way ANOVA followed by a Dunnett's test) with a significant reduction in withdrawal latency compared to contralateral values (*, $p \leq 0.05$; **, $p \leq 0.01$, Student's t-test) while no significant differences reflecting thermal hyperalgesia were seen in the mutants following CCI (d).

Wild-type mice (b) showed significant differences between pre- and post-operative values on the ipsilateral side for the mechanical stimulus (‡, $p \leq 0.05$; Kruskal-Wallis ANOVA followed by a Dunn's test) with a significant ipsilateral reduction in withdrawal threshold compared to contralateral values (**, $p < 0.01$, Mann-Whitney Rank Sum Test), while no significant differences were seen on any day of testing for the PSD-95 mutant (e) indicating the lack of development of mechanical allodynia.

Wild-type mice in (c) showed significant differences between pre- and post-operative values for the cold test (‡, $p \leq 0.05$; ‡, $p \leq 0.01$, One-way ANOVA followed by a Dunnett's test) with a significant ipsilateral increase in withdrawal compared to contralateral values (*, $p \leq 0.05$; **, $p \leq 0.01$, Student's t-test). The SPET in response to a cold (4°C) thermal stimulus is shown for PSD-95 mutant mice (f).

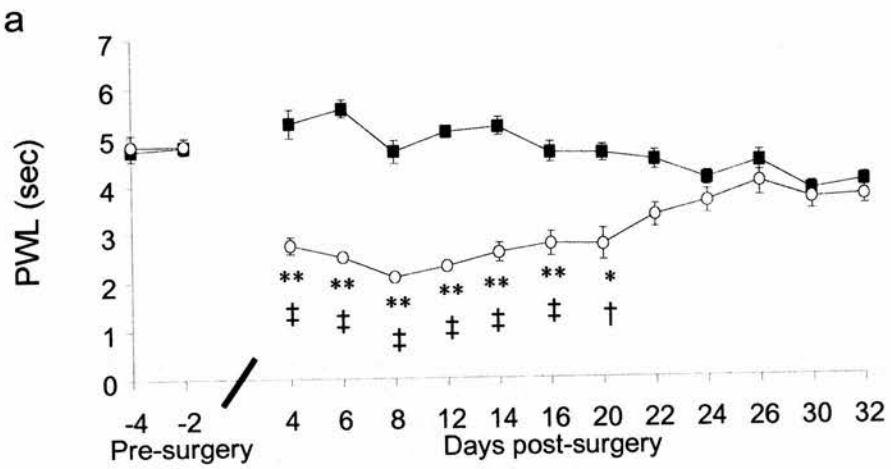
a
PWL (sec)
7
6
5
4
3
2
1
0
-4 -2
Pre-surgery
4 6 8 12 14 16 20 22 24 26 30 32
Days post-surgery

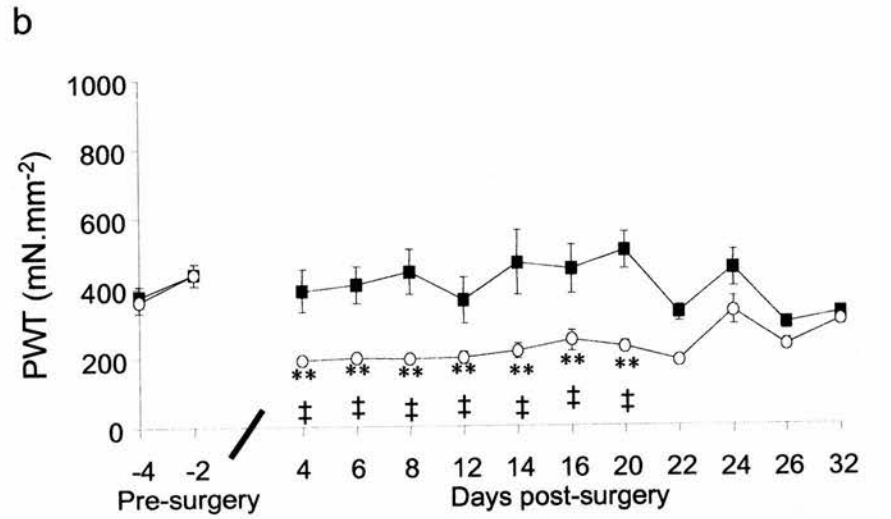
b
PWT (mN.mm-2)
1000
800
600
400
200
0
-4 -2
Pre-surgery
4 6 8 12 14 16 20 22 24 26 32
Days post-surgery

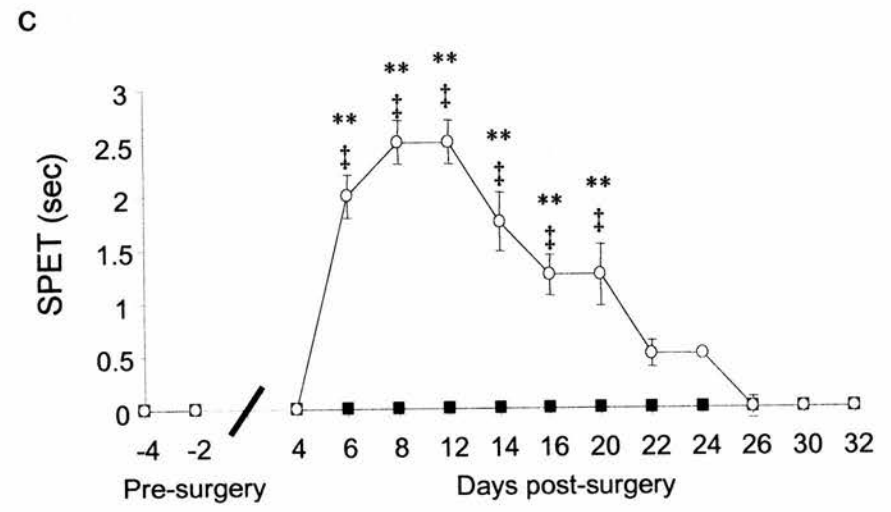
c
SPET (sec)
3
2.5
2
1.5
1
0.5
0
-4 -2
Pre-surgery
4 6 8 12 14 16 20 22 24 26 30 32
Days post-surgery

d

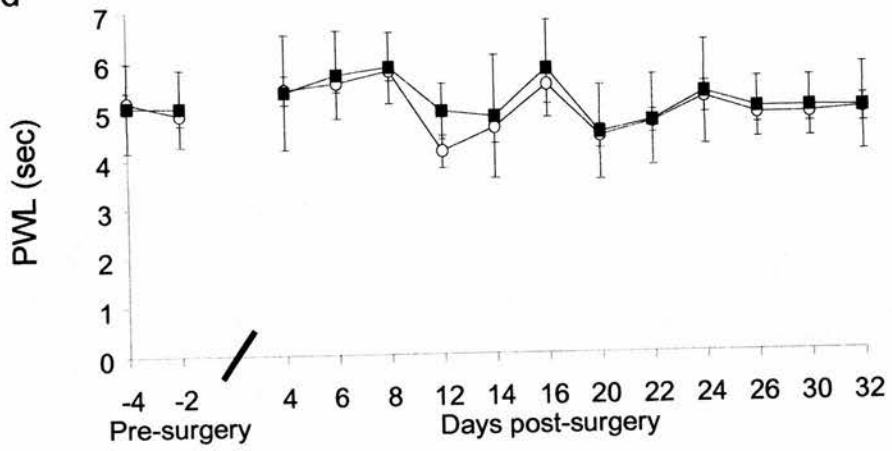
PWL (sec)
7
6
5
4
3
2
1
0
-4 -2
Pre-surgery
4 6 8 12 14 16 20 22 24 26 30 32
Days post-surgery

e

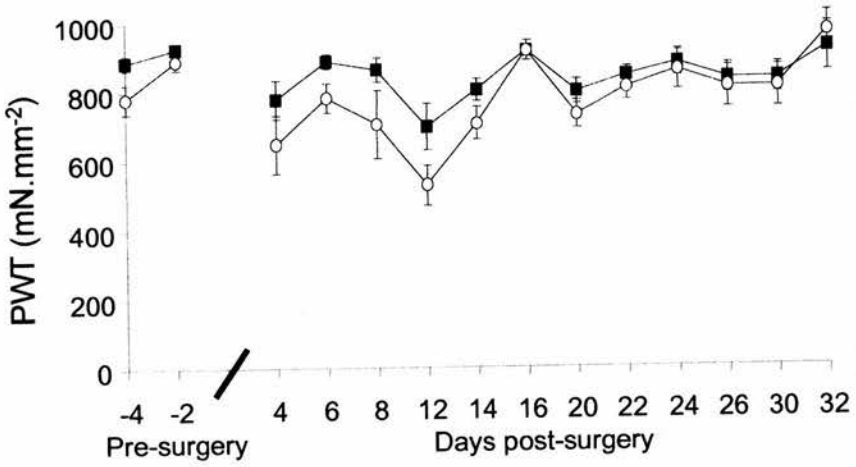
PWT (mN.mm-2)
1000
800
600
400
200
0
-4 -2
Pre-surgery
4 6 8 12 14 16 20 22 24 26 30 32
Days post-surgery

f

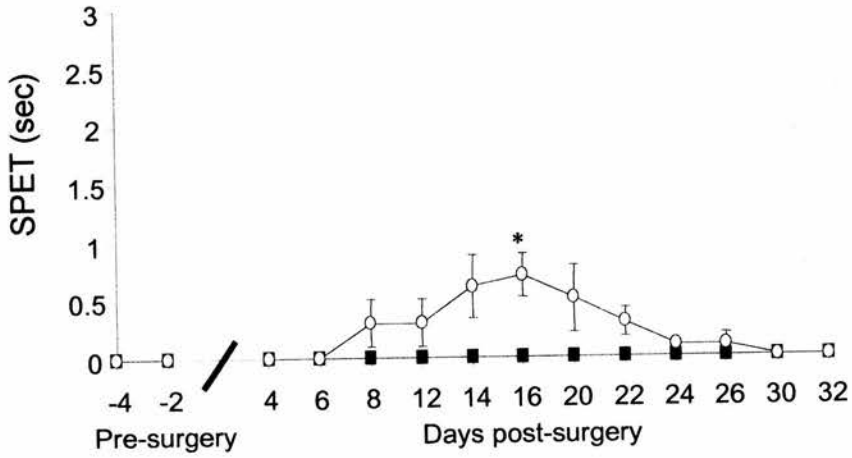
SPET (sec)
3
2.5
2
1.5
1
0.5
0
*
-4 -2
Pre-surgery
4 6 8 12 14 16 20 22 24 26 30 32
Days post-surgery

ratio (axon diameter/ external myelin diameter) showed little variation between wild-type and PSD-95 mutant mice under normal conditions (Fig. 4.5b and e, respectively). Finally, electron microscopic analysis of the diameters of unmyelinated C fibres indicated little variation between naïve wild-type and homozygous PSD-95 mutant mice (Fig. 4.5c and f, respectively) with no significant difference between the two groups (Chi^2 test and Kolmogorov-Smirnov test for normality). The morphological similarity is shown in photomicrographs for wild-type (Fig. 4.6a) and PSD-95 mutant (Fig. 4.6b) mice. The size, distribution and numbers of myelinated and unmyelinated axons seen were in accordance with previous reports (Sommer et al., 1995; Guilbaud et al., 1993).

In order to rule out the possibility that morphological differences in the demyelination of primary afferents were contributing to the lack of sensitivity in mutant mice, we carried out identical experiments to those described above on the sciatic nerve of both groups of mice following CCI (see Sections 2.4.3, 2.4.4 and Fig. 2.3, pgs. 86-89). Following constriction, light microscopic analysis showed that wild-type and PSD-95 mutant mice had a similar amount of demyelination distal to the ligation site with the same extent of large myelinated fibre loss (Fig. 4.7a and b; Fig. 4.8a and b, respectively) and no significant difference in the extent of demyelination observed (Chi^2 test and Kolmogorov-Smirnov test for normality). There was little variation in the number and size of unmyelinated C-fibres distal to the site of ligation for wild-type and PSD-95 mutant mice (Fig. 4.7c and d respectively; Chi^2 test and Kolmogorov-Smirnov test for normality) in accordance with previous reports (Guilbaud et al., 1993). No significant alterations in any fibre type could be detected proximal to ligation (data not shown).

These analyses indicated that there were no significant morphological differences in axons either under normal conditions or following constriction injury between wild-type and PSD-95 mutant mice that might account for the lack of behavioural development seen in the PSD-95 mutant mice.

Figure 4.5 Morphological analysis of the tibial branch of the sciatic nerve of naïve wild-type and PSD-95 mutant mice

The frequency distribution of the axon diameters of myelinated fibres in the Aδ/Aβ diameter range from the tibial branch of the sciatic nerve in naïve wild-type (a, n=3) and naïve PSD-95 mutant mice (d, n=3). In each nerve, 750 fibres were used for diameter measurement. No significance differences were observed at the light microscopy level for myelinated A fibre diameter distributions between wild-type and PSD-95 mutant mice (χ^2 test).

The myelin sheath thickness of myelinated fibres in terms of G ratio (internal/external diameter) as a function of the external diameter is shown in naïve wild-type (b, n=3) and naïve PSD-95 mutant (e, n=3) mouse sciatic nerve. No significant difference in the G ratio range of myelinated fibres was observed.

The frequency distribution of the axon diameters of unmyelinated C-fibres from the tibial branch of the sciatic nerve in naïve wild-type (c, n=2) and naïve PSD-95 mutant mice (f, n=2) is shown. In each nerve, 250 unmyelinated fibres were used for axon diameter measurement. At the electron microscope level, C-fibre clusters were consistently of normal appearance in wild-type and PSD-95 mutant nerves.

a

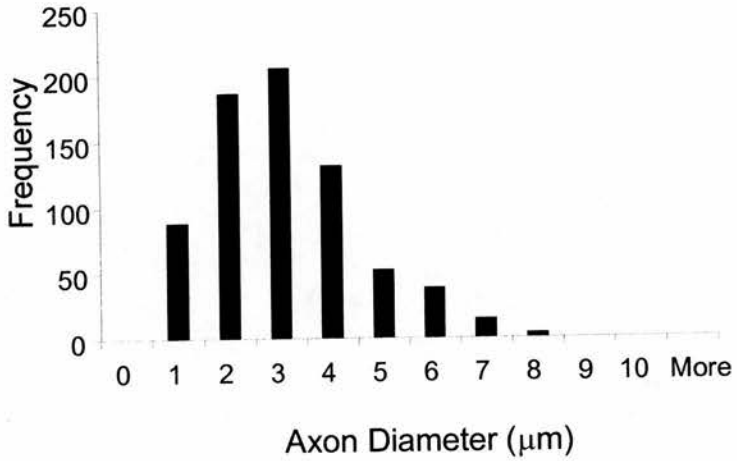
250
200
150
100
50
0
Frequency
0 1 2 3 4 5 6 7 8 9 10 More
Axon Diameter (μm)

b

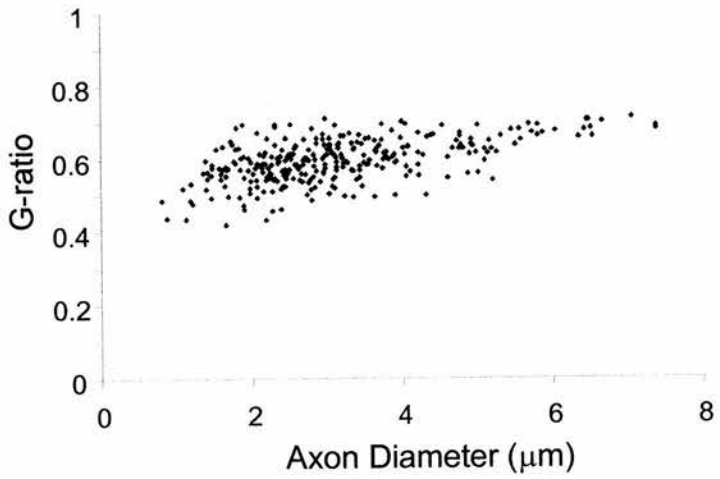
1
0.8
0.6
0.4
0.2
0
G-ratio
0 2 4 6 8
Axon Diameter (μm)

c

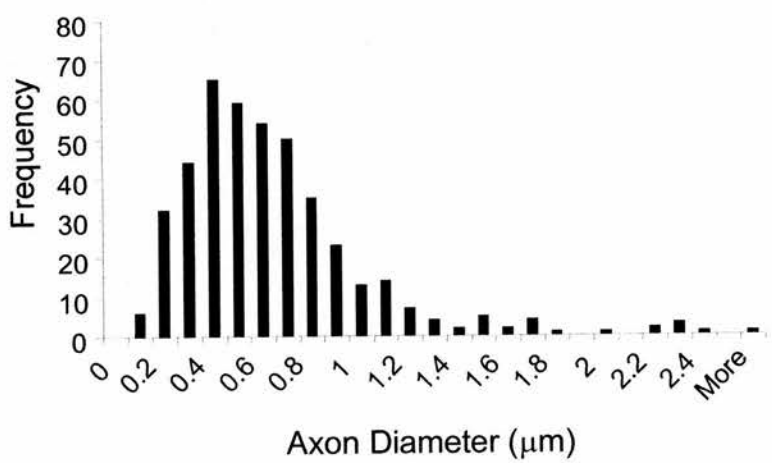
80
70
60
50
40
30
20
10
0
Frequency
0 0.2 0.4 0.6 0.8 1 1.2 1.4 1.6 1.8 2 2.2 2.4 More
Axon Diameter (μm)

d

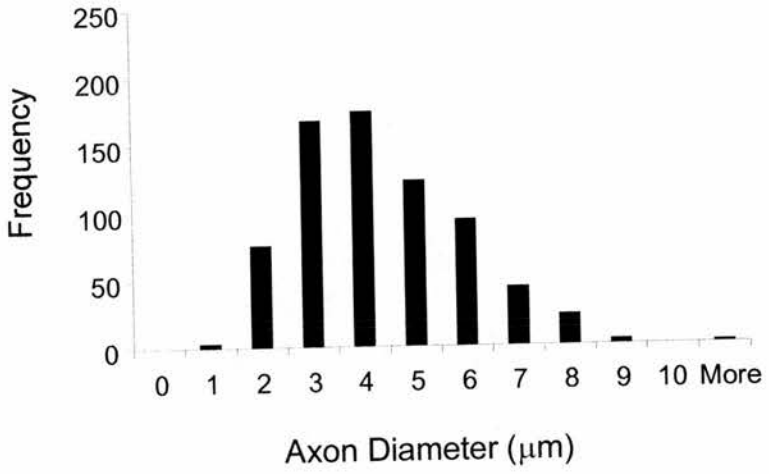
250
200
150
100
50
0
Frequency
0 1 2 3 4 5 6 7 8 9 10 More
Axon Diameter (μm)

e

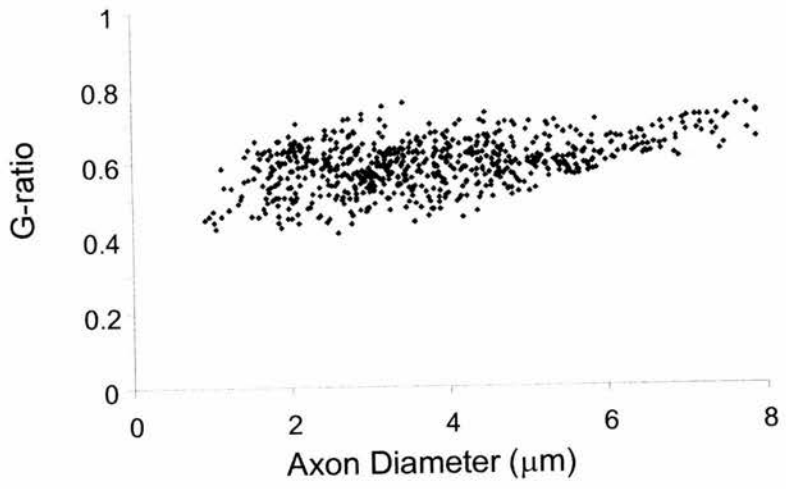
1
0.8
0.6
0.4
0.2
0
G-ratio
0 2 4 6 8
Axon Diameter (μm)

f

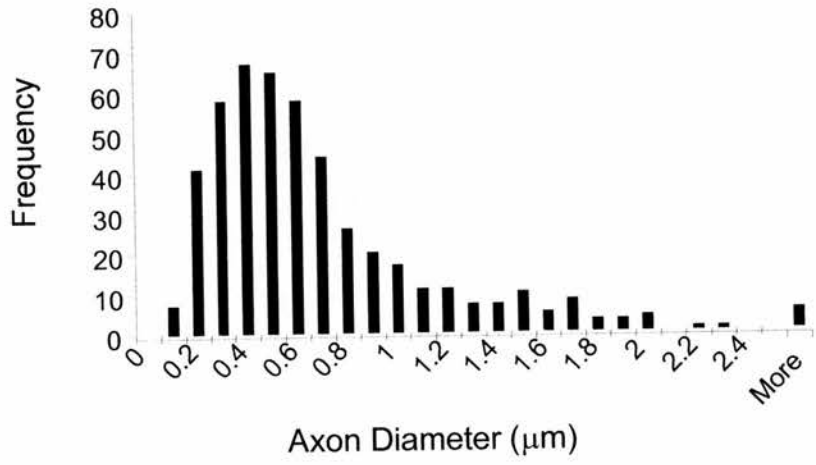
80
70
60
50
40
30
20
10
0
Frequency
0 0.2 0.4 0.6 0.8 1 1.2 1.4 1.6 1.8 2 2.2 2.4 More
Axon Diameter (μm)

Figure 4.6 Photomicrographs of the tibial branch of the sciatic nerve of naïve wild-type and PSD-95 mutant mice

(a) shows a photomicrograph of the tibial branch of the sciatic nerve of naïve wild-type mice observed by electron microscopy, showing a normal distribution of both small and large myelinated fibres and unmyelinated C-fibre clusters.

(b) shows a photomicrograph of the tibial branch of the sciatic nerve of naïve PSD-95 mutant mice observed by electron microscopy also showing a normal distribution of myelinated fibres and C-fibre clusters. These represent typical examples of fibre morphology

Scale bar = 10μm

a

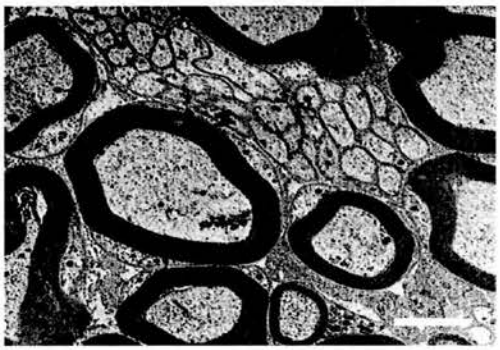

b

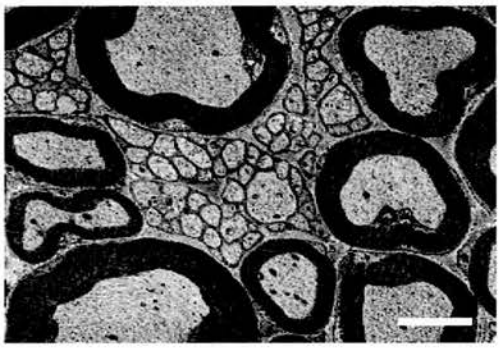

Figure 4.7 Morphological analysis following CCI of the tibial branch of the sciatic nerve of wild-type and PSD-95 mutant mice distal to ligation

(a) and (b) show the frequency distribution of the axon diameters of myelinated fibres from the tibial branch of the sciatic nerve in wild-type (a, n=3) and PSD-95 mutant (b, n=3) mice following CCI, showing a reduction in the number of medium and large diameter fibres distal to the site of ligation. There was no significant difference between the two groups and both wild-type and PSD-95 mice showed similar levels of demyelination.

(c) and (d) show the frequency distribution of the axon diameters of unmyelinated C-fibres from the tibial branch of the sciatic nerve in naïve wild-type (c, n=2) and PSD-95 mutant (d, n=2) mice following CCI. There was no significant difference in frequency distribution when compared to naïve results and there was no significant difference when the PSD-95 mutant distribution was compared to the wild-type distribution.

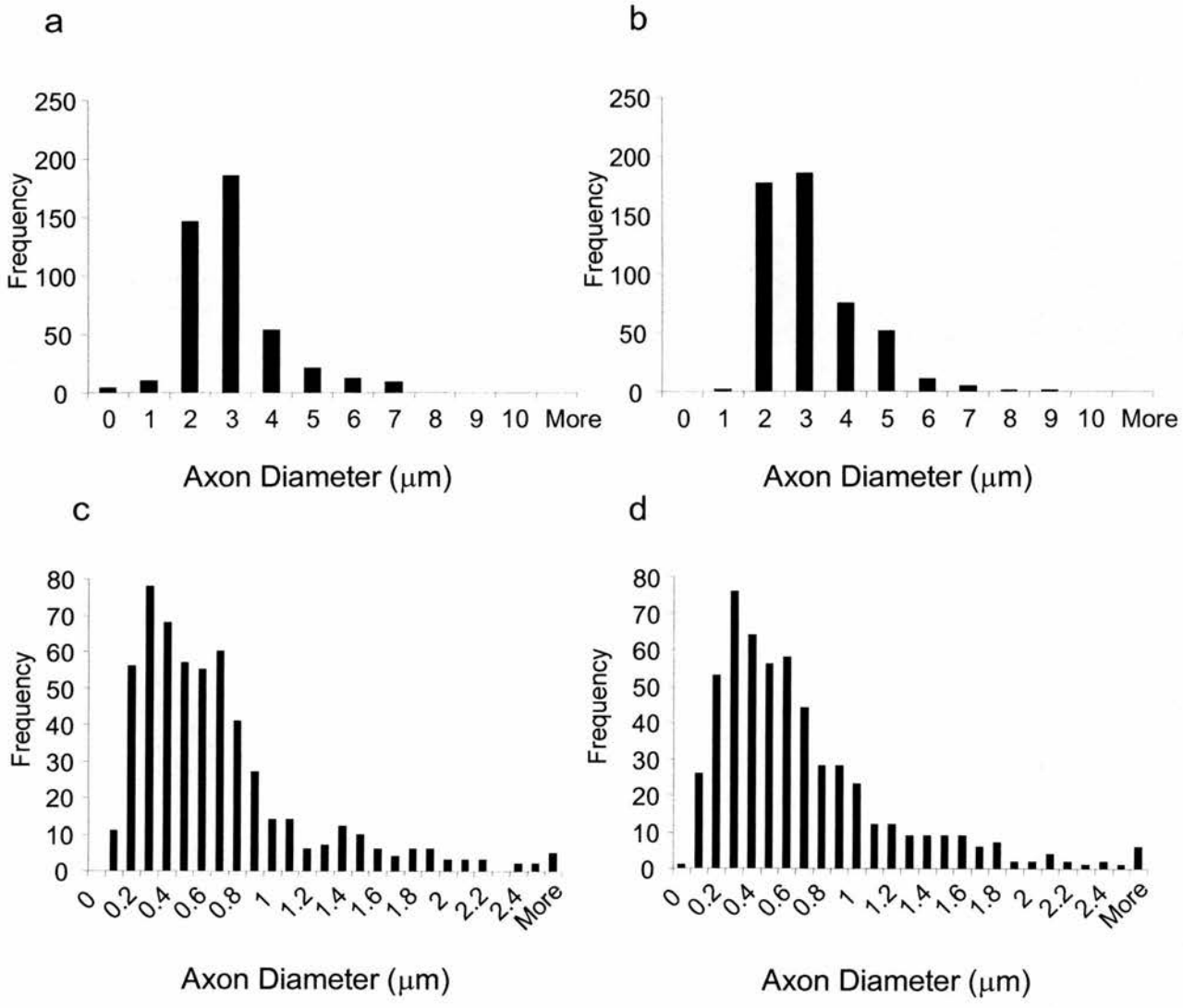
a
Frequency
250
200
150
100
50
0
0 1 2 3 4 5 6 7 8 9 10 More
Axon Diameter (μm)
b
Frequency
250
200
150
100
50
0
0 1 2 3 4 5 6 7 8 9 10 More
Axon Diameter (μm)
c
Frequency
80
70
60
50
40
30
20
10
0
0 0.2 0.4 0.6 0.8 1 1.2 1.4 1.6 1.8 2 2.2 2.4 More
Axon Diameter (μm)
d
Frequency
80
70
60
50
40
30
20
10
0
0 0.2 0.4 0.6 0.8 1 1.2 1.4 1.6 1.8 2 2.2 2.4 More
Axon Diameter (μm)

Figure 4.8 Light microscopy images of the tibial branch of the sciatic nerve of wild-type and PSD-95 mutant mice following CCI distal to ligation

In (a), a light micrograph image of wild-type tibial nerve distal to ligation shows a loss of larger myelinated fibres as represented in Figure 4.6 (a) and in (b), an image of PSD-95 mutant tibial nerve distal to ligation shows a similar loss of larger myelinated fibres as represented in Figure 4.7 is shown. These represent typical examples of fibre morphology.

Scale bar = 10μm

a

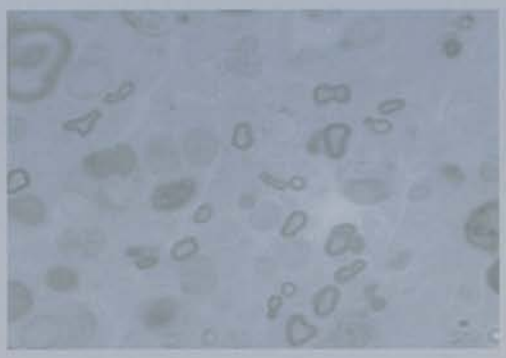

b

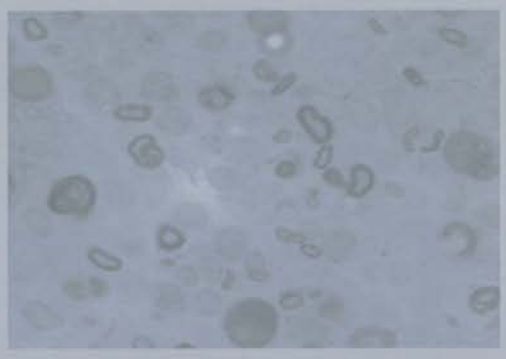

4.2.5 Behavioural reflex effects of the NMDA receptor antagonist (R)-CPP following CCI

The NMDA receptor is consistently documented to be involved in the central sensitisation of pain pathways following afferent nerve damage. To examine whether the lack of injury-induced sensitisation in pain behaviours in the homozygous PSD-95 mutant mice might relate to the role of PSD-95 as an NMDA receptor adapter protein, we assessed the contribution of spinal NMDA receptors to the CCI-induced changes here by the local administration of a highly selective NMDA receptor antagonist, (R)-CPP (see Section 2.2.4 and compound details in Table 2.1, pgs. 60-63).

In wild-type mice, the ipsilateral thermal hyperalgesia brought about by CCI was reversed by (R)-CPP with dose-dependent effects in each case from 50-200pmole/in 10μl saline, while the drug had no significant effect on responses elicited from the uninjured hindlimb of wild-type mice (Fig. 4.9a, b, and c). Again, in wild-type mice, the ipsilateral mechanical allodynia brought about by CCI could be reversed by (R)-CPP with dose-dependent effects in each case from 50-200pmole/in 10μl, although there was a trend toward elevated paw withdrawal thresholds in the von Frey test (Fig. 4.10a, b and c) on the contralateral side.

Intrathecal injection of (R)-CPP in PSD-95 mutant mice following CCI had no effect on responses from either hindlimb of PSD-95 mutants (where the development of neuropathic sensitisation had failed to occur) to either thermal or mechanical stimuli (Fig. 4.11a and b, respectively). The elevated baseline threshold for mechanical withdrawal reflexes seen bilaterally in the PSD-95 mutants was unaffected by (R)-CPP, indicating that this change is not caused by contralateral NMDA receptor activation (Fig. 4.11b).

As a control, the intrathecal injection of (R)-CPP in naïve wild-type mice had no effect on thermal or mechanical withdrawal responses (Fig. 4.12a and b, respectively). Similarly, the intrathecal injection of (R)-CPP in naïve PSD-95 mutant mice had no effect on thermal or mechanical withdrawal responses (Fig. 4.13a and b,

respectively). As a further control, the intrathecal injection of the saline vehicle in wild-type mice following CCI had no effect on the presence of thermal and mechanical reflex sensitivity (Fig. 4.14a and b, respectively) and did not affect withdrawal thresholds of PSD-95 mutant mice at any time (Fig. 4.15a and b).

These findings show that the prevention of neuropathic sensitisation seen in PSD-95 mutant mice can be mimicked by spinal NMDA receptor blockade in wild-type mice, consistent with the idea that disruption of some aspect of spinal NMDA receptor function in the mutant may be responsible for the failure of sensitisation.

4.2.6 Intrathecal administration of the agonist NMDA in naïve mice

Behavioural changes following CCI were bilaterally mimicked in naïve wild-type mice by acute intrathecal administration of 0.25nmol/in 10µl NMDA (see Section 2.2.4 and compound details in Table 2.1, pgs 60-63). Statistically significant development of thermal hyperalgesia in wild-type mice could be seen following intrathecal NMDA (Fig. 4.16a). In striking contrast, behavioural responses of PSD-95 mutant mice to the noxious thermal stimulus were unaffected by intrathecal administration of NMDA (Fig. 4.16a). Similarly, in naïve wild-type mice, intrathecal administration of NMDA mimicked (bilaterally) the mechanical allodynia seen unilaterally after CCI (Fig. 4.16b). In PSD-95 mutant mice, the effect of NMDA was completely abrogated (Fig. 4.16b).

These findings indicate that spinal NMDA receptor function (as monitored by a physiological read-out of neuropathic pain behaviour) is profoundly disrupted in PSD-95 mutant mice and spinal NMDA receptor activation adequately mimics neuropathic sensitisation in wild-type mice in a manner that is disrupted by PSD-95 mutation. The observations suggest that failure of proper NMDA receptor function in the dorsal horn of PSD-95 mutants is responsible for the lack of neuropathic sensitisation observed.

Figure 4.9 Effects of the intrathecal administration of the selective NMDA receptor antagonist (R)-CPP on thermal hyperalgesia in wild-type mice at the peak of neuropathic reflex sensitivity

Data represent the average hindlimb withdrawal latency ± SEM to a noxious thermal stimulus of wild-type mice (n=7) for each time point following the intrathecal injection of 50ρmol (a), 100ρmol (b) or 200ρmol (c) of (R)-CPP.

Wild-type mice at the peak of ipsilateral thermal hyperalgesia, as determined by a significant reduction in ipsilateral paw withdrawal latency ('PWL') compared to contralateral withdrawal latency (*, $p < 0.05$, Student's t-test), were intrathecally injected with (R)-CPP (at arrow). 10 min following injection, 50ρmol (a), 100ρmol (b) or 200ρmol (c) of (R)-CPP significantly attenuated ipsilateral thermal hyperalgesia in comparison to pre-injection ipsilateral values (†, $p<0.05$, One-way ANOVA followed by a Dunnett's test) while there was no significant alteration in the pre-/post- injection contralateral responses. The duration of the drug effect varied in a dose-dependent manner, with 50ρmol (R)-CPP reversing the sensitisation of ipsilateral paw withdrawal for 20 min, whereas 100ρmol and 200ρmol (R)-CPP had significant effects for around 50 min. As the drug effect wore off, ipsilateral PWL returned to baseline withdrawal latencies indicative of thermal hyperalgesia.

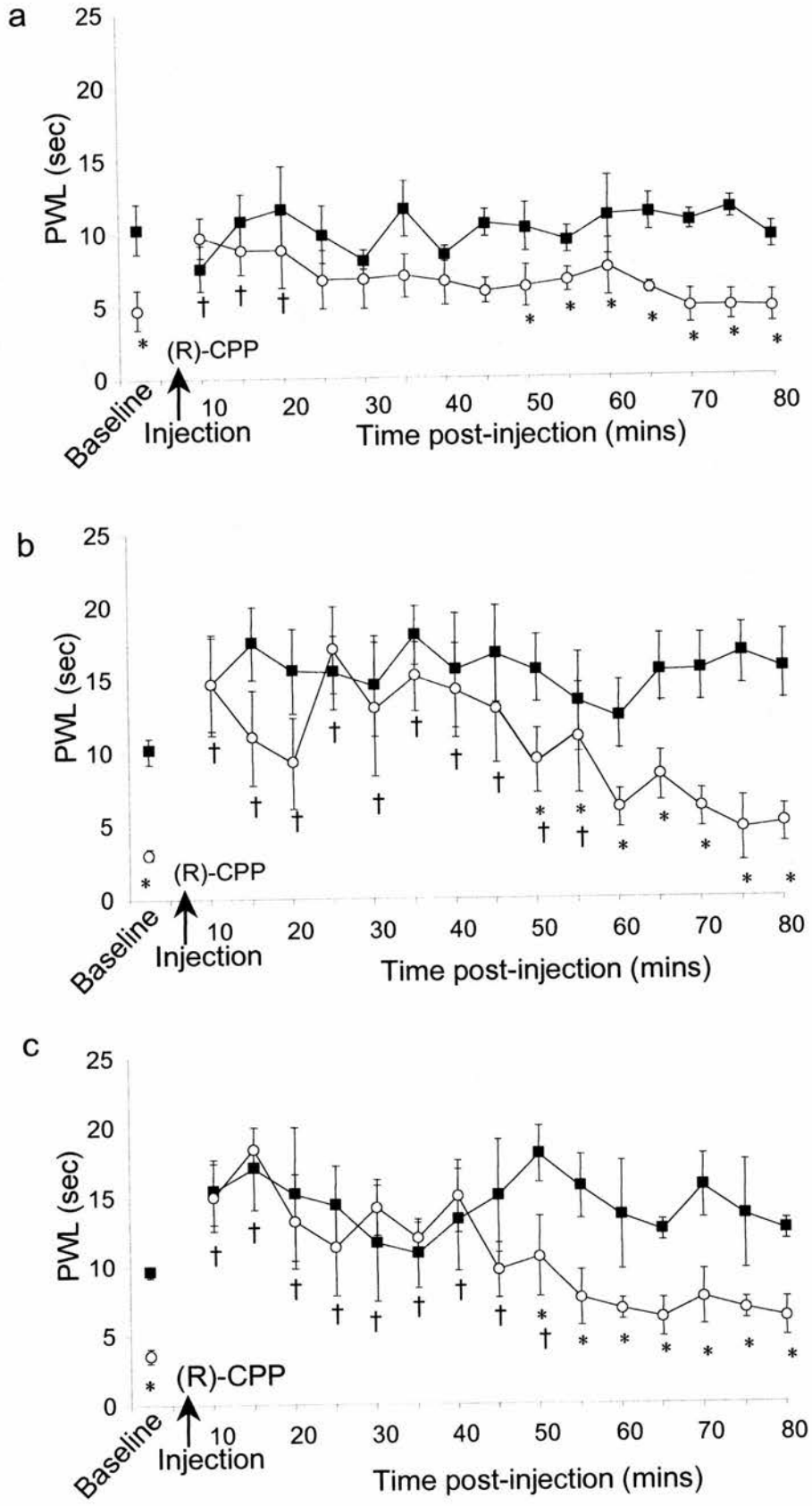
a
b
c
PWL (sec)
25
20
15
10
5
0
(R)-CPP
Baseline
Injection
10
20
30
40
50
60
70
80
Time post-injection (mins)

Figure 4.10 Effects of the intrathecal administration of the selective NMDA receptor antagonist (R)-CPP on mechanical allodynia in wild-type mice at the peak of neuropathic reflex sensitivity

Data represent the average hindlimb withdrawal threshold ± SEM to a normally innocuous mechanical stimulus of wild-type mice (n=7) for each time point following the intrathecal injection of 50pmol (a), 100pmol (b) or 200pmol (c) of (R)-CPP.

Wild-type mice at the peak of ipsilateral mechanical allodynia, as determined by a significant reduction in ipsilateral paw withdrawal latency ('PWL') compared to contralateral withdrawal latency (*, $p < 0.05$, Mann-Whitney Rank Sum test), were intrathecally injected with (R)-CPP (at arrow). 10 min following injection, 50pmol (a), 100pmol (b) or 200pmol (c) of (R)-CPP significantly attenuated ipsilateral mechanical allodynia in comparison to pre-injection ipsilateral values (†, $p<0.05$, Kruskal-Wallis ANOVA followed by a Dunn's test) while there was no significant alteration in the pre-/post- injection contralateral responses. The duration of the drug effect varied in a dose-dependent manner, with 50pmol (R)-CPP reversing the sensitisation of ipsilateral paw withdrawal for 20 min, whereas 100pmol reversed ipsilateral sensitisation for 40 min and 200pmol (R)-CPP had significant effects for up to 50 min. However, at this highest dose (c) there were variations in the contralateral response, indicative of effects on motor co-ordination. As the drug effect wore off, ipsilateral PWL returned to baseline withdrawal thresholds indicative of mechanical allodynia.

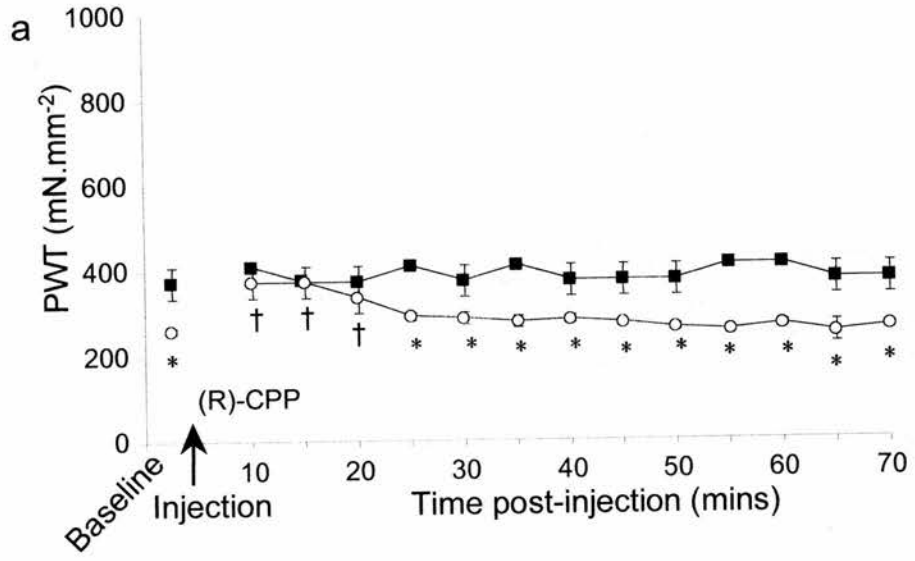
a
1000
800
600
400
200
0
PWT (mN.mm-2)
(R)-CPP
Baseline
Injection
10
20
30
40
50
60
70
Time post-injection (mins)

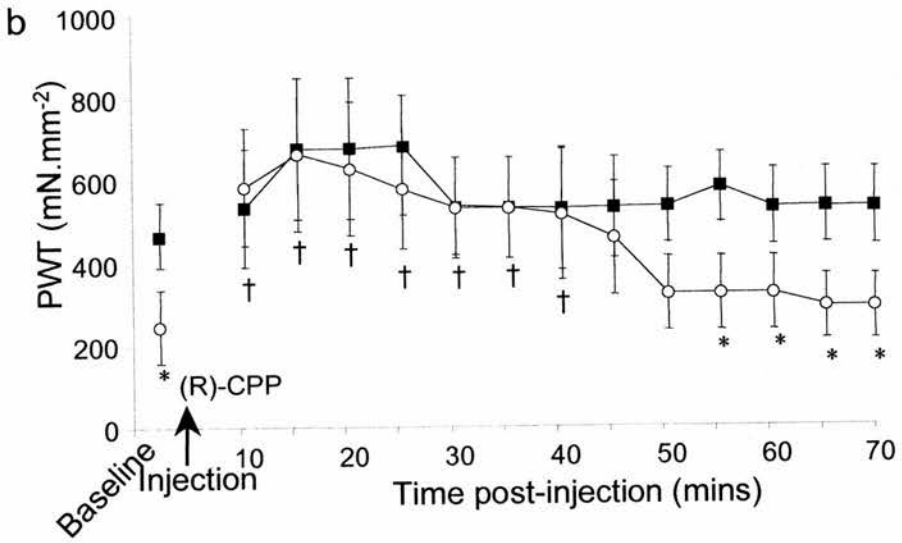
b
1000
800
600
400
200
0
PWT (mN.mm-2)
(R)-CPP
Baseline
Injection
10
20
30
40
50
60
70
Time post-injection (mins)

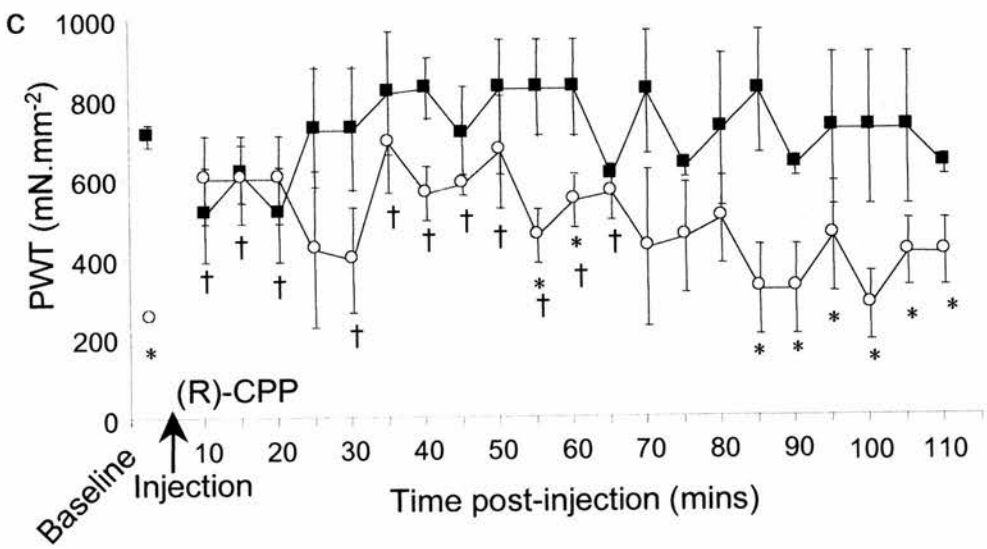
c
1000
800
600
400
200
0
PWT (mN.mm-2)
(R)-CPP
Baseline
Injection
10
20
30
40
50
60
70
80
90
100
110
Time post-injection (mins)

Figure 4.11 Effects of the intrathecal administration of the selective NMDA receptor antagonist (R)-CPP in PSD-95 mutant mice following CCI

Data represent the average (a) hindlimb withdrawal threshold to noxious heat and (b) withdrawal threshold to mechanical (von Frey filament) stimuli ± SEM for each time point in PSD-95 mutant mice that had previously undergone CCI (n=7), following the intrathecal injection of 100ρmol of (R)-CPP.

There was no significant difference in either withdrawal latency or threshold (a and b, respectively) of either hindpaw in PSD-95 mutant mice that had undergone CCI when testing resumed 10 min following injection of the antagonist (Student's t-test and Mann-Whitney Rank Sum test, respectively). The intrathecal injection of (R)-CPP (at arrow) had no significant effect on the withdrawal latency or withdrawal threshold in either hindlimb.

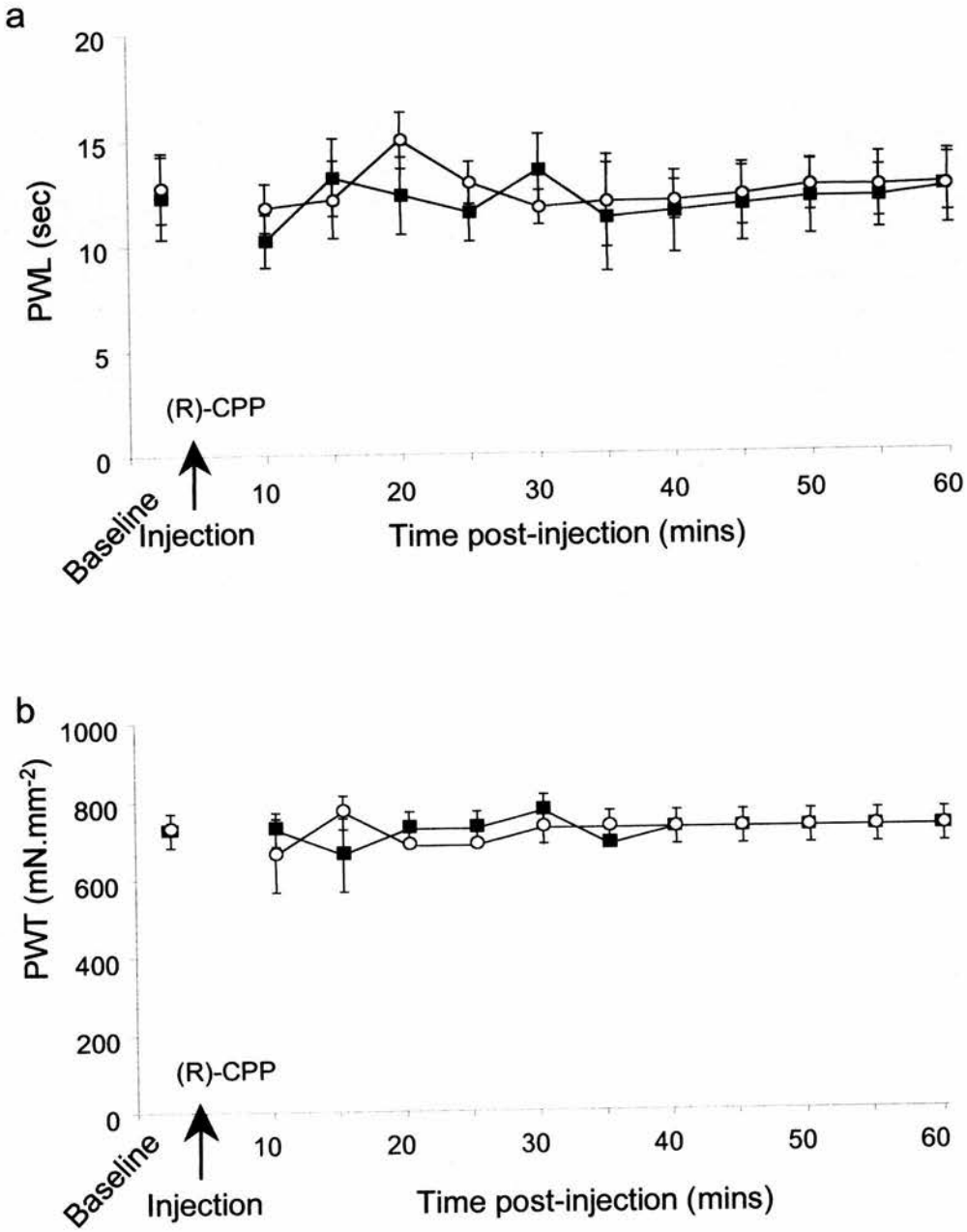
a
20
15
10
5
0
PWL (sec)
(R)-CPP
Baseline
Injection
10
20
30
40
50
60
Time post-injection (mins)
b
1000
800
600
400
200
0
PWT (mN.mm-2)
(R)-CPP
Baseline
Injection
10
20
30
40
50
60
Time post-injection (mins)

Figure 4.12 Effects of the intrathecal administration of the selective NMDA receptor antagonist (R)-CPP in naïve wild-type mice

Data represent the average (a) hindlimb withdrawal threshold to noxious heat and (b) withdrawal threshold to mechanical (von Frey filament) stimuli ± SEM for each time point in naïve wild-type mice (n=5) following the intrathecal injection of 100ρmol of (R)-CPP.

There was no significant difference in either withdrawal latency or threshold (a and b, respectively) of either hindpaw in naïve wild type mice when testing resumed 10 min following injection (Student's t-test and Mann-Whitney Rank Sum test, respectively). The intrathecal injection of (R)-CPP (at arrow) had no significant effect on the withdrawal latency or withdrawal threshold in either hindlimb.

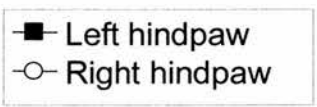

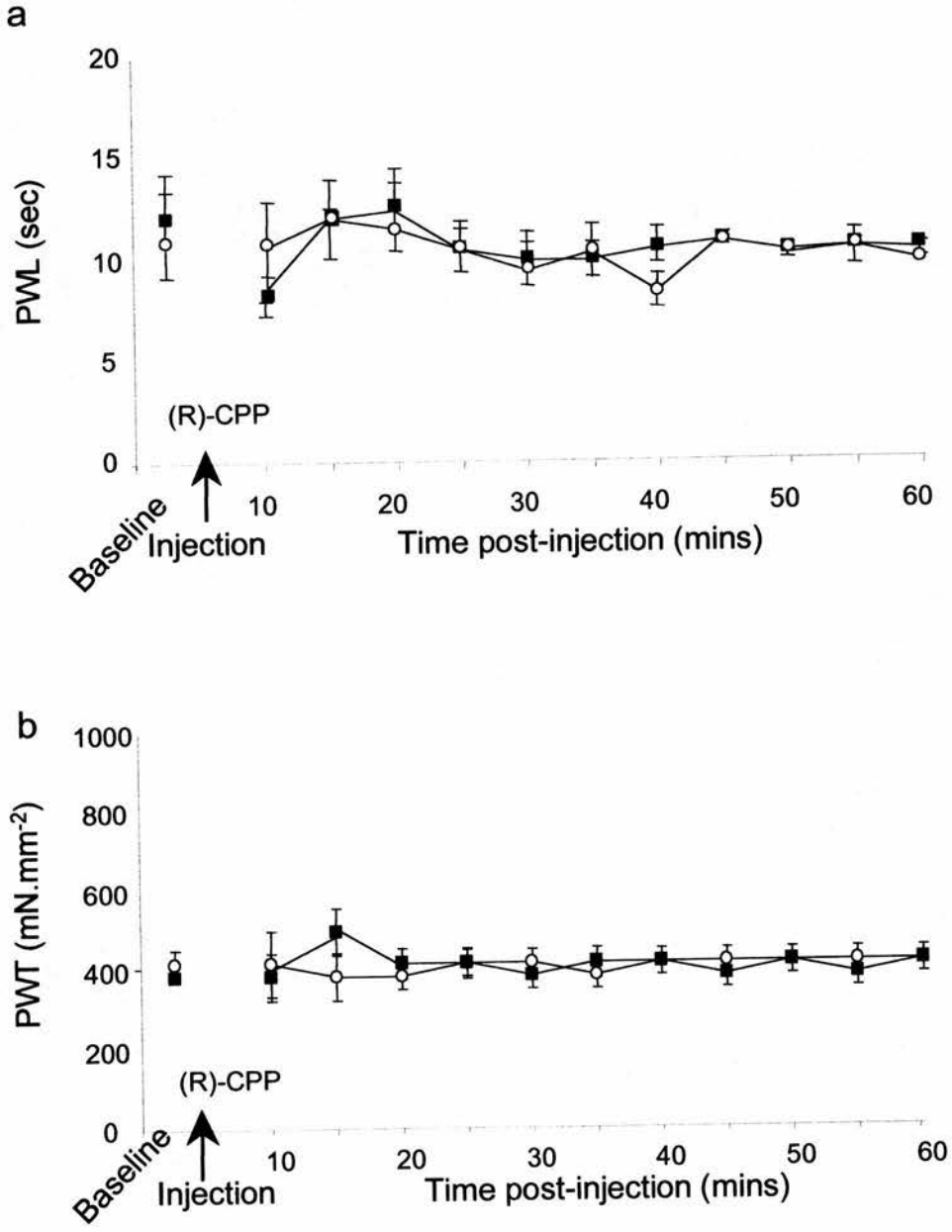
a
20
15
10
5
0
PWL (sec)
(R)-CPP
Baseline
Injection
10
20
30
40
50
60
Time post-injection (mins)
b
1000
800
600
400
200
0
PWT (mN.mm-2)
(R)-CPP
Baseline
Injection
10
20
30
40
50
60
Time post-injection (mins)

Figure 4.13 Effects of the intrathecal administration of the selective NMDA receptor antagonist (R)-CPP in naïve PSD-95 mutant mice

Data represent the average (a) hindlimb withdrawal threshold to noxious heat and (b) withdrawal threshold to mechanical (von Frey filament) stimuli ± SEM for each time point in naïve PSD-95 mutant mice (n=5) following the intrathecal injection of 100ρmol of (R)-CPP.

There was no significant difference in either withdrawal latency or threshold (a and b, respectively) of either hindpaw in naïve PSD-95 mutant mice when testing resumed 10 min following injection (Student's t-test and Mann-Whitney Rank Sum test, respectively). The intrathecal injection of (R)-CPP (at arrow) had no significant effect on the withdrawal latency or withdrawal threshold in either hindlimb.

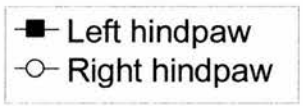

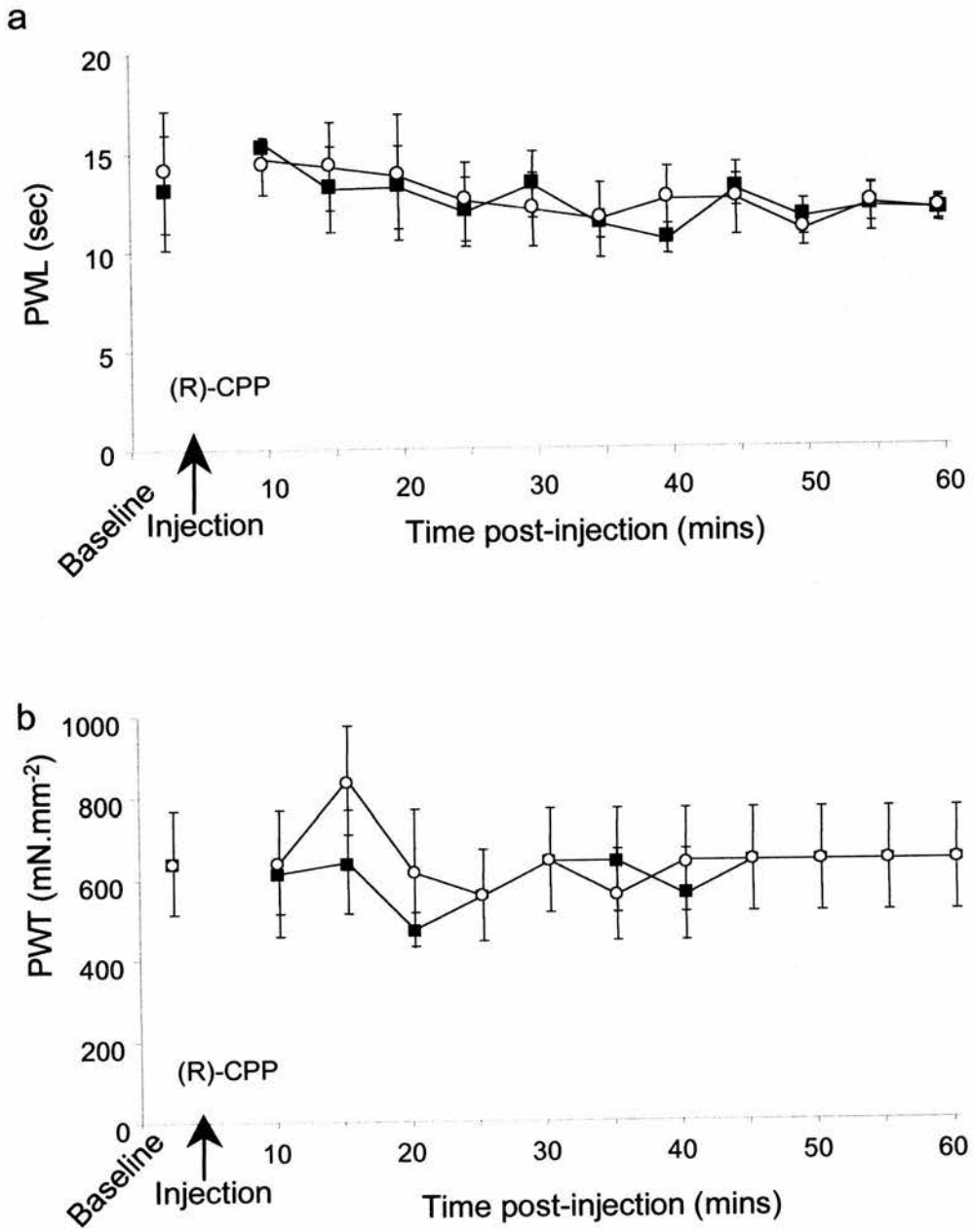
a
20
15
10
5
0
PWL (sec)
(R)-CPP
Baseline
Injection
10
20
30
40
50
60
Time post-injection (mins)
b
1000
800
600
400
200
0
PWT (mN.mm-2)
(R)-CPP
Baseline
Injection
10
20
30
40
50
60
Time post-injection (mins)

Figure 4.14 Effects of the intrathecal administration of saline in wild-type mice at the peak of neuropathic reflex sensitivity

Data represent the average (a) hindlimb withdrawal to noxious heat and (b) withdrawal threshold to mechanical (von Frey filament) stimuli ± SEM for each time point in wild type mice (n=6) at the peak of behavioural reflex sensitivity following the intrathecal injection of saline vehicle.

Wild type mice at the peak of ipsilateral thermal hyperalgesia, as determined by a significant reduction in ipsilateral paw withdrawal latency (a, 'PWL'; *, $p<0.05$ Student's t-test) or paw withdrawal threshold (b, 'PWT'; *, $p<0.05$ Mann-Whitney Rank Sum test) compared to contralateral withdrawal latency, were intrathecally injected with saline (at arrow). 10 min following injection, saline had no discernible effect on the withdrawal latency or the withdrawal threshold in either hindlimb and there was no significant effect on hindlimb withdrawal post-injection when compared to pre-injection, baseline withdrawal.

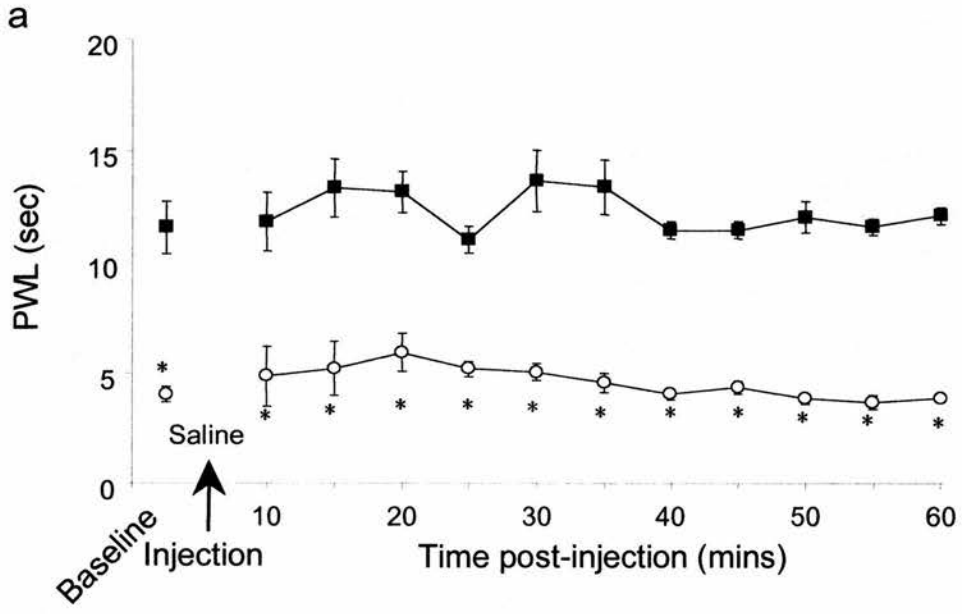
a
PWL (sec)
20
15
10
5
0
Saline
Baseline
Injection
10
20
30
40
50
60
Time post-injection (mins)

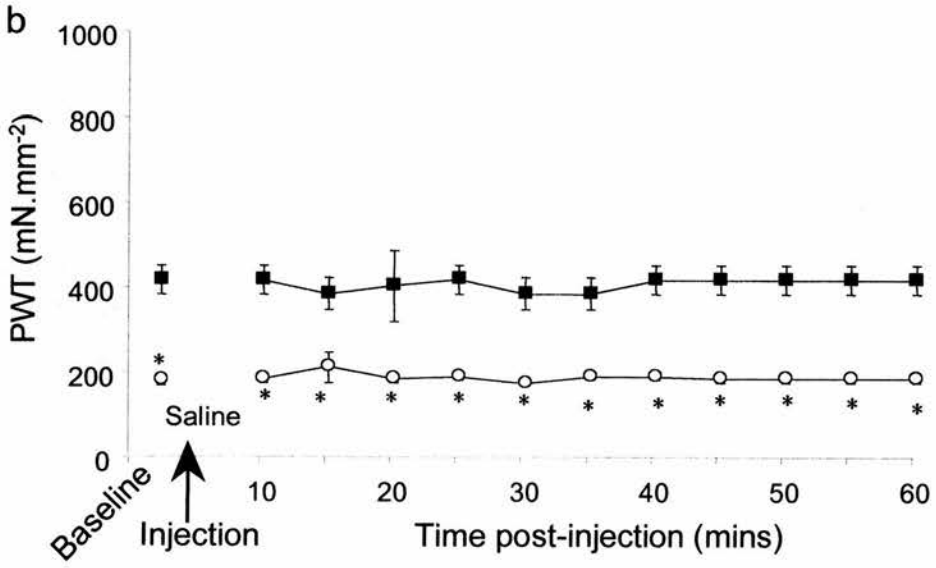
b
PWT (mN.mm-2)
1000
800
600
400
200
0
Saline
Baseline
Injection
10
20
30
40
50
60
Time post-injection (mins)

Figure 4.15 Effects of the intrathecal administration of saline in PSD-95 mutant mice following CCI

Data represent the average (a) hindlimb withdrawal to noxious heat and (b) withdrawal threshold to mechanical (von Frey filament) stimuli ± SEM for each time point in PSD-95 mutant mice that had previously undergone CCI surgery (n=6) following the intrathecal injection of saline vehicle.

There was no significant difference in either withdrawal latency or threshold (a and b, respectively) of either hindpaw in PSD-95 mutant mice following CCI (Student's t-test and Mann-Whitney Rank Sum test, respectively). Saline (at arrow) had no discernible effect on the withdrawal latency or the withdrawal threshold in either hindlimb and there was no significant effect in hindlimb withdrawal post-injection when compared to pre-injection, baseline withdrawal.

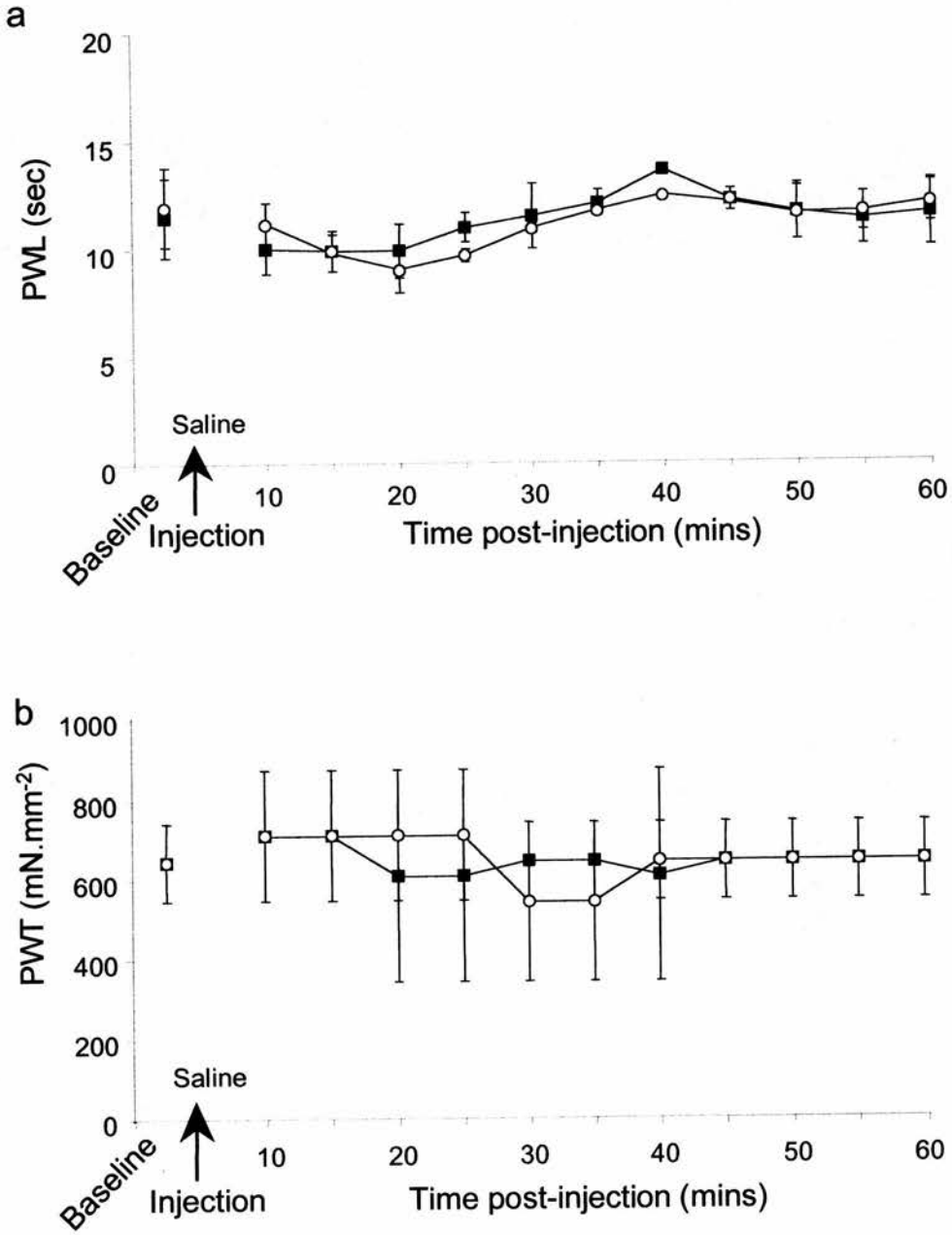
a
20
15
10
5
0
PWL (sec)
Saline
Baseline
Injection
10
20
30
40
50
60
Time post-injection (mins)
b
1000
800
600
400
200
0
PWT (mN.mm-2)
Saline
Baseline
Injection
10
20
30
40
50
60
Time post-injection (mins)

Figure 4.16 Effects of the intrathecal administration of the agonist NMDA in naïve wild-type and PSD-95 mutant mice

Data are represented as the mean bilateral response ± SEM to the paw withdrawal latency to noxious thermal stimulation (a) and the paw withdrawal threshold to mechanical stimulation (b) for each time point prior to ('baseline') and 10 min following the intrathecal administration of NMDA (0.25nmol in 10µl, at arrow) to naïve wild-type (▲) and naïve PSD-95 mutant (△) mice (n=6 wild-type; n=7 for PSD-95 mutant mice).

Wild-type mice showed significant development of thermal hyperalgesia following intrathecal injection of NMDA when compared to pre-drug administration values in response to thermal stimulation (a, *, $p<0.01$, One-way ANOVA) and in response to mechanical stimulation (b, *, $p<0.01$, Kruskal-Wallis one-way ANOVA). No development of thermal hyperalgesia post-NMDA administration was seen in PSD-95 mutant mice when compared to pre-injection values (One-way ANOVA), nor was there any development of mechanical allodynia post-drug administration when compared to pre-drug values (Kruskal-Wallis one-way ANOVA).

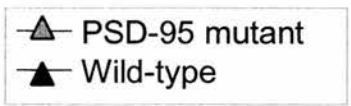

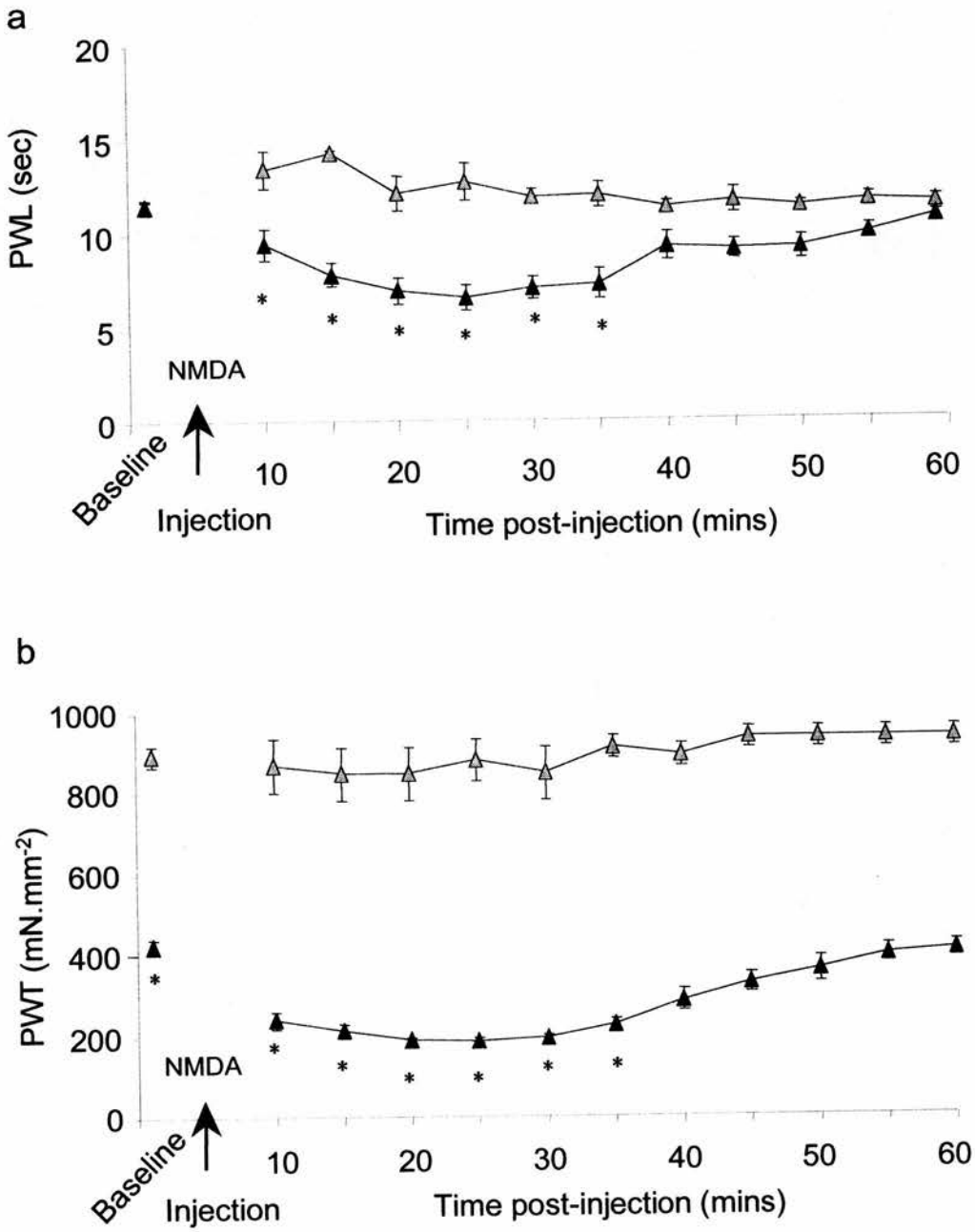
a
20
15
10
5
0
PWL (sec)
NMDA
Baseline
Injection
10
20
30
40
50
60
Time post-injection (mins)
b
1000
800
600
400
200
0
PWT (mN.mm-2)
NMDA
Baseline
Injection
10
20
30
40
50
60
Time post-injection (mins)

4.2.7 Behavioural reflex effects of intrathecal injection of CaMKII inhibitors

Since the primary action of activated NMDA receptors is the gating of Ca^{2+} entry, which can stimulate the Ca^{2+}-activated protein kinase, CaMKII, we investigated whether CaMKII activity is necessary for the NMDA-dependent sensitisation of spinal neurones by the intrathecal injection of CaMKII inhibitors in wild-type mice following CCI (see Section 2.2.4 and compound details in Table 2.1, pgs 60-63).

Intrathecal injection of the potent, selective CaMKII inhibitor myristoyl-autocamtide 2-related inhibitory peptide (myr-AIP) clearly reversed the neuropathic thermal hyperalgesia for up to 70 min (Fig. 4.17a) and mechanical allodynia for up to 45 min (Fig. 4.17b) seen in wild-type mice following CCI. Similarly, intrathecal injection of the selective CaMKII inhibitor KN-93 reversed thermal hyperalgesia for 45 min (Fig. 4.18a) and mechanical allodynia for up to 65 min (Fig. 4.18b) in wild-type mice following CCI.

An analogue of KN-93 with reduced activity against CaMKII, KN-92, showed less effects on neuropathic sensitisation to the noxious thermal stimulus (Fig. 4.19a) and to the mechanical stimulus (Fig. 4.19b).

These observations support the behavioural reflex evidence for a key role of the NMDA receptor and its downstream target CaMKII in neuropathic sensitisation and indicate that acute blockade at either point in this pathway is effective in reversing established neuropathic sensitisation.

Figure 4.17 Effects of the selective CaMKII inhibitor myristoyl-autocamtide 2-related inhibitory peptide on thermal hyperalgesia and mechanical allodynia in wild-type mice at the peak of neuropathic reflex sensitivity

Data represent the average (a) hindlimb withdrawal latency to noxious heat and (b) withdrawal threshold to von Frey filament stimuli ± SEM (n=8) for each time point before and following the intrathecal injection of 1nmol myristoyl-autocamtide 2-related inhibitory peptide ('myr-AIP', 1nmol in 10µl saline).

Wild-type mice at the peak of ipsilateral thermal hyperalgesia as determined by a significant reduction in ipsilateral paw withdrawal latency (a, 'PWL'; *, $p<0.05$ Student's t-test) or paw withdrawal threshold (b, 'PWT'; *, $p<0.05$ Mann-Whitney Rank Sum test) compared to contralateral withdrawal latency were intrathecally injected with myristoyl-autocamtide 2-related inhibitory peptide (at arrow). 10 min following injection, myristoyl-autocamtide 2-related inhibitory peptide significantly attenuated ipsilateral thermal hyperalgesia (a) in comparison to pre-injection ipsilateral values (†, $p<0.05$, One-way ANOVA followed by a Dunnett's test) while there was no significant alteration in the contralateral response. The effect lasted for up to 70 min for the thermal test and 45 min for the mechanical test before the ipsilateral withdrawal returned to pre-injection, baseline thresholds (*, $p<0.05$ Student's t-test, †, $p<0.05$ Mann-Whitney Rank Sum test, respectively).

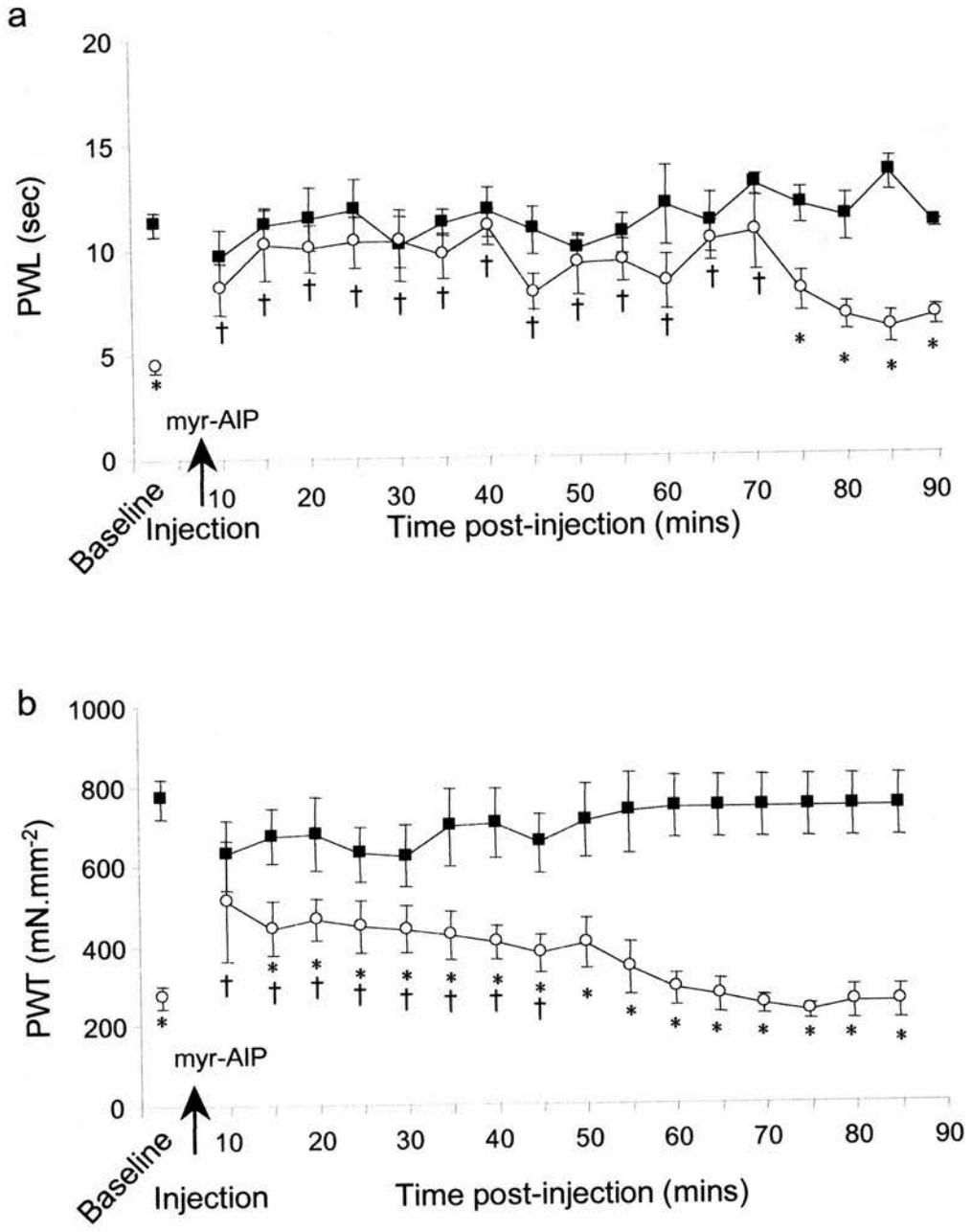
a
PWL (sec)
20
15
10
5
0
myr-AIP
Baseline
10
20
30
40
50
60
70
80
90
Injection
Time post-injection (mins)
b
PWT (mN.mm-2)
1000
800
600
400
200
0
myr-AIP
Baseline
10
20
30
40
50
60
70
80
90
Injection
Time post-injection (mins)

Figure 4.18 Effects of the CaMKII inhibitor KN-93 on thermal hyperalgesia and mechanical allodynia in wild-type mice at the peak of neuropathic reflex sensitivity

Data represent the average (a) hindlimb withdrawal latency to noxious heat and (b) withdrawal threshold to von Frey stimuli ± SEM to a noxious thermal or normally innocuous mechanical stimulus (n=9) for each time point before and following the intrathecal injection of 120ρmol KN-93.

Wild-type mice at the peak of ipsilateral thermal hyperalgesia as determined by a significant reduction in ipsilateral paw withdrawal latency (a, 'PWL'; *, $p<0.05$ Student's t-test) or paw withdrawal threshold (b, 'PWT'; *, $p<0.05$ Mann-Whitney Rank Sum test) compared to contralateral withdrawal latency, were intrathecally injected with KN-93 (at arrow). 10 min following injection, 120ρmol KN-93 significantly attenuated ipsilateral thermal hyperalgesia in (a) in comparison to pre-injection ipsilateral values (†, $p<0.05$, One-way ANOVA followed by a Dunnett's test) while there was no significant alteration in the contralateral response. In (b), the ipsilaterally reduced paw withdrawal threshold to mechanical stimulation was significantly increased (†, $p<0.05$, Kruskal-Wallis ANOVA followed by a Dunn's test) with no change in contralateral responses. The effect of KN-93 lasted for up to 45 min for the thermal test and 65 min for the mechanical test before the ipsilateral withdrawal returned to pre-injection, baseline values indicative of hyperalgesia/ allodynia.

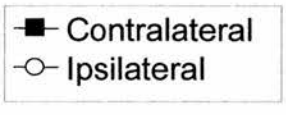

a

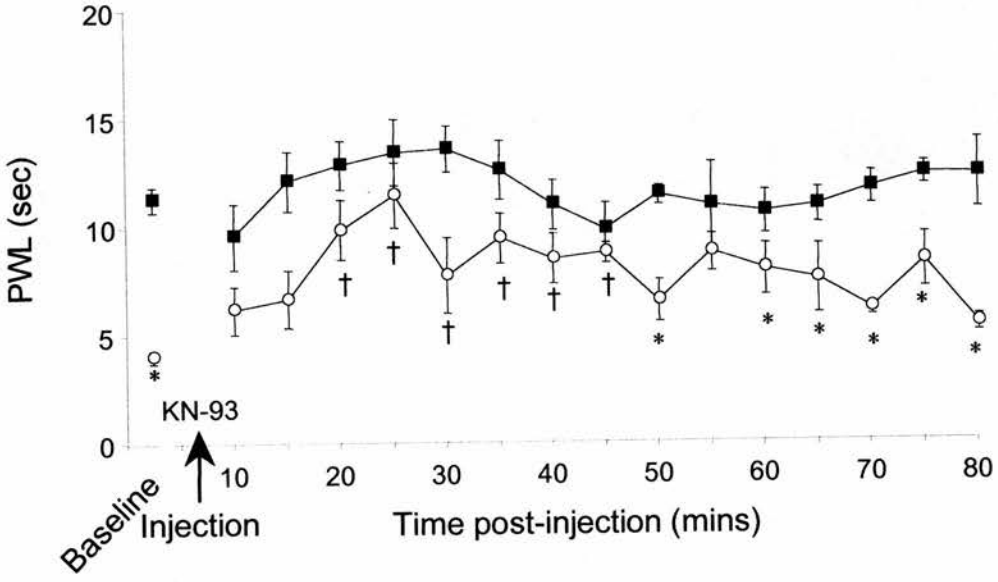
PWL (sec)
20
15
10
5
0
KN-93
Baseline
Injection
10
20
30
40
50
60
70
80
Time post-injection (mins)

b

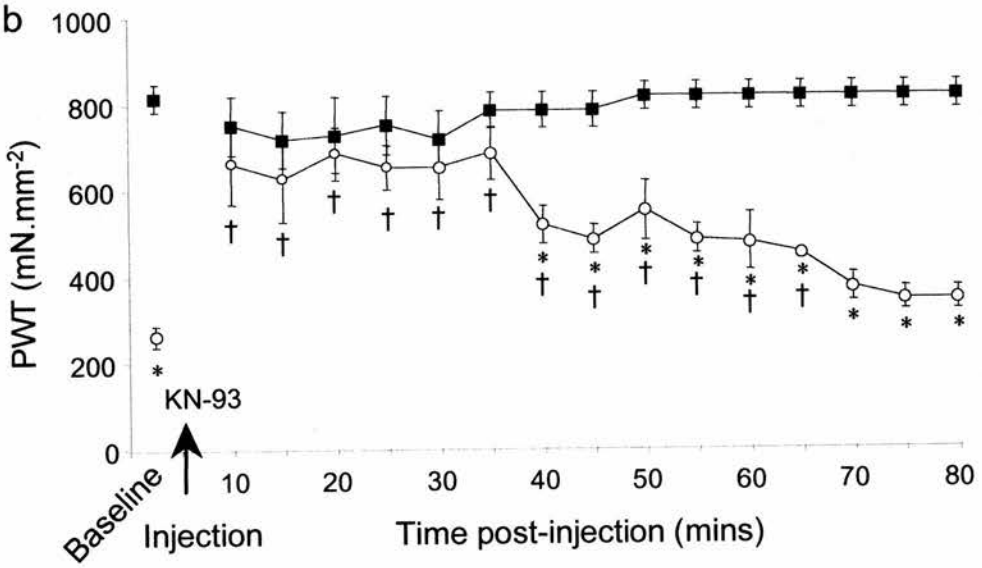
PWT (mN.mm-2)
1000
800
600
400
200
0
KN-93
Baseline
Injection
10
20
30
40
50
60
70
80
Time post-injection (mins)

Figure 4.19 Effects of the less active control analogue KN-92 on thermal hyperalgesia and mechanical allodynia in wild-type mice at the peak of neuropathic reflex sensitivity

Data represent the average (a) hindlimb withdrawal latency to noxious heat and (b) withdrawal threshold to von Frey stimuli ± SEM to a noxious thermal or normally innocuous mechanical stimulus (n=8) for each time point before and following the intrathecal injection of 120ρmol of the less active KN-93 analogue, KN-92 as indicated....

Wild-type mice at the peak of ipsilateral thermal hyperalgesia as determined by a significant reduction in ipsilateral paw withdrawal latency (a, 'PWL'; *, $p<0.05$ Student's t-test) or paw withdrawal threshold (b, 'PWT'; *, $p<0.05$ Mann-Whitney Rank Sum test) compared to contralateral withdrawal latency, were intrathecally injected with KN-92 (at arrow). 10 min following injection, 120ρmol KN-92 moderately attenuated ipsilateral thermal hyperalgesia in (a) in comparison to pre-injection ipsilateral values (†, $p<0.05$, One-way ANOVA followed by a Dunnett's test) while there was no significant alteration in the contralateral response. In (b), the ipsilaterally reduced paw withdrawal threshold to mechanical stimulation was moderately increased (†, $p<0.05$, Kruskal-Wallis ANOVA followed by a Dunn's test) with no change in contralateral responses. The effect of KN-92 lasted for up to 35 min for the thermal test and 40 min for the mechanical test before the ipsilateral withdrawal returned to pre-injection, baseline values indicative of hyperalgesia/ allodynia.

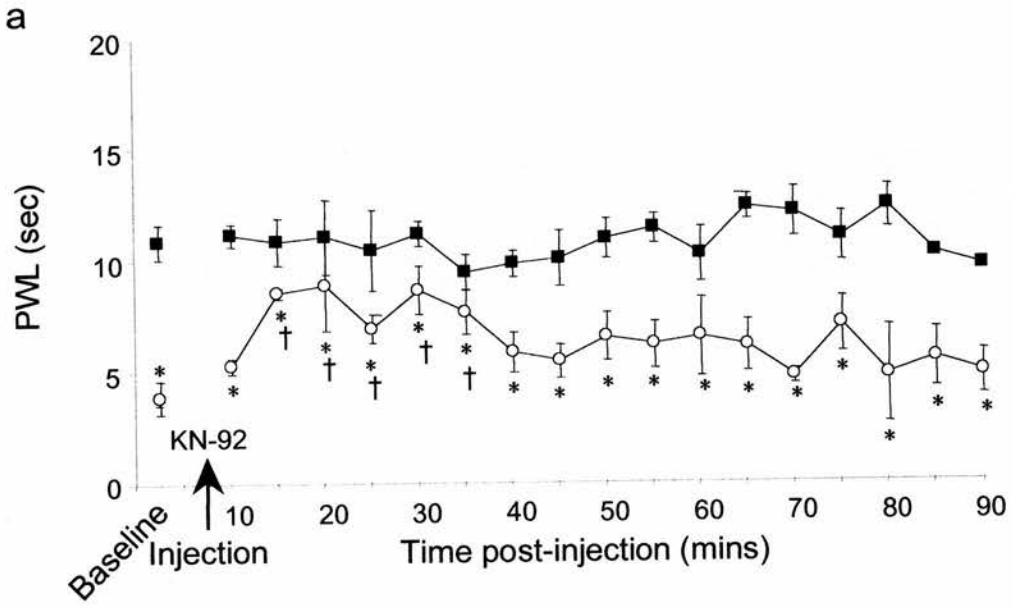
a
PWL (sec)
20
15
10
5
0
KN-92
Baseline
Injection
10
20
30
40
50
60
70
80
90
Time post-injection (mins)

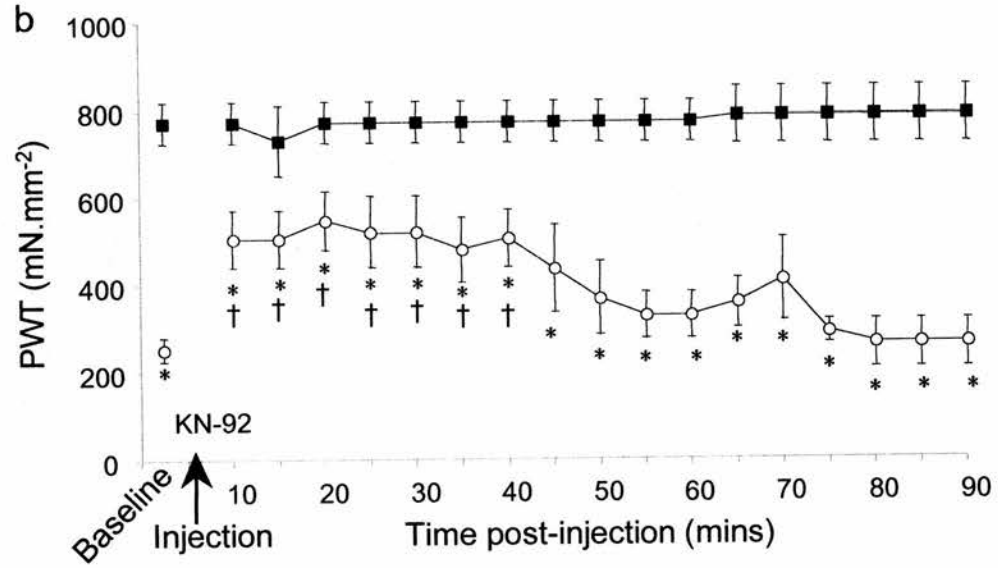
b
PWT (mN.mm-2)
1000
800
600
400
200
0
KN-92
Baseline
Injection
10
20
30
40
50
60
70
80
90
Time post-injection (mins)

4.2.8 CaMKII activity in wild-type and PSD-95 mutant mice

Following activation, CaMKII autophosphorylates at Thr^{286} to produce a constitutively active form of the enzyme (Hanson et al., 1989). To provide a biochemical index of the activation state of CaMKII, we isolated CaMKII by immunoprecipitation from spinal cord extracts and measured the proportion of its activity that was constitutive in order to monitor NMDA receptor-mediated Ca^{2+} entry. We assessed CaMKII activation responses in PSD-95 mutant mice to establish whether functional communication between the NMDA receptor and CaMKII might be disrupted by the PSD-95 mutation (see Section 2.4.5, pgs 90-91).

The proportion of immunoprecipitated CaMKII activity that was constitutive (rather than maximally evoked by Ca^{2+} addition in vitro) was measured after topical application of NMDA (with its co-agonist glycine), of the Ca^{2+} ionophore, ionomycin or of saline vehicle to dorsal surface of the spinal cord of naïve wild-type and PSD-95 mutant mice. There was no significant difference in the proportion of constitutive CaMKII activity in the increased response to either NMDA or ionomycin between wild-type and PSD-95 mutant mice (Table 4.1a). This response to NMDA/glycine was similar to that of ionomycin, and so must be assumed to represent a ceiling level of response. Also, the mean maximal CaMKII activity (evoked by Ca^{2+}/calmodulin addition in vitro) in immunoprecipitates from PSD-95 mutant mice spinal cord was unaltered from that seen in wild-type mice (108.3 ± 13.7 and 97.8 ± 13.1 pmoles/min/μg original extract protein, respectively), indicating that CaMKII expression is not likely to be altered in the mutant mice. So, spinal NMDA receptor function at the level of acute agonist-induced Ca^{2+} entry in response to agonist stimulation is not affected in naïve PSD-95 mutant mice, a result that is consistent with earlier studies in the hippocampus of these animals (Migaud et al., 1998).

In wild-type mice with chronic constriction injury, there was a clear increase in constitutive CaMKII activity ipsilateral, but not contralateral to injury (Table 4.1b). This increase was reversed by topical application of the selective NMDA

Table 4.1 Effects of acute intrathecal drug administration and of chronic nerve injury (CCI) on CaMKII activation in spinal cord of wild-type and PSD-95 mutant mice

(a) Saline vehicle, NMDA (500 μM) with the co-agonist glycine (100 μM), or ionomycin (10 μM), were topically applied to the dorsal surface of L3-L6 spinal cord in naïve wild-type and PSD-95 mutants. Data are expressed as the percentage of maximal CaMKII activity and are means ± SEM (n=4/6). Statistically significant differences are shown as *, $p<0.05$ by Mann-Whitney U test, compared to corresponding saline values.

(b) Saline vehicle or (R)-CPP (10 μM) or saline vehicle were applied in a volume of 500μl to the dorsal surface of L3-L6 spinal cord in wild-type and PSD-95 mutant mice at the peak of neuropathic reflex sensitivity following CCI. Data are expressed as the percentage of maximal CaMKII activity and are means ± SEM (n=4/6). Statistically significant differences are shown as *, $p<0.05$ by Mann-Whitney Rank Sum test compared to corresponding contralateral values.

Acute administration of drug to spinal dorsal horn	Constitutive CaMKII activity (% of maximal activity)			
(a) In naïve mice	Wild-type		PSD-95 Mutant	
Saline	25.4 ± 3.9		21.1 ± 3.0	
NMDA/glycine	36.2 ± 3.7 *		32.4 ± 4.1 *	
Ionomycin	33.5 ± 2.1 *		30.0 ± 2.8 *	
(b) In mice with established CCI	Wild-type		PSD-95 Mutant	
	Ipsilateral CCI	Contralateral CCI	Ipsilateral CCI	Contralateral CCI
Saline	35.0 ± 2.8 *	16.3 ± 2.3	16.9 ± 1.8	13.9 ± 1.6
(R)-CPP	12.9 ± 1.6	18.1 ± 3.6	-	-

receptor antagonist (R)-CPP to the spinal cord for 15 min immediately prior to removal. This increase in constitutive CaMKII activity was absent in PSD-95 mutant mice following CCI (Table 4.1b).

Since both acute NMDA-induced Ca^{2+} entry and the ability of CaMKII to respond to Ca^{2+} elevation appear to be normal in the mutant mice, it seems likely that a factor facilitating the functional coupling between the NMDA receptor and CaMKII is the key element altered in CCI.

4.2.9 NMDA receptor modulation by phosphorylation

Disruption of the function of an NMDA receptor modulatory factor in PSD-95 mutant mice is likely to be responsible for the non-sensitising phenotype observed. One possible candidate for such a modulatory factor might be the regulatory phosphorylation of NMDA receptor subunits by kinases such as PKC and PKA, which may specifically increase the degree of Ca^{2+} entry evoked by a given concentration of NMDA (Tingley et al., 1997; Westphal et al., 1999).

In order to directly assess whether the phosphorylation state of the NMDA receptor was altered following CCI, we utilised phospho-specific antibodies for key channel-regulating residues in NR1 at Ser^{896} and Ser^{897} (PKC and PKA targets, respectively, see Sections 2.2.6 and 2.4.6 and antibody details in Table 2.3, pgs. 64-66, 69, 91). Small reductions in the levels of pan-NR1 immunoreactivity were seen ipsilateral to CCI (Fig. 4.20a; in accordance with a previous report (Hama et al., 1995) and our unpublished data from the rat CCI model). These reductions were similar in PSD-95 mutant mice to those in wild-type mice (Fig. 4.20a). Figure 4.20 shows that the extent to which Ser^{897} of the NR1 subunit was phosphorylated was specifically increased ipsilateral to CCI in wild-type mice (Fig. 4.20b). 4-5 fold greater ratios of phospho-Ser^{897}-NR1:pan-NR1 immunoreactivity were seen ipsilateral to CCI compared to those on the contralateral side (Fig. 4.20c). In PSD-95 mutant mice, the corresponding CCI-induced increment in Ser^{897}-NR1 phosphorylation was almost completely prevented (Fig. 4.20b).

Figure 4.20 Immunoblots for phospho-Ser^{897}-NR1 and pan-NR1 in NR1 immunoprecipitates from wild-type and PSD-95 mutant mice following CCI surgery

Western blot analysis of hemisected spinal cord pan-NR1 immunoprecipitates following sciatic CCI induced 12 days previously.

(a) Immunoprecipitated samples derived from either two wild-type (+/+) or two PSD-95 mutant (-/-) mice, ipsilateral or contralateral to the injury were probed with antibodies for pan-NR1.

(b) Immunoprecipitated samples derived from either two wild-type (+/+) or two PSD-95 mutant (-/-) mice, ipsilateral or contralateral to the injury were probed with antibodies for phospho-Ser^{897}-NR1 (same samples as in a) above). Non-specific bands seen at ~40-70 kDa represent cross-reactivity with the immunoprecipitating IgG and were similar in all samples and in extract-free blanks.

(c) ECL films from 4 separate determinations were scanned and the specific densities of the ~120 kDa NR1 bands were analysed by densitometry. Arbitrary grey scale values were normalised to the wild-type contralateral values in each case and then mean relative phospho-Ser^{897}-NR1: pan-NR1 immunoreactivity ratios were calculated.

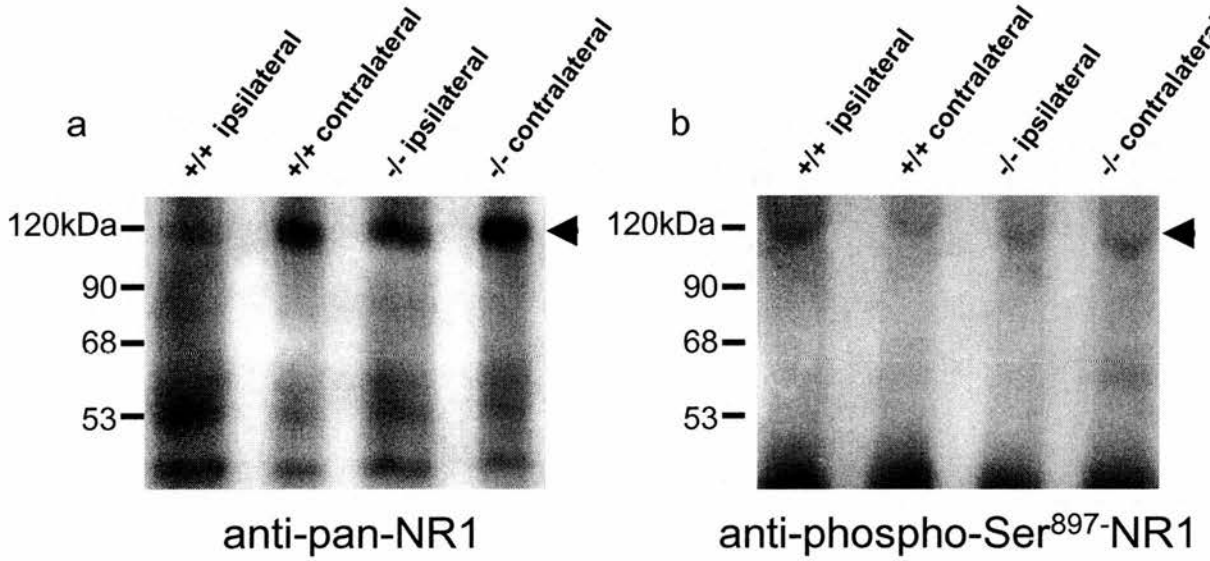

c

	+/+ ipsi	+/+ contra	-/- ipsi	-/- contra
Mean relative phospho-Ser^{897}-NR1:pan NR1 immunoreactivity (grey scale ratios relative to +/+ contra)	4.67±0.63	1.0 (as defined)	1.35±0.22	1.02±0.17

Phospho-Ser^{896}-NR1 immunoreactivity could not be reliably detected in these experiments. These results suggest that a mechanism of regulatory phosphorylation of NR subunits is a prime candidate for the mechanism of facilitated NMDA receptor function which is necessary for neuropathic sensitisation and which is disrupted in PSD-95 mutants.

4.2.10 Further examination of PKA signalling

NMDA receptor phosphorylation by PKA is implicated in the regulation of neuropathic sensitisation. PSD-95 can link kinase-docking adapters such as AKAP79/150 to the NMDA receptor (Colledge et al., 2000), and such adapters, together with relevant kinases can be isolated in association with NMDA receptor:PSD-95 complexes (Husi et al., 2000). As the SH3 and GK domains of PSD-95 are absent in the PSD-95 mutant mice, and the presence of these two domains is believed to be important for AKAP79/150 association with the NMDA receptor, it was of interest to determine whether there were any alterations in the protein: protein interactions whereby PKA is targeted to the postsynaptic membrane via a PSD-95 interaction. Given the apparent increase in PKA phosphorylation at Ser^{897} on NR1 ipsilateral to injury in wild-type mice, and the lack of this injury-induced increase in PSD-95 mutant mice, we hypothesised that there may be some interruption of PKA targeting to the NMDA receptor as a consequence of the PSD-95 mutation, possibly due to a disrupted linkage via AKAP79/150. We examined this question by isolating spinal cord multiprotein complexes from naïve wild-type and naïve PSD-95 mutant samples using the peptide-based affinity separations, targeting the SIESDV site in NR2 subunits as described in Section 4.2.2 (Husi and Grant, Husi et al., 2000) and carried out a small-scale analysis of the NR2-associated PKA-related proteins that may be altered as a consequence of the mutation. We used antibodies against the regulatory PKA subunits, RIIα and RIIβ, which bind to AKAP79/150 (Coghlan et al., 1995) as well as an antibody targeted against AKAP150 (the rat isoform) itself, and an antibody against the NMDA receptor subunit NR1 as well as GAPDH were used as controls for protein levels (Fig. 4.21).

Figure 4.21 Immunoblots for NR1, RIIα, RIIβ and AKAP150 in 'pep6' NR2 C-terminal resin immunoprecipitates from naïve wild-type and PSD-95 mutant mice

Western blot analysis of spinal cord 'pep6' C-terminal (SIESDV) resin of NR2 immunoprecipitates derived from either 8 wild-type (+/+) or 8 PSD-95 mutant (-/-) mice were probed with antibodies for NR1 (a), RIIα (b), RIIβ (c) and AKAP150 (d). Levels of NR1 protein were used as a relative indication of NMDA receptor levels in +/+ and -/- samples and the ubiquitous housekeeping enzyme GAPDH was used as an internal control (lower panels). There was no significant difference in the levels of any of these proteins when wild-type extracts were compared to PSD-95 mutant extracts.

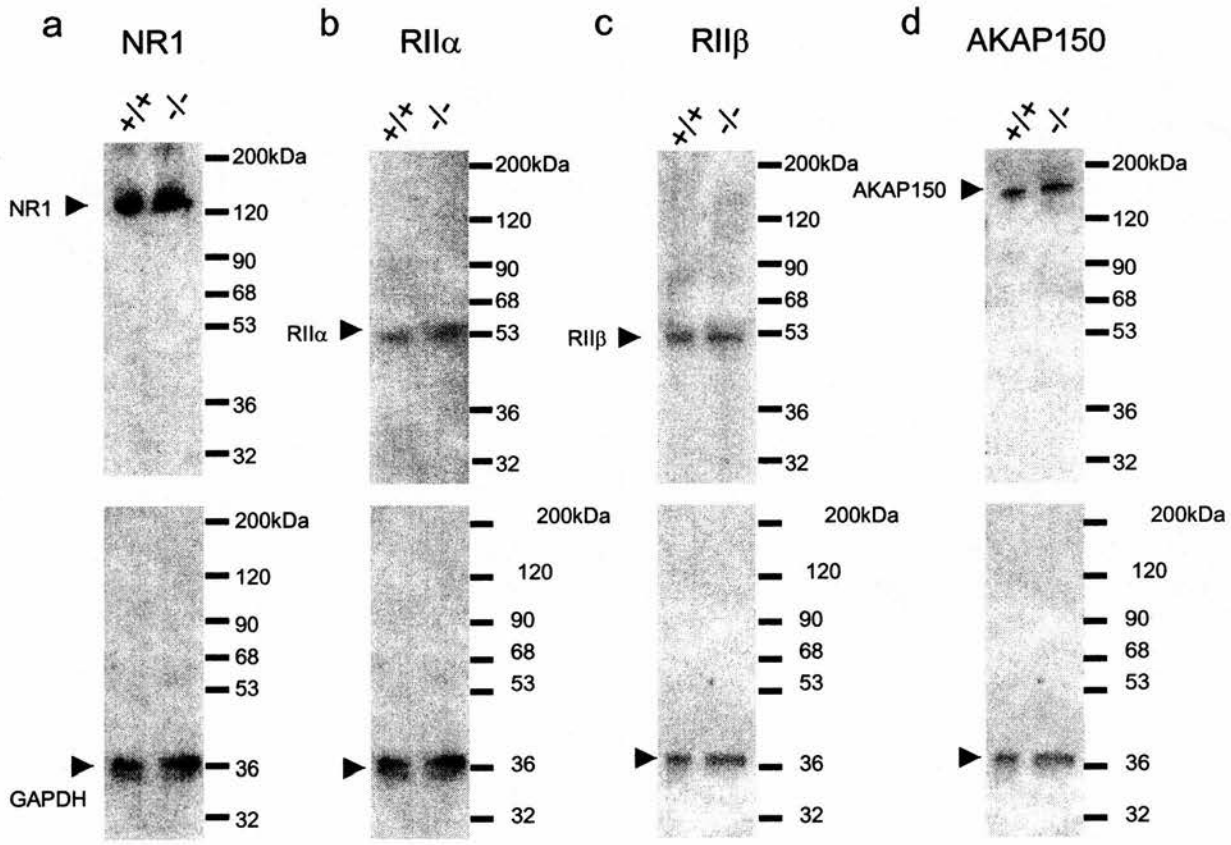
a
NR1
b
RIIα
c
RIIβ
d
AKAP150
+/+
-/-
200kDa
120
90
68
53
36
32
NR1
RIIα
RIIβ
AKAP150
GAPDH

There were no discernible alterations in the levels of NR1 (Fig. 4.21a), RIIα (Fig. 4.21b), RIIβ (Fig. 4.21c) or AKAP150 (Fig. 4.21d) when naïve wild-type samples were compared to naïve PSD-95 mutant samples (see Sections 2.2.6 and 2.4.6 and antibody details in Table 2.3, pgs. 64-66, 69).

4.3: Discussion

Spinal NMDA receptors have a well-established role in the central mechanisms of neuropathic pain. Intrathecal application of selective NMDA receptor antagonists inhibit the behavioural reflex thermal hyperalgesia and mechanical allodynia that are characteristic of neuropathic pain models (Chaplan, Malmberg and Yaksh, 1997; Tal and Bennett, 1993; Boyce et al., 1999; Mao et al., 1993) and the mRNA and protein for NMDA receptor subunits are all expressed in dorsal spinal cord (Luque et al., 1994; Boyce et al., 1999; Yung, 1998). We addressed the potential role of the NMDA receptor-adapter protein PSD-95. Generation of transgenic mice expressing a truncating mutation part way through the sequence of the PSD-95 gene (Migaud et al., 1998) enabled us to address the spinal distribution, the relation to NMDA receptors and the functional role of PSD-95 in neuropathic pain.

Histochemical staining for the β-galactosidase reporter incorporated into the mutant construct showed expression in many cells within lamina II of the superficial dorsal horn of heterozygous mice. This corresponds to known regions of high NMDA receptor expression and to zones of termination of fine afferents in the regulation of sensory processing (and matches a recent report of the immunoreactivity for native PSD-95 in spinal cord; Tao et al., 2000). No evidence was found for β-galactosidase staining in dorsal root entry zones, DRG or afferent fibres. NMDA receptors have been proposed to regulate afferent transmitter release (Liu, Mantyh and Basbaum, 1997), and NR1 as well as NR2B subunits have been detected in primary afferent neurones and DRG (Watanabe, Mishina, and Inoue, 1994; Ma and Hargreaves, 2000). However, our evidence suggests that any such peripheral NMDA receptor complexes that occur would lack the adapter PSD-95. In the spinal cord of wild-type mouse, protein: protein interaction studies using immuno- or affinity- reagents (Husi et al., 2000) for NR1, NR2B or PSD-95 confirmed that each of these could harvest complexes showing immunoreactivity for NR1, NR2A, NR2B and PSD-95.

The functional impact of the truncated PSD-95 construct on neuropathic pain-related behaviours was striking. Thermal hyperalgesia, mechanical allodynia and cold allodynia brought about by peripheral nerve ligation injury were completely (or almost completely) abrogated in homozygous PSD-95 mutant mice. There was no evidence for motor deficit in these mice as locomotion, motor grip function and the ability to execute the behavioural reflex responses appeared normal. The pre-nerve injury response sensitivity and that of the contralateral paw after injury was no different between mutant and wild-type mice in the thermal hyperalgesia and cold allodynia tests. The basal response thresholds to mechanical stimuli appeared to be elevated in the PSD-95 mutant mice. This would be consistent with the idea that some PSD-95-mediated function was contributing to maintaining the sensitivity of the basal reflex to mechanical stimuli. Nevertheless, the lower threshold in wild-type mice was insensitive to the NMDA receptor antagonist (R)-CPP suggesting lack of direct involvement of this receptor. It is important to note that different strains of mice have been shown to exhibit different responses in a variety of nociceptive behavioural reflex tests (Mogil et al., 1999). Further work would be necessary to confirm and extend this observation here. These results indicate that the cellular role(s) of PSD-95, which are disrupted by the truncation mutation, are essential for the processes that underlie hyperaesthesia in a neuropathic pain model.

Since alterations and degeneration of afferent myelin sheaths could potentially elicit changes that contribute to the development of pain-related behaviours (Guilbaud et al., 1993; Sommer et al., 1995; Coggeshall et al., 1993; Campbell et al., 1988), we investigated the morphology of sciatic nerve fibres in PSD-95 mutant mice. No alterations in axon profiles, myelination or local responses to constriction injury were apparent, consistent with the idea that central sites, where PSD-95 is expressed, are likely to be the location of the key changes.

Studies utilising the intrathecal injection of NMDA receptor antagonist and agonist confirmed that the hyperalgesia and allodynia of the CCI model (as adapted by us for use in mice) are indeed dependent on NMDA receptors at a spinal site. The selective NMDA receptor antagonist (R)-CPP showed a concentration-dependent and

reversible inhibition of the neuropathic hyperalgesia and allodynia in wild-type mice. Its specificity was indicated by the lack of effect on contralateral responses in wild-type mice and on responses from either side in PSD-95 mutants where the sensitisation had failed to develop. Conversely, the intrathecal injection of the agonist, NMDA, mimicked the thermal hyperalgesia and mechanical allodynia that could be caused by nerve injury in wild-type mice, but appeared ineffective in the PSD-95 mutant mice. This is consistent with a recent preliminary report of attenuated tail flick responses to NMDA in rats treated with PSD-95 antisense oligonucleotide (Tao et al., 2000). Beyond implicating NMDA receptor function in the injury-induced sensory changes, these data suggest that the failure of a key ligand-gated signal from spinal NMDA receptors in the PSD-95 mutant mice may be responsible for their lack of neuropathic sensitisation.

Since the primary action of NMDA receptor complexes is the gating of Ca^{2+}/ Na^{+} entry, we examined the role of a major Ca^{2+}-regulated kinase, CaMKII, in neuropathic sensitisation. CaMKII is an abundant protein of the postsynaptic density complex, which contains NMDA receptors (Kennedy, 1997), can be isolated in molecular complexes associated with NR1 or NR2 subunits (Husi et al., 2000) and may dock directly to NR2A or B subunits (Gardoni et al., 1999). This location, as well as data implicating NMDA receptor-mediated CaMKII activation in the cellular sensitisation occurring during long-term potentiation in hippocampus (Nicoll and Malenka, 1995; Lisman et al., 1997), suggests that the enzyme may be a good candidate as a contributor to neuropathic sensitisation. Consistent with this hypothesis, the thermal hyperalgesia and mechanical and cold allodynia following CCI in wild-type mice were attenuated by the selective CaMKII inhibitors, myristoyl-autocamtide 2-related inhibitory peptide, KN-93 and to a lesser extent by KN-92 (a less active congener of KN-93).

Following its activation by Ca^{2+}, CaMKII becomes autophosphorylated to generate a constitutively active, Ca^{2+}-independent form of the enzyme (Hanson et al., 1989). We therefore measured the fraction of authentic CaMKII activity that was constitutive as a monitor of the recent history of Ca^{2+} elevation. Increments in the

fraction of constitutively active CaMKII were no different when a high concentration of NMDA, and its co-agonist glycine, was topically applied to the dorsal spinal cord between wild-type and PSD-95 mutant mice. These responses were similar in extent to those elicited by the Ca^{2+} ionophore, ionomycin, and are therefore likely to be at ceiling level. This suggests that the maximally-activated Ca^{2+} entry function of the NMDA receptor is unaltered by the PSD-95 mutation and that NMDA receptor complexes do not appear to be incorrectly assembled or dysfunctional in the mutant, with regard to Ca^{2+} entry.

Nevertheless, CCI caused a clear increment in constitutive CaMKII activity (that was NMDA receptor-dependent) in spinal cord tissue from the ipsilateral compared to the contralateral side of wild-type mice and this response was minimal in PSD-95 mutants. Total CaMKII kinase activity and immunoreactivity was unaltered by CCI or by the PSD-95 mutation. It therefore seems possible that a critical role of PSD-95 with regard to neuropathic hyperalgesia/ allodynia could be in enabling a mechanism whereby the sensitivity of the NMDA-mediated Ca^{2+} entry response is enhanced by CCI. In such a situation, the sensitivity of NMDA receptor Ca^{2+} entry to relatively low concentrations of agonist (as during CCI in vivo) might well be greater, while the maximal extent of the response may be unaltered. Adapter-mediated contributions to cellular compartmentalisation of relevant proteins or actions as molecular scaffolds to facilitate intracellular signalling could potentially underlie such modulation.

The interaction between NMDA and PSD-95 potentially increases the complexity of signalling networks at excitatory synapses and may provide a structural framework that permits preferential targeting of kinases to NMDA receptors. Presumably, such a highly organized kinase-substrate complex might ensure rapid and efficient phosphorylation of NMDA receptor ion channels in response to local synaptic signals (Colledge et al., 2000). One basis for a facilitation of NMDA receptor function during CCI might be its regulatory protein phosphorylation through kinases such as PKC (Chen and Huang, 1992) or PKA (Westphal et al., 1999).

Here, we report a specific increase in the levels of PKA phosphorylation ipsilateral to CCI in wild-type mice, with no alteration in PKC phosphorylation. In spinal cord neurones, PKC can potentiate NMDA-mediated current (Gerber and Randić, 1989) and there is evidence for a facilitation of NMDA receptor responses in dorsal horn neurones by concurrent neuropeptide and metabotropic glutamate receptor activation, that may occur in neuropathic and other chronic pain models (Heppenstall and Fleetwood-Walker, 1997; Bleakman et al., 1992) and which may involve PKC and/or PKA (Kolaj et al., 1994). Moreover, in vitro, expression of PSD-95 may act to inhibit PKC-induced potentiation of the NMDA receptor ion channel (Yamada et al., 1999). Therefore, the lack of PKC-induced phosphorylation may not be too surprising as previous reports have shown that NMDA receptors assembled from subunits that lack all known PKC sites can still show PKC-induced potentiation thereby indicating that PKC may be acting indirectly (Zheng et al., 1999).

NMDA receptor-ligand binding sites and NR1 protein levels are reduced in the dorsal horn following peripheral nerve injury (CCI) and inflammation (Aanonsen et al., 1990; Hama et al., 1995; Sloan et al., 1991). The NR1 subunit contains three regions of alternative splicing, N1, C1 and C2 (Zukin and Bennett, 1995). As mentioned in the introduction, the AKAP, Yotiao interacts with the C1 exon of NR1 subunits, and may act to induce a stable Yotiao: PKA: NR1 complex that could promote PKA-mediated modulation of NMDA receptor activity (Lin et al., 1998; Feliciello et al., 1999). Through interaction with the C1 splice variant, Yotiao targets both PKA and active PP1 phosphatase to NMDA receptor complexes, conferring bi-directional regulation of NMDA receptor activity (Westphal et al., 1999). While NR1 is highly expressed throughout the spinal cord and sensory ganglion (Kus, Saxon and Beitz, 1995), the C1 is present in only ~10% of total NR1 protein in the spinal cord and spinal cord injury causes no significant change in overall NR1 or CI cassette expression (Grossman et al., 2000; Prybylowski et al., 2001). Moreover, the expression of Yotiao is very low in spinal cord tissue (Husi, unpublished). Thus, a different mechanism of PKA-mediated potentiation of NMDA receptors may account for increased PKA phosphorylation ipsilateral to injury in wild-type mice.

One potential explanation for these observations is that the AKAP79/150 signalling scaffold no longer can be recruited to glutamate receptors through interaction with MAGUK proteins (Colledge et al., 2000). AKAP79/150 previously has been shown to provide a scaffold for three signalling enzymes: PKA, PKC, and calcineurin (PP2B). Interestingly, PSD-95 competes with calcineurin for binding to AKAP79/150 in vitro so that when bound to MAGUKs, AKAP79/150 may preferentially target kinases but not phosphatases to NMDA receptors (Colledge et al., 2000). However, there were no alterations in the levels of NMDA receptor-associated AKAP150 or PKA subunits in the PSD-95 mutant mice, although we cannot rule out the possibility that they may be bound to other NMDA receptor complex-related interaction partners. The precise basis for the PSD-95-dependent facilitation of NMDA receptor function caused by CCI remains to be elucidated.

The site of truncation of the PSD-95 molecule may give some clue as to the protein docking events that may be crucial to the functional disruption of neuropathic pain. The first and second PDZ domains of PSD-95 are unaltered in the mutant although part of its third PDZ domain, and the SH3 and the guanylate kinase (GK) domains are deleted (Migaud et al., 1998). Interactions of NR2 subunits, Shaker K^+ channels and nNOS (which involve PDZ1 and 2 domains) should in principle be retained (Kornau et al., 1995; Sheng and Wyszynski, 1997; Christopherson et al., 1999). PDZ3 domain interactions such as with the microtubule binding protein CRIPT, neuroligin and citron may be prevented (Passafarro et al., 1999; Irie et al., 1997; Zhang et al., 1999). SynGAP, which can interact with PDZ1, 2 and 3 of PSD-95 and may regulate the MAPK pathway (Chen et al., 1998), shows no detectable expression in spinal cord (data not shown). The influences of the PSD-95 mutation on in vivo cellular interactions between proteins may be more complex. Intermolecular interactions between the SH3 and GK domains of PSD-95 may restrict its intermolecular binding (McGee and Bredt, 1999), although such interactions have reportedly no effects on the ability of PSD-95 to cluster K^+ channels (Shin et al., 2000). Further complexities may be present if the truncated PSD-95 mutant protein does not undergo identical intracellular trafficking and localisation to that of the wild-type protein (Migaud et al., 1998).

Figure 4.22 Summary schematic of the main findings with PSD-95 mutant mice following CCI

This schematic represents a summary of the results presented in this chapter. PSD-95 is exclusively expressed in the superficial laminae of the dorsal horn and associates with NR2 subunits of NMDA receptor as has been shown in other regions of the nervous system. PSD-95 mutant mice fail to develop the characteristic behavioural sensitivity to thermal and mechanical stimuli following CCI although this is not a consequence of differential demyelination following CCI as a result of the mutation, as the constriction injury does cause demyelination to the same extent as that noted in wild-type littermate controls. In addition, activation of spinal NMDA receptors by local intrathecal application failed to result in behavioural sensitisation in the PSD-95 mutant mice as it does in the wild-type mice.

Despite this, Ca^{2+} entry through the NMDA receptor in PSD-95 mutant mice functions normally, although the increment in CaMKII activity that normally follows ipsilateral to injury in wild-type mice was absent in the PSD-95 mutant mice. This may indicate that the mechanisms responsible for the lack of sensitivity lies downstream of PSD-95, such as with the PKA anchoring protein AKAP79/150 which localises PKA to its site of action and which is dislocated from the complex as a result of the mutation. We noted that levels of PKA activation of the NR1 subunit, as measured by examination of the levels of phospho-Ser^{897} protein, were elevated ipsilateral to CCI in the spinal cord of wild-type mice but not in PSD-95 mutant mice. However, the underlying cause of this difference is unknown as there was no apparent difference in the expression of spinal cord AKAP79/150 or of RIIα, RIIβ PKA subunit protein levels in PSD-95 mouse when compared to wild-type controls.

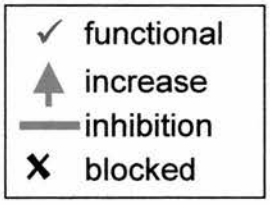

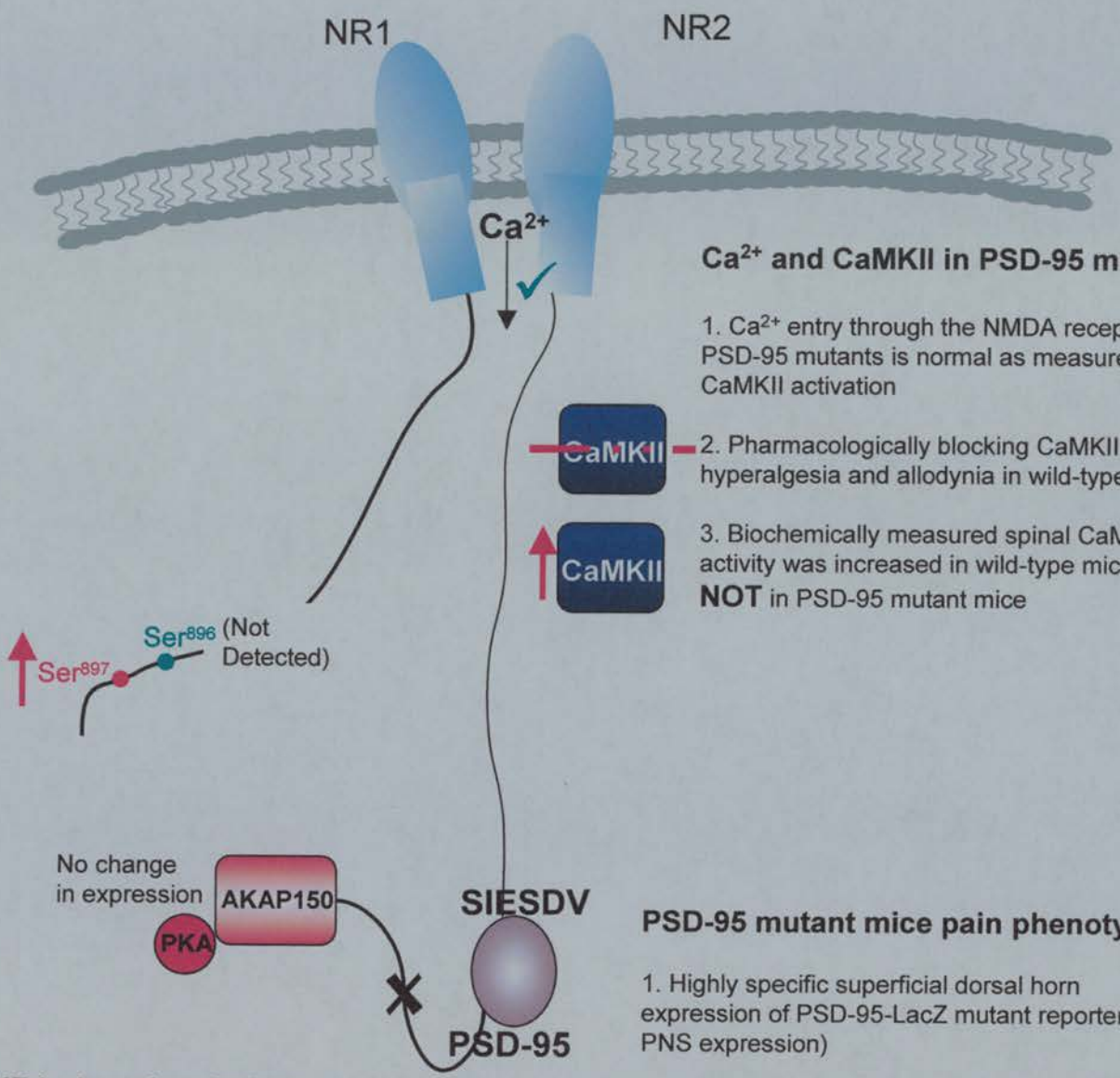

Ca^{2+} and CaMKII in PSD-95 mutants:

1. Ca^{2+} entry through the NMDA receptor in PSD-95 mutants is normal as measured by CaMKII activation

2. Pharmacologically blocking CaMKII inhibits hyperalgesia and allodynia in wild-type mice

3. Biochemically measured spinal CaMKII activity was increased in wild-type mice but **NOT** in PSD-95 mutant mice

NR1 phosphorylation:

1. Increased PKA phosphorylation ipsilateral in wild-type mice but **NOT** in PSD-95 mutants

2. This is not due to a loss of PKA localisation as a result of the mutations as there was no difference between wild-type and PSD-95 mutant mice in the levels of PKA subunits or the PKA anchoring protein AKAP79/150

PSD-95 mutant mice pain phenotype:

1. Highly specific superficial dorsal horn expression of PSD-95-LacZ mutant reporter (no PNS expression)

2. PSD-95 associates with NMDA receptor subunits in wild-type the spinal cord

3. **No** behavioural sensitivity following CCI despite normal myelination and expected levels of demyelination associated with wild-type CCI

4. Behavioural sensitivity could not be induced in PSD-95 mutants with in vivo NMDA receptor activation

There is the possibility that postsynaptic densities lacking PSD-95 may use Chapsyn110/PSD-93 or SAP102 for ligand localisation. However, little is known about the physiological diversity that may derive from differences in MAGUK content at glutamatergic synapses. SAP97 and PSD-95 PDZ domains 1 and 2 have similar binding affinities for the NR2 C-terminal sequence which may indicate that both are comparable in their capability to interact with NMDA receptors, while all three PDZ domains of SAP102 are capable of binding the NR2 motif (Müller et al., 1996). So, which interaction actually occurs in vivo depends primarily on which member of the MAGUK family co-distributes with the receptors in neuronal cells (Müller et al., 1996).

While data for the other MAGUK members is lacking, they contain the same domains, and share NR2 subunits and K^+ channels as common targets such that it might be expected that, if present in the spinal cord, other MAGUKs of this family might compensate in the regulation of NMDA receptor pathway. However, this possibility is not supported here, given the complete absence of neuropathic reflex sensitivity development following peripheral nerve injury. Proteomic analysis of the NMDA receptor complex in the forebrain of wild-type and PSD-95 mutant mice indicate that there is no alteration in the levels of Chapsyn110/PSD-93 or SAP97 as a consequence of the mutation, whereas there is an increase in SAP102 (Husi et al., 2000). Moreover, evidence from Chapsyn110/PSD-93 knockout mice suggests that MAGUKs may not be essential for the normal development of structure and function of certain central synapses but may participate during extreme physiological situations (McGee et al., 2001).

In addition, forebrain analysis of the PSD-95 mutant indicates that there are no overall alterations in the levels of GKAP, Yotiao, PKC, PKA CaMKII, or the phosphatases PP1, PP2A or PP2B. Nor were there apparent alterations in any of the molecules involved in the MAPK pathway or nNOS levels associated with the NMDA receptor complex (Husi et al., 2000). It is possible that PSD-95 may be the only functional MAGUK as far as the spinal cord is concerned, although this remains to be shown.

Although the critical docking partner for PSD-95 in its role in neuropathic sensitisation cannot be readily discerned at present, the present studies firmly establish that this molecule plays a key role in the facilitation of NMDA receptor function which underlies neuropathic pain-related behaviours. The neuropathic sensitisation of spinal sensory reflexes is therefore dependent on spinal NMDA receptors and the failure of this sensitisation in PSD-95 mutant mice indicates that NR: PSD-95 interactions in spinal cord play a key role in the development of neuropathic pain.

CHAPTER 5: Summary and Conclusions

Neuropathic pain encompasses a group of painful disorders due to peripheral or central nervous system dysfunction as a result of injury to the nervous system. The chronic pain that develops manifests as hyperalgesia, allodynia and spontaneous pain. The mechanisms underlying neuropathic pain are complex, involving both peripheral and central anatomical and neurochemical changes that can persist long after the injury has healed. The morphological and functional alterations that occur in the central nervous system during neuropathic pain highlight the neuroplasticity inherent in the CNS. Animal models that reproduce the mechanisms underlying neuropathic pain have led to a better understanding of the cellular events involved. Here, we have used the chronic constriction injury model (CCI, Bennett and Xie, 1988), which mimics many of the behavioural changes symptomatic of neuropathy. Basic research with this animal model has shown that a number of pathophysiological and biochemical changes occur in the nervous system as a result of the peripheral nerve injury.

The AMPA and NMDA subtypes of ionotropic glutamate receptors have long been the focus of research in the mechanisms of spinal nociceptive transmission. The AMPA receptors have widespread expression in the spinal cord and not only mediate the fast synaptic currents arriving at the dorsal horn of the spinal cord in response to acute primary afferent stimulation, but also participate in mediating chronic neuropathic transmission (Aanonsen, Lei and Wilcox, 1990; Budai and Larson, 1994; Mao et al., 1992a). NMDA receptor subunits are also present in the spinal cord tissue with differential regional expression. However, postsynaptic membranes must undergo sufficient depolarisation, such as in response to high threshold primary afferent stimulation as in the case of peripheral nerve injury, before the NMDA receptor ion channel becomes activated. Spinal administration of AMPA or NMDA receptor agonists can enhance dorsal horn neurone responses to noxious stimulation (Aanonsen, Lei and Wilcox, 1990) and produce spontaneous pain behaviours and hyperalgesia (Zhou, Bonesara and Carlton, 1996). In addition, NMDA receptor

antagonists can reduce the frequency dependent wind-up of dorsal horn neurones following repetitive C-fibre stimulation (Davies and Lodge, 1987) and attenuate the raised behavioural sensitivity characteristic of peripheral neuropathy (Mao et al., 1993; Tal and Bennett, 1993). To this date, the factors determining the relative contribution of AMPA and NMDA receptors to neuropathic pain mechanisms are poorly understood.

The work presented here has been concerned with an examination of the mechanisms underlying neuropathic pain following peripheral nerve injury, focussing on the ionotropic glutamate receptors AMPA and NMDA, their respective intracellular interacting proteins and regulation of specific subunits by phosphorylation under conditions of peripheral nerve injury. This research has utilised behavioural, pharmacological, histochemical and biochemical techniques to investigate the role of recently identified proteins differentially interacting with the C-terminal domains of the ionotropic AMPA and NMDA glutamate receptors in mediating neuropathic sensitivity at the behavioural and cellular level.

5.1 AMPA receptor involvement in neuropathic pain

Firstly, the involvement of AMPA receptors in mediating hyperalgesia and mechanical allodynia was examined by the intrathecal injection of the AMPA receptor antagonists, NBQX, NS-257 and SYM 2206 in rats with established neuropathic reflex sensitisation following chronic constriction injury (Bennett and Xie, 1988). These AMPA receptor antagonists all alleviated thermal hyperalgesia and mechanical allodynia to varying degrees and in a dose-dependent manner with no effects in uninjured animals; observations consistent with a particular role for AMPA receptors in the persistent pain behaviours that develop following induction of CCI (Budai and Larson, 1994; Mao et al., 1992a).

The expression of the AMPA receptor subunits GluR1 and GluR2, with reported predominant dorsal over ventral horn expression (Harris et al., 1996; Tölle et al., 1995) was examined using in situ hybridisation histochemistry for mRNA level

analysis and Western blot for protein level analysis. mRNA expression was examined in rats with maximal development of neuropathic reflex sensitivity as indicated by behavioural reflex sensitisation following CCI. We confirmed that the mRNAs for the GluR1 and GluR2 subunits were specifically localised in the dorsal horn of the spinal cord with moderate to weak labelling in ventral horn under normal conditions. We noted an ipsilateral reduction in the levels of GluR1 mRNA in the superficial laminae of the dorsal horn as compared to control contralateral, sham and naïve expression levels, whereas overall levels of GluR2 mRNA in the spinal cord increased significantly in the superficial laminae. Western blot analysis, carried out to further characterise AMPA receptor subunit protein levels, revealed similar results to that described for mRNA, whereby GluR1 protein levels were diminished ipsilateral to CCI as compared to control levels, while GluR2 levels increased in ipsilateral spinal cord. While the increased GluR2 levels ipsilateral to CCI agrees, the GluR1 result is in disagreement with one previously published paper reporting that levels of GluR1 (as assessed by immunohistochemistry) increase ipsilateral to CCI (Harris et al., 1996). The reason for this is unclear although here both ISHH levels of GluR1 mRNA and Western blot of GluR1 protein were consistent in showing decreases ipsilateral to CCI. Western blot of whole spinal cord may mask lamina-specific alterations in GluR1 protein levels ipsilateral to CCI although regionally identified GluR1 mRNA levels were also diminished ipsilateral to CCI. While alterations in mRNA do not necessarily imply similar alterations in protein levels, the consistent decrease in both GluR1 protein and mRNA in the ipsilateral dorsal horn following CCI in comparison to increases of GluR1 protein in the report of Harris et al. (1996) suggest that further study is required to resolve the issue.

It is possible that changes in the relative expression of the GluR1 and 2 subunits throughout the dorsal horn or even within individual neurones may contribute to the functional changes occurring in the established neuropathic state following CCI. The presence of GluR2 subunits renders the AMPA receptor ion channel impermeable to Ca^{2+} (Burnashev et al., 1992a). However, there appears to be a differential expression of GluR1 and GluR2 in the superficial dorsal horn (as examined by AMPA-induced cobalt loading), whereby cells expressing Ca^{2+}-permeable AMPA

receptors (so presumably lacking the GluR2 subunit) can be found in LI and LII_o, while there are low numbers of Ca^{2+}-permeable AMPA receptors in LII_i corresponding to the high expression of GluR2 subunits in this region (Engelman, Allen and MacDermott, 1999; Tölle et al., 1993).

We examined the possibility of modulation of AMPA receptors by kinases such as CaMKII/PKC and/or PKA, which are known to target the GluR1 subunit. Following CCI, spinal cord GluR1-directed immunoprecipitates were probed with phospho-specific antibodies targeted against phospho-Ser^{831} (CaMKII/PKC site) and phospho-Ser^{845} (PKA site) on the C-terminus of GluR1 subunits. Previous studies have shown that dorsal horn responses to ionotropic glutamate receptor agonists can be enhanced by PKA and PKC activation and may result in hyperalgesia (Cerne, Jiang and Randić, 1992; Aley and Levine, 1999; Munro, Fleetwood-Walker and Mitchell, 1994; Coderre, 1993; Mao, et al., 1992b). In addition, GluR1 phosphorylation of Ser^{831} by CaMKII potentiates GluR1 current in the hippocampus (Derkach, Barria and Soderling, 1999) while PKA-mediated phosphorylation at Ser^{845} increases AMPA responsiveness through a modulation of channel gating and channel open probability without affecting channel conductance (Banke et al., 2000). Here, following CCI, we document increases in phospho-Ser^{831}-GluR1 immunoreactivity in GluR1 immunoprecipitates in the ipsilateral spinal cord, compared to contralateral, sham and naïve controls. This suggests that peripheral nerve injury may preferentially promote CaMKII/PKC phosphorylation of AMPA receptors although the underlying mechanisms mediating this are unknown to date.

5.2 GluR1 and GluR2 receptor subunit interactions with additional proteins potentially involved in neuropathic pain

We examined here for the first time, using a number of complementary approaches, the in vivo function of GRIP, PICK1 and NSF (which are known to interact with the GluR2 C-terminus) and SAP97 (which is known to interact with the GluR1 C-terminus). The vast majority of studies to date on these docking proteins have been biochemical with very little in vivo functional data. The use of motif-targeted

myristoylated peptides enabled us to investigate functional, in vivo roles for the proteins interacting with the GluR1 C-terminus (SAP97) and the GluR2 C-terminus (GRIP/PICK1 or NSF). These results showed that blocking the GluR2 C-termini motifs for interactions with either GRIP/PICK1 or NSF was effective at alleviating thermal hyperalgesia following CCI, with minimal effects on mechanical allodynia behaviours. In contrast, blocking the interaction of SAP97 with GluR1 attenuated both hyperalgesia and allodynia following CCI. None of the myristoylated peptides had any effects when administered to naïve animals. The data presented here indicate that the interaction of GRIP/PICK1 and NSF with the C-terminus of the GluR2 subunit and the interaction of SAP97 with the C-terminus of the GluR1 subunit of AMPA receptor may well play a role in the mechanisms underlying neuropathic pain reflex sensitisation following peripheral nerve injury.

Infusion of the same peptide used here to block GRIP and PICK1 into cultured spinal neurones has shown that PKC and the interaction of GRIP and PICK1 with the GluR2/3 C-terminus may be important for unmasking silent glutamatergic synapses between sensory afferents and spinal cord dorsal horn neurones (Li et al., 1999). In culture, induction of cerebellar LTD causes phosphorylation of Ser^{880} within the GluR2 C-terminal PDZ motif (Matsuda et al., 2000) and this phosphorylation causes dissociation of GRIP from GluR2 without affecting PICK1 binding, disruption of GluR2 clusters and internalisation of GluR2 subunits (Matsuda et al., 2000). Hence, blocking Ser^{880} phosphorylation has been reported to attenuate cerebellar LTD (Xia, 2000; Matsuda et al., 2000).

In situ hybridisation histochemistry enabled us to localise GRIP, and NSF mRNA in the spinal cord under basal conditions and following CCI, as well as documenting Narp mRNA levels, a protein proposed to cause clustering of GluR1-containing AMPA receptor subunits. Western blot analyses of protein levels were carried out in parallel where possible. In situ hybridisation analysis of GRIP, NSF and Narp mRNA expression in the spinal cord indicated that all were present to varying degrees under normal conditions with all showing moderate expression in the superficial laminae of the dorsal horn (at prime sites for mediating the processing of

nociceptive information) as well as throughout the lower dorsal horn laminae III-V. Expression of these interacting proteins was differentially altered following CCI. GRIP and Narp mRNA expression were significantly increased specifically in the superficial dorsal horn ipsilateral to CCI, and Western blot analysis of GRIP immunoreactivity revealed a similar increase in GRIP protein levels. Increases in GRIP levels at the peak of neuropathic reflex sensitisation and the anti-hyperalgesic and allodynic effects of blocking the GRIP interaction with the GluR2 C-terminal domain suggest this is an important molecule that becomes activated following the induction of CCI. Though our in situ hybridisation analysis indicated an ipsilateral increase in Narp mRNA following CCI, corresponding Western blot analysis could not be carried out due to the lack of commercially available antibodies. NSF mRNA was decreased in the superficial laminae ipsilateral to CCI, as was NSF ipsilateral spinal cord protein expression as indicated by Western blot analysis. PICK1 mRNA analysis could not be carried out due to the lack of published sequence for the rat cDNA, although Western blot analysis revealed no significant alteration of overall PICK1 protein levels as a result of peripheral nerve injury. Overall, levels of SAP97 protein were also apparently unaltered in the spinal cord in response to CCI.

The specific location of GluR2 in LII_i, as well as increases in GluR2 and GRIP mRNA (with corresponding increases in protein levels of GluR2 and GRIP) in areas innervated by specific subsets of capsaicin-sensitive afferents suggests that they may play a key role in mediating neuropathic pain. Decreases in the levels of NSF mRNA and protein in this region may imply a reduction in AMPA receptor recycling and this hypothetical lack of rundown of AMPA receptor activity could influence the maintenance of the persistent pain state.

The functional implications of the GluR2: NSF interaction are unclear. Decreases in mRNA and protein levels could affect the receptor's ability to relay nociceptive information (Song et al., 1998; Lüthi et al., 1999). Loading of peptides corresponding to the NSF-binding domain of GluR2 into rat hippocampal CA1 pyramidal neurones results in a marked, progressive decrement of AMPA receptor-mediated synaptic transmission (Nishimune et al., 1998). A downregulation of NSF may imply a

reduction in AMPA receptor recycling and this hypothetical lack of rundown of AMPA receptor activity could influence the maintenance of the persistent pain state although it is likely that only one facet of the change in NSF relates to the role of GluR2.

Limited information is available for Narp at this time and although we show levels of Narp mRNA increasing ipsilateral to CCI, the functional significance of this is difficult to elucidate. It has been reported that >90% of GluR1 clusters have associated Narp immuno-staining and the over-expression of Narp increases the number of pre-synaptic terminals in spinal neurones (O'Brien et al., 1999). Narp is dramatically upregulated in neurones in response to patterned synaptic activity so that it may play a critical role in linking activity with the development and plasticity of excitatory synapses. So, it is plausible, based on this information, that an increase in Narp following the development of neuropathic pain behaviours in CCI could lead to an increase in AMPA receptor-related synapses in neurones in the spinal cord and facilitate their responsiveness, although this remains to be determined.

Physical association of GRIP/PICK1 with the GluR2 C-terminus in the spinal cord under normal conditions was confirmed by probing GluR2-directed immunoprecipitates for the presence of docking proteins. This same approach was used to uncover any alterations in GRIP and PICK1 association with GluR2 following either CCI or the direct activation of spinal AMPA receptors by the topical application of the agonist, AMPA. In contrast to the mRNA and protein analyses showing ipsilateral increases in overall levels of GRIP, the amount of GRIP associated with GluR2 subunits appeared to diminish bilaterally following CCI. PICK1 levels directly associated with GluR2 also diminished but unilaterally in the ipsilateral spinal cord. This indicates that association of these two proteins with GluR2 is differentially altered under conditions of peripheral nerve injury. It is possible that the apparent relative dissociation of GRIP and PICK1 from GluR2 in CCI reflects a process resulting from activation of the receptor. The fact that similar observations were made following application of the agonist AMPA would be consistent with this. The bilateral changes in GRIP rather than PICK1 may reflect an

associated bilateral activation of AMPA receptors, although the results with intrathecal AMPA receptor antagonists do not suggest any major contralateral activation (at least at the time of testing). There is now some evidence for GRIP having additional non-AMPA receptor-related roles (Dong et al., 1999b), so additional demands on cellular pools of GRIP in CCI may complicate the factors influencing GluR2:GRIP association (and perhaps contribute to the contralateral changes observed).

Overall levels of GRIP and PICK1 protein in membrane and cytosolic fractions were examined in response to the dorsal topical application of either saline or AMPA to assess whether stimulation-induced intracellular translocation of these proteins might play a role in influencing their GluR2 association and overall function. In agreement with previous work (Wyszynski et al., 1998), we found that a large proportion of GRIP appeared to be cytosolic and indeed, stimulation of AMPA receptors caused a translocation of GRIP from a GluR2 membrane-associated location to the cytosol. A similar translocation from the membrane to the cytosol was noted for PICK1. Activation-induced translocation of these docking proteins is therefore an important factor to consider in their possible roles during neuropathic pain states.

5.3 PSD-95 in NMDA receptor-mediated neuropathic pain

Several techniques were utilised to examine the role of the NMDA receptor interacting protein PSD-95, which docks to the NR2 subunits of the NMDA receptor, in neuropathic pain. The expression of PSD-95 in the spinal cord was specifically localised to the superficial dorsal horn LII of the spinal cord. Small-scale NR and PSD-95-directed immunoprecipitations were undertaken and confirmed a direct association of PSD-95 with NMDA receptor subunits in the spinal cord.

Mutant mice expressing a truncated form of the PSD-95 molecule were utilised to determine any potential role of PSD-95 in the development of neuropathic reflex sensitivity. We have shown that the interaction of PSD-95 with the NR2 subunits of NMDA receptors plays a crucial part in the transmission of (NMDA-related)

nociceptive information as PSD-95 mutant mice displayed a striking lack of neuropathic sensitisation normally associated with peripheral nerve injury in comparison to the development of sensitised behavioural reflexes seen in wild-type mice. This lack of behavioural sensitisation in PSD-95 mutant mice was not due to either basal morphological differences in the peripheral nerve as a general result of the mutation, as axon profiles of myelinated and unmyelinated fibres appeared normal when compared to wild-type, nor found to be due to a differential demyelination in comparison to wild-type mice as a result of CCI surgery.

Studies utilising NMDA receptor antagonist and agonist were used to confirm NMDA receptor-associated mediation of behavioural sensitivity. The intrathecal injection of the NMDA antagonist (R)-CPP significantly alleviated thermal hyperalgesia in wild type mice at the peak of CCI-induced behavioural alterations in a dose-dependent manner, while no effects were seen in parallel experiments with PSD-95 mutant mice. Additionally, intrathecal injection of NMDA, to act as an in vivo activator of spinal NMDA receptors, resulted in the well-characterised hyperalgesic and allodynic response in wild-type mice only, with no apparent alterations in PSD-95 mutant behavioural responses.

The specific distribution of PSD-95 in LII suggests an important role for this molecule in mediating neuropathic sensitisation. However, PSD-95 is a member of the MAGUK family of proteins that have high homology between their PDZ domains. Little is known about the physiological diversity that may derive from differences in MAGUK content at glutamatergic synapses although it is likely that the NR2 subunits expressed throughout the spinal cord interact with other members of the MAGUK family of proteins and which interaction actually occurs in vivo depends primarily on which member of the MAGUK family co-distributes with NMDA receptors in neuronal cells (Müller et al., 1996). NR2 subunits and K^+ channels are common targets for MAGUKS and it might be expected that, if present in the spinal cord, other MAGUKs of this family might compensate in the regulation of NMDA receptor pathway. However, here postsynaptic densities lacking PSD-95 do not appear to use any other members of the MAGUK family of proteins such as

Chapsyn110/PSD-93 or SAP102 instead, given the complete absence of neuropathic reflex sensitivity development following peripheral nerve injury. Thus, it is possible that PSD-95, given its highly specific localisation, is key to neuropathic behavioural sensitisation while the localisation and functional role of other MAGUKS in the spinal cord remains to be determined.

5.4 NMDA receptor-mediated Ca^{2+} entry and phosphorylation

NMDA receptor- mediated rises in intracellular calcium can activate CaMKII and the NMDA receptor: PSD-95 complex (in the forebrain) incorporates CaMKII, which docks to NR2 subunits and is predicted to respond readily to NMDA receptor-mediated Ca^{2+} entry (Gardoni et al., 1999; Husi and Grant, 2001). CaMKII inhibitors inhibit dorsal horn neurone responses to mustard oil applications (Young, et al., 1995) and the active autophosphorylated form of CaMKII can increase excitatory transmission in dorsal horn neurones (Kolaj et al., 1994). To examine any potential role of CaMKII in mediating behavioural reflex sensitisation following CCI, we used the intrathecal injection of two CaMKII inhibitors, myristoyl-autocamtide-2 related inhibitory peptide and KN-93, in mice at the peak of neuropathic reflex sensitisation. We report here that intrathecally applied CaMKII inhibitors can alleviate thermal hyperalgesia and mechanical allodynia that occurs following CCI in wild-type mice.

Given this evidence supporting a role for CaMKII in neuropathic sensitisation, we used CaMKII activation as a biochemical marker for Ca^{2+} entry in response to NMDA receptor stimulation elicited by the topical application of the agonist NMDA in wild-type and PSD-95 mutant mice. There was a significant increase in CaMKII enzymic activity of spinal cord extracts from both wild-type and PSD-95 mutant mice following topical application of maximally-effective concentrations of either NMDA or the Ca^{2+} ionophore, ionomycin. This indicated that the overall ability of the NMDA receptor to mediate Ca^{2+} entry into the postsynaptic cell was unaffected by the PSD-95 mutation, suggesting an intact NMDA receptor ion channel, an observation consistent with previous electrophysiological observations on hippocampal neurones in these mutant mice (Migaud et al., 1998). Using the same

protocols, CaMKII activity was increased in the ipsilateral dorsal horn of wild-type mice following CCI and this increment could be prevented by topical application of the NMDA receptor antagonist (R)-CPP. No such alteration in CaMKII activity was seen in PSD-95 mutant mice following CCI. These observations suggest that while NMDA-activated Ca^{2+} entry mechanisms are still basically intact in PSD-95 mutant mice, some mechanism which facilitates the involvement or activation of NMDA receptors after CCI becomes selectively prevented in the PSD-95 mutants.

We examined modulation of NMDA receptors by the kinases PKC and/or PKA following CCI at NR1 C-terminal sites by immunoprecipitation with phospho-specific antibodies targeted against phospho-Ser^{896} (PKC site) and phospho-Ser^{897} (PKA site) on the C-terminus of NR1 subunits of the NMDA receptor. Regulatory phosphorylation of NMDA receptor subunits by kinases such as PKC and PKA may increase the degree of Ca^{2+} entry evoked by NMDA receptor stimulation (Tingley et al., 1997; Westphal et al., 1999). Electrophysiological responses of spinal neurones to NMDA are facilitated by PKC and PKA activation (Cerne, Rusin and Randić 1993; Heppenstall and Fleetwood-Walker, 1997) and NR1 phosphorylation at the PKA Ser^{897} site is reported to increase following capsaicin injection in spinothalamic tract cells (Zou, Lin and Willis, 2000).

The levels of phospho-Ser^{897}-NR1 associated with NR1 immunoprecipitates were increased in wild type mice ipsilateral to injury following CCI, with no apparent alterations in levels in PSD-95 mutant mice following CCI. To identify a possible underlying cause for the apparent inability of PKA to phosphorylate phospho-Ser^{897}-NR1 residues in PSD-95 mutant mice, we carried out small scale NR2B-directed immunoprecipitates of naïve wild-type and PSD-95 mutant spinal cord. The site of truncation of the PSD-95 molecule in the mutants removes a site of interaction with the AKAP, AKAP79/150, a PKA anchoring protein that is believed to localise PKA to target sites. We hypothesised that a disrupted linkage via PSD-95 of AKAP79/150 to target sites may have accounted for the lack of injury-induced increases in phospho-Ser^{897}-NR1 in the PSD-95 mutant mice. Nevertheless, we could detect no alterations in the levels of NR2B-associated AKAP79/150 or of two PKA subunits

RIIα and RIIβ, which bind to AKAP79/150. The lack of CCI-induced NR1 phosphorylation at Ser^{897} and of sensitised reflex function in the PSD-95 mutant mice therefore does not seem to be due to a disrupted AKAP79/150 linkage.

5.6 Potential therapeutic implications

This project provides new insight into the mechanisms by which AMPA and NMDA receptor subunits, by virtue of their intermolecular interaction, might contribute to neuropathic pain processing. Regulation of AMPA and NMDA receptors following peripheral nerve damage is likely to be influenced by the ability of their intracellular interacting proteins to dictate specificity of targeting and/or linkages to additional signalling pathways. Although many of the underlying mechanisms are still unknown, we showed not only that intracellular proteins acting directly at AMPA and NMDA receptor subunit C-terminal motifs are localised at spinal sites of nociceptive processing but also that synthetic peptide blockers or knockout of these proteins can specifically attenuate behavioural sensitisation following nerve injury. The apparently more restricted localisation of these proteins, in comparison to the more widespread expression of AMPA and NMDA receptors themselves may be advantageous for specificity of action. While analgesic/anti-hyperalgesic targeting is now focussing on the development of subunit selective pharmacological manipulations of regionally localised AMPA and NMDA receptors in the spinal cord (Sorkin, Yaksh and Doom, 1999; Boyce et al., 1999), the work presented here contributes to an understanding of how AMPA and NMDA receptor subunit function may be regulated in response to peripheral nerve injury.

BIBLIOGRAPHY

Aanonsen LM, Wilcox GL (1987) Nociceptive action of excitatory amino acids in the mouse: effects of spinally administered opioids, phencyclidine and sigma agonists. J Pharmacol Exp Ther 243: 9-19.

Aanonsen LM, Lei S, Wilcox GL (1990) Excitatory amino acid receptors and nociceptive transmission in rat spinal cord. Pain 41: 309-321.

Aanonsen LM, Sloan SI, Kajander, KC, Bennett GJ, Seybold VS (1990) Changes in PCP binding sites in rat spinal cord in a chronic constriction injury. Soc for Neurosci Abstr 16, 1073.

Aanonsen LM, Kajander KC, Bennett GJ, Seybold VS (1992) Autoradiographic analysis of ^{125}I-substance P binding in rat spinal cord following chronic constriction injury of the sciatic nerve. Brain Res 596: 259-268.

Abbadie C, Brown JL, Mantyh PW, Basbaum AI (1996) Spinal cord substance P receptor immunoreactivity increases in both inflammatory and nerve injury models of persistent pain. Neurosci 70: 201-209.

Abe T, Sugihara H, Nawa H, Shigemoto R, Mizuno N, Nakanishi S (1992) Molecular characterization of a novel metabotropic glutamate receptor mGluR5 coupled to inositol phosphate/Ca^{2+} signal transduction. J Biol Chem 267: 13361-13368.

Agrawal SG, Evans RH (1986) The primary afferent depolarizing action of kainate in the rat. Br J Pharmacol 87: 345-355.

Al Ghoul WM, Volsi GL, Weinberg RJ, Rustioni A (1993) Glutamate immunocytochemistry in the dorsal horn after injury or stimulation of the sciatic nerve of rats. Brain Res Bull 30: 453-459.

Aley KO, Levine JD (1999) Role of protein kinase A in the maintenance of inflammatory pain. J Neurosci 19: 2181-2186.

Angaut-Petit D (1975) The dorsal column system: II. Functional properties and bulbar relay of the postsynaptic fibres of the cat's fasciculus gracilis. Exp Brain Res 22: 471-493.

Aramori I, Nakanishi S (1992) Signal transduction and pharmacological characteristics of a metabotropic glutamate receptor, mGluR1, in transfected CHO cells. Neuron 8: 757-765.

Attal N, Jazat F, Kayser V, Guilbaud G (1990a) Further evidence for 'pain-related' behaviours in a model of unilateral peripheral mononeuropathy. Pain 41: 235-251.

Attal N, Neil A, Chen L, Guilbaud G (1990b) Effects of adrenergic depletion with guanethidine before and after the induction of a peripheral neuropathy on subsequent mechanical-, heat-, and cold sensitivities in rats. Pain (Suppl) 5: S464.

Banke TG, Bowie D, Lee H, Huganir RL, Schousboe A, Traynelis SF (2000) Control of GluR1 AMPA receptor function by cAMP-dependent protein kinase. J Neurosci 20: 89-102.

Barber RP, Vaughn JE, Roberts E (1982) The cytoarchitecture of GABAergic neurons in rat spinal cord. Brain Res 238: 305-328.

Barbut D, Polak JM, Wall PD (1981) Substance P in spinal cord dorsal horn decreases following peripheral nerve injury. Brain Res 205: 289-298.

Basbaum AI, Fields HL (1978) Endogenous pain control mechanisms: review and hypothesis. Ann Neurol 4: 451-462.

Basbaum AI, Gautron M, Jazat F, Mayes M, Guilbaud G (1991) The spectrum of fiber loss in a model of neuropathic pain in the rat: An electron microscopic study. Pain 47: 359-367.

Battaglia G, Rustioni A (1988) Co-existence of glutamate and substance P in dorsal root ganglion neurons of the rat and monkey. J Comp Neurol 277: 302-312.

Bennett GJ, Mayer DJ (1979) Inhibition of spinal cord interneurons by narcotic microinjection and focal electrical stimulation in the periaqueductal central gray matter. Brain Res 172: 243-257.

Bennett GJ, Xie YK (1988) A peripheral mononeuropathy in rat that produces disorders of pain sensation like those seen in man. Pain 33: 87-107.

Berthele A, Boxall SJ, Urban A, Anneser JM, Zieglgänsberger W, Urban L, Tölle TR (1999) Distribution and developmental changes in metabotropic glutamate receptor messenger RNA expression in the rat lumbar spinal cord. Brain Res Dev Brain Res 112: 39-53.

Bessou P, Perl ER (1969) Response of cutaneous sensory units with unmyelinated fibers to noxious stimuli. J Neurophysiol 32: 1025-1043.

Bessou P, Burgess PR, Perl ER, Taylor CB (1971) Dynamic properties of mechanoreceptors with unmyelinated (C) fibers. J Neurophysiol 34: 116-131.

Bevan S, Szolcsanyi J (1990) Sensory neuron-specific actions of capsaicin: mechanisms and applications. Trends Pharmacol Sci 11: 330-333.

Biella G, Panara C, Pecile A, Sotgiu ML (1991) Facilitatory role of calcitonin gene-related peptide (CGRP) on excitation induced by substance P (SP) and noxious stimuli in rat spinal dorsal horn neurons: An iontophoretic study in vivo. Brain Res 559: 352-356.

Bleakman D, Rusin KI, Chard PS, Glaum SR, Miller RJ (1992) Metabotropic glutamate receptors potentiate ionotropic glutamate responses in the rat dorsal horn. Mol Pharmacol 42: 192-196.

Bleazard L, Hill RG, Morris R (1994) The correlation between the distribution of the NK_1 receptor and the actions of tachykinin agonists in the dorsal horn of the rat

indicates that substance P does not have a functional role on substantia gelatinosa (lamina II) neurons. J Neurosci 14: 7655-7664.

Bortolotto ZA, Collingridge GL (1998) Involvement of calcium/calmodulin-dependent protein kinases in the setting of a molecular switch involved in hippocampal LTP. Neuropharm 37: 535-544.

Boulter J, Hollmann M, O'Shea-Greenfield A, Hartley M, Deneris E, Maron C, Heinemann S (1990) Molecular cloning and functional expression of glutamate receptor subunit genes. Sci 249: 1033-1037.

Boxall SJ, Thompson SW, Dray A, Dickenson AH, Urban L (1996) Metabotropic glutamate receptor activation contributes to nociceptive reflex activity in the rat spinal cord in vitro. Neurosci 74: 13-20.

Boyce, S, Wyatt, A, Webb, JK, O'Donnell, R, Mason, G, Rigby, M, Sirinathsinghji, D, Hill, RG, Rupniak, NMJ (1999) Selective NMDA NR2B antagonists induce antinociception without motor dysfunction: correlation with restricted localisation of NR2B subunit in dorsal horn. Neuropharm 38: 611-623.

Brenman JE, Topinka JR, Cooper EC, McGee AW, Rosen J, Milroy T, Ralston HJ, Bredt DS (1998) Localization of postsynaptic density-93 to dendritic microtubules and interaction with microtubule-associated protein 1A. J Neurosci 18: 8805-8813.

Brown AG, Iggo A (1967) A quantitative study of cutaneous receptors and afferent fibres in the cat and rabbit. J Physiol 193: 707-733.

Brown AG (1971) Effects of descending impulses on transmission through the spinocervical tract. J Physiol 219: 103-125.

Brown AG, Brown PB, Fyffe REW, Publos LM (1983) Receptive field organisation and response properties of spinal neurons with axons ascending the dorsal columns in the cat. J Physiol 337: 575-588.

Brown AG (1981) The spinocervical tract. Prog Neurobiol 17: 59-96.

Brown PB, Fuchs JL (1975) Somatotopic representation of hindlimb skin in cat dorsal horn. J Neurophysiol 38: 1-9.

Brückner, K, Labrador, JP, Scheiffele, P, Herb, A, Seeburg, PH, Klein, R (1999) EphrinB ligands recruit GRIP family PDZ adaptor proteins into raft membrane microdomains. Neuron 22: 511-524.

Budai D, Wilcox GL, Larson AA (1992) Enhancement of NMDA-evoked neuronal activity by glycine in the rat spinal cord in vivo. Neurosci Lett 135: 265-268.

Budai D, Larson AA (1994) GYKI 52466 inhibits AMPA/kainate and peripheral mechanical sensory activity. Neuroreport 5: 881-884.

Burgess PR, Perl ER (1967) Myelinated afferent fibers responding specifically to noxious stimulation of skin. J Physiol 190: 541-562.

Burnashev N, N, Schoepfer R, Monyer H, Ruppersberg JP, Gunther W, Seeburg PH, Sakmann (1992a) Control by asparagine residues of calcium permeability and magnesium blockade in the NMDA receptor. Sci 257: 1415-1419.

Burnashev N, Khodorova N, Jonas P, Helm P, Wisden W, Monyer H, Seeburg PH, Sak N (1992b) Calcium-permeable AMPA-kainate receptors in fusiform cerebellar glial-cells. Sci 256: 1566-1570.

Campbell JN, Raja SN, Meyer RA, MacKinnon SE (1988) Myelinated afferents signal the hyperalgesia associated with nerve injury. Pain 32: 89-94.

Carlton SM, McNeill DL, Chung K, Coggeshall RE (1988) Organization of calcitonin gene-related peptide-immunoreactive terminals in the primate dorsal horn. J Comp Neurol 276: 527-536.

Carlton SM, Hargett GL, Coggeshall RE (1995) Localization and activation of glutamate receptors in unmyelinated axons of rat glabrous skin. Neurosci Lett 197: 25-28.

Cerne R, Jiang M, Randić M (1992) Cyclic adenosine 3'5'-monophosphate potentiates excitatory amino acid and synaptic responses of rat spinal dorsal horn neurons. Brain Res 596: 111-123.

Cerne R, Randić M (1992) Modulation of AMPA and NMDA responses in rat spinal dorsal horn neurons by trans-1-aminocyclopentane-1,3-dicarboxylic acid. Neurosci Lett 144: 180-184.

Cerne R, Rusin KI, Randić M (1993) Enhancement of the *N*-methyl-D-aspartate response in spinal dorsal horn neurons by cAMP-dependent protein kinase. Neurosci Lett 161: 124-128.

Cervero F, Iggo A, Ogawa H (1976) Nociceptor-driven dorsal horn neurones in the lumbar spinal cord of the cat. Pain 2: 5-24.

Cervero F, Iggo A, Molony V (1977) Responses of SCT neurones to noxious stimulation of the skin. J Physiol 267: 537-558.

Cervero F, Molony V, Iggo A (1979) Supraspinal linkage of substantia gelatinosa neurones: effects of descending impulses. Brain Res 175: 351-355.

Cervero F, Iggo A (1980) The substantia gelatinosa of the spinal cord. Brain Res 103, 717-772.

Cervero F (1988) The superficial dorsal horn. In: Processing of Sensory Information in the Superficial Dorsal Horn of the Spinal Cord (Cervero F, Bennett GJ, Headley PM, eds), pp 1-9. New York: Plenum Press.

Chan SF, Sucher NJ (2001) An NMDA receptor signaling complex with protein phosphatase 2a. J Neurosci 21: 7985-7992.

Chaplan SR, Malmberg AB, Yaksh TL (1997) Efficacy of spinal NMDA receptor antagonism in formalin hyperalgesia and nerve injury evoked allodynia in the rat. J Pharm Expt Ther 280: 829-838.

Che YH, Tamatani M, Tohyama M (2000) Changes in mRNA for post-synaptic density-95 (PSD-95) and carboxy-terminal PDZ ligand of neuronal nitric oxide synthase following facial nerve transection. Brain Res Mol Brain Res 76: 325-335.

Chen, NS, Luo, T, Raymond, LA (1999) Subtype-dependence of NMDA receptor channel open probability. J Neurosci 19: 6844-6854.

Chen HJ, RojasSoto M, Oguni A, Kennedy MB (1998) A synaptic Ras-GTPase activating protein (p135 SynGAP) inhibited by CaM kinase II. Neuron 20: 895-904.

Chen L, Huang LY (1992) Protein kinase C reduces Mg^{2+} block of NMDA-receptor channels as a mechanism of modulation. Nature 356: 521-523.

Christensen BN, Perl ER (1970) Spinal neurones specifically excited by noxious or thermal stimuli: marginal zone of the dorsal horn. J Neurophysiol 33: 293-307.

Christopherson KS, Hillier BJ, Lim WA, Bredt DS (1999) PSD-95 assembles a ternary complex with the *N*-Methyl-D-aspartatic acid receptor and a bivalent neuronal NO synthase PDZ domain. J Biol Chem 274: 27467-27473.

Chung HJ, Xia J, Scannevin RH, Zhang X, Huganir RL (2000) Phosphorylation of the AMPA receptor subunit GluR2 differentially regulates its interaction with PDZ domain-containing proteins. J Neurosci 20: 7258-7267.

Coderre TJ, Melzack R (1991) Central neural mediators of secondary hyperalgesia following heat injury in rats: Neuropeptides and excitatory amino acids. Neurosci Lett 131: 71-74.

Coderre TJ, Melzack R (1992) The contribution of excitatory amino acids to central sensitization and persistent nociception after formalin-induced tissue injury. J Neurosci 12: 3665-3670.

Coderre TJ (1993) The role of excitatory amino-acid receptors and intracellular messengers in persistent nociception after tissue-injury in rats. Mol Neurobiol 7: 229-246.

Coggeshall RE, Dougherty PM, Pover CM, Carlton SM (1993) Is large myelinated fiber loss associated with hyperalgesia in a model of experimental peripheral neuropathy in the rat? Pain 52: 233-242.

Coghlan VM, Perrino BA, Howard M, Langeberg LK, Hicks JB, Gallatin WM, Scott JD (1995) Association of protein kinase A and protein phosphatase 2B with a common anchoring protein. Sci 267: 108-111.

Colledge M, Dean RA, Scott GK, Langeberg LK, Huganir RL, Scott JD (2000) Targeting of PKA to glutamate receptors through a MAGUK-AKAP complex. Neuron 27: 107-119.

Collingridge GL, Kehl SJ, McLennan H (1983) Excitatory amino acids in synaptic transmission in the Schaffer-commissural pathway of the rat hippocampus. J Physiol 334: 35-46.

Colvin LA, Mark MA, Duggan AW (1997) The effect of a peripheral mononeuropathy on immunoreactive (ir)- galanin release in the spinal cord of the rat. Brain Res 766: 259-261.

Cook AJ, Woolf CJ, Wall PD, McMahon SB (1987) Dynamic receptive field plasticity in rat spinal cord dorsal horn following C-primary afferent input. Nature 325: 151-153.

Coudore-Civiale MA, Courteix C, Eschalier A, Fialip J (1998) Effect of tachykinin receptor antagonists in experimental neuropathic pain. Eur J Pharmacol 361: 175-184.

Courteix C, Lavarenne J, Eschalier A (1993) RP-67580, a specific tachykinin NK_1 receptor antagonist, relieves chronic hyperalgesia in diabetic rats. Eur J Pharmac 241: 267-270.

Couture R, Boucher S, Picard P, Regoli D (1993) Receptor characterization of the spinal action of neurokinins on nociception: A three receptor hypothesis. Regul Pept 46: 426-429.

Craven SE, Bredt DS (1998) PDZ proteins organize synaptic signaling pathways. Cell 93: 495-498.

Craven SE, El-Husseini AE, Bredt DS (1999) Synaptic targeting of the postsynaptic density protein PSD-95 mediated by lipid and protein motifs. Neuron 22: 497-509.

Cridland RA, Henry JL (1988) Effects of intrathecal administration of neuropeptides on a spinal nociceptive reflex in the rat: VIP, galanin, CGRP, TRH, somatostatin and angiotensin II. Neuropep 11: 23-32.

Cruz L, Basbaum AI (1985) Multiple opioid peptides and the modulation of pain: Immunohistochemical analysis of dynorphin and enkephalin in the trigeminal nucleus candalis and spinal cord of the cat. J Comp Neurol 240: 331-348.

Cumberbatch MJ, Chizh BA, Headley PM (1994) AMPA receptors have an equal role in spinal nociceptive and non-nociceptive transmission. Neuroreport 5: 877-880.

Curtis DR, Phillis JW, Watkins JC (1960) The chemical excitation of spinal neurones by certain acidic amino acids. J Physiol 150: 656-682.

Curtis DR, Hosli L, Johnston GA (1967) Inhibition of spinal neurons by glycine. Nature 215: 1502-1503.

Curtis DR, Duggan AW, Felix D, Johnston GA (1970) GABA, bicuculline and central inhibition. Nature 226: 1222-1224.

Davies J, Evans RH, Francis AA, Watkins JC (1979) Excitatory amino acid receptors and synaptic excitation in the mammalian central nervous system. J Physiol 75: 641-654.

Davies S, Lodge D (1987) Evidence for involvement of *N*-methyl-aspartate receptors in wind-up of class-2 neurons in the dorsal horn of the rat. Brain Res 424: 402-406.

Davis KD (1998) Cold-induced pain and prickle in the glabrous and hairy skin. Pain 75: 47-57.

De Biasi S, Rustioni A (1988) Glutamate and substance P coexist in primary afferent terminals in the superficial laminae of spinal cord. Proc Natl Acad Sci U S A 85: 7820-7824.

de Quidt ME, Emson PC (1986) Distribution of neuropeptide Y-like immunoreactivity in the rat central nervous system-II. Immunohistochemical analysis. Neurosci 18: 545-618.

Derkach V, Barria A, Soderling TR (1999) Ca^{2+}/calmodulin-kinase II enhances channel conductance of α-amino-3-hydroxy-5-methyl-4-isoxazolepropionate type glutamate receptors. Proc Natl Acad Sci U S A 96: 3269-3274.

Dev KK, Nishimune A, Henley JM, Nakanishi S (1999) The protein kinase C alpha binding protein PICK1 interacts with short but not long form alternative splice variants of AMPA receptor subunits. Neuropharm 38: 635-644.

Devor M, Wall PD (1990) Cross-excitation in dorsal root ganglia of nerve-injured and intact rats. J Neurophysiol 64: 1733-1746.

Devor M (1991) Neuropathic pain and injured nerve: peripheral mechanisms. Br Med Bull 47: 619-630.

Dickenson AH, Sullivan AF (1990) Differential effects of excitatory amino acid antagonists on dorsal horn nociceptive neurones in the rat. Brain Res 506: 31-39.

Dickenson AH, Aydar E (1991) Antagonism at the glycine site on the NMDA receptor reduces spinal nociception in the rat. Neurosci Lett 121: 263-266.

Dickinson T, Mitchell R, Robberecht P, Fleetwood-Walker SM (1999) The role of VIP/PACAP receptor subtypes in spinal somatosensory processing in rats with an experimental peripheral mononeuropathy. Neuropharm 38: 167-180.

Dong HL, Zhang PS, Liao DZ, Huganir RL (1999a) Characterization, expression, and distribution of GRIP protein. ANYAS 868: 535-540.

Dong HL, Zhang PS, Song IS, Petralia RS, Liao DZ, Huganir RL (1999b) Characterization of the glutamate receptor-interacting proteins GRIP1 and GRIP2. J Neurosci 19: 6930-6941.

Dong HL, O'Brien RJ, Fung ET, Lanahan AA, Worley PF, Huganir RL (1997) GRIP: A synaptic PDZ domain-containing protein that interacts with AMPA receptors. Nature 386: 279-284.

Dougherty PM, Willis WD (1991) Enhancement of spinothalamic neuron responses to chemical and mechanical stimuli following combined micro-iontophoretic application of *N*-methyl-D-aspartic acid and substance P. Pain 47: 85-93.

Dougherty PM, Palecek J, Paléckova V, Sorkin LS, Willis WD (1992) The role of NMDA and non-NMDA excitatory amino acid receptors in the excitation of primate spinothalamic tract neurons by mechanical, chemical, thermal, and electrical stimuli. J Neurosci 12: 3025-3041.

Dubner R, Bennett GJ (1983) Spinal and trigeminal mechanisms of nociception. Ann Rev Neurosci 6: 381-418.

Duggan AW, Griersmith BT (1979) Inhibition of the spinal transmission of nociceptive information by supraspinal stimulation in the cat. Pain 6: 149-161.

Duggan AW, Johnston GA (1970) Glutamate and related amino acids in cat spinal roots, dorsal root ganglia and peripheral nerves. J Neurochem 17: 1205-1208.

Duggan AW, Morton CR, Zhao ZQ, Hendry IA (1987) Noxious heating of the skin releases immunoreactive substance P in the substantia gelatinosa of the cat: a study with antibody microprobes. Brain Res 403: 345-349.

Duggan AW, Hope PJ, Jarrott B, Schiable H-D, Fleetwood-Walker SM (1990) Release, spread and persistence of immunoreactive Neurokinin A in the dorsal horn of the cat following noxious cutaneous stimulation: Studies with antibody microprobes. Neurosci 35: 195-202.

Duggan AW, Riley RC, Mark MA, MacMillan SJA, Schaible H-G (1995) Afferent volley patterns and the spinal release of immunoreactive substance P in the dorsal horn of the anaesthetized spinal cat. Neurosci 65: 849-858.

Ehlers MD, Zhang S, Bernhardt JP, Huganir RL (1996) Inactivation of NMDA receptors by direct interaction of calmodulin with the NR1 subunit. Cell 84: 745-755.

Elliott AM, Smith BH, Penny KI, Smith WC, Chambers WA (1999) The epidemiology of chronic pain in the community. Lancet 354: 1248-1252.

Emson PC, Fahrenkrug J, Schaffalitzky de Muckadell OB, Jessell TM, Iversen LL (1978) Vasoactive intestinal polypeptide (VIP): vesicular localization and potassium evoked release from rat hypothalamus. Brain Res 143: 174-178.

Engelman, HS, Allen, TB, MacDermott, AB (1999) The distribution of neurons expressing calcium-permeable AMPA receptors in the superficial laminae of the spinal cord dorsal horn. J Neurosci 19: 2081-2089.

Fanning AS, Anderson JM (1996) Protein-protein interactions: PDZ domain networks. Curr Biol 6: 1385-1388.

Feldmeyer D, Kask K, Brusa R, Kornau HC, Kolhekar R, Rozov A, Burnashev N, Jensen V, Hvalby O, Sprengel R, Seeburg PH (1999) Neurological dysfunctions in mice expressing different levels of the Q/R site-unedited AMPAR subunit GluR-B. Nat Neurosci 2: 57-64.

Feliciello A, Cardone L, Garbi C, Ginsberg MD, Varrone S, Rubin CS, Avvedimento EV, Gottesman ME (1999) Yotiao protein, a ligand for the NMDA receptor, binds and targets cAMP-dependent protein kinase II. FEBS Lett 464: 174-178.

Fields HL, Heinricher MM (1985) Anatomy and physiology of a nociceptive modulatory system. Philos Trans R Soc Lond B Biol Sci 308: 361-374.

Firestein BL, Brenman JE, Aoki C, SanchezPerez AM, ElHusseini AED, Bredt DS (1999) Cypin: A cytosolic regulator of PSD-95 postsynaptic targeting. Neuron 24: 659-672.

Fisher K, Coderre TJ (1998) Hyperalgesia and allodynia induced by intrathecal (RS)-dihydroxyphenylglycine in rats. Neuroreport 9: 1169-1172.

Fleetwood-Walker SM, Mitchell R, Hope PJ, El-Yassir N, Molony V, Bladon CM (1990) The involvement of neurokinin receptor subtypes in somatosensory processing in the superficial dorsal horn of the cat. Brain Res 519: 169-182.

Florenzano F, DeLuca B (1999) Nociceptive stimulation induces glutamate receptor down- regulation in the trigeminal nucleus. Neurosci 90: 201-207.

Fong, DK, Craig, AM (1999) The Narp hypothesis? Neuron 23: 195-197.

Foong FW, Duggan AW (1986) Brain-stem areas tonically inhibiting dorsal horn neurones: studies with microinjection of the GABA analogue piperidine-4-sulphonic acid. Pain 27: 361-371.

Frost SA, Raja SN, Campbell JN, Mayer RA, Khan AA (1988) Does hyperalgesia to cooling stimuli characterize patients with sympathetically maintained pain (reflex sympathetic dystrophy)? Proc Vth World Congress Pain 151-156.

Fuji K, Senba E, Ueda Y, Tohyama M (1983) Vasoactive intestinal polypeptide (VIP)-containing neurons in the spinal cord of the rat and their projections. Neurosci Lett 37: 51-55.

Fukunaga K, Rich DP, Soderling TR (1989) Generation of the Ca^{2+}-independent form of Ca^{2+}/calmodulin-dependent protein kinase II in cerebellar granule cells. J Biol Chem 264: 21830-21836.

Furuyama T, Kiyama H, Sato K, Park HT, Maeno H, Takagi H, Tohyama M (1993) Region-specific expression of subunits of ionotropic glutamate receptors (AMPA-type, KA-type and NMDA receptors) in the rat spinal- cord with special reference to nociception. Mol Br Res 18: 141-151.

Furuyashiki T, Fujisawa K, Fujita A, Madaule P, Uchino S, Mishina M, Bito H, Narumiya S (1999) Citron, a Rho-target, interacts with PSD-95/SAP-90 at glutamatergic synapses in the thalamus. J Neurosci 19: 109-118.

Garces YI, Rabito SF, Minshall RD, Sagen J (1993) Lack of potent antinociceptive activity by substance P antagonist CP-96,345 in the rat spinal cord. Life Sci 52: 353-360.

Garcia EP, Mehta S, Blair LAC, Wells DG, Shang J, Fukushima T, Fallon JR, Garner CC, Marshall J (1998) SAP90 binds and clusters kainate receptors causing incomplete desensitization. Neuron 21: 727-739.

Gardoni F, Schrama LH, van Dalen JJ, Gispen WH, Cattabeni F, Di Luca M (1999) αCaMKII binding to the C-terminal tail of NMDA receptor subunit NR2A and its modulation by autophosphorylation. FEBS Lett 456: 394-398.

Gautron M, Jazat F, Ratinahirana H, Hauw JJ, Guilbaud G (1990) Alterations in myelinated fibers in the sciatic-nerve of rats after constriction - possible relationships between the presence of abnormal small myelinated fibers and pain-related behavior. Neurosci Lett 111: 28-33.

Gerber G, Randić M (1989) Excitatory amino acid-mediated components of synaptically evoked input from dorsal roots to deep dorsal horn neurons in the rat spinal cord slice. Neurosci Lett 106: 211-219.

Gibson SJ, Polak JM, Bloom SR, Wall PD (1981) The distribution of nine peptides in rat spinal cord with special emphasis on the substantia gelatinosa and on the area around the central canal (lamina X). J Comp Neurol 201: 65-79.

Gibson SJ, Polak JM, Allen JM, Adrian TE, Kelly JS, Bloom SR (1984) The distribution and origin of a novel brain peptide, neuropeptide Y, in the spinal cord of several mammals. J Comp Neurol 227: 78-91.

Giesler GJ, Menétrey D, Guilbaud G, Besson JM (1976) Lumbar cord neurons at the origin of the spinothalamic tract in the rat. Brain Res 118: 320-324.

Giesler GJ, Nahin RL, Masden AM (1984) Postsynaptic dorsal column pathway of the rat: Anatomical studies. J Neurophysiol 51: 260-275.

Giesler GJ, Cannon JT, Urca G, Liebeskind JC (1978) Long ascending projections from substantia gelatinosa Rolandi and the subjacent dorsal horn in the rat. Sci 202: 984-986.

Gillespie CS, Sherman DL, Fleetwood-Walker SM, Cottrell DF, Tait S, Garry EM, Wallace VC, Ure J, Griffiths IR, Smith A, Brophy PJ (2000) Peripheral demyelination and neuropathic pain behavior in periaxin-deficient mice. Neuron 26: 523-531.

Glazer EJ, Basbaum AI (1981) Immunohistochemical localization of leucine - enkephalin in the spinal cord of the cat: enkephalin - containing marginal neurones and pain modulation. J Comp Neurol 196: 377-390.

Go VL, Yaksh TL (1987) Release of substance P from the cat spinal cord. J Physiol 391:141-167.

Grond S, Zech D, Diefenbach C, Bischoff A (1994) Prevalence and pattern of symptoms in patients with cancer pain: a prospective evaluation of 1635 cancer patients referred to a pain clinic. J Pain Symptom Manag 9: 372-382.

Grossman SD, Wolfe BB, Yasuda RP, Wrathall JR (2000) Changes in NMDA receptor subunit expression in response to contusive spinal cord injury. J Neurochem 75: 174-184.

Grossman SD, Wolfe BB, Yasuda RP, Wrathall JR (1999) Alterations in AMPA receptor subunit expression after experimental spinal cord contusion injury. J Neurosci 19: 5711-5720.

Guan Y, Guo W, Dubner R, Ren K (2001) Enhanced AMPA receptor GluR1 subunit expression and phosphorylation within brain stem pain modulatory circuitry after persistent inflammation. Soc Neurosci Abstr 509.12: 261-261.

Guilbaud G, Oliveras JL, Giesler GJ, Besson JM (1977) Effects induced by stimulation of the centralis inferior nucleus of the raphe on dorsal horn interneurons in cat's spinal cord. Brain Res 126: 355-360.

Guilbaud G, Gautron M, Jazat F, Ratinahirana H, Hassig R, Hauw JJ (1993) Time-course of degeneration and regeneration of myelinated nerve- fibers following chronic loose ligatures of the rat sciatic-nerve - can nerve lesions be linked to the abnormal pain-related behaviors. Pain 53: 147-158.

Hama AT, Unnerstall JR, Siegan JB, Sagen J (1995) Modulation of NMDA receptor expression in the rat spinal cord by peripheral nerve injury and adrenal medullary grafting. Brain Res 687: 103-113.

Hanson PI, Kapiloff MS, Lou LL, Rosenfeld MG, Schulman H (1989) Expression of a multifunctional Ca^{2+}/calmodulin-dependent protein kinase and mutational analysis of its autoregulation. Neuron 3: 59-70.

Hao JX, Shi TJ, Xu IS, Kaupilla T, Xu XJ, Hökfelt T, Bartfai T, Wiesenfeld-Hallin Z (1999) Intrathecal galanin alleviates allodynia-like behaviour in rats after partial peripheral nerve injury. Eur J Neurosci 11: 427-432.

Hardy JD, Wolff HG, Goodell H (1950) Experimental evidence on the nature of cutaneous hyperalgesia. J Clin Invest 29: 115-140.

Hargreaves K, Dubner R, Brown F, Flores C, Joris J (1988) A new and sensitive method for measuring thermal nociception in cutaneous hyperalgesia. Pain 32: 77-88.

Harmar A, Keen P (1982) Synthesis, and central and peripheral axonal transport of substance P in a dorsal root ganglion-nerve preparation in vitro. Brain Res 231: 379-385.

Harris JA, Corsi M, Quartaroli M, Arban R, Bentivoglio M (1996) Upregulation of spinal glutamate receptors in chronic pain. Neurosci 74: 7-12.

Hayashi Y, Shi SH, Esteban JA, Piccini A, Poncer JC, Malinow R (2000) Driving AMPA receptors into synapses by LTP and CaMKII: requirement for GluR1 and PDZ domain interaction. Sci 287: 2262-2267.

Hayes RL, Price DD, Ruda MA, Dubner R (1979) Suppression of nociceptive responses in the primate by electrical stimulation of the brain or morphine administration: behavioural and electrophysiological comparisons. Brain Res 167: 417-421.

Hayes AG, Tyers MB (1979) Effects of intrathecal and intracerebroventricular injections of substance P on nociception in the rat and mouse. Br J Pharmacol 66: 488P.

Hayes AG, Skingle M., Tyers M.B. (1981) Effects of single doses of capsaicin on nociceptive thresholds in the rodent. Neuropharm 20: 505-512.

Helgren, ME, Arsenault, K, Kapadia, SE, LaMotte, CC (1999) Deafferentation-induced regulation of AMPA receptors in the spinal cord of the adult rat. Som Motor Res 16: 39-48.

Helke CJ, Charlton CG, Wiley RG (1986) Studies on the cellular localisation of spinal cord substance P receptors. Neurosci 19: 523-533.

Henley JM, Jenkins R, Hunt SP (1993) Localization of glutamate receptor-binding sites and messenger RNAs to the dorsal horn of the rat spinal-cord. Neuropharm 32: 37-41.

Henry JL (1976) Effects of substance P on functionally identified units in cat spinal cord. Brain Res 114: 439-451.

Heppenstall PA, Fleetwood-Walker SM (1997) The glycine site of the NMDA receptor contributes to neurokinin1 receptor agonist facilitation of NMDA receptor agonist-evoked activity in rat dorsal horn neurons. Brain Res 744: 235-245.

Hill R (2000) NK1 (substance P) receptor antagonists-why are they not analgesic in humans? Trends Pharmacol Sci 21: 244-246.

Hiraga K, Mizuguchi T, Takeda F (1991) The incidence of cancer pain and improvement of pain management in Japan. Postgrad Med J 67 (Suppl) 2:S14-25: S14-S25.

Hisatsune C, Umemori H, Inoue T, Michikawa T, Kohda K, Mikoshiba K, Yamamoto T (1997) Phosphorylation-dependent regulation of *N*-methyl-D-aspartate receptors by calmodulin. J Biol Chem 272: 20805-20810.

Hökfelt T, Wiesenfeld-Hallin Z, Villar M, Melander T (1987) Increase of galanin-like immunoreactivity in rat dorsal root ganglion cells after peripheral axotomy. Neurosci Lett 83: 217-220.

Hökfelt T, Elde RP, Johansson B, Luft, Nilsson, Arimura (1976) Immunohistochemical evidence for separate populations of somatostatin-containing and substance P-containing primary afferent neurons in the rat. Neurosci 1: 131-136.

Hökfelt T, Zhang X, Wiesenfeld-Hallin Z (1994) Messenger plasticity in primary sensory neurons following axotomy and its functional implications. Trends Neurosci 17: 22-30.

Hollmann M, Boulter J, Maron C, Beasley L, Sullivan J, Pecht G, Heinemann S (1993) Zinc potentiates agonist-induced currents at certain splice variants of the NMDA receptor. Neuron 10: 943-954.

Hollmann M, Heinemann S (1994) Cloned glutamate receptors. Annu Rev Neurosci 17:31-108: 31-108.

Hope PJ, El-Yassir N, Fleetwood-Walker SM, Mitchell R (1989) Opioid and serotonergic effects on lamina I and deeper dorsal horn neurones. In: Processing of Sensory Information in the Superficial Dorsal Horn of the Spinal Cord (Cervero F, Bennett GJ, Headley PM, eds), pp 399-403. New York: Plenum Press.

Hosoya M, Kimura C, Ogi K, Ohkubo S, Miyamoto Y, Kugoh H, Shimizu M, Onda H, Oshimura M, Arimura A (1997) Structure of the human pituitary adenylate cyclase activating polypeptide (PACAP) gene. Biochimica et Biophysica Acta 1992 Jan 6;1129(2):199-206 199-206.

Hsueh YP, Kim E, Sheng M (1997) Disulfide-linked head-to-head multimerization in the mechanism of ion channel clustering by PSD-95. Neuron 18: 803-814.

Huettner JE (1990) Glutamate receptor channels in rat DRG neurons: activation by kainate and quisqualate and blockade of desensitization by Con A. Neuron 5: 255-266.

Husi H, Ward MA, Choudhary JS, Blackstock WP, Grant SG (2000) Proteomic analysis of NMDA receptor-adhesion protein signaling complexes. Nat Neurosci 3: 661-669.

Husi H, Grant SG (2001) Isolation of 2000-kDa complexes of N-methyl-D-aspartate receptor and postsynaptic density-95 from mouse brain. J Neurochem 77: 281-291.

Hylden JLK, Wilcox GL (1982) Intrathecal opioids block a spinal action of substance P in mice: functional importance of both mu and delta receptors. Eur J Pharmac 86: 95-98.

Iggo A (1959) Cutaneous heat and cold receptors with slowly conducting (C) afferent fibres. Quart J Exp Physiol 44: 362-370.

Iggo A (1974) Activation of cutaneous nociceptors and their action on dorsal horn neurones. In: Advances in Neurology (Bonica J, ed), pp 1-9. New York: Raven.

Irie M, Hata Y, Takeuchi M, Ichtchenko K, Toyoda A, Hirao K, Takai Y, Rosahl TW, Sudhof TC (1997) Binding of neuroligins to PSD-95. Sci 277: 1511-1515.

Ishihara T, Shigemoto R, Mori K, Takahashi K, Agata S (1992) Functional expression and tissue distribution of a novel receptor for vasoactive intestinal polypeptide. Neuron 8: 811-819.

Jackson DL, Graff CB, Richardson JD, Hargreaves KM (1995) Glutamate participates in the peripheral modulation of thermal hyperalgesia in rats. Eur J Pharmacol 284: 321-325.

Jänig W, Levine JD, Michaelis M (1996) Interactions of sympathetic and primary afferent neurons following nerve injury and tissue trauma. Prog Brain Res 113: 161-184.

Jeftinija S, Murase K, Nedeljkov V, Randić M (1982) Vasoactive intestinal polypeptide excites mammalian dorsal horn neurons both in vivo and in vitro. Brain Res 243: 158-164.

Jessell T, Tsunoo A, Kanazawa I, Otsuka M (1979) Substance P: depletion in the dorsal horn of rat spinal cord after section of the peripheral processes of primary sensory neurons. Brain Res 168: 247-259.

Jia H, Rustioni A, Valtschanoff JG (1999) Metabotropic glutamate receptors in superficial laminae of the rat dorsal horn. J Comp Neurol 410: 627-642.

Jia Z, Agopyan N, Miu P, Xiong Z, Henderson J, Gerlai R, Taverna FA, Velumian A, MacDonald J, Carlen P, Abramow-Newerly W, Roder J (1996) Enhanced LTP in mice deficient in the AMPA receptor GluR2. Neuron 17: 945-956.

Johnson MS, Lutz EM, MacKenzie CJ, Wolbers WB, Robertson DN, Holland PJ, Mitchell R (2000) Gonadotropin-releasing hormone receptor activation of extracellular signal-regulated kinase and tyrosine kinases in transfected GH3 cells and in alphaT3-1 cells. Endocrin 141: 3087-3097.

Jones PM, Persaud SJ (1998) Ca^{2+}-induced loss of Ca^{2+}/calmodulin-dependent protein kinase II activity in pancreatic beta-cells. Am J Physiol 274: E708-E715.

Ju G, Hökfelt T, Brodin E, Fahrenkrug J, Fischer JA, Frey P, Elde RP, Brown JC (1987) Primary sensory neurons of the rat showing calcitonin gene-related peptide immunoreactivity and their relation to substance P-, somatostatin-, galanin-, vasoactive intestinal polypeptide- and cholecystokinin-immunoreactive ganglion cells. Cell Tiss Res 247: 417-431.

Kajander KC, Bennett GJ (1992) Onset of a painful peripheral neuropathy in rat: a partial and differential deafferentation and spontaneous discharge in A beta and A delta primary afferent neurons. J Neurophysiol 68: 734-744.

Kajander KC, Xu J (1995) Quantitative evaluation of calcitonin gene-related peptide and substance P levels in rat spinal cord following peripheral nerve injury. Neurosci Lett 186: 184-188.

Kar S, Quirion R (1995) Neuropeptide receptors in developing and adult rat spinal cord: An in vitro quantitative autoradiography study of calcitonin gene-related peptide, neurokinins, μ-opioid, galanin, somatostatin, neurotensin and vasoactive intestinal polypeptide receptors. J Comp Neurol 354: 253-281.

Kasahara J, Fukunaga K, Miyamoto E (1999) Differential effects of a calcineurin inhibitor on glutamate-induced phosphorylation of Ca^{2+}/calmodulin-dependent protein kinases in cultured rat hippocampal neurons. J Biol Chem 274: 9061-9067.

Keinänen K, Wisden W, Sommer B, Werner P, Herb A, Verdoorn TA, Sakmann B, Seeburg PH (1990) A family of AMPA-selective glutamate receptors. Sci 249: 556-560.

Kennedy MB (1997) The postsynaptic density at glutamatergic synapses. Trends Neurosci 20: 264-268.

Khasar SG, Lin YH, Martin A, Dadgar J, McMahon T, Wang D, Hundle B, Aley KO, Isenberg W, McCarter G, Green PG, Hodge CW, Levine JD, Messing RO (1999) A novel nociceptor signaling pathway revealed in protein kinase Cε mutant mice. Neuron 24: 253-260.

Kim CH, Chung HJ, Lee HK, Huganir RL (2001) Interaction of the AMPA receptor subunit GluR2/3 with PDZ domains regulates hippocampal long-term depression. Proc Natl Acad Sci U S A 98: 11725-11730.

Kim E, Niethammer M, Rothschild A, Jan YN, Sheng M (1995) Clustering of Shaker-type K^+ channels by interaction with a family of membrane-associated guanylate kinases. Nature 378: 85-88.

Kim E, Cho KO, Rothschild A, Sheng M (1996) Heteromultimerization and NMDA receptor-clustering activity of Chapsyn-110, a member of the PSD-95 family of proteins. Neuron 17: 103-113.

Kim E, Sheng M (1996) Differential K^+ channel clustering activity of PSD-95 and SAP97, two related membrane-associated putative guanylate kinases. Neuropharm 35: 993-1000.

Kim JH, Liao DZ, Lau LF, Huganir RL (1998) SynGAP: a synaptic RasGAP that associates with the PSD-95/SAP90 protein family. Neuron 20: 683-691.

Kleckner NW, Dingledine R (1988) Requirement for glycine in activation of NMDA-receptors expressed in Xenopus oocytes. Sci 241: 835-837.

Klein CM, Coggeshall RE, Carlton SM, Sorkin LS (1992) The effects of A- and C-fiber stimulation on patterns of neuropeptide immunostaining in the rat superficial dorsal horn. Brain Res 580: 121-128.

Knyihár-Csillik E, Kreutzberg GW, Raivich G, Csillik B (1991) Vasoactive intestinal polypeptide in dorsal root terminals of the rat spinal cord is regulated by the axoplasmic transport in the peripheral nerve. Neurosci Lett 131: 83-87.

Kolaj M, Cerne R, Cheng G, Brickey DA, Randić M (1994) Alpha subunit of calcium/calmodulin-dependent protein kinase enhances excitatory amino acid and synaptic responses of rat spinal dorsal horn neurons. J Neurophysiol 72: 2525-2531.

Koltzenburg M, Torebjörk HE, Wahren LK (1994) Nociceptor modulated central sensitization causes mechanical hyperalgesia in acute chemogenic and chronic neuropathic pain. Brain 117: 579-591.

Kornau HC, Schenker T, Kennedy MB, Seeburg PH (1995) Domain interaction between NMDA receptor subunits and the postsynaptic density protein PSD-95. Sci 269: 1737-1740.

Kornau HC, Seeburg PH, Kennedy MB (1997) Interaction of ion channels and receptors with PDZ domain proteins. Curr Op Neurobiol 7: 368-373.

Krupp JJ, Vissel B, Heinemann SF, Westbrook GL (1998) N-terminal domains in the NR2 subunit control desensitization of NMDA receptors. Neuron 20: 317-327.

Kus L, Saxon D, Beitz AJ (1995) NMDAR1 mRNA distribution in motor and thalamic-projecting sensory neurons in the rat spinal cord and brain stem. Neurosci Lett 196: 201-204.

Laemmli UK (1970) Cleavage of structural proteins during the assembly of the head of bacteriophage T4. Nature 227: 680-685.

Laing I, Todd AJ, Heizmann CW, Schmidt HW (1994) Subpopulations of GABAergic neurons in laminae I-III of rat spinal dorsal horn defined by coexistence with classical transmitters, peptides, nitric oxide synthase or parvalbumin. Neurosci 61: 123-132.

LaMotte RH, Shain CN, Simone DA, Tsai E-FP (1991) Neurogenic hyperalgesia: Psychophysical studies of underlying mechanisms. J Neurophysiol 66: 190-211.

Lau LF, Huganir RL (1995) Differential tyrosine phosphorylation of *N*-methyl-D-aspartate receptor subunits. J Biol Chem 270: 20036-20041.

Laube B, Hirai H, Sturgess M, Betz H, Kuhse J (1997) Molecular determinants of agonist discrimination by NMDA receptor subunits: analysis of the glutamate binding site on the NR2B subunit. Neuron 18: 493-503.

Lee HK, Barbarosie M, Kameyama K, Bear MF, Huganir RL (2000) Regulation of distinct AMPA receptor phosphorylation sites during bidirectional synaptic plasticity. Nature 405: 955-959.

Lee Y, Takami K, Kawai Y, Girgis S, Hillyard CJ, MacIntyre I, Emson PC, Tohyama M (1985) Distribution of calcitonin gene-related peptide in the rat peripheral nervous system with reference to its coexistence with substance P. Neurosci 15: 1227-1237.

Legendre P, Rosenmund C, Westbrook GL (1993) Inactivation of NMDA channels in cultured hippocampal neurons by intracellular calcium. J Neurosci 13: 674-684.

Leonard AS, Hell JW (1997) Cyclic AMP-dependent protein kinase and protein kinase C phosphorylate *N*-methyl-D-aspartate receptors at different sites. J Biol Chem 272: 12107-12115.

Leonard AS, Davare MA, Horne MC, Garner CC, Hell JW (1998) SAP97 is associated with the α-amino-3-hydroxy-5-methylisoxazole- 4-propionic acid receptor GluR1 subunit. J Biol Chem 273: 19518-19524.

Li P, Kerchner GA, Sala C, Wei F, Huettner JE, Sheng M, Zhuo M (1999) AMPA receptor-PDZ interactions in facilitation of spinal sensory synapses. Nat Neurosci 2: 972-977.

Light AR, Perl ER (1979) Spinal termination of functionally identified primary afferent neurones with slowly conducting myelinated fibres. J Comp Neurol 186: 117-132.

Lima D, Coimbra A (1986) A Golgi-study of the neuronal population of the marginal zone (Lamina-I) of the rat spinal cord. J Comp Neurol 244: 53-71.

Lin JW, Wyszynski M, Madhavan R, Sealock R, Kim JU, Sheng M (1998) Yotiao, a novel protein of neuromuscular junction and brain that interacts with specific splice variants of NMDA receptor subunit NR1. J Neurosci 18: 2017-2027.

Lisman J, Malenka RC, Nicoll RA, Malinow R (1997) Learning mechanisms: the case for CaMKII. Sci 276: 2001-2002.

Liu H, Mantyh PW, Basbaum AI (1997) NMDA-receptor regulation of substance P release from primary afferent nociceptors. Nature 386: 721-724.

Liu X-G, Sandkühler J (1995) Long-term potentiation of C-fiber-evoked potentials in the rat spinal dorsal horn is prevented by spinal *N*-methyl- D-aspartic acid receptor blockage. Neurosci Lett 191: 43-46.

Llinás R, McGuinness TL, Leonard CS, Sugimori M, Greengard P (1985) Intraterminal injection of synapsin I or calcium/calmodulin-dependent protein kinase II alters neurotransmitter release at the squid giant synapse. Proc Natl Acad Sci USA 82: 3035-3039.

Loren I, Emson PC, Fahrenkrug J, Björklund A, Alumets J, Hakanson R, Sundler F (1979) Distribution of vasoactive intestinal polypeptide in the rat and mouse brain. Neurosci 4: 1953-1976.

Lu X, Wyszynski M, Sheng M, Baudry M (2001) Proteolysis of glutamate receptor-interacting protein by calpain in rat brain: implications for synaptic plasticity. J Neurochem 77: 1553-1560.

Lu WY, Xiong ZG, Lei S, Orser BA, Dudek E, Browning MD, MacDonald JF (1999) G-protein-coupled receptors act via protein kinase C and Src to regulate NMDA receptors. Nat Neurosci 2: 331-338.

Lundberg JM, Terenius L, Hökfelt T, Goldstein M (1983) High levels of neuropeptide Y in peripheral noradrenergic neurons in various mammals including man. Neurosci Lett 42: 167-172.

Luque JM, Bleuel Z, Malherbe P, Richards JG (1994) Alternatively spliced isoforms of the *N*-methyl-D-aspartate receptor subunit-1 are differentially distributed within the rat spinal cord. Neurosci 63: 629-635.

Lüthi A, Chittajallu R, Duprat F, Palmer MJ, Benke TA, Kidd FL, Henley JM, Isaac JTR, Collingridge GL (1999) Hippocampal LTD expression involves a pool of AMPARs regulated by the NSF-GluR2 interaction. Neuron 24: 389-399.

Lutz EM, Sheward WJ, West KM, Morrow JA, Fink G, Harmar AJ (1993) The VIP2 receptor: molecular characterisation of a cDNA encoding a novel receptor for vasoactive intestinal peptide. FEBS Lett 334: 3-8.

Lynn B (1994) The fibre composition of cutaneous nerves and the classification and response properties of cutaneous afferents, with particular reference to nociception. Pain Rev 1: 172-183.

Lynn B, Carpenter SE (1982) Primary afferent units from hairy skin of the rat hindlimb. Brain Res 238: 29-43.

Lynn B, Shakhanbeh J (1988) Properties of A delta high threshold mechanoreceptors in the rat hairy and glabrous skin and their response to heat. Neurosci Lett 85: 71-76.

Ma QP, Hargreaves RJ (2000) Localization of *N*-methyl-D-aspartate NR2B subunits on primary sensory neurons that give rise to small-caliber sciatic nerve fibers in rats. Neurosci 101: 699-707.

Ma W, Bisby MA (1998) Increase of preprotachykinin mRNA and substance P immunoreactivity in spared dorsal root ganglion neurons following partial sciatic nerve injury. Eur J Neurosci 10: 2388-2399.

Ma W, Bisby MA (1997) Differential expression of galanin immunoreactivities in the primary sensory neurons following partial and complete sciatic nerve injuries. Neurosci 79: 1183-1195.

Malmberg AB, Brandon EP, Idzerda RL, Liu H, McKnight GS, Basbaum AI (1997a) Diminished inflammation and nociceptive pain with preservation of neuropathic pain in mice with a targeted mutation of the type I regulatory subunit of cAMP-dependent protein kinase. J Neurosci 17: 7462-7470.

Malmberg AB, Chen C, Tonegawa S, Basbaum AI (1997b) Preserved acute pain and reduced neuropathic pain in mice lacking PKCγ. Sci 278: 279-283.

Mammen AL, Kameyama K, Roche KW, Huganir RL (1997) Phosphorylation of the α-3-hydroxy-5-methylisoxazole4-propionic acid receptor GluR1 subunit by calcium/ calmodulin-dependent kinase II. J Biol Chem 272: 32528-32533.

Mao J, Price DD, Hayes RL, Lu J, Mayer DJ (1992a) Differential roles of NMDA and non-NMDA receptor activation in induction and maintenance of thermal hyperalgesia in rats with painful peripheral mononeuropathy. Brain Res 598: 271-278.

Mao J, Price DD, Mayer DJ, Hayes RL (1992b) Pain-related increases in spinal cord membrane-bound protein kinase C following peripheral nerve injury. Brain Res 588: 144-149.

Mao J, Price DD, Hayes RL, Lu J, Mayer DJ, Frenk H (1993) Intrathecal treatment with dextrorphan or ketamine potently reduces pain-related behaviors in a rat model of peripheral mononeuropathy. Brain Res 605: 164-168.

Masu M, Tanabe Y, Tsuchida K, Shigemoto R, Nakanishi S (1991) Sequence and expression of a metabotropic glutamate receptor. Nature 349: 760-765.

Matsuda S, Mikawa S, Hirai H (1999) Phosphorylation of serine-880 in GluR2 by protein kinase C prevents its C-terminus from binding with glutamate receptor-interacting protein. J Neurochem 73: 1765-1768.

Matsuda S, Launey T, Mikawa S, Hirai H (2000) Disruption of AMPA receptor GluR2 clusters following long-term depression induction in cerebellar Purkinje neurons. EMBO J 19: 2765-2774.

McGee AW, Bredt DS (1999) Identification of an intramolecular interaction between the SH3 and guanylate kinase domains of PSD-95. J Biol Chem 274: 17431-17436.

McGee AW, Topinka JR, Hashimoto K, Petralia RS, Kakizawa S, Kauer F, Aguilera-Moreno A, Wenthold RJ, Kano M, Bredt DS (2001) PSD-93 knock-out mice reveal that neuronal MAGUKs are not required for development or function of parallel fiber synapses in cerebellum. J Neurosci 21: 3085-3091.

McMahon SB, Wall PD (1983) Receptive fields of lamina I projection cells move to incorporate a nearby region of injury. Pain 19: 234-247.

Medhurst AD, Harrison DC, Read SJ, Campbell C.A, Robbins MJ, Pangalos MN (2000) The use of TaqMan RT-PCR assays for semi-quantitative analysis of gene expression in CNS tissues and disease models. J Neurosci Meth 98: 9-20.

Melcher T, Maas S, Herb A, Sprengel R, Seeburg PH, Higuchi M (1996) A mammalian RNA editing enzyme. Nature 379: 460-464.

Meller ST, Dykstra CL, Gebhart GF (1993) Acute mechanical hyperalgesia is produced by co-activation of AMPA and metabotropic glutamate receptors. Neuroreport 4: 879-882.

Melzack R, Wall PD (1965) Pain mechanisms: a new theory. Sci 150: 971-979.

Mendell LM, Wall PD (1965) Responses of dorsal cord cells to peripheral cutaneous unmyelinated fibres. Nature 206: 97-99.

Mendell LM (1966) Physiological properties of unmyelinated fiber projection to the spinal cord. Exp Neurol 16: 316-332.

Menétrey D, Chaouch A, Binder D, Besson JM (1982) The origin of the spinomesencephalic tract in the rat: an anatomical study using the retrograde transport of horseradish peroxidase. J Comp Neurol 206: 193-207.

Merskey H (1986) Classification of chronic pain; Descriptions of chronic pain syndromes and definitions of pain terms. Pain (Suppl) 3: S1-S226.

Migaud M, Charlesworth P, Dempster M, Webster LC, Watabe AM, Makhinson M, He Y, Ramsay MF, Morris RGM, Morrison JH, Odell TJ, Grant SGN (1998) Enhanced long-term potentiation and impaired learning in mice with mutant postsynaptic density-95 protein. Nature 396: 433-439.

Mogil JS, Wilson SG, Bon K, Lee SE, Chung K, Raber P, Pieper JO, Hain HS, Belknap JK, Hubert L, Elmer GI, Chung JM, Devor M (1999) Heritability of nociception I: responses of 11 inbred mouse strains on 12 measures of nociception. Pain 80: 67-82.

Molander C, Xu H, Grant G (1984) The cytoarchitectonic organisation of the spinal cord in the rat. I. The lower thoracic and lumbrosacral cord. J Comp Neurol 230: 133-141.

Monyer H, Sprengel R, Schoepfer R, Herb A, Higuchi M, Lomeli H, Burnashev N, Sakmann B, Seeburg PH (1992) Heteromeric NMDA receptors - molecular and functional distinction of subtypes. Sci 256: 1217-1221.

Moon IS, Apperson ML, Kennedy MB (1994) The major tyrosine-phosphorylated protein in the postsynaptic density fraction is *N*-methyl-D-aspartate receptor subunit 2B. Proc Natl Acad Sci U S A 91: 3954-3958.

Moriyoshi K, Masu M, Ishii T, Shigemoto R, Mizuno N, Nakanishi S (1991) Molecular cloning and characterization of the rat NMDA receptor. Nature 354: 31-37.

Morris RGM (1989) Synaptic plasticity and learning: selective impairment of learning in rats and blockade of long-term potentiation in vivo by NMDA receptor antagonist AP5. J Neurosci 9: 3040-3058.

Morton CR, Johnson SM, Duggan AW (1983) Lateral reticular regions and the descending control of dorsal horn neurones of the cat: selective inhibition by electrical stimulation. Brain Res 275: 13-21.

Morton CR, Hutchison WD (1989) Release of sensory neuropeptides in the spinal cord: studies with CGRP and galanin. Neurosci 31: 807-815.

Müller BM, Kistner U, Kindler S, Chung WJ, Kuhlendahl S, Fenster SD, Lau LF, Veh RW, Huganir RL, Gundelfinger ED, Garner CC (1996) SAP102, a novel postsynaptic protein that interacts with NMDA receptor complexes in vivo. Neuron 17: 255-265.

Munger BL, Bennett GJ, Kajander KC (1992) An experimental painful peripheral neuropathy due to nerve constriction: Axonal pathology in the sciatic nerve. Exp Neurol 118: 204-214.

Munro FE, Fleetwood-Walker SM, Mitchell R (1994) Evidence for a role of protein kinase C in the sustained activation of rat dorsal horn neurons evoked by cutaneous mustard oil application. Neurosci Lett 170: 199-202.

Murase K, Nedeljkov V, Randić M. (1982) The actions of neuropeptides on dorsal horn neurones in the rat spinal cord slice preparation: an intracellular study. Brain Res 234: 170-176.

Nagy JI, Hunt SP, Iversen LL, Emson PC (1981) Biochemical and anatomical observations on the degeneration of peptide-containing primary afferent neurons after neonatal capsaicin. Neurosci 6: 1923-1934.

Nagy JI, Hunt SP (1982) Fluoride resistant acid phosphatase - containing neurones in dorsal root ganglia are separate from those containing substance P or somatostatin. Neurosci 7: 89-98.

Nahin RL, Ren K, De León M, Ruda M (1994) Primary sensory neurons exhibit altered gene expression in a rat model of neuropathic pain. Pain 58: 95-108.

Naisbitt S, Kim E, Weinberg RJ, Rao A, Yang FC, Craig AM, Sheng M (1997) Characterization of guanylate kinase-associated protein, a postsynaptic density protein at excitatory synapses that interacts directly with postsynaptic density-95 synapse- associated protein 90. J Neurosci 17: 5687-5696.

Neugebauer V, Rumenapp P, Schaible HG (1997) The role of spinal neurokinin-2 receptors in the processing of nociceptive information from the joint and in the generation and maintenance of inflammation-evoked hyperexcitability of dorsal horn neurons in the rat. Eur J Neurosci 249-260.

Neugebauer V, Lucke T, Schaible HG (1994) Requirement of metabotropic glutamate receptors for the generation of inflammation-evoked hyperexcitability in rat spinal cord neurons. Eur J Neurosci 6: 1179-1186.

Nicoll RA, Malenka RC (1995) Contrasting properties of two forms of long-term potentiation in the hippocampus. Nature 377: 115-118.

Niethammer M, Kim E, Sheng M (1996) Interaction between the C-terminus of NMDA receptor subunits and multiple members of the PSD-95 family of membrane-associated guanylate kinases. J Neurosci 16: 2157-2163.

Nishimune A, Isaac JTR, Molnar E, Noel J, Nash SR, Tagaya M, Collingridge GL, Nakanishi S, Henley JM (1998) NSF binding to GluR2 regulates synaptic transmission. Neuron 21: 87-97.

Noel, J, Ralph, GS, Pickard, L, Williams, J, Molnar, E, Uney, JB, Collingridge, GL, Henley, JM (1999) Surface expression of AMPA receptors in hippocampal neurons is regulated by an NSF-dependent mechanism. Neuron 23: 365-376.

Nuytten D, Kupers R, Lammens M, Dom R, Van Hees J, Gybels J (1992) Further evidence for myelinated as well as unmyelinated fibre damage in a rat model of neuropathic pain. Exp Brain Res 91: 73-78.

O'Brien RJ, Lau LF, Huganir RL (1998) Molecular mechanisms of glutamate receptor clustering at excitatory synapses. Curr Op Neurobiol 8: 364-369.

O'Brien RJ, Xu DS, Petralia RS, Steward O, Huganir RL, Worley P (1999) Synaptic clustering of AMPA receptors by the extracellular immediate- early gene product Narp. Neuron 23: 309-323.

Ogawa T, Karazawa I, Kimura S (1985) Regional distribution of Substance P, NKA and NKB in rat spinal cord, nerve roots and dorsal root ganglia, and the effects of dorsal root section or spinal transection. Brain Res 359: 152-157.

Oku, Satoh, Fujii, Otaka, Yajima, Takagi (1987) CGRP promotes mechanical nociception by potentiating release of SP from the spinal dorsal horn in rats. Brain Res 403: 350-354.

Oliveras JL, Besson JM, Guilbaud G, Liebeskind JC (1974) Behavioural and electrophysiological evidence of pain inhibition from midbrain stimulation in the cat. Exp Brain Res 20: 32-44.

Osten P, Srivastava S, Inman GJ, Vilim FS, Khatri L, Lee LM, States BA, Einheber S, Milner TA, Hanson PI, Ziff EB (1998) The AMPA receptor GluR2 C-terminus can mediate a reversible, ATP- dependent interaction with NSF and α- and β-SNAPs. Neuron 21: 99-110.

Osten P, Khatri L, Perez JL, Kohr G, Giese G, Daly C, Schulz TW, Wensky A, Lee LM, Ziff EB (2000) Mutagenesis reveals a role for ABP/GRIP binding to GluR2 in synaptic surface accumulation of the AMPA receptor. Neuron 27: 313-325.

Paleckova V, Palecek J, McAdoo DJ, Willis WD (1992) The non-NMDA antagonist CNQX prevents release of amino acids into the rat spinal cord dorsal horn evoked by sciatic nerve stimulation. Neurosci Lett 148: 19-22.

Passafarro M, Sala C, Niethammer M, Sheng M (1999) Microtubule binding by CRIPT and its potential role in the synaptic clustering of PSD-95. Nat Neurosci 2: 1063-1069.

Pellegrini-Giampietro DE, Fan S, Ault B, Miller BE, Zukin RS (1994) Glutamate receptor gene expression in spinal cord of arthritic rats. J Neurosci 14: 1576-1583.

Perrot S, Attal N, Ardid D, Guilbaud G (1993) Are mechanical and cold allodynia in mononeuropathic and arthritic rats relieved by systemic treatment with calcitonin or guanethidine? Pain 52: 41-47.

Picard P, Boucher S, Regoli D, Gitter BD, Howbert JJ, Couture R (1993) Use of non-peptide tachykinin receptor antagonists to substantiate the involvement of NK_1 and NK_2 receptors in a spinal nociceptive reflex in the rat. Eur J Pharmacol 232: 255-261.

Popratiloff A, Weinberg RJ, Rustioni A (1996) AMPA receptor subunits underlying terminals of fine-caliber primary afferent fibers. J Neurosci 16: 3363-3372.

Popratiloff A, Weinberg RJ, Rustioni A (1998) AMPA receptors at primary afferent synapses in substantia gelatinosa after sciatic nerve section. Eur J Neurosci 10: 3220-3230.

Procter MJ, Houghton AK, Faber ESL, Chizh BA, Ornstein PL, Lodge D, Headley PM (1998) Actions of kainate and AMPA selective glutamate receptor ligands on nociceptive processing in the spinal cord. Neuropharm 37: 1287-1297.

Prybylowski KL, Grossman SD, Wrathall JR, Wolfe BB (2001) Expression of splice variants of the NR1 subunit of the *N*-methyl-D-aspartate receptor in the normal and injured rat spinal cord. J Neurochem 76: 797-805.

Püschel AW, O'Connor V, Betz H (1994) The *N*-ethylmaleimide-sensitive fusion protein (NSF) is preferentially expressed in the nervous system. FEBS Lett 347: 55-58.

Quirion R, Shults CW, Moody TW, Pert CB, Chase TN, O'Donohue TL (1983) Autoradiographic distribution of substance P receptors in rat central nervous system. Nature 303: 714-716.

Quirion R, Dam T-V (1988) Multiple tachykinin receptors: recent developments. Regul Pept 22: 18-25.

Ramer MS, Bisby MA (1997) Rapid sprouting of sympathetic axons in dorsal root ganglia of rats with a chronic constriction injury. Pain 70: 237-244.

Randić M, Miletic (1978) Depressant actions of methionine-enkephalin and somatostatin in cat dorsal horn neurones activated by noxious stimuli. Brain Res 152: 196-202.

Rao A, Kim E, Sheng M, Craig AM (1998) Heterogeneity in the molecular composition of excitatory postsynaptic sites during development of hippocampal neurons in culture. J Neurosci 18: 1217-1229.

Ray SK, Matzelle DD, Wilford GG, Hogan EL, Banik NL (2000) Increased calpain expression is associated with apoptosis in rat spinal cord injury: calpain inhibitor provides neuroprotection. Neurochem Res 25: 1191-1198.

Rees H, Sluka KA, Urban L, Walpole CJ, Willis WD (1998) The effects of SDZ NKT 343, a potent NK1 receptor antagonist, on cutaneous responses of primate spinothalamic tract neurones sensitized by intradermal capsaicin injection. Exp Brain Res 121: 355-358.

Réthelyi M (1977) Preterminal and terminal axon arborization in the substantia gelatinosa of the cat's spinal cord. J Comp Neurol 172: 511-528.

Reti IM, Baraban JM (2000) Sustained increase in Narp protein expression following repeated electroconvulsive seizure. Neuropsychopharm 23: 439-443.

Rexed B (1952) The cytoarchitectonic organization of the spinal cord in the cat. J Comp Neurol 96: 415-495.

Reynolds DV (1969) Surgery in the rat during electrical analgesia induced by focal brain stimulation. Sci 164: 444-445.

Rizzoli AA (1968) Distribution of glutamic acid, aspartic acid, aminobutyric acid and glycine in six areas of cat spinal cord before and after transection. Brain Res 11: 11-18.

Robertson B, Grant G (1985) A comparison between wheat germ agglutinin-and choleragenoid-horseradish peroxidase as anterogradely transported markers in central branches of primary sensory neurones in the rat with some observations in the cat. Neurosci 14: 895-905.

Roche KW, O'Brien RJ, Mammen AL, Bernhardt J, Huganir RL (1996) Characterization of multiple phosphorylation sites on the AMPA receptor GluR1 subunit. Neuron 16: 1179-1188.

Rose MA, Kam PC (2002) Gabapentin: pharmacology and its use in pain management. Anaesthesia 57: 451-462.

Rosenmund C, Westbrook GL (1993) Calcium-induced actin depolymerization reduces NMDA channel activity. Neuron 10: 805-814.

Rosenmund C, Carr DW, Bergeson SE, Nilaver G, Scott JD, Westbrook GL (1994) Anchoring of protein kinase A is required for modulation of AMPA/kainate receptors on hippocampal-neurons. Nature 368: 853-856.

Rowan S, Todd AJ, Spike RC (1993) Evidence that neuropeptide Y is present in GABAergic neurons in the superficial dorsal horn of the rat spinal cord. Neurosci 53: 537-545.

Ruda MA (1982) Opiates and pain pathways: demonstration of enkephalin synapses on dorsal horn projection neurones. Sci 215: 1523-1525.

Rudin NJ (2001) Chronic pain rehabilitation: principles and practice. WMJ 100: 36-43, 66.

Rusin KI, Ryu PD, Randić M (1992) Modulation of excitatory amino acid responses in rat dorsal horn neurons by tachykinins. J Neurophysiol 68: 265-286.

Rusin KI, Jiang MC, Cerne R, Randić M (1993) Interactions between excitatory amino acids and tachykinins in the rat spinal dorsal horn. Brain Res Bull 30: 329-338.

Rustioni A, Weinberg RJ (1989) Somatosensory system. In: Handbook of chemical neuroanatomy. Integrated systems of the CNS, Pt II. (Björklund A, Hökfelt T, Swanson LW, eds).

Salt TE, Hill RG (1981) Vasoactive intestinal polypeptide (VIP) applied by microiontophoresis excites single neurones in the trigeminal nucleus caudalis of the rat. Neuropep 1: 403-408.

Salt TE, Hill RG (1983) Neurotransmitter candidates of somatosensory primary afferent fibres. Neurosci 10: 1083-1103.

Sang CN, Hostetter MP, Gracely RH, Chappell AS, Schoepp DD, Lee G, Whitcup S, Caruso R, Max MB (1998) AMPA/Kainate antagonist LY293558 reduces capsaicin-evoked hyperalgesia but not pain in normal skin in humans. Anesthes 89: 1060-1067.

Sattler, R, Xiang, ZG, Lu, WY, Hafner, M, MacDonald, JF, Tymianski, M (1999) Specific coupling of NMDA receptor activation to nitric oxide neurotoxicity by PSD-95 protein. Sci 284: 1845-1848.

Scadding J (1984) Peripheral Neuropathies. In: Textbook of Pain (Wall PD, Melzack R, eds), pp 413-425. Edinburgh: Churchill Livingstone.

Scannevin RH, Huganir RL (2000) Postsynaptic organization and regulation of excitatory synapses. Nat Rev Neurosci 1: 133-141.

Schaible HG, Schmidt RF (1985) Development, Organization and Processing in Somatosensory Pathways. New York: Liss.

Schmalbruch H (1986) Fiber composition of the rat sciatic nerve. Anat Rec 215: 71-81.

Schopperle WM, Holmqvist MH, Zhou Y, Wang J, Wang Z, Griffith LC, Keselman I, Kusinitz F, Dagan D, Levitan IB (1998) Slob, a novel protein that interacts with the Slowpoke calcium-dependent potassium channel. Neuron 20: 565-573.

Seeburg PH (1993) The TIPS/TINS lecture -The molecular-biology of mammalian glutamate receptor channels. Trends Pharm Sci 14: 297-303.

Seguin L, Le Marouille-Girardon S, Millan MJ (1995) Antinociceptive profiles of non-peptidergic neurokinin$_1$ and neurokinin$_2$ receptor antagonists: A comparison to other classes of antinociceptive agent. Pain 61: 325-343.

Shehab SA, Atkinson ME (1986) Vasoactive intestinal polypeptide increases in areas of the dorsal horn of the spinal cord from which other neuropeptides are depleted following peripheral axotomy. Exp Brain Res 62: 422-430.

Sheng M (1996) PDZs and receptor/channel clustering: Rounding up the latest suspects. Neuron 17: 575-578.

Sheng M, Wyszynski M (1997) Ion channel targeting in neurons. Bioessays 19: 847-853.

Sherrington CS (1906) The integrative action of the nervous system. New York: Scribner.

Shibata T, Watanabe M, Ichikawa R, Inoue Y, Koyanagi T (1999) Different expressions α-3-hydroxy-5-methyl-4-isoxazole propionic acid and *N*-methyl-D-aspartate receptor subunit mRNAs between visceromotor and somatomotor neurons of the rat lumbosacral spinal cord. J Comp Neurol 404: 172-182.

Shin H, Hsueh YP, Yang FC, Kim E, Sheng M (2000) An intramolecular interaction between Src homology 3 domain and guanylate kinase-like domain required for channel clustering by postsynaptic density-95/SAP90. J Neurosci 20: 3580-3587.

Silva AJ, Stevens CF, Tonegawa S, Wang Y (1992) Deficient hippocampal long-term potentiation in α-calcium-calmodulin kinase II mutant mice. Sci 257: 201-206.

Silva E, Cleland CL, Gebhart GF (1997) Contributions of glutamate receptors to the maintenance of mustard oil-induced hyperalgesia in spinalized rats. Exp Brain Res 117: 379-388.

Simmons RMA, Li DL, Hoo KH, Deverill M, Ornstein PL, Iyengar S (1998) Kainate GluR5 receptor subtype mediates the nociceptive response to formalin in the rat. Neuropharm 37: 25-36.

Simone DA, Kajander KC (1996) Excitation of rat cutaneous nociceptors by noxious cold. Neurosci Lett 213: 53-56.

Sloan SI, Stucky CL, Jansen EM, Galeazza MT, Seybold VS, Aanonsen L (1991) Changes in PCP binding sites in rat spinal cord in an experimental model of acute, peripheral inflammation. Soc Neurosci Abstr 17, 435.

Smith GD, Seckl JR, Harmar AJ (1993) Distribution of neuropeptides in dorsal root ganglia of the rat; substance P, somatostatin and calcitonin gene-related peptide. Neurosci Lett 153: 5-8.

Sommer B, Keinänen K, Verdoorn TA, Wisden W, Burnashev N, Herb A, Kohler M, Takagi T, Sakmann B, Seeburg PH (1990) Flip and flop - a cell-specific functional switch in glutamate operated channels of the CNS. Sci 249: 1580-1585.

Sommer C, Lalonde A, Heckman HM, Rodriguez M, Myers RR (1995) Quantitative neuropathology of a focal nerve injury causing hyperalgesia. J Neuropath Exp Neurol 54: 635-643.

Song I, Kamboj S, Xia, J., Dong H, Liao D, Huganir RL (1998) Interaction of the *N*-ethylmaleimide-sensitive factor with AMPA receptors. Neuron 21: 393-400.

Songyang Z, Fanning AS, Fu C, Xu J, Marfatia SM, Chishti AH, Crompton A, Chan AC, Anderson JM, Cantley LC (1997) Recognition of unique carboxyl-terminal motifs by distinct PDZ domains. Sci 275: 73-77.

Sorkin LS, Yaksh TL, Doom CM (1999) Mechanical allodynia in rats is blocked by a Ca^{2+} permeable AMPA receptor antagonist. Neuroreport 10: 3523-3526.

Sotgiu ML, Biella G (2000) Differential effects of MK-801, an *N*-methyl-D-aspartate non-competitive antagonist, on the dorsal horn neuron hyperactivity and hyperexcitability in neuropathic rats. Neurosci Lett 283: 153-156.

Srivastava S, Osten P, Vilim FS, Khatri L, Inman G, States B, Daly C, DeSouza S, Abagyan R, Valtschanoff JG, Weinberg RJ, Ziff EB (1998) Novel anchorage of GluR2/3 to the postsynaptic density by the AMPA receptor-binding protein ABP. Neuron 21: 581-591.

Staudinger J, Lu JR, Olson EN (1997) Specific interaction of the PDZ domain protein PICK1 with the COOH terminus of protein kinase C-α. J Biol Chem 272: 32019-32024.

Strack S, Colbran RJ (1998) Autophosphorylation-dependent targeting of calcium/ calmodulin-dependent protein kinase II by the NR2B subunit of the *N*-methyl- D-aspartate receptor. J Biol Chem 273: 20689-20692.

Sugihara H, Moriyoshi K, Ishii T, Masu M, Nakanishi S (1992) Structures and properties of seven isoforms of the NMDA receptor generated by alternative splicing. Biochem Biophys Res Commun 185: 826-832.

Sugimoto T, Bennett GJ, Kajander KC (1990) Transsynaptic degeneration in the superficial dorsal horn after sciatic nerve injury: Effects of a chronic constriction injury, transection, and strychnine. Pain 42: 205-213.

Sugiura Y, Terui N, Hosoya T, Kohno K (1988) Distribution of unmyelinated primary afferent fibers in the dorsal horn. In: Processing of Sensory Information in the Superficial Dorsal Horn of the Spinal Cord (Cervero F, Bennett GJ, Headley PM, eds), pp 15-29.

Sutton, JL, Maccecchini, ML, Kajander, KC (1999) The kainate receptor antagonist 2S,4R-3-methylglutamate attenuates mechanical allodynia and thermal hyperalgesia in a rat model of nerve injury. Neurosci 91: 283-292.

Swett JE, Woolf CJ (1985) The somatotopic organization of primary afferent terminals in the superficial laminae of the dorsal horn of the rat spinal cord. J Comp Neurol 231: 66-77.

Tal M, Bennett GJ (1993) Dextrorphan relieves neuropathic heat-evoked hyperalgesia in the rat. Neurosci Lett 151: 107-110.

Tal M, Eliav E (1996) Abnormal discharge originates at the site of nerve injury in experimental constriction neuropathy (CCI) in the rat. Pain 64: 511-518.

Tao Y, Huang Y, Mei L, Johns RA (2000) Expression of PSD-95/SAP90 is critical for *N*-methyl-D-aspartate receptor-mediated thermal hyperalgesia in the spinal cord. Neurosci 98: 201-206.

Tezuka T, Umemori H, Akiyama T, Nakanishi S, Yamamoto T (1999) PSD-95 promotes Fyn-mediated tyrosine phosphorylation of the *N*- methyl-D-aspartate receptor subunit NR2A. Proc Natl Acad Sci U S A 96: 435-440.

Tingley WG, Ehlers MD, Kameyama K, Doherty C, Ptak JB, Riley CT, Huganir RL (1997) Characterization of protein kinase A and protein kinase C phosphorylation of the *N*-methyl-D-aspartate receptor NR1 subunit using phosphorylation site-specific antibodies. J Biol Chem 272: 5157-5166.

Todd AJ, McKenzie J (1989) GABA-immunoreactive neurons in the dorsal horn of the rat spinal cord. Neurosci 31: 799-806.

Todd AJ (1990) An electron microscope study of glycine-like immunoreactivity in laminae I-III of the spinal dorsal horn of the rat. Neurosci 39: 387-394.

Topinka JR, Bredt DS (1998) N-terminal palmitoylation of PSD-95 regulates association with cell membranes and interaction with K^+ channel Kv1.4. Neuron 20: 125-134.

Torres R, Firestein BL, Dong H, Staudinger J, Olson EN, Huganir RL, Bredt DS, Gale NW, Yancopoulos GD (1998) PDZ proteins bind, cluster, and synaptically colocalize with Eph receptors and their ephrin ligands. Neuron 21: 1453-1463.

Tölle, Berthele A, Zieglgänsberger W, Seeburg PH, Wisden W (1995) Flip and flop variants of AMPA receptors in the rat lumbar spinal cord. Eur J Neurosci 7: 1414-1419.

Tölle TR, Berthele A, Zieglgänsberger W, Seeburg PH, Wisden W (1993) The differential expression of 16 NMDA and non-NMDA receptor subunits in the rat spinal-cord and in periaqueductal gray. J Neurosci 13: 5009-5028.

Treede RD, Magerl W (1995) Modern concepts of pain and hyperalgesia: Beyond the polymodal C-nociceptor. News Physiol Sci 10: 216-228.

Tsui CC, Copeland NG, Gilbert DJ, Jenkins NA, Barnes C, Worley PF (1996) Narp, a novel member of the pentraxin family, promotes neurite outgrowth and is dynamically regulated by neuronal activity. J Neurosci 16: 2463-2478.

Urban L, Naeem S, Patel IA, Dray A (1994) Tachykinin induced regulation of excitatory amino acid responses in the rat spinal cord in vitro. Neurosci Lett 168: 185-188.

van Rossum D, Hanisch UK (1999) Cytoskeletal dynamics in dendritic spines: direct modulation by glutamate receptors? Trends Neurosci 22: 290-295.

Verdoorn TA, Burnashev N, Monyer H, Seeburg PH, Sakmann B (1991) Structural determinants of ion flow through recombinant glutamate receptor channels. Sci 252: 1715-1718.

Villar MJ, Cortes R, Theodorsson E, Wiesenfeld-Hallin Z, Schalling M, Fahrenkrug J, Emson PC, Hökfelt T (1989) Neuropeptide expression in rat dorsal root ganglion cells and spinal cord after peripheral nerve injury with special reference to galanin. Neurosci 33: 587-604.

Wakisaka S, Kajander KC, Bennett GJ (1991) Increased neuropeptide Y (NPY)-like immunoreactivity in rat sensory neurons following peripheral axotomy. Neurosci Lett 124: 200-203.

Wall PD (1991) Neuropathic pain and injured nerve: central mechanisms. Br Med Bull 47: 631-643.

Wall PD (1960) Cord cells responding to touch, damage and temperature of skin. J Neurophysiol 23: 197-210.

Wall PD (1967) The laminar organisation of dorsal horn and effects of descending impulses. J Physiol 188: 403-423.

Walpole C, Ko SY, Brown M, Beattie D, Campbell E, Dickenson F, Ewan S, Hughes GA, Lemaire M, Lerpiniere J, Patel S, Urban L (1998) 2-Nitrophenylcarbamoyl-(S)-prolyl-(S)-3-(2-naphthyl)alanyl-N-benzyl-N - methylamide (SDZ NKT 343), a potent human NK1 tachykinin receptor antagonist with good oral analgesic activity in chronic pain models. J Med Chem 41: 3159-3173.

Wanaka A, Shiotani Y, Kiyama H, Matsuyama T, Kamada T, Shiosaka S, Tohyama M (1987) Glutamate-like immunoreactive structures in primary sensory neurons in the rat detected by a specific antiserum against glutamate. Exp Brain Res 65: 691-694.

Wang YT, Salter MW (1994) Regulation of NMDA receptors by tyrosine kinases and phosphatases. Nature 369: 233-235.

Watanabe M, Mishina M, Inoue Y (1994) Distinct gene expression of the *N*-methyl-D-aspartate receptor channel subunit in peripheral neurons of the mouse sensory ganglia and adrenal gland. Neurosci Lett 165: 183-186.

Weinberg RJ (1999) Glutamate: an excitatory neurotransmitter in the mammalian CNS. Brain Res Bull 50: 353-354.

Wenthold RJ, Yokotani N, Doi K, Wada K (1992) Immunochemical characterization of the non-NMDA glutamate receptor using subunit-specific antibodies - evidence for a heterooligomeric structure in rat-brain. J Biol Chem 267: 501-507.

Wenthold RJ, Trumpy VA, Zhu WS, Petralia RS (1994) Biochemical and assembly properties of GluR6 and KA2, two members of the kainate receptor family, determined with subunit-specific antibodies. J Biol Chem 269: 1332-1339.

Westlund KN, McNeill DL, Coggeshall RE (1989) Glutamate immunoreactivity in rat dorsal root axons. Neurosci Lett 96: 13-17.

Westphal RS, Tavalin SJ, Lin JW, Alto NM, Fraser IDC, Langeberg LK, Sheng M, Scott JD (1999) Regulation of NMDA receptors by an associated phosphatase-kinase signaling complex. Sci 285: 93-96.

Wiesenfeld-Hallin Z, Villar MJ, Hökfelt T (1988) Intrathecal galanin at low doses increases spinal reflex excitability in rats more to thermal than mechanical stimuli. Exp Brain Res 71: 663-666.

Wiesenfeld-Hallin Z, Xu XJ, Hakanson R, Feng DM, Folkers K (1991a) Low-dose intrathecal morphine facilitates the spinal flexor reflex by releasing different neuropeptides in rats with intact and sectioned peripheral nerves. Brain Res 551: 157-162.

Wiesenfeld-Hallin Z, Xu XJ, Hakanson R, Feng DM, Folkers K, Kristensson K, Villar MJ, Fahrenkrug J, Hökfelt T (1991b) On the role of substance P, galanin, vasoactive intestinal peptide, and calcitonin gene-related peptide in mediation of spinal reflex excitability in rats with intact and sectioned peripheral nerves. ANYAS 632: 198-211.

Wiesenfeld-Hallin Z (1986) Substance P and somatostatin modulate spinal cord excitability via physiologically different sensory pathways. Brain Res 372: 172-175.

Wiesenfeld-Hallin Z (1987) Intrathecal vasoactive intestinal polypeptide modulates spinal reflex excitability primarily to cutaneous thermal stimuli in rats. Neurosci Lett 80: 293-297.

Willis WD (1977) Inhibition of spinothalamic tract cells and interneurons by brain stem stimulation in the monkey. J Neurophysiol 40: 968-981.

Willis WD, Coggeshall RE (1991) Sensory mechanisms of the spinal cord. New York and London: Plenum Press.

Willis WD, Haber LH, Martin RF (1977) Inhibition of spinothalamic tract cells and interneurons by brain stem stimulation in the monkey. J Neurophysiol 40: 968-981.

Willis WD, Leonard RB (1979) Spinothalamic tract neurones in the substantia gelantinosa. Sci 202: 986-988.

Woolf CJ, Wall PD (1982) Chronic peripheral nerve section diminishes the primary afferent A-fibre mediated inhibition of rat dorsal horn neurones. Brain Res 242: 77-85.

Woolf CJ, Shortland P, Coggeshall RE (1992) Peripheral nerve injury triggers central sprouting of myelinated afferents. Nature 355: 75-78.

Woolf CJ, Hardy JD (1941) Studies on pain: Observations on pain due to a local cooling and on factors involved in the 'cold pressor'. J Clin Invest 20: 521-533.

Woolf CJ, Fitzgerald M (1983) The properties of neurones recorded in the superficial dorsal horn of the rat spinal cord. J Comp Neurol 221: 313-328.

Woolf CJ (1983) Evidence for a central component of post-injury pain hypersensitivity. Nature 306: 686-688.

Woolf CJ (1986) Are excitatory amino acids the fast neurotransmitters in cutaneous C- primary afferent neurones. Neurosci Lett (Suppl) 24: 537.

Woolf CJ, Wall PD (1986) Relative effectiveness of C primary afferent fibers of different origins in evoking a prolonged facilitation of the flexor reflex in the rat. J Neurosci 6: 1433-1442.

Woolf CJ, Thompson SWN (1991) The induction and maintenance of central sensitization is dependent on *N*-methyl-D-aspartic acid receptor activation; Implications for the treatment of post-injury pain hypersensitivity states. Pain 44: 293-299.

Wyszynski M, Lin J, Rao A, Nigh E, Beggs AH, Craig AM, Sheng M (1997) Competitive binding of α-actinin and calmodulin to the NMDA receptor. Nature 385: 439-442.

Wyszynski M, Kim E, Yang FC, Sheng M (1998) Biochemical and immunocytochemical characterization of GRIP, a putative AMPA receptor anchoring protein, in rat brain. Neuropharm 37: 1335-1344.

Wyszynski M, Valtschanoff JG, Naisbitt S, Dunah AW, Kim E, Standaert DG, Weinberg R, Sheng M (1999) Association of AMPA receptors with a subset of glutamate receptor-interacting protein in vivo. J Neurosci 19: 6528-6537.

Xia J, Zhang XQ, Staudinger J, Huganir RL (1999) Clustering of AMPA receptors by the synaptic PDZ domain- containing protein PICK1. Neuron 22: 179-187.

Xia J, Chung HJ, Wihler C, Huganir RL, Linden DJ (2000) Cerebellar long-term depression requires PKC-regulated interactions between GluR2/3 and PDZ domain-containing proteins. Neuron 28: 499-510.

Xu XJ, Wiesenfeld-Hallin Z, Villar MJ, Fahrenkrug J, Hokfelt T (1990) On the role of galanin, substance P and other neuropeptides in primary sensory neurons of the rat: studies on spinal reflex excitability and peripheral axotomy. Eur J Neurosci 2: 733-743.

Xu X-J, Hao J-X, Hökfelt T, Wiesenfeld-Hallin Z (1994) The effects of intrathecal neuropeptide Y on the spinal nociceptive flexor reflex in rats with intact sciatic nerves and after peripheral axotomy. Neurosci 63: 817-826.

Yaksh TL, Farb DH, Leeman SE, Jessell TM (1979) Intrathecal capsaicin depletes substance P in the rat spinal cord and produces prolonged thermal analgesia. Sci 206: 481-483.

Yaksh TL, Abay EO, Go VL (1982) Studies on the location and release of cholecystokinin and vasoactive intestinal peptide in rat and cat spinal cord. Brain Res 242: 279-290.

Yamada Y, Chochi Y, Takamiya K, Sobue K, Inui M (1999) Modulation of the channel activity of the ξ2/ζ1-subtype *N*-methyl D-aspartate receptor by PSD-95. J Biol Chem 274: 6647-6652.

Yamamoto T, Nozaki-Taguchi N, Sakashita Y, Kimura S (1999) Nociceptin/orphanin FQ: role in nociceptive information processing. Prog Neurobiol 57: 527-535.

Yamamoto T, Yaksh TL (1992) Effects of intrathecal capsaicin and an NK-1 antagonist, CP,96- 345, on the thermal hyperalgesia observed following unilateral constriction of the sciatic nerve in the rat. Pain 51: 329-334.

Yashpal K, Sarrieau A, Quirion R (1991) ^{125I}Vasoactive intestinal polypeptide binding sites: quantitative autoradiographic distribution in the rat spinal cord. J Chem Neuroanat 4: 439-446.

Yashpal K, Hui-Chan CWY, Henry JL (1996) SR 48968 specifically depresses neurokinin A- vs substance P-induced hyperalgesia in a nociceptive withdrawal reflex. Eur J Pharmacol 308: 41-48.

Yasphal K, Wright DM, Henry JL (1982) Substance P reduces tail-flick latency: implications for chronic pain syndromes. Pain 14: 155-167.

Ye B, Liao D, Zhang X, Zhang P, Dong H, Huganir RL (2000) GRASP-1: a neuronal RasGEF associated with the AMPA receptor/GRIP complex. Neuron 26: 603-617.

Yoshimura M, Jessell T (1990) Amino acid-mediated EPSPs at primary afferent synapses with substantia gelatinosa neurones in the rat spinal cord. J Physiol 430:315-35.

Yoshimura M, Nishi S (1992) Excitatory amino acid receptors involved in primary afferent- evoked polysynaptic EPSPs of substantia gelatinosa neurons in the adult rat spinal cord slice. Neurosci Lett 143: 131-134.

Young MR, Fleetwood-Walker SM, Mitchell R, Munro FE (1994) Evidence for a role of metabotropic glutamate receptors in sustained nociceptive inputs to rat dorsal horn neurons. Neuropharm 33: 141-144.

Young MR, Fleetwood-Walker SM, Mitchell R, Dickinson T (1995) The involvement of metabotropic glutamate receptors and their intracellular signaling pathways in sustained nociceptive transmission in rat dorsal horn neurons. Neuropharm 34: 1033-1041.

Yu XM, Askalan R, Keil GJ, Salter MW (1997) NMDA channel regulation by channel-associated protein tyrosine kinase Src. Sci 275: 674-678.

Yung KKL (1998) Localization of glutamate receptors in dorsal horn of rat spinal cord. Neuroreport 9: 1639-1644.

Zhang S, Ehlers MD, Bernhardt JP, Su CT, Huganir RL (1998) Calmodulin mediates calcium-dependent inactivation of *N*-methyl-D- aspartate receptors. Neuron 21: 443-453.

Zhang X, Nicholas AP, Hökfelt T (1993) Ultrastructural studies on peptides in the dorsal horn of the spinal cord-I. Co-existence of galanin with other peptides in primary afferents in normal rats. Neurosci 57: 365-384.

Zhang X, Ji RR, Nilsson S, Villar M, Ubink R, u G, Wiesenfeld-Hallin Z, Hokfelt T (1995) Neuropeptide Y and galanin binding sites in rat and monkey lumbar dorsal root ganglia and spinal cord and effect of peripheral axotomy. Eur J Neurosci 7: 367-380.

Zhang WD, Vazquez L, Apperson M, Kennedy MB (1999) Citron binds to PSD-95 at glutamatergic synapses on inhibitory neurons in the hippocampus. J Neurosci 19: 96-108.

Zheng X, Zhang L, Wang AP, Bennett MV, Zukin RS (1999) Protein kinase C potentiation of *N*-methyl-D-aspartate receptor activity is not mediated by phosphorylation of *N*-methyl-D-aspartate receptor subunits. Proc Natl Acad Sci U S A 96: 15262-15267.

Zhou S, Bonasera L, Carlton SM (1996) Peripheral administration of NMDA, AMPA or KA results in pain behaviors in rats. Neuroreport 7: 895-900.

Zieglgänsberger W, Sutor B (1983) Responses of substantia gelatinosa neurons to putative neurotransmitters in an in vitro preparation of the adult rat spinal cord. Brain Res 279: 316-320.

Zieglgänsberger W, Herz A (1971) Changes of cutaneous receptive fields of spinocervical tract neurones and other dorsal horn neurones by microelectrophorectically administered amino acids. Exp Brain Res 13: 111-126.

Zou X, Lin Q, Willis WD (2000) Enhanced phosphorylation of NMDA receptor 1 subunits in spinal cord dorsal horn and spinothalamic tract neurons after intradermal injection of capsaicin in rats. J Neurosci 20: 6989-6997.

Zukin RS, Bennett MV (1995) Alternatively spliced isoforms of the NMDAR1 receptor subunit. Trends Neurosci 18: 306-313.